

**THE UNIVERSITY OF HULL & THE
UNIVERSITY OF YORK**

**Proteomic Identification of Putative Biomarkers
of Neo-adjuvant Chemotherapy Resistance in
Luminal (ER+) Breast Cancer**

Thesis being submitted for the degree of

Doctorate of Medicine

by

Tasadooq Hussain

BA (Edu.) PGCert.(Research) MRCS MBBS (Hons)

The University of Hull and The University of York
Hull York Medical School

November 2013

Abstract:

Background:

Neoadjuvant chemotherapy is a standard treatment for locally advanced breast cancer however chemoresistance can be a major obstacle in ER+ cancers. Using comparative proteomic approaches (antibody microarray/AbMA and 2D-PAGE with MALDI-TOF/TOF MS) to investigate a pilot series of breast cancer samples our research group recently identified 14-3-3 theta/tau, tBID and Bcl-XL as putative biomarkers of response to neoadjuvant chemotherapy (Hodgkinson et al J Prot 2012, 75:1276-1283 and 75:2745-2752). Here we aimed to analyse further samples using the AbMA approach and to re-analyse the combined data.

Methods:

Samples from chemoresistant and chemosensitive breast cancers were selected following anthracycline-taxane chemotherapy and 4 experiments were performed using ductal ER+ tumours. Differential protein expression was compared between chemoresistant and chemosensitive samples using the Panorama XPRESS Profiler725 AbMA kit. The combined data from 9 AbMA assays and 3 2D-PAGE/MS experiments was then analysed using Ingenuity Pathway Analysis (IPA; Ingenuity Systems). A pilot series of archival samples was used for clinical validation of putative predictive biomarkers.

Results:

89 differentially expressed proteins (DEPs) were seen in the 4 further AbMA experiments. In the combined dataset (12 experiments from 2 proteomic platforms), 8 DEPs were seen in at least 3 experiments. These were 14-3-3 theta, 14-3-3 epsilon, 14-3-3 gamma, Bcl-xl, Bid, Phosphokinase B, Vimentin and FAK. 121 DEPs from the combined data were analysed using IPA; 13 DEPs were mapped onto the PI3K/AKT pathway. Clinical validation in a pilot series of archival samples revealed Akt-1 Ser473 and FAKY397 alongside the previously identified and validated 14-3-3 theta/tau, and tBID to be significantly associated with chemotherapy resistance.

Conclusion:

We have now identified at least 8 proteins which could play a role in breast chemoresistance. We propose a potential role for Akt-1, FAK, 14-3-3 theta/tau and tBID as predictive biomarkers of neoadjuvant chemotherapy resistance in breast cancer. Further validation in a larger sample series is now required.

Publications and Presentations:

Hussain T; Kneeshaw P; Cawkwell L (2013); Molecular Mechanisms of Breast Cancer Chemotherapy Resistance; *Journal of Oncology News*: Vol 7, Issue 6, January 2013; ISSN: 1751-4975

Hussain T; Scaife L; Hodgkinson V.C.; P. Kneeshaw; Prof. Mike Lind Prof. P. Drew, Cawkwell L (2013); Proteomic biomarker discovery: review of the science, its challenges with clinical samples in cancer research – *British Journal of Medicine and Medical Research*, 4(1): 1-33, 2014

Garimella V; Agarwal V; **Hussain T;** Radhakrishnan S; Long E; Mahapatra T; McManus P; Kneeshaw P; Drew P; Lind M; Cawkwell L (2013); Clinical response to primary Letrozole therapy in women over 70 years with early breast cancer: possible role of p53 as a biomarker - *Journal of Clinical Oncology- Submitted November 2013*

Hussain T; Scaife L; Hodgkinson V.C.; Agarwal V; Long E; Mahapatra T; McManus P.L. Kneeshaw P; Cawkwell L (2013) *14-3-3 proteins, tBID, Akt1 and FAKY397 may be predictive biomarkers of response to neoadjuvant chemotherapy in oestrogen receptor positive breast cancer as revealed by combined antibody microarray and 2D-PAGE/MALDI/TOF/TOF/MS proteomics. Abstract- Society of Academic Research and Surgery, Cambridge, January 2014 (Oral Presentation, Patey Prize Paper Session)*

Hussain T; Scaife L; Hodgkinson V.C.; Agarwal V; Long E; Mahapatra T; McManus P.L. Kneeshaw P; Cawkwell L (2013) Proteomic Identification of Predictive Biomarkers of Neo-adjuvant Chemotherapy Resistance in Breast Cancer: A possible role of Akt-1, FAKY397, 14-3-3 theta/tau and tBID? *Abstract- British Association of Surgical Oncology~ACS Conference, London, November 2013 (Oral Presentation, Roland Raven Prize Paper Session)*

Hussain T; Scaife L; Hodgkinson V.C.; Agarwal V; Long E; Mahapatra T; McManus P.L. Kneeshaw P; Cawkwell L (2013) A Comparative Proteomic Approach for Identification of Putative Biomarkers of Neo-adjuvant Chemotherapy Resistance in Breast Cancer *Abstract - American Society of Clinical Oncology (ASCO) 2013 Annual Meeting, Chicago, US, May 2013*

Hussain T; Scaife L; Hodgkinson V.C.; Agarwal V; Long E; Mahapatra T; McManus P.L. Kneeshaw P; Cawkwell L (2013) Assessment of neoadjuvant chemotherapy responses for locally advanced breast cancer patients: DCE-MRI vs. Resection histology- *Abstract-Presented at the Association of Breast Surgeons ~ACS Conference Manchester 2013; EJSO; Volume 39, Issue 5 , Page 480-81, May 2013*

Hussain T; Scaife L; Hodgkinson V.C.; Agarwal V; Long E; Mahapatra T; McManus P.L. Kneeshaw P; Cawkwell L (2013) Proteomic identification of putative biomarkers of breast neo-adjuvant chemotherapy resistance *Abstract-Presented at the Association of Breast Surgeons ~ACS Conference Manchester 2013; EJSO; Volume 39, Issue 5 , Page 493, May 2013*

Hussain T; Scaife L; Hodgkinson V.C.; Agarwal V; Long E; Mahapatra T; McManus P.L. Kneeshaw P; Cawkwell L (2013); Comparative proteomic approach for the identification of putative biomarkers of neoadjuvant chemotherapy resistance in luminal A breast molecular subtype – *Abstract-Presented at the Association of Surgeons in Training Conference Manchester 2013;*

Hussain T; Hodgkinson V.C.; Agarwal V; Long E; Mahapatra T; McManus P.L. Kneeshaw P; Cawkwell L (2013) Clinical response to primary Letrozole therapy in women over 70 years with early breast cancer: a retrospective study with a 5 year follow up - *European Journal of Surgical Oncology, Volume 38, Issue 5, pg. 433, 2012 Abstract-Presented at the Association of Breast Surgeons ~ACS Conference Bournemouth 2012*

Table of Contents:

Chapter 1. 26

1.1 BREAST ANATOMY:.....	26
1.1.1 Gross Anatomy:.....	26
1.1.2 Breast Structure:.....	26
1.1.3 The Terminal Ductal Lobular Unit:	27
1.2 CLINICAL INTRODUCTION TO BREAST CANCER:.....	29
1.2.1 Epidemiology:	29
1.2.2 Aetiology:.....	29
1.2.3 Breast Cancer Risk Factors:	29
1.3 BREAST CANCER CLASSIFICATIONS:.....	32
1.3.1 Histological Classification:	33
1.3.2 Breast Cancer Histological Grade Classification:.....	34
1.3.3 Breast TNM classification:.....	35
1.4 MANAGEMENT OF BREAST CANCER:	36
1.4.1 Treatment of Breast Cancer:	36
1.5 BREAST CANCER CHEMOTHERAPY:	37
1.5.1 Breast Cancer Chemotherapeutic Agents:.....	37
1.5.2 Predicative Markers of Therapy Response:	44

1.6 MOLECULAR INTRODUCTION TO BREAST CANCER:.....	46
1.6.1 Cell Cycle:.....	47
1.6.2 Cellular Apoptosis:.....	49
1.7 BREAST CANCER & SURFACE RECEPTORS:	53
1.7.1 Oestrogen Receptor (ER):	54
1.7.2 Progesterone Receptor (PR):.....	54
1.8 MOLECULAR CLASSIFICATION OF BREAST CANCER:.....	54
1.8.1 Breast Cancer Molecular Subtypes & Clinical Outcomes:	56
1.8.2 Breast Molecular Subtypes & Neoadjuvant Therapy Response:	57
1.8.3 Why Biomarkers for ER+ (Luminal A) Breast Cancer?	59
1.9 CHEMOTHERAPY RESISTANCE:.....	60
1.9.1 Intracellular Defence Mechanisms:.....	60
1.9.2 Enhanced DNA Repair:.....	62
1.9.3 Chemotherapy-Induced Apoptosis and Drug Resistance:.....	62
1.9.4 Alteration of Molecular Pathways & Drug Resistance:	65
1.10 PROTEOMICS FOR BIOMARKER DISCOVERY:.....	69
1.11 BIOMARKER:.....	70
1.11.1 Proteomics Vs. Other Omic Studies:.....	70
1.12 PROTEOMICS:	72
1.13 Workflow of Proteomic Discovery Pathway:	73

1.13.1 Proteomic Discovery Phase:.....	75
1.14 Clinical Samples in Proteomic Cancer Research:	80
1.15 PROJECT AIMS & OBJECTIVES:	83
Chapter 2.	85
2.1 INTRODUCTION:.....	85
2.2 STUDY DESIGN:.....	85
2.3 SAMPLE COLLECTION AND PATIENT SELECTION:.....	87
2.3.1 Response Evaluation From Clinical Samples:	89
2.3.2 Sample Collection at Surgery:.....	90
2.3.3 Archival Series Pre-treatment Core Biopsy Patient Selection:	97
2.4 SAMPLE PREPARATION FOR MICROARRAY ANALYSIS:	100
2.4.1 Introduction:	100
2.5 Protein Extraction Methodology:	100
2.5.1 Mechanical Homogenisation for Small Sample Volumes:	104
2.6 BRADFORD PROTEIN QUANTIFICATION METHOD:	105
2.6.1 Determination of Protein Concentration:	106
2.6.2 Plotting BSA Standard Protein Curve:.....	107
2.7 ANTIBODY MICROARRAY:.....	109
2.7.1 Panorama [®] Antibody Microarray-XPRESS Profiler 725 Kit:	109
2.8 ANTIBODY MICROARRAY EXPERIMENT PROTOCOL:	111

2.8.1 Sample Dilution and Protein Labelling:.....	111
2.9 OPTIMISATION OF HALF-LABELLING PROTOCOL:.....	118
2.9.1 Introduction:.....	118
2.9.2 Half-Labeling Microarray Protocol:.....	118
2.9.3 Protein Labelling for the Half-Protocol:.....	118
2.10 DATA MINING:.....	121
2.10.1 Introduction:.....	121
2.10.2 Ingenuity Pathway Analysis:.....	121
2.11 IMMUNOBLOTTING:.....	123
2.11.1 Western Blotting:.....	123
2.11.2 Protein Extraction and Quantification:.....	123
2.11.3 One-Dimensional Electrophoresis:.....	124
2.11.4 Transfer of Proteins to Nitrocellulose Membrane:.....	124
2.11.5 Blocking Non-specific Binding Sites on Membrane:.....	126
2.11.6 Adding Primary and Secondary Antibodies:.....	126
2.11.7 Loading Control:.....	126
2.11.8 Protein Detection:.....	127
2.11.9 Densitometry:.....	127
2.12 IMMUNOHISTOCHEMISTRY.....	128
2.12.1 Archival Samples used in Pilot Clinical Validations:.....	128

2.12.2 Blocking and Antigen Retrieval Methods:.....	128
Chapter 3.	138
3.1 INTRODUCTION:.....	138
3.1.1 Results from the Bradford Quantification Assay:	139
3.2 HALF PROTOCOL OPTIMISATION EXPERIMENTS USING BREAST TUMOUR SAMPLES:.....	142
3.2.1 Introduction:	142
3.3 EXPERIMENT # 1: SAMPLE #16B (CS) vs. #1B (CR)	143
3.3.1 Introduction:	143
3.3.2 Sample Dilutions and Protein Labelling:	144
3.3.3 D/P Ratio, Slide Hybridisation & Quality Control:	145
3.3.4 Discussion:	147
3.4 EXPERIMENT #1b: LABELLED Cy 3 #16B (CS) vs. Cy 5 #1B (CR).....	149
3.4.1 D/P ratio, Slide Hybridisation & Quality Control:.....	150
3.4.2 Discussion:	150
3.5 EXPERIMENT 2b: SAMPLE #38 (CS) vs. #15B (CR).....	152
3.5.1 Introduction:	152
3.5.2 Protein labelling and Dye Solubilisation:.....	153
3.5.3 D/P Ratio, Slide Hybridisation & Quality Control:	155

3.6 EXPERIMENT #2: SAMPLE #38 (CS) vs #15B (CR).....	156
3.6.1 Protein Labelling for Samples:.....	156
3.6.2 D/P Ratio & Quality Control:.....	158
3.7 EXPERIMENT 1c: SAMPLE 16B (CS) vs. 1B (CR)	160
3.7.1 Protein labelling and Dye Solubilisation:.....	160
3.7.2 D/P Ratio and Quality Control:	161
3.8 EXPERIMENT #3: SAMPLE #12B (CS) vs. #1 (CR).....	163
3.8.1 Protein labelling and Dye Solubilisation:.....	163
3.8.2 D/P Ratio and Quality Control:	164
3.9 MICROARRAY DATA ANALYSIS:.....	166
3.9.1 Discussion:	170
3.9.2 Data Analysis : Combined Approach.....	174
3.10 PILOT OPTIMISATION EXPERIMENTS USING SMALL TUMOUR SAMPLES: .	190
3.10.1 Introduction:	190
3.10.2 Experiment Protocol:.....	190
3.10.3 Discussion:	192
Chapter 4.	195
4.1 INTRODUCTION:.....	195
4.1.1 Data Mining Approaches:	195
4.1.2 DEP selections for IPA Analysis:	196

4.2 RESULTS:	201
4.2.1 Combined Antibody Microarray (9 experiments) Data Mining Results:	201
4.2.2 Combined Antibody Microarray & 2D-PAGE/MS Data Mining Results:	204
4.2.3 Confirmed DEPs from the Combined Data: VH Study	207
4.3 DISCUSSION:	214
4.4 DEPs For Confirmations and Validations: Current Study	215
Chapter 5.	218
5.1 INTRODUCTION:	218
5.1.1 Optimisations of Primary Phospho-Antibodies:	219
5.1.2 Reasons for Failed Optimisations:	221
5.2 RESULTS:	225
5.3 IMMUNOHISTOCHEMISTRY:	226
5.3.1 Introduction:	226
5.4 CLINICAL VALIDATION OF VIMENTIN PROTEIN:	227
5.5 CLINICAL VALIDATION OF AKT1 PhosphoSer473 PROTEIN:	230
5.6 CLINICAL VALIDATION OF FAK PosphoY397 PROTEIN:	233
5.7 CLINICAL VALIDATION OF 14-3-3 theta/tau ISOFORM:	235
5.8 CLINICAL VALIDATION OF 14-3-3 epsilon ISOFORM:	239
5.9 CLINICAL VALIDATION OF 14-3-3 beta/alpha ISOFORM:	240
5.10 CLINICAL VALIDATION OF 14-3-3 zeta/delta ISOFORM:	241

5.11 DISCUSSION:	242
5.11.1 Role of 14-3-3 in Breast Chemoresistance:.....	242
5.11.2 Role of Vimentin in Breast Chemoresistance:	243
5.11.3 Role of Akt1 in Breast Chemoresistance:	246
5.11.4 Role of FAK in Breast Chemoresistance:	248
5.11.5 Study Limitations:	250
Chapter 6. 255	
6.1 SUMMARY FROM MICROARRAY ANALYSIS:.....	255
6.2 FUTURE CONFIRMATIONS AND VALIDATIONS:.....	257
6.3 SUMMARY FROM THE NEW MICROARRAY PROTOCOL:.....	257
6.4 SUMMARY FROM POTEIN EXTRACTION EXPERIMENTS:	257
6.5 PROTEOMICS-FUTURE PERSPECTIVE:.....	258
6.5.1 Monitoring for Chemoresistance: Intrinsic Vs Acquired.....	258
6.5.2 Developing Pre-Clinical Models:.....	259
6.5.3 Concluding Remarks:.....	259
REFERENCES.....	260-270

List of Appendices:

Appendix 1.....271-280

Appendix 2.....281-297

Appendix 3.....298

Appendix 4.....299

Appendix 5.....300

Appendix 6.....301-302

Appendix 7.....303-306

List of Tables:

	Page no.	
Table 1	Summary of Breast Cancer Risk factors	30
Table 2	Histological Classification of Breast Cancers	33
Table 3	Breast Cancer Chemotherapy Regimens	38
Table 4	RECIST Criteria	43
Table 5	Multivariate Analysis of pCR within Different Biological Groups	58
Table 6	Limitations and Benefits of Clinical Samples	82
Table 7	Samples Selected for Antibody Microarray Analysis	90
Table 8	Table Listing Clinical Tumour Samples – Current study	95
Table 9	Table Listing for Clinical Tumour Samples – VH study	96
Table 10	EC-D series Samples Clinico-pathological Status	99
Table 11	Bradford Assay Commaise Plus Reagent Contents	106
Table 12	IHC Scoring system for Cytoplasmic staining	134
Table 13	IHC Scoring system for Cell membrane staining	135
Table 14	IHC Scoring for Nuclear membrane staining	135
Table 15	Project Samples Recorded Weights & Dilution Volumes	139
Table 16	Final protein Concentrations for Six Clinical Samples- TH analysis	140
Table 17	Final protein Concentrations for Six Clinical Samples- VH analysis	141
Table 18	TH/VH Average Protein Combinations	142
Table 19	The Summary of Samples Characteristics for Therapy Response	143
Table 20	Final Sample & Dilution Buffer Volumes for Sample #16B vs #1B	144
Table 21	Results from 2nd Bradford Assay using Labelled Samples	145
Table 22	Results from 2nd Bradford Assay using Labelled Samples	149
Table 23	The Summary of Samples Characteristics for Therapy Response	152
Table 24	Final Sample & Dilution Buffer Volumes for Sample #38 vs #15B	153
Table 25	Results from 2nd Bradford Assay using Labelled Samples	153

Table 26	Final Sample & Dilution Buffer Volumes for Sample #38 vs #15B	157
Table 27	Results from 2nd Bradford Assay using Labelled Samples	157
Table 28	Final Sample & Dilution Buffer Volumes for Sample #16B vs #1B	160
Table 29	Results from 2nd Bradford Assay using Labelled Samples	161
Table 30	Final Sample & Dilution Buffer Volumes for Sample #38 vs #15B	163
Table 31	Results from 2nd Bradford Assay using Labelled Samples	164
Table 32	A Summary of Optimisation & Research Experimental Protocols & Quality Control Data	165
Table 33	Antibody Microarray Data (4 experiments)	167
Table 34	Total Number of DEPs identified :Current Study	169
Table 35	List of Significantly Expressed DEPs : 1/4 discovery microarray experiments	171
Table 36	List of Significantly Expressed DEPs : 2/4 discovery microarray experiments	172
Table 37	List of Significantly Expressed DEPs : 3/4 discovery microarray experiments	172
Table 38	List of Significantly Expressed DEPs : Full vs Half Protocols	173
Table 39	Antibody Microarray Data : Current Study + VH Study	175
Table 40	Combined AbMA DEP Data : Current Study + VH Study	177
Table 41	Total Number of DEPs identified-Combined TH + VH Microarray Analysis	181
Table 42	Total number of DEPs identified in >2 experiments: Combined AbMA data TH + VH study	182
Table 43	The DEP data from 2D-PAGE/MS Experiments : VH study	183
Table 44	Combined DEP Data from 2D-PAGE/MS + AbMA experiments : IPA Analysis	186
Table 45	Pilot Series Samples :Tissue Weights and Dilution Volumes	190

Table 46	Bradford Quantification Results AbMA extraction buffer & Water Sonicator Method	191
Table 47	IPA: Data Selection & Proteomic Method	198
Table 48	Canonical Pathways for Protein Matches Identified in Combined Analysis #1	202
Table 49	Canonical Pathways for Protein Matches Identified in Combined Analysis #2	205
Table 50	Relevant Pathways Selected from Combined Analysis # 2 Data	207
Table 51	Previously Confirmed DEPs on Immunoblotting	207
Table 52	Details of Primary Antibodies used for Western Blotting	218
Table 53	AkT1 phosphoSer473 : Optimisation Experiments	220
Table 54	FAKphosphoY397 : Optimisation Experiments	220
Table 55	AbCAM Trouble Shooting Guide	221
Table 56	AbCAM Trouble Shooting Guide	221
Table 57	Primary Antibodies used for IHC	226
Table 58	IHC Scoring assessment for Vimentin : ECD series	229
Table 59	IHC Scoring assessment for Akt1phosphoser473: ECD series	232
Table 60	IHC Scoring assessment for FAK phosphoY397: ECD series	235
Table 61	IHC Scoring assessment for 14-3-3 theta/tau: ECD series	238
Table 62	IHC Scoring assessment for 14-3-3 theta/tau: Combined Analysis	238
Table 63	IHC Scoring assessment for 14-3-3 epsilon: MRI-iFEC series	239
Table 64	IHC Scoring assessment for 14-3-3 beta/alpha: MRI-iFEC series	240
Table 65	IHC Scoring assessment for 14-3-3 zeta/delta: MRI-iFEC series	241

List of Figures:

	Page no.
Gross Anatomy of Breast	27
Breast TDLU unit	28
Graph showing Breast Cancer Incidence Rates	31
Cell Cycle	48
Apoptosis Pathways (Extrinsic and Intrinsic)	51
Kaplan Mier Curves for DFS and OS: Intrinsic Molecular Subtypes	57
The p53 Apoptosis and Cell Cycle Arrest Pathways	64
PIP3/AkT Pathway	66
Integrin PIP3/AkT Pathway	68
Workflow of Biomarker Discover Pipelines	74
Forward Phase Antibody Microarray Illustration	79
Study Design	87
Consort Chart of Samples Collected : VH project	92
Consort Chart of Total Samples Collected : VH + TH project	93
Consort of Current Study	94
Pictures of Sample Preparation and Protein Extraction	103
BSA Standard Curve	108
Panorama XPRESS Profiler 725 Kit	110
Workflow of Full-Labeling Protocol	113
Panorama XPRESS Profiler 725 Kit: Scanned Images	117

Workflow of Half-Labeling Protocol	120
i-Blot Image	125
IHC samples and Archival Series	129
Fishers Exact Test	136
Half-Labeling Protocol Exp #1	146
Spot morphologies from scanned failed Expt#1 slide	148
Half-Labeling Protocol Exp #1b	151
Half-Labeling Protocol Exp #2b	154
Full- Labeling Protocol Exp #2	161
Half-Labeling Protocol Exp #1c	162
Flowchart of DEPs eligible for combines IPA analysis	199
Flowchart of DEPs eligible for combines IPA analysis: sample source	200
DEPs matches onto PIP3/AKT pathway	208
DEPs matches onto ERK/MAPK pathway	209
DEPs matches onto Death Receptor pathway	210
DEPs matches onto P70s6k pathway	211
DEPs matches onto cell cycle G2M CHK pathway	212
DEPs matches onto 14-3-3 mediated pathway	213
Western blot image of Akt1 phosphoSer473 antibody	223
Western blot image of FAKphosphoY397 antibody	224
Western blot image of Vimentin	225
IHC image of Vimentin	228

IHC image of Akt1 phosphoSer473 antibody	231
IHC image of FAKphosphoY397 antibody	234
IHC image of 14-3-3 theta/tau	237

Abbreviations:

2D-PAGE/MS	Polyacramide Gel Electrophoresis/Mass Spectrometry
AbMA	Antibody Microarray
AJCC	American Joint Committee on Cancer
ALDH	Aldehyde Dehydrogenase
BCRP	Breast Cancer Resistance Protein
BCS	Breast Conserving Surgery
BER	Base Excision Repair
BSA	Bovine Serum Albumin
CdK	Cyclin-dependent kinase
CDKI	Cyclin-dependent kinase-Inhibitors
CMF	Cyclophosphamide, Methotrexate, 5-Flourouracil
CR	Chemoresistant
CS	Chemosensitive
DAB	Diaminobenzidine
DCE	Dynamic Contrast Enhanced
DEP	Differentially Expressed Protein
DFS	Disease Free Survival
DMSO	Dimethyl Sulphoxide
DoH	Department of Health
EBCTCG	Early Breast Cancer Trialist Collaborative Group
ECM	Extra Cellular Matrix
ECTO	European Cooperative Trial in Operable Breast Cancer
EGFR	Epidermal Growth Factor Receptor
ELISA	Enzyme-Linked-Immunsorbent Assay
ER	Oestrogen Receptor
ESI	Electrospray Ionisation
FAK	Focal Adhesion Kinase
FEC	5-Flourouracil, Epirubicin, Cyclophosphamide,
FFPE	Formalin Fixed Paraffin Embedded Tissue

HER2	Human Epidermal Growth Factor Receptor 2
HRP	Horseradish Peroxidase
IDC	Invasive Ductal Carcinoma
IF	Intermediate Filament
IHC	Immunohistochemistry
ILC	Invasive Lobular Carcinoma
IPA	Ingenuity Pathway Analysis
iTRAQ	Isobaric Tagging Relative and Absolute Quantification
LCM	Laser Capture Microdissection
MAC	Mitochondrial Apoptosis Channel
MALDI	Matrix-Assisted Laser Desorption/Ionisation
MDR	Multi Drug Resistance
MMR	Mismatch repair
MRI	Magnetic Resonance Imaging
NACT	Neoadjuvant Breast Chemotherapy
NCCN	National Comprehensive Cancer Network
NER	Nucleotide Excision Repair
NGS	Nottingham Grading System
NHEJ	Non-Homologous End Joining
NICE	National Institute of Clinical Excellence
NPI	Nottingham Prognostic Index
NSABP	National Surgical Adjuvant Breast and Bowel Project
OCP	Oral Contraceptive Pill
OS	Overall survival
PBS	Phosphate-Buffered Saline
pCR	Pathological Complete Response
PET	Positron Emission Tomography
PR	Progesterone Receptor
PTEN	Phospho Tensin Analog
QC	Quality Control

REC	Research Ethics Committee
RECIST	Response Evaluation Criteria In Solid Tumours
RIDEP	Repeatedly Identified Differentially Expressed Protein
TBS	Tris-Buffered Saline
TDLU	Terminal Ductal Lobular Unit
TIF	Tumour Interstitial Fluid
TNBC	Triple Negative Breast Cancer
TNFR	Tumour Necrosis Factor Receptor
TNM	Tumour-Node-Metastasis
TOF	Time of Flight
US	Ultrasound
WB	Western Blot

Acknowledgements

Firstly, I would like to thank my research supervisors Dr. Lynn Cawkwell, Prof. Mike Lind, and Mr. Peter Kneeshaw for their support and guidance throughout the project and for making this project possible for me. I would also like to thank Prof. John Greenman for his help and guidance during the last stages of this project. A big thank you to Dr. Victoria Hodgkinson (PhD) and Dr. Lucy Scaife (Post doctoral fellow) for their involvement in collecting tissue samples, for the help, and guidance throughout the project. Also thanks to all the surgeons at the Breast Unit for providing the clinical samples and supporting the project. I would also like to thank the clinical secretaries and the breast out-patient nurses for supporting me and making my clinical experience enjoyable and pleasant. I am thankful to Dr. Ann Campbell (Pathologist) for her clinical involvement in the project, especially her valuable inputs and guidance during the immuno validation work. I am also thankful to Veronica M O'Donnell (Bio-Med student) for her involvement with the project and help with clinical validations. I am ever so grateful to all the patients who agreed to take part in the study and would like to thank them all. A special thank you must also go to all my colleagues and friends at the Daisy Building, especially, Vijay Agarwal, Elena Kashuba, and Rishi Shrivastava for the support and friendship throughout the project.

I would like to thank my mum and dad for keeping faith in my abilities and for blessing me as always with your prayers, love and affection. To my friends, especially Bilal Elahi for his valuable friendship, help and support; without you, my operating skills would have been lost ! Finally, a massive thank you must go to Farheen, my wife, for the huge amount of support and encouragement she has given me, and not to forget her sacrifices and patience – I shall always remember that and cannot thank you enough.

AUTHOR'S DECLARATION

I confirm that this work is original and that if any passage(s) or diagram(s) have been copied from academic papers, books, the internet or any other sources these are clearly identified by the use of quotation marks and the reference(s) is fully cited. I certify that, other than where indicated, this is my own work and does not breach the regulations of HYMS, the University of Hull or the University of York regarding plagiarism or academic conduct in examinations. I have read the HYMS Code of Practice on Academic Misconduct, and state that this piece of work is my own and does not contain any unacknowledged work from any other sources'. I also confirm that patient information obtained to produce this piece of work has been appropriately anonymised'.

X

Signature:

Tasadoq Hussain
Clinical Research Fellow Surgery

Date: 20/10/2013

CHAPTER I

CLINICAL INTRODUCTION TO BREAST CANCER

Chapter 1.

1.1 BREAST ANATOMY:

The mammary gland is a modified sweat gland situated in the superficial fascia on the anterior wall of axilla. It overlies the pectoralis muscles. It is rudimentary in males, in females it start enlarging at the age of puberty. The primary function of mammary glands is to produce milk during lactation; milk is produced in the glandular acini of the lobules and transferred via the intralobular ducts into the extralobular and finally the lactiferous duct. The contraction of myoepithelial cells at the basement membrane of the acini ejects the milk into the intralobular ducts.

1.1.1 Gross Anatomy:

A well developed female adult breast is conical in shape; its base extending transversely from the lateral border of the sternum medially to the mid axillary line laterally. Vertical extension is from the 2nd to 6th rib on the anterior chest wall (Figure 1). The breast has an extension directed towards the axilla called the axillary process of spence or axillary tail. This is important clinically because it can contain abnormal breast masses.

1.1.2 Breast Structure:

The fibrous connective tissue that forms the breast fascia extends between skin and pectoral fascia through the substance of the gland and is called the suspensory ligaments of Astley Cooper. This provides internal support to the gland and divides it into 8-10 radially arranged lobules. Each lobule is drained by a lactiferous duct which converges to the nipple like spokes of

a wheel; lobules produce milk during breast feeding which is transported by lactiferous ducts. There are 8-10 openings depending on the gland lobulation on the surface of the nipple, the duct presents as dilatation under the areola called lactiferous sinus (Figure 1).

GROSS ANATOMY OF THE BREAST

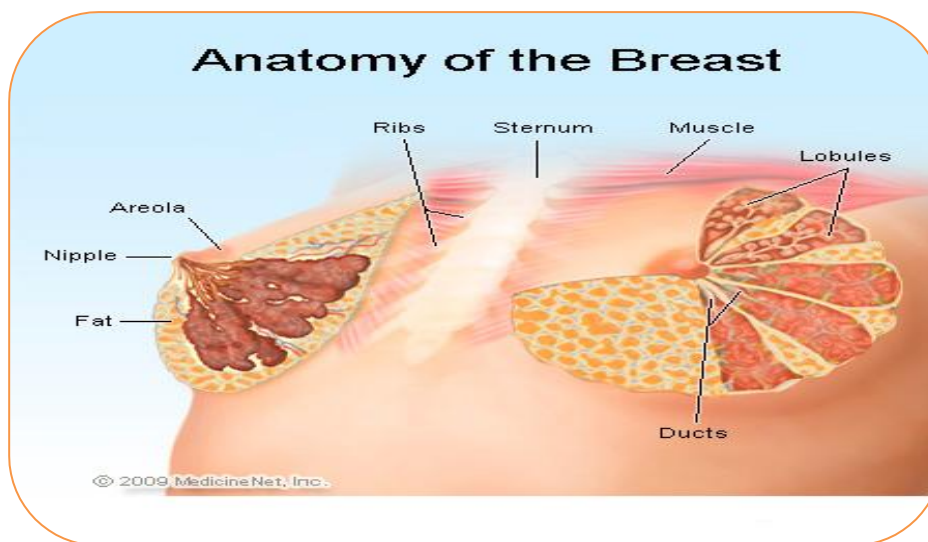


Figure 1: Gross anatomy of the breast showing division of the gland into lobules. Each of the breast lobule is drained by its own lactiferous duct and all the ducts from different lobules join to form a mammary duct. Atlas of Anatomy.com (c) (2004) J Artner MD.

1.1.3 The Terminal Ductal Lobular Unit:

The distal terminus of the ductal network is the terminal ductal lobular unit (TDLU). Each of the lobes in the breast contains thousands of TDLUs, which form the functional secretory unit. The secretory units produce milk, which drains via the branching ducts to their terminus as the

ampullae at the surface of the nipple (Figure 2). The TDLU is complex and consists of the extralobular and intralobular terminal ducts, and the blindly ending lobules (or ductules). Each TDLU is lined by an inner layer of secretory cells and an outer layer of myoepithelial cells containing contractile fibers that eject the milk into the ducts during lactation (Shaaban AM 2002).

THE TERMINAL DUCTAL LOBULAR UNIT (TDLU)

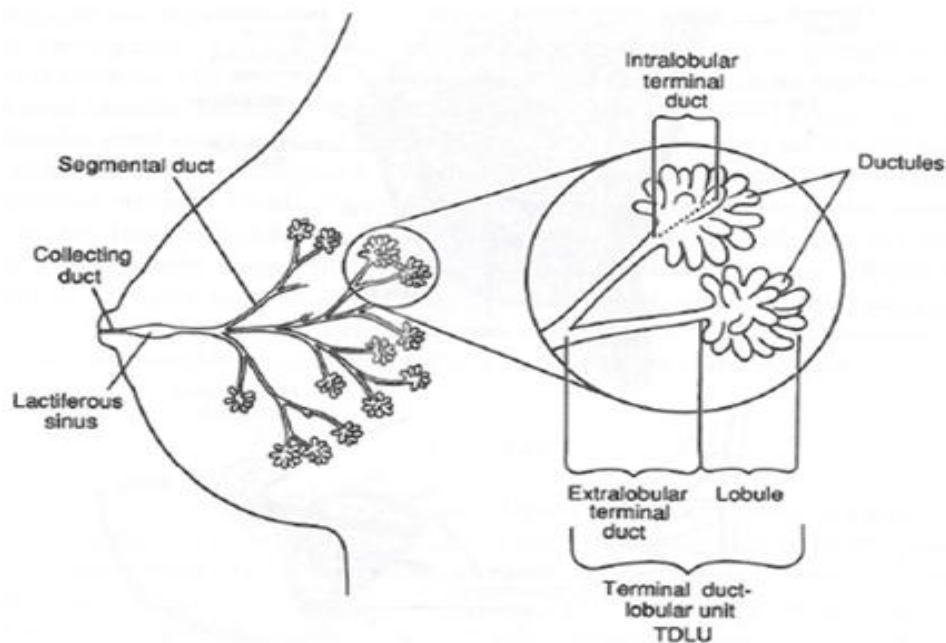


Figure 2: show an illustration of terminal ductal lobular unit. Each TDLU is made up of distal terminus of the duct and a breast lobule. It is lined by inner secretory and outer myoepithelial cells and produce milk during lactation. Hindle, W, Mokbel, K, Glob. Libr. Women's med., (ISSN: 1756-2228) 2009.

1.2 CLINICAL INTRODUCTION TO BREAST CANCER:

1.2.1 Epidemiology:

Breast cancer accounts for about 31% of all cancer cases in women worldwide and is the second most common cancer in the UK. The UK Department of Health (DoH) Office of national statistics data from 2010 shows, 49,961 new cases of breast cancer diagnosed that year. About 99% of them were in women and less than 1% in men (2011). In the year 2008, the estimated worldwide incidence of breast cancer was 1.38 million. This accounted for around a tenth (10.9%) of all new cancers and nearly 23% of all female cancer cases (Westlake S 2008).

1.2.2 Aetiology:

The aetiology of breast cancer is multi factorial and poorly understood as various risk factors modulate the development of breast cancer in women through reproductive age and after menopause (Dumitrescu and Cotarla 2005). This section summarizes breast cancer risk associated with each factor in detail (summarised in the Table 1).

1.2.3 Breast Cancer Risk Factors:

1.2.3.1 Age:

Breast cancer risk increases with age. Nearly 80% of diagnosed cancers occur in women 50 and over (Figure 3). The estimated lifetime risk of developing breast cancer for women in the UK is 1 in 10 below 65 years and 1 in 8 between 65 to 80 years (2005; Glass AG 2007).

Table 1: Summary of Breast Cancer Risk Factors
(Adapted from Dumitrescu and Cotarla 2005)

	Breast Cancer Risk Factors	Magnitude of Risk
Well confined Risk Factors	Increasing age	++
	Geographical region (western countries)	++
	Family history of breast cancer	++
	Mutations in BRCA1 and BRCA2 genes	++
	Mutations in other high-penetrance genes (Li Fraumeni syndrome, ATM, NBS1, LKB1)	++
	Ionizing radiation exposure (in childhood)	++
	History of benign breast disease	++
	Late age of menopause (>54)	++
	Early age of menarche (<12)	++
	Nulliparity and older age at first birth	++
	High mammographic breast density	+
	Hormonal replacement therapy	+
	Oral contraceptives recent use	
	Obesity in postmenopausal women	
	Tall stature	
Probable Factors	Alcohol consumption (~1 drink/day)	
		++
	High insulin-like growth factor I (IGF-I) levels	+
	High prolactin levels	+
	High saturated fat and well-done meat intake	+
	Polymorphisms in low-penetrance genes	+
	High socioeconomic status	

++ (moderate to high increase in risk);

-- (moderate to high decrease in risk);

+ (low to moderate increase in risk)

- (low to moderate decrease in risk)

AGE RELATED INCIDENCE RATE OF BREAST CANCER

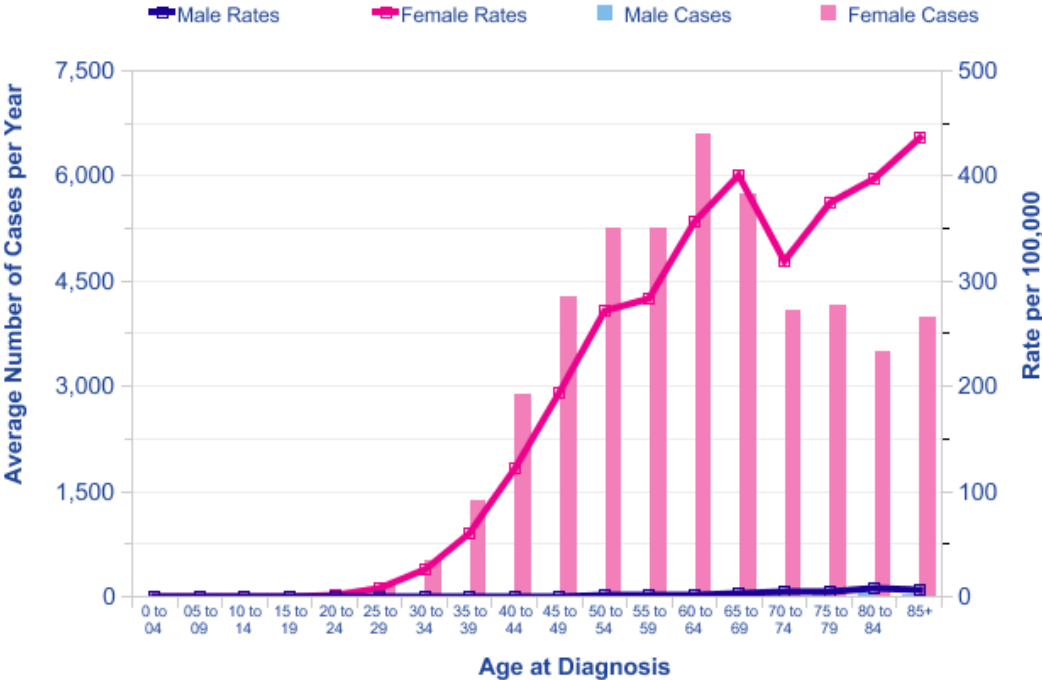


Figure 3: The graph shows an age related specific incidence rate for breast cancer between 2006 and 2008. As shown from the figure the incidence of breast cancer increase after age 50 with a peak in the rates of breast cancers at 65 years. Adapted from The Office of National Statistics, 2008.

1.2.3.2 Hormonal factors:

Long uninterrupted exposure to Oestrogen and Progesterone hormones can affect the chance of developing breast cancer (Farquhar C ; 2003). Individual hormonal factors that increase the risk include:

- Hormone replacement treatment containing oestrogen and progesterone over several years
- Nulliparity or late motherhood
- Absence of breastfeeding or breastfeeding for less than a year
- Early menarche (under 12) or late menopause (after 50)

1.2.3.3 Familial Breast Cancers:

Hereditary or familial breast cancers accounts for 25% of all breast cancer cases. Germline gene mutations in BRCA1, BRCA2, CHEK2, PTEN and TP53 increase the risk of both breast and ovarian cancers by 5-7%. Higher prevalence is noted in women with a family history of breast or ovarian cancer at a young age or multiple tumours and in certain ethnic groups such as Ashkenazi Jews. The mutant protein cannot carry out the normal cell functions of cell regulation growth, DNA repair and apoptosis. As a result, cells grow in an uncontrolled fashion increasing the chances of malignant transformation.

1.3 BREAST CANCER CLASSIFICATIONS:

Breast cancers can be classified under four different classification schemes, or groups. Each type of classification is based on different criteria and serves a different purpose. The most commonly used classification systems are based on:

- Histological appearance
- Tumour Grade
- Protein and Gene expression status
- Tumour Stage

1.3.1 Histological Classification:

The classification of breast cancer into different histological sub-types is based on the microscopic anatomy and tumour spread. Breast cancers can be broadly divided into two major histological subtypes: ductal and lobular (summarised in the Table 2). Ductal disease originates from milk ducts and lobular disease from breast lobules. Further, depending on the spread of tumour cells beyond the basement layer, it can be invasive or non-invasive.

1.3.1.1 Invasive Breast Cancer:

Invasive breast cancers by definition spread beyond the basement layer and can be divided into ductal and lobular sub-types. Invasive ductal carcinoma (IDC) no-specific type is the most common form (80%) of all the invasive sub-types. Invasive lobular carcinoma is less common and account for only 10% of invasive cancers.

Table 2: Histological Classification of Breast Cancers

<i>Type</i>	<i>Invasive</i>	<i>Non-Invasive (In-situ)</i>
Ductal	Invasive Ductal Carcinoma (IDC)	Ductal Carcinoma In-situ (DCIS)
Lobular	Invasive Lobular Carcinoma (ILC)	Lobular Carcinoma In-situ (LCIS)

1.3.2 Breast Cancer Histological Grade Classification:

Histological grade in breast cancer has an independent prognostic significance, as it, along with other predictive factors such as receptor status, guides patient treatment management (El-Sayed et al. 2008). The three commonly used prognostic determinants for breast cancer include: axillary node (LN) status, primary tumour size, and tumour histologic grade. The most widely used histologic grading system of breast cancer is the Nottingham combined histologic grade (Elston-Ellis modification of Scarff-Bloom-Richardson grading system), also known as the Nottingham Grading System. Originally proposed by Bloom-Richardson in 1957, it is a numerical grading system categorizing breast tumours into three pathological grades of grade 1 to 3 based on the degree of tubule formation, nuclear pleomorphism and hyperchromatic mitotic nuclei. This classification system is more commonly used in Europe, including the UK.

1.3.2.1 Prediction of Prognosis based on Histological Grade:

The Nottingham Grading System has undergone a rigorous validation in number of other independent studies to determine its usefulness in predicting cancer. Furthermore, NGS has been combined with lymph nodal status and tumour sizes to develop a prognostic index. One such index created by the Nottingham Study Group is called Nottingham Prognostic Index (NPI) taking into account tumour size, grade and lymph node status. The histological grade and lymph node status are awarded an equal weighting in the NPI scoring them similarly on a scale of 1 to 3. The combined score from the above two is then added to the multiplied score of 0.2 and tumour size (in centimetres). Cut-off points of 2.4, 3.4, 4.4, 5.4 and 6.4 can be used to stratify the patients into groups excellent, good, moderate I, moderate II, poor and very poor prognosis respectively.

$$\text{NPI} = 0.2 \times \text{tumour size in cm} + \text{Tumour grade} + \text{Lymph node status}$$

Despite the usefulness of histological grading in predicting the prognosis, tumour gene signatures have been found to have superior predictive and prognostic powers (Sotiriou, Wirapati et al. 2006; Peppercorn, Perou et al. 2008). For histological grading, factors such as subjectivity of histologic technique, reproducibility and inter/ intra-observer variability can all preclude its applicability at all times (Rakha, Reis-Filho et al. 2010).

1.3.3 Breast TNM classification:

The tumour node metastasis (TNM) staging system is a universally accepted staging system for breast cancer. This classification is based on a retrospective analysis of diverse population groups representing all stages of disease and correlation of tumour characteristics with survival data. TNM classification is periodically updated to incorporate changes from evolving imaging and treatment options which impact patient survival. The American Joint Committee on Cancer (AJCC) outlines TNM staging, which is also accepted by International Union Against Cancer (UICC). In this classification, breast cancers are classified based on extent of tumour (T); spread to the lymph nodes (N) and presence of distant Metastasis (M). A numerical designate is added against each letter to indicate the size of primary tumour or its extent and the extent of cancer spread. The updated version (7th edition) of the breast cancer TNM staging was proposed by AJCC in 2003. In this edition, amendments were made to incorporate nodal *micro*-metastasis with a size-based discrimination between *micro*-metastases and isolated tumour cells. Also a classification of lymph node status by the number of involved axillary lymph nodes and inclusion of metastasis to the infraclavicular, internal mammary, and supraclavicular lymph nodes were included (Cancer). With the quantification of nodal metastasis with new

classification, it was expected that there could be a raised possibility of finding more evidence of nodal micrometastases than before thereby creating a discrepancy between the clinical axillary nodal status and its pathological state. Therefore, in the revised TNM staging the pathological staging system has been reorganized to classify patients with one to three positive axillary lymph nodes (with at least one tumour deposit > 2.0 mm and all tumour deposits > 0.2 mm) as pN1a; patients with four to nine positive axillary lymph nodes as pN2a, and patients with 10 or more positive axillary lymph nodes as pN3a. Furthermore, the infraclavicular disease was staged as pN3a in the revised version following evidence from the Newman *et al.* study of 146 locally advanced breast cancers showing poor correlations of disease free and overall survivals with infraclavicular metastasis (Newman, Kuerer et al. 2001).

1.4 MANAGEMENT OF BREAST CANCER:

Triple assessment is a formalized clinical approach undertaken to diagnose breast cancer. This approach consists of three key assessments: clinical breast examination, radiological examination (e.g. mammogram, ultrasound, magnetic resonance imaging) and pathological assessment (e.g. biopsy or cytology).

1.4.1 Treatment of Breast Cancer:

Breast cancers treatment involves combination of medical (e.g. chemotherapy) and hormonal therapies with surgery. Surgical options for breast cancers depend on the patient age, tumour size, grade and location. Breast Conserving Surgery (BCS) options include: lumpectomy and wide local excisions. For locally advanced breast cancers, administration of neo-adjuvant treatment before surgery may increase the chances of BCS and avoid mastectomy (Steger and Bartsch 2011). At the time of surgery, axillary staging is performed by taking a sentinel lymph

node biopsy or axillary node sampling following the injection of a radioactive tracer and blue dye. In the event of finding a sentinel lymph node(s) positive for *macro*-metastasis (> 2 mm), the National Institute of Clinical Guidance (NICE) breast management guidelines of 2009, recommend axillary therapy in the form of clearance or radiotherapy (2009). In order to further reduce the chances of local recurrence, all patients treated with BCS are offered radiotherapy to the breast as adjuvant treatment.

1.5 BREAST CANCER CHEMOTHERAPY:

Breast cancer chemotherapy was first administered in mid 1970s as an adjuvant treatment following mastectomy and radiotherapy (DeVita and Chu 2008). Since then, the long term benefits of breast cancer adjuvant chemotherapy have been demonstrated in the meta-analysis of different adjuvant chemotherapy regimens by the Early Breast Cancer Trialist Collaborative Group (EBCTCG) (2005). Of the different combination used, anthracycline-based poly-therapy with 5-fluorouracil, adriamycin and cyclophosphomide (FAC) or 5-fluorouracil, epirubicin and cyclophosphomide (FEC) was found to show the highest rates of overall (15 years) and disease free (5 year) survival. Breast chemotherapy consists of different chemotherapeutic agents. A short summary of some of the popular regimens is illustrated in the Table 3.

1.5.1 Breast Cancer Chemotherapeutic Agents:

Anthracyclines:

Anthracyclines (or anthracycline antibiotics) are a class of drugs derived from *Streptomyces* bacterium species and are commonly used for cancer chemotherapy (Fujiwara 2000). Drugs from this that are used in breast cancer chemotherapy regimens include: doxorubicin and epirubicin. The mechanism of action of anthracyclines agents is via multiple pathways and include,

inhibition of cytoplasmic proteases activity leading to the inhibition of degradation of proteins involved in cell growth and metabolism thereby inducing apoptosis; inhibition of DNA and RNA synthesis by intercalating between base pairs of the DNA/RNA strand, preventing the replication of rapidly-growing cancer cells (Takimoto CH 2008).

Table 3: Breast Cancer Chemotherapy Regimens

<i>Chemotherapeutic agent</i>	<i>Combination Regimens</i>
Cyclophosphamide	CMF- Cyclophosphamide, Methotrexate, Fluorouracil
Epirubicin	FEC- Epirubicin, Cyclophosphamide, Fluorouracil
Fluorouracil (5FU)	FEC-T- Epirubicin, Cyclophosphamide, Fluorouracil and Taxotere
	E-CMF- Epirubicin followed by CMF
	EC- Epirubicin and Cyclophosphamide
Doxorubicin (Adriamycin)	AC- Doxorubicin (Adriamycin) and Cyclophosphamide
Methotrexate	MMM- Methotrexate, Mitozantrone and Mitomycin
Mitomycin	MM- Methotrexate and Mitozantrone
Mitozantrone	
Docetaxel (Taxotere)	EC- Docetaxel

Cyclophosphamide:

Cyclophosphamide is a nitrogen mustard alkylating agent, from the oxazaphorines group. It comes as a 'pro-drug' and is converted to its active metabolite in liver by the action of Cytochrome P4503A4. The formed active metabolite, 4-hydroxycyclophosphamide exists in equilibrium with its tautomer, aldophosphamide. Most of the aldophosphamide is oxidised by the enzyme aldehyde dehydrogenase (ALDH) to produce carboxyphosphamide and a small proportion is converted into phosphoramidate mustard and acrolein. The main effect of cyclophosphamide comes from its metabolite phosphoramidate mustard which forms DNA crosslinks both between and within DNA strands at guanine N-7 positions that are irreversible and lead to cell death (Takimoto CH 2008).

5-Fluorouracil:

5-fluorouracil (5-FU) is a pyrimidine analog belonging to the family of drugs called antimetabolites. 5-FU acts in several ways, but principally it is a prodrug for FdUMP which acts as a thymidylate synthase inhibitor. Interrupting the action of this enzyme, blocks synthesis of the pyrimidine thymidine, which is a nucleoside required for DNA replication. Thymidylate synthase methylates deoxyuridine monophosphate (dUMP) into thymidine monophosphate (dTMP). Therefore in the presence of 5-FU, dTMP levels are decreased resulting in cell death (Longley, Harkin et al. 2003).

Taxanes:

The taxanes are class of anticancer drugs, originally derived from the bark of the Pacific yew, *Taxus brevifolia*. The cytotoxic action of taxanes is exerted principally by inhibition of mitosis. Taxanes disrupt the microtubule function by stabilizing the GDP-bound tubulin in the

microtubule which then inhibit the process of cell division in rapidly growing cells (Miller and Sledge 1999).

1.5.1.1 BREAST NEOADJUVANT CHEMOTHERAPY:

Neo-adjuvant chemotherapy (NACT) has become a standard treatment for locally advanced breast cancers. It was introduced in the last ten years to treat locally advanced breast cancers with an aim to facilitate breast conserving surgery and improve 5 year survival. However, compared to adjuvant treatment it offers no added survival benefits (Steger and Bartsch 2011). Multiple chemotherapeutic regimens were studied in combination for the neo-adjuvant setting; however, desired clinical benefits from a particular specific 'tailored' regimen could not be established (Hudis and Modi 2007). Hence, tested and standardized adjuvant breast chemotherapy regimens with established safety profiles were introduced for the neo-adjuvant setting (Mauri, Pavlidis et al. 2005). The clinico-pathological criteria to give neo-adjuvant chemotherapy treatment rest solely on the local advancement of breast cancer, tumour size (large operable breast cancer) and/or proven lymph node metastases (Fisher, Bryant et al. 1998). Tumours showing a complete pathological response to neo-adjuvant treatment were found to show better clinical outcomes than to those with residual disease (Wolmark, Wang et al. 2001).

The major advantage of breast neo-adjuvant chemotherapy in locally advanced breast tumour is that it down-stages the disease and allows breast conservation surgery (BCS). The National Surgical Adjuvant Breast and Bowel Project (NSABP) B-18 trial assessing clinical and operative outcomes of women receiving pre-operative chemotherapy with operable breast cancers showed neo-adjuvant treatment reduce tumour bulk thereby allowing 12% more lumpectomies in tumours ≥ 5 cm (Fisher, Brown et al. 1997). Further, a pathological complete response (pCR) to

neo-adjuvant treatment was found associated with an improved disease free (DFS) and overall survival (OS) at nine years of follow-up (Wolmark, Wang et al. 2001). Furthermore, the ability to monitor therapy responses on treatment with imaging (e.g. MRI) allows adjustments to chemotherapy regimen and/or drug dosages according to responses (Loo, Teertstra et al. 2008). Another major gain from neo-adjuvant approach is that it identifies non-responders early in the course of treatment and spares them from the unnecessary side effects of chemotherapeutic drugs for no obvious clinical gains. Therefore using this approach, non-responders can be streamlined early in the course of the treatment to receive alternative treatments minimizing the risk of disease becoming inoperable. Taxanes were added to anthracycline-based regimens to improve their clinical effectiveness and achieve pathological complete response (pCR) (Bonnetterre, Dieras et al. 2004).

1.5.1.2 Advantages of adding Taxanes:

Taxanes have been assessed in three randomized controlled trials B-27, CVAP and GEPARDUO (Bear, Anderson et al. 2003; von Minckwitz, Kummel et al. 2008) for early-stage breast cancer neo-adjuvant chemotherapy in combination (Taxane with Anthracyclines) or sequential regimens (Taxanes after Anthracyclines). Docetaxel was used in all three trials; while B-27 and CVAP used docetaxel in sequential regimens with anthracyclines, GEPARDUO assessed it in both combination and sequential regimens. Results from all the three trials confirmed a significantly higher clinical and pCR rates after adding taxanes to anthracyclines. The objective and complete pathological response rates (ORR and CpR) of 90% and 26% was seen in B-27 trial with AC and Taxane sequential therapy in 805 patients (Crown, O'Leary et al. 2004). In the GEPARDUO trial with AC and Taxane sequential therapy in 458 patients ORR and pCR were found to be 87% and 22.4% respectively.

The results from NSABP-27 randomised phase III trial showed higher rates of pathological complete response with 4 cycles of anthracycline-cyclophosphamide (AC) and 4 cycles of docetaxel (Bear, Anderson et al. 2006). Furthermore, docetaxel when used in sequential regimen with AC was found to increase the disease-free survival in patients who have had partial response to AC regimen (DFS: Hazard ratio [HR] = 0.71; 95% CI, 0.55 to 0.91; $p = .007$; OS: HR = 0.33; 95% CI, 0.23 to 0.47; $p < .0001$). The National Comprehensive Cancer Network Guidance following the evidence, favoured using AC-docetaxel in sequential regimen for neoadjuvant treatment (2012). Keeping in with the above guidance, the neoadjuvant regimen used within the Hull and East Yorkshire Hospitals NHS trust includes a sequential administration of 4 cycles of epirubicin/cyclophosphamide followed by 4 cycles of docetaxel.

1.5.1.3 Assessing Response to NACT:

Response to chemotherapy is generally assessed by clinical examination and/or radiological imaging. Several guidelines to define tumour response on radiological imaging have been proposed. Among these, the criteria validated by the Response Evaluation Criteria in Solid Tumours (RECIST) group (Therasse, Arbuck et al. 2000) and the UICC (International Union Against Cancer) are widely accepted and frequently used. Based on these guidelines, responses can be classified as a complete response, partial response, stable disease and progressive disease (Table 4).

In general, 60-90% of breast cancers show clinical response (complete or partial) to neo-adjuvant therapy (Wolmark, Wang et al. 2001). A complete clinical response is defined as a complete disappearance of tumour following NACT; a 30% reduction in size of tumour from the baseline measurement is considered a partial response.

Table 4: RECIST CRITERIA

(Adapted European Journal of Cancer 45 (2009) 228-247)

<i>Response</i>	<i>Definition</i>
Complete Response (CR)	Disappearance of all target lesions
Partial Response (PR)	At least a 30% decrease in the sum of diameters of target lesions, taking as reference the baseline sum diameters
Progressive Disease (PD)	At least a 20% increase in the sum of diameters of target lesions, taking as reference the smallest sum on study (this includes the baseline sum if that is the smallest on study) In addition to the relative increase of 20%, the sum must also demonstrate an absolute increase of at least 5mm OR Appearance of one or more new lesions
Stable Disease (SD)	Neither sufficient shrinkage to qualify for PR nor sufficient increase to qualify for PD, taking as reference the smallest sum diameters

A pathological complete response (pCR) as defined by some studies is absence of invasive disease from breast only. However, majority of others report pCR as absence of invasive disease from both breast and axillary lymph nodes thereby leading to variation in pCR reporting rates (3-30%) between various studies (Jones and Smith 2006). Furthermore, a pCR in axillary nodes after NACT is shown to correlate with improved overall (OS) and relapse free survival (RFS) (OS and RFS: 93% and 87% vs 72%) at 5 years in contrast to patients not achieving axillary pCR

(OS and RFS: 72% vs 60%; $p < 0.001$) (Hennessy, Hortobagyi et al. 2005). Therefore, a pathological complete response to neo-adjuvant therapy may be considered as a surrogate for prognosis based on the above evidence. However, different tumour subtypes are associated with different responses to neoadjuvant therapies. Generally, tumours containing high levels of Ki67, ER- and HER2+ status respond effectively to anthracycline and taxane-containing neoadjuvant chemotherapy but tend to have a poor clinical outcome (Yoshioka, Hosoda et al. 2013).

1.5.1.4 Monitoring Neo-adjuvant Therapy Response:

As defined by the RECIST criteria (section 1.5.1.3), a complete radiological response to NACT is defined as disappearance of all target lesions on imaging. Traditionally, a NACT therapy response has been monitored on clinical examination, mammogram and ultrasound. Dynamic contrast enhanced-magnetic resonance imaging (DCE-MRI) has recently emerged as another useful investigating modality to monitor responses to NACT (Garimella, Qutob et al. 2007). Compared to mammogram and ultrasound, the DCE-MRI has higher sensitivity and specificity and hence is a good investigation tool to monitor therapy responses (Partridge, Gibbs et al. 2002; Bhattacharyya 2008). However, the predictive value of DCE-MRI is found to depend on patient's age, tumour histology and receptor status (Hsiang et al. 2007; Chen, Feig et al. 2008).

1.5.2 Predictive Markers of Therapy Response:

Many clinical markers have been identified that help predict response to neo-adjuvant chemotherapy. This section highlights briefly some of the most commonly used clinical markers to predict therapy responses. These markers although more routinely used, are not absolute, as molecular sub-typing and axillary staging are also important predictors of therapy responses.

1.5.2.1 Tumour Size and stage:

Similar to age and menstrual status, tumour size and stage is found to have an inverse relationship with therapy response. High stage (nodal involvement) disease and/or large size tumours (> 5 cm) have less likelihood of a complete response compared to smaller tumours and lower stage disease (Stage IIA, IIB and IIIA) (Keam, Im et al. 2007).

1.5.2.2 Hormone Receptor Status:

Oestrogen (ER) and Progesterone (PR) receptor status can independently predict pathological complete responses following neo-adjuvant therapy (Guarneri, Broglio et al. 2006). This effect, independent of type of neo-adjuvant regimen employed, has been found consistently across many studies. Response (pCR) rates can vary between ER+ and ER- tumours and are generally found to be superior with ER- sub-types. The European Cooperative Trial in Operable breast cancer (ECTO) study from their analysis of 1355 patients showed, 42% of ER- tumours had pCR compared to 12% of ER+ tumours (Gianni, Baselga et al. 2005). Similarly, Guarneri *et al.*; in their retrospective analysis of 1731 patients had 24% of ER – tumours showing pCR with different neoadjuvant regimens compared to 8% of ER+ tumours (Guarneri, Broglio et al. 2006). Ring *et al.*; in their retrospective analysis of 435 patients treated with anthracycline-combination regimen and mitoxantrone achieved pCR in 21.6% of ER- tumours compared to 8.1% of ER+ tumours ($p < 0.001$). In the same study, ER- tumours with pCR were found to have superior 5 year overall survival thereby confirming the prognostic significance of pCR in ER- tumours (Ring, Smith et al. 2004). The therapy responses in the PR- tumours have been observed to follow a similar trend to ER- tumours. Daidone *et al.* from their study of 231 T2 tumours

reported, a higher response rate with PR- tumours compared to PR+ (86% vs. 68%) (Daidone, Veneroni et al. 1999).

1.5.2.3 Tumour Proliferation Marker (The Ki67 Index Status):

The Ki-67 nuclear antigen is expressed in rapidly proliferating cells in all phases of cell cycle and is a marker of cellular proliferation. Many studies have been carried out to determine the relationship between tumour cell proliferation, analysed by Ki67 expression, and chemotherapy response. A 25% decrease in proliferation fraction as assessed by Ki-67 staining of the fine needle aspirates in 51 patients receiving anthracycline neo-adjuvant treatment was found to be associated with decrease risk of cancer recurrence (Pathmanathan and Balleine 2013). Burcombe *et al.* from their study of 118 patients treated with anthracycline based NACT found an increased likelihood of achieving pCR from >75% reduction in Ki-67 index from the pre-treatment baseline (Burcombe, Makris et al. 2005). From a study of 119 breast tumours, a >20% expression of Ki-67 was found to predict pCR in patients treated with anthracycline based neo-adjuvant chemotherapy (Petit, Wilt et al. 2004). However, there is currently no evidence based protocol established to derive a reliable and informative Ki67 score for routine clinical use. In this circumstance, pathologists must establish a standardised framework for scoring Ki67 and communicating results to a multidisciplinary team.

1.6 MOLECULAR INTRODUCTION TO BREAST CANCER:

The molecular aetiology of tumourigenesis is multi-factorial and thought to result from a series of progressive changes such as activation of oncogenes, inactivation of tumour suppressor genes and loss of DNA repair genes. Therefore, in order to fully understand the natural progression of

tumours and their responses to chemotherapy, cellular processes that trigger, regulate and affect cell proliferation and apoptosis (programmed cell death) has to be clearly understood.

1.6.1 Cell Cycle:

A eukaryotic cell cycle is divided into a series of sequential phases; the G_1 , S, G_2 and M phases with a G_0 resting phase between M and G_1 . A cell progresses through various phases, in response to growth factors or onco-proteins. This transition occurs by inactivating distinct checkpoints at G_1 and G_2 stages so that the cell growth occurs in favourable environment and with genetic integrity (Hilakivi-Clarke, Wang et al. 2004). The DNA replication and cell mitosis occur in S and M phases of the cell cycle. The cells enter G_0 resting phase from G_1 when fully differentiated or in the presence of DNA damage, which otherwise precludes cell cycle progression. Two classes of regulatory molecules belonging to family of serine threonine kinases, cyclin and cyclin-dependent kinases (CDK) drive cell cycle progression (Nigg 1995). Effector proteins that include cyclin-dependent kinase inhibitors (CDKIs) drive cell progression through checkpoints and can reversibly halt cell cycle progression in event of an aberrant cell cycle event (Bartek, Lukas et al. 2004).

Figure 4 gives a graphic illustration of the cell cycle with the cyclin/CDK regulators and CDKIs.

THE MAMMALIAN EUKARYOTIC CELL CYCLE PATHWAY

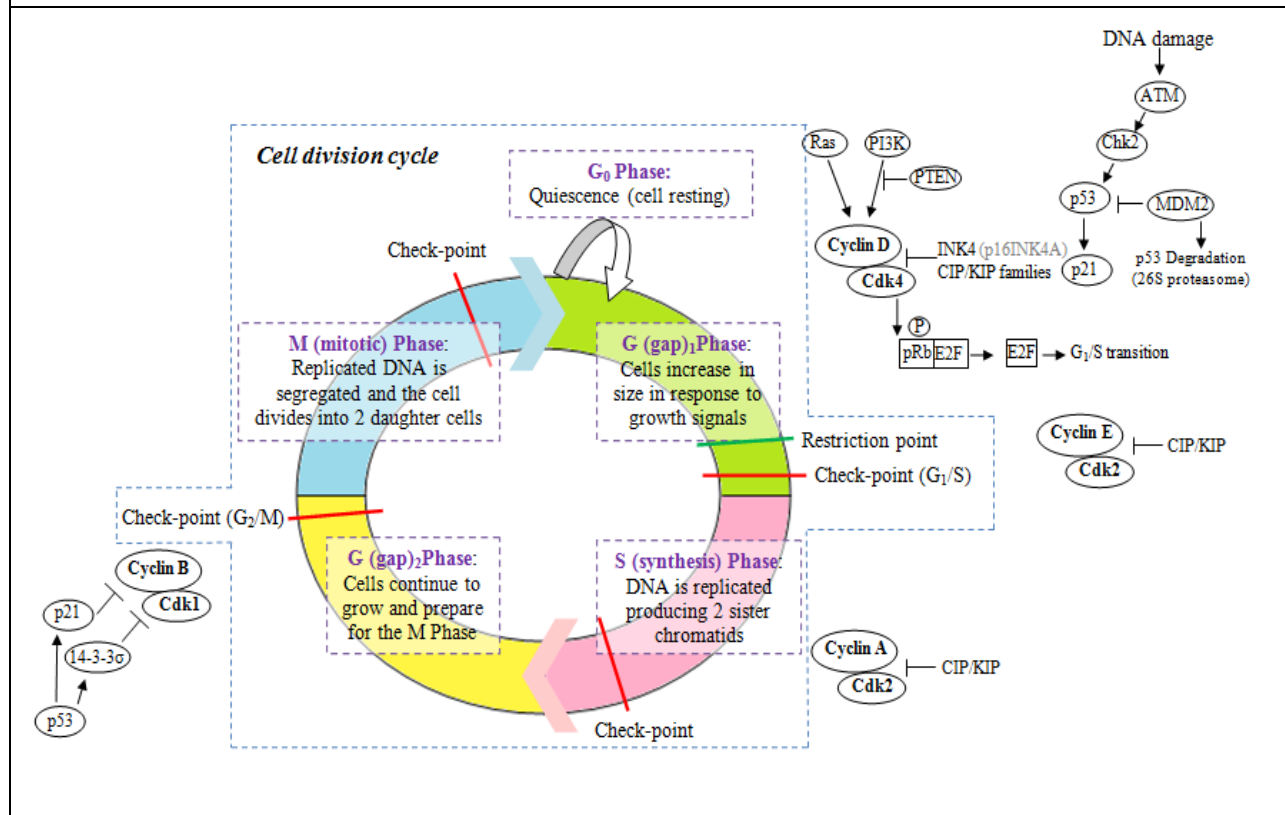


Figure 4: The mammalian cell cycle progresses sequentially through G₁ S G₂ and M phases. Cell preparation to progress through different phases occurs at the G₁ phase. This occurs in response to growth factors such as cyclin and cyclin-dependent kinases (CDK). There is a G₁ Checkpoint that can detect DNA damages and halt cell progression. This is controlled by cyclin-dependent kinase inhibitor proteins belonging to INK and Cip/Kip family. The DNA synthesis occurs in the S phase controlled by cyclin A-CDK2. The cell progresses to G₂ phase where further growth in preparation to cell division occurs. The cell has to go through the G₂ Checkpoint at this stage which act as another filter to any DNA damages occurred during the DNA synthesis. In the M phase cell division occurs and two sister chromatids are formed by the process of meiosis. Following cell division the cell enters either the G₁ to complete another cycle or a G₀ resting phase. (Courtesy V.C.Hodgkison, PhD thesis)

1.6.2 Cellular Apoptosis:

Apoptosis is a genetically controlled mechanism of cell death, it is important for the regulation of tissue homeostasis. In cancers this mechanism is commonly associated with aberrations, thereby, allowing cancer cells to continually proliferate and proceed unregulated with damages to DNA. Apoptosis occurs via two major pathways, the extrinsic and the intrinsic pathway. The extrinsic pathway is activated in response to external stimuli (e.g. hypoxia, infection, toxins etc.) and is initiated by the binding of extracellular death ligands with Fas and tumour necrosis factor receptor (TNFR) super family proteins. The intrinsic mitochondrial pathway is initiated in response to an internal stimulus (e.g. stress) and on activation releases cytochrome C from the mitochondria. The execution of both pathways is mediated through the activation of caspases, a family of cysteine proteases present in the cytosol as inactive precursors (pro-caspases). Activation of caspases cleaves regulatory and structural molecules of the cell, culminating in cell death.

At the initiation of the intrinsic pathway, internal (DNA damage and reactive oxygen species) and external (chemotherapeutic drugs, radiation, infection etc) apoptotic stimuli form a mitochondrial apoptosis-induced channel (MAC) to trigger the release of cytochrome C (Dejean, Martinez-Caballero et al. 2006). Further, in response to these stimuli, mitochondrial proteins called small mitochondria-derived activator of caspases (SMACs) are released into the cytosol to bind with the inhibitor of apoptosis proteins (IAPs). This binding of SMACs with IAPs deactivates IAPs, which in turn activate pro-caspases to continue the process of apoptosis (Fesik and Shi 2001). Released cytochrome C binds with the Apoptotic protease activating factor - 1 (Apaf-1) and adenosine triphosphate (ATP), which then bind to the pro-caspase-9 to create a

protein complex known as an apoptosome. The apoptosome cleaves the pro-caspase to its active form of caspase-9, which in turn activates caspase-3, the final effector enzyme of the apoptotic cascade. The active caspase-3 cleaves an inhibitor of caspase activated DNAase lamins, several cytoskeleton binding proteins and poly (ADP-ribose) polymerase (PARP). Cleavage of these proteins causes DNA fragmentation, inhibition of DNA synthesis and repair, nuclear membrane disruption, chromatin condensation, and cytoskeleton collapse (Chaudhry and Asselin 2009).

The extrinsic or direct signal transduction pathway is triggered when the tumour necrosis factor released in response to external stimuli binds with the TNF-Receptor 1. This binding initiate a signalling cascade via the intermediate membrane proteins, the TNF receptor-associated death domain (TRADD) and Fas-associated death domain (FADD) (Chen and Goeddel 2002). Further, a second independent extrinsic pathway involving Fas- Fas ligand (FasL) also activates caspase-8 by forming the death-inducing signalling complex (DISC) which contains FADD, caspase-8 and caspase-10. The activated caspase-8 feeds directly into caspase-3 activation which in turn contributes to degradation of cellular proteins important for cell survival and integrity (Wajant 2002) (Figure 5).

CELLULAR APOPTOTIC PATHWAYS (EXTRINSIC AND INTRINSIC)

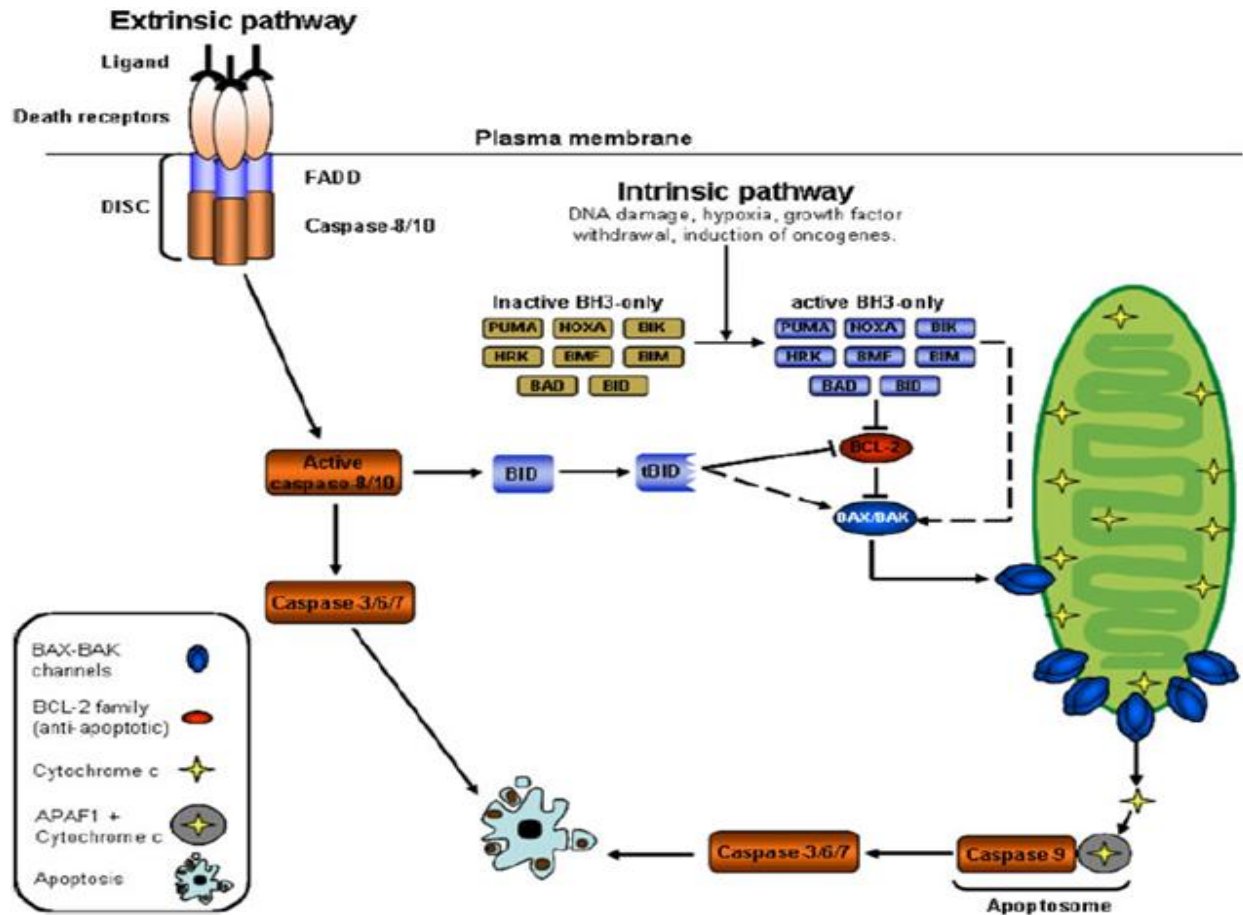


Figure 5: The apoptotic extrinsic pathway as shown in the figure is activated by the binding of TNF with the TNFR1 in response to external stimuli. Upon activation, a death induced signalling complex (DISC) is formed which activate caspases 8/10 and 3. In contrast, the intrinsic pathway is activated by pro-apoptotic proteins (Bax, Bid, and Bad), hypoxia, and DNA damage by radiation exposure. Similarly, activation of intrinsic pathway releases the cytochrome c from the mitochondrial membrane that binds with Apoptotic Protease Activating Factor-1 in presence of ATP to form apoptosome. The apoptosome in the cytosol binds to pro-caspase 9 to activate pro-caspase 3 to caspase-3. The formation of caspase-3, the final effector enzyme that cleaves regulatory and structural cell proteins to bring cell death remains the final common pathway for both extrinsic and intrinsic apoptotic pathways. (Adapted from David Erikson; Tumour Biol. (2010) 31:363–372).

1.6.2.1 APOPTOTIC PROTEINS:

The BCL-2 Protein:

The Bcl-2 gene (18q21.3) was initially identified at a breakpoint in a chromosomal translocation (t14:18) in human B-cell lymphomas (Tsujimoto, Finger et al. 1984). The gene codes a family of proteins that regulate cell apoptosis. Bcl-2 proteins are usually expressed in every tissue during the developmental period. However, in adults, their expression is restricted to proliferating cells. The Bcl-2 family members can be both pro and anti-apoptotic (Al-Mansouri and Alokail 2006). The anti-apoptotic members such as Bcl-2 and Bcl-xL and the pro-apoptotic members such as Bax, Bad and Bid exists with different domains.

A balance between cell proliferation and apoptosis drives the normal development of tissue. In normal adult cells, pro-apoptotic members of Bcl-2 family exist as heterodimers with anti-apoptotic members in order to maintain the cell homeostasis in a resting state. In the pro-apoptotic conditions an increased cytoplasmic Bax concentration shifts the equilibrium to the Bax homodimer formation and increases the mitochondrial permeability to release cytochrome C (Quinn, Henshall et al. 2005). Similarly, an increased formation of Bcl-2 homodimer in anti-apoptotic conditions shifts the equilibrium towards inhibition of apoptosis by blocking the MAC activity of Bax protein.

In breast tissue, Bcl-2 is known to be expressed in normal mammary epithelial cells and in early pregnancy but remains undetectable in lactating and involuting glands (Kumar, Vadlamudi et al. 2000). In breast carcinomas, Bcl2 persistent expression was found in about 61-70% of invasive ductal carcinomas, 66% of micro-papillary carcinomas and 2.9% of apocrine carcinoma (Leal, Henrique et al. 2001).

Studies have shown Bcl-2 protein promotes cell survival but not proliferation in breast cancer cells (Kumar, Vadlamudi et al. 2000). Studies analysing mechanisms of anticancer therapies have shown phosphorylation of Bcl-2 protein at serine residue in response to anticancer therapy renders the protein functionally inactive. This decreases its binding with Bax protein and confers the protective effect (Simstein, Burow et al. 2003). Over-expression of Bcl2 protein has been shown to cause resistance to anticancer therapy by inhibiting apoptosis (Olopade, Adeyanju et al. 1997). Evidence to such a hypothesis, comes from a breast cancer cell line study that showed improved responses to breast cancer chemotherapeutic agents including doxorubicin, docetaxel and mitomycin C by knocking down the expression of Bcl-2 and Bcl-xL proteins using anti-sense oligodeoxynucleotides (Nuki and Simkin 2006). Similarly, a loss or down-regulation of pro-apoptotic Bcl-2 family member may result in resistance to anticancer therapy (Radetzki, Kohne et al. 2002) as shown by forced expression of pro-apoptotic proteins such as Bak and Nbk/Bik showing reversal of chemotherapy resistance by manipulating the downstream signalling cascade.

1.7 BREAST CANCER & SURFACE RECEPTORS:

Breast tumours show expression of Oestrogen (ER), Progesterone (PR) and Human Epidermal Growth Factor-2 (HER2) on their cell surface. These receptors promote tumour growth from their interaction with the Oestrogen and Progesterone hormones. Therefore, a thorough understanding of these interactions at the molecular level can help develop therapy strategies and determine long term cancer prognosis.

1.7.1 Oestrogen Receptor (ER):

The oestrogen receptor (ER) is a nuclear ligand activated transcription factor belonging to steroid hormone receptor family. It is an important molecular marker in breast cancer as it promotes cell proliferation and differentiation via 17 β -estradiol (E2) interaction. There are two types of ERs characterised to date: ER α and ER β .

Breast tumours express both ER receptors. However, expression of ER β is reportedly decreased with carcinogenesis (Gustafsson 1999). Approximately 70-80% of breast cancers show ER positivity (Keen and Davidson 2003) and ER α plays the predominant mediator of mitogenic effects of oestrogen (Hewitt, Harrell et al. 2005). More recently, expression of ER β has been found to be associated with breast cancers in pre-menopausal with high oestradiol levels (Murillo-Ortiz, Perez-Luque et al. 2008).

1.7.2 Progesterone Receptor (PR):

The progesterone receptor (PR) a member of steroid hormone receptor super family is a protein found inside cells. PR exists naturally in two isoforms: PR-A and PR-B. As the majority of ER α positive tumours also express PR; presence of normal PR levels in the breast cancer cells suggests an intact ER signal transduction pathway (Sandhu, Parker et al. 2010).

1.8 MOLECULAR CLASSIFICATION OF BREAST CANCER:

The receptor based breast cancer classification uses immuno-histo-chemistry (IHC) to confirm individual cell receptor (ER, PR, and HER) status. Gene expression profiling studies by Perou et al. analysed cell receptors and tumour grade alongside the biologic heterogeneity from molecular alterations (Geyer, Marchio et al. 2009; Prat and Perou 2011) classifying breast cancers into

distinct molecular sub-types. Even though, similar in morphology, molecular sub-types differed markedly in their biologic characteristics making them a genetically diverse group (Bertucci and Birnbaum 2008).

Using gene expression profiling techniques such as cDNA microarray and oligonucleotide two-dimensional array, breast tumours, can be clustered into different groups based on differential gene expressions (Liu and Sotiriou 2002). Sorlie *et al.* and Sotiriou *et al.* were the first to classify breast cancers using this technique into 5 distinct subtypes; Luminal A (ER+); Luminal B (ER/PR+); erbB2 over-expressive (HER2+), Basal-like (triple negative); and Normal-like (Sorlie, Perou et al. 2001; van 't Veer, Dai et al. 2002; van de Vijver, He et al. 2002; Sotiriou, Neo et al. 2003). The dominant factor emerging from these molecular studies showed remarkably different gene-expression phenotypes for the ER positive and negative tumours. Based on this feature, a further sub-division of molecular subtypes was undertaken by Sorlie *et al.* from a selected intrinsic gene set of 456 cDNA clones based on decrease or absent ER gene expression and other additional transcriptional factors. Groups with the lowest ER expression were: basal-like, normal epithelial and erbB2 subtypes each with specific expression characteristics. The basal-like subtype had a high expression of keratins 5, 17, laminin, and fatty acid binding protein 7. The erbB2 showed a high expression of genes in the ERBB2 amplicon including ERBB2 and GRB7. The normal breast-like, showed a highest expression of adipose tissue and nonepithelial cell types type proteins (Sorlie, Perou et al. 2001). The luminal group, with the highest ER gene expression pattern was further categorized into 'A' and 'B' sub-groups. This classification was based on the level of luminal specific genes and ER cluster expression. The luminal-A subgroup demonstrated the highest expression of the ER gene. A further division of luminal group into two smaller units of luminal B and C was undertaken depending on a

moderate to low expression of the luminal specific genes. After the initial molecular classification into subtypes of breast cancer, a new intrinsic subtype was identified in 2007 called claudin-low subtype (Herschkowitz, Simin et al. 2007). It is characterized by a low expression of genes involved in tight junctions and intercellular adhesion such as claudin-3, 4 and 7, cingulin, occludin, and E-cadherin. This subtype is located in the hierarchical clustering near the basal-like tumors, suggesting both subtypes may share some characteristic gene expression such as low expression of HER2 and luminal gene cluster.

1.8.1 Breast Cancer Molecular Subtypes & Clinical Outcomes:

As discussed in the section 1.5.1.3, the clinical and molecular subtypes of breast cancers show a wide variation in responses to neoadjuvant chemotherapy and clinical prognosis. The correlation of specific gene expressions to the clinical outcomes was first demonstrated from the work of van't Veer and colleagues using the cDNA microarray analysis of 70 core genes (van 't Veer, Dai et al. 2002; van de Vijver, He et al. 2002). Further, Sorlie, Perou *et al.* (2001), analysed clinical outcomes for each of the intrinsic breast molecular sub-type in a univariate survival analysis and found basal-like and ERBB2 were associated with shortest relapse-free and overall survival (n=49; OS: Luminal A 96 months, Basal like 36 months and ERBB2 72 months; P<0.01; RFS: Luminal A 96 months, Basal like 24 months and ERBB2 72 months P<0.01) (Sorlie, Perou et al. 2001). Similar differences in relapse-free and overall survival between the basal-like, ERBB2 and luminal sub-types were also found by Sotiriou *et al.* in a larger study involving 99 breast tumours. The luminal subtype was found to show better relapse-free and overall survival compared to basal like and ERBB2 sub-types (RFS: Luminal 3000 vs Basal like 2000 days; P< 0.013; OS: Luminal 3500 vs Basal like 2200 days; P <0.022) (Sotiriou, Neo et al. 2003) (Figure

6). In conclusion, molecular classification classifies breast cancers into six distinct sub-types each with a unique characteristic representing the breast tumour heterogeneity in its entirety.

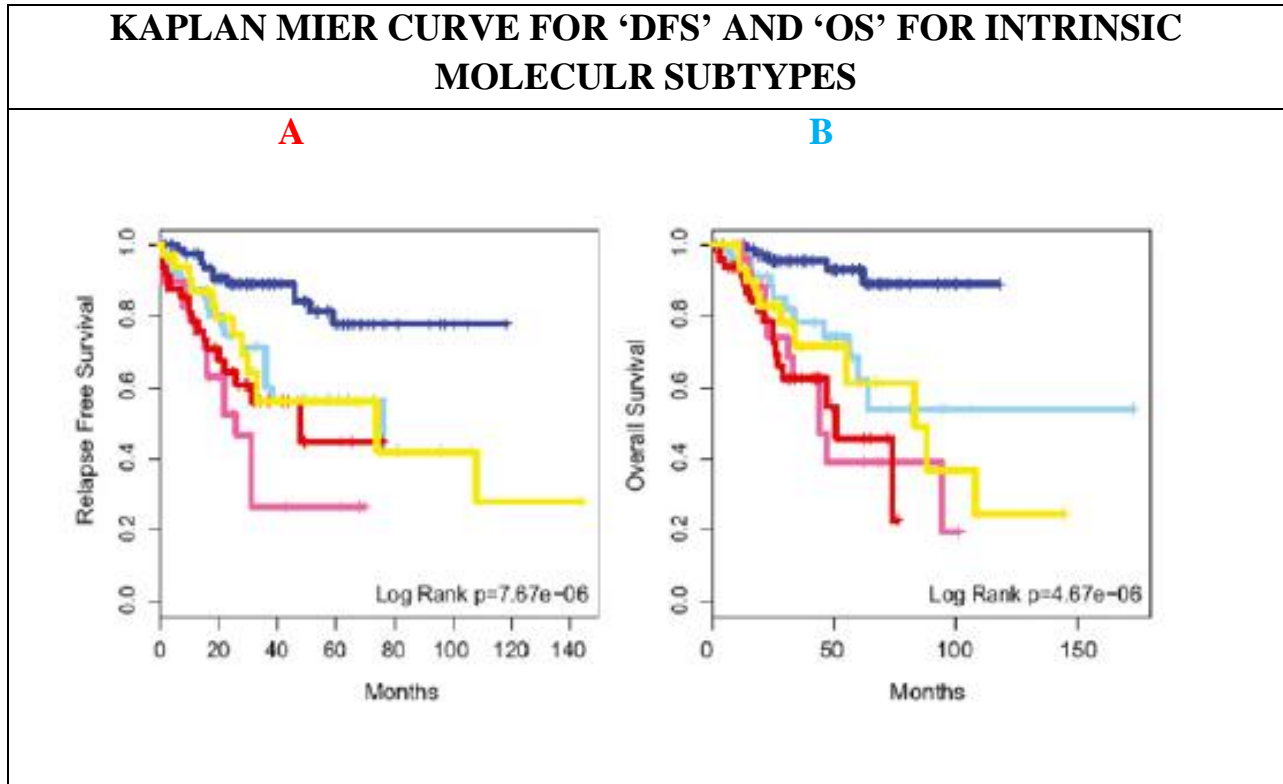


Figure 6: The graph illustrates Kaplan–Meier curves of disease-free survival (A) and overall survival (B) Dark blue, luminal A; light blue, luminal B; red, basal-like; pink, HER2-enriched; yellow, Claudin-low; red. From the above data, Luminal A is found to show the best and HER2 + the worse disease free and overall survivals amongst all the molecular subtypes (Herschkowitz, Simin et al. 2007).

1.8.2 Breast Molecular Subtypes & Neoadjuvant Therapy Response:

The effects of anthracycline-taxane based NACT in different biological phenotypes were examined in the GeparTRio study involving 2,072 locally advanced breast cancers (Huober, von Minckwitz et al. 2010). Findings from the study showed highest pCR rate of 57% in patients age < 40 years with triple negative (basal-like) status compared to 35% pCR rate for luminal subtypes (Table 5).

Table 5: Multivariate analysis for pCR within different biological groups
(Adapted from GeparTrio Study; Huober von Minckwitz et al. 2010)

Factor	Luminal A, pCR at surgery (n=562)		Luminal B, pCR at surgery (n=462)		HER2 like, pCR at surgery (n=193)		Triple negative, pCR at surgery (n=351)	
	pCR (%)	P value	pCR (%)	P value	pCR (%)	P value	pCR (%)	P value
Age (years)								
<40	10.1	0.256	24.1	0.163	33.3	0.441	57.0	0.01
>40	6.6		17.8		28.2		34.1	
Tumour Grade								
III	16.2	<0.0001	24.3	0.018	31.3	0.164	39.5	0.137
I + II	3.8		17.8		25.3		30.5	
Histological Type								
Ductal/others	7.8	0.376	20.0	0.058	31.0	0.164	38.9	0.702
Lobular	4.3		11.9		7.7		39.1	

Further, Rouzier *et al.* evaluated the gene expression profiles of 82 breast cancer patients treated with anthracycline-taxane NACT and reported pCR rates of 45% for the basal-like and HER2-positive sub-types and 6% for the luminal sub-types (Rouzier, Perou et al. 2005). Kim *et al.* from their series of 257 patients treated with adriamycin-taxane NACT showed similar findings of a higher pCR rates 21.1% vs 10.5% vs 8.9% $p=0.001$ for basal-like, HER2+ and luminal sub-type (Kim, Sohn et al. 2010). Carey *et al.* from their 107 patients series showed 36% of HER2+ and 27% of basal-like sub-types achieved pCR ($p=0.01$) compared to only 7% of luminal tumours following anthracycline only NACT (Carey, Dees et al. 2007). Lv *et al.* from their analysis of 102

tumours treated with anthracycline-taxane-carboplatin NACT regimens found pCR rates of 24.4% ,22.2% and 8.7% ($p=0.041$) for basal-like, HER2+ and luminal sub-types respectively (Lv, Li et al. 2011). In a more recent follow up study of 512 patients who received anthracycline-based therapy (epirubicin or doxorubicin) or an antimetabolic based-therapy (including taxanes and vinca-alkaloids) pCR was shown to be significantly lower in HR+/HER2- tumors ($P < 0.0001$) at 7 year follow up (Guiu, Arnould et al. 2013). Further, in the same study the OS rates at 7 years were found to be significantly higher in HR+/HER2- (76.1%) followed by 60.1% (TNBC), 72.4% (HR+/HER2+), and 49.9% (HR-/HER2). From the above findings, it is safe to conclude that luminal, basal-like, normal-like, and erbB2+ subgroups have different responses to neoadjuvant chemotherapy and clinical outcomes: basal-like (mostly hormone receptor negative) and erbB2+ (mostly HER2 overexpressed/amplified and ER-) respond well to neoadjuvant therapy but have the worst outcomes with the shortest DFS and OS rates. At a molecular level, the differential chemosensitivities between different molecular subtypes can be explained from a lower expression of proliferation cluster genes in the luminal A subtype (Perou, Sorlie et al. 2000; Sorlie, Perou et al. 2001).

1.8.3 Why Biomarkers for ER+ (Luminal A) Breast Cancer?

According to the NCCN breast cancer guidance 2012, patients presenting with a locally advanced breast cancer up to the age of 70 years are routinely offered neoadjuvant chemotherapy to down stage the disease and facilitate BCS ((Guidelines)TM 2012). Currently, this practice remains uniform across all the breast cancer molecular subtypes. However, as evidenced from the above studies (sections 1.8.1 and 1.8.2), ER+ (Luminal A) breast cancer subtype tend to have poor pathological response after neoadjuvant chemotherapy. Therefore, using molecular signatures (e.g. gene or protein biomarkers) and/or radiological imaging (e.g. MRI, PET scan) if

chemotherapy responses in ER+ (Luminal A) subtype can be predicted, patients unlikely to respond to therapy can be selected early in the treatment course. These patients then can be streamlined to alternative treatment strategies sparing them from unnecessary side-effects of therapies for no therapeutic gains.

1.9 CHEMOTHERAPY RESISTANCE:

Drug resistance of tumour cells is a major obstacle in effective neo-adjuvant chemotherapy treatment and a common cause of primary treatment failure. Although exact mechanisms of resistance to anticancer therapy remain unclear, multiple factors are believed to act in interrelated or independent pathways which result in intrinsic and acquired therapy resistance. In general, the common mechanisms implicated with chemo resistance include:

1. Intra-cellular defence factors which decrease the drug concentrations at the target level by activating transporter protein and detoxification mechanisms within the cells
2. Enhanced DNA repair
3. Resistance to chemotherapy-induced apoptosis

1.9.1 Intracellular Defence Mechanisms:

Drug Transporter Protein:

The intracellular concentrations of a drug are managed by a fine balance of drug influx and efflux mechanisms. Changes to drug accumulation in the cell occur by a decrease in drug influx or an increase in efflux mechanisms. As most of the cytotoxic drugs enter cells via passive diffusion, alterations in the bio-physical properties of the plasma membrane and changes in the lipid fluidity due to Ca^{2+} concentration can all decrease the rate of drug uptake into the cells

(Liang and Huang 2002; Laura Gatti 2005). This mechanism is primarily implicated in cisplatin, and methotrexate drug resistance, but is less effective in preventing lipid soluble drugs such as anthracyclines from entering the cell. (Ramu, Glaubiger et al. 1983; Stavrovskaya 2000).

Multi-Drug Resistance Protein:

The multi-drug resistance proteins (MRP) are a subfamily of the ‘ABC super-family’ of transporter proteins. Similar to the P-gp protein, the MRP family is also functionally ATP dependent and are mostly involved in the transport of glutathione (GSH)-conjugated derivatives of toxic compounds (GS-X pump) (Ishikawa, Kuo et al. 2000). A total of seven protein members (MRP-1 to 7) belong to the MRP family. MRP-2 is implicated in anthracycline resistance. The MRP-1 protein was detected in 49% of breast cancers (Leonessa and Clarke 2003) using immunohistochemical studies and over-expression was associated with reduced overall and disease free survival (Filipits, Malayeri et al. 1999).

Breast Cancer Resistant Protein:

The breast cancer resistant protein (BCRP) is a 72 kDa protein that belongs to the G sub-family of ABC super-family proteins. Evidence of BCRP over-expression in multi-drug resistance was confirmed in transfection studies involving MCF-7 breast cell lines transfected with BCRP cDNA. Collectively, BCRP over-expression was found to confer resistance to mitoxantrone, topotecan, and flavopiridol, paclitaxel, cisplatin/ or *vinca* alkaloids (Allen, Brinkhuis et al. 1999) (Doyle, Yang et al. 1998). The BCRP/ABCP mediates mitoxantrone and anthracyclines (doxorubicin) cell efflux, an action which is dependent on the presence of threonine or glycine substrate at position 482 of the BCRP cDNA (Honjo, Hrycyna et al. 2001). Mutation in the

BRCP/ABCP gene causes arginine substitution at position 482 changes the substrate specificity and anthracyclines are accumulated in the cells thus conferring drug resistance.

1.9.2 Enhanced DNA Repair:

Cytotoxic medications can also activate several other distinct cellular mechanisms that lead to drug resistance. One such example is the up-regulation of DNA repair mechanisms which has been associated with resistance to alkylating agents in leukaemia and topoisomerase inhibitors in breast cancers. The DNA repair mechanisms involve excision or repair of damaged strands. Excision of damaged base pairs involves, nucleotide excision repair (NER) and base excision repair (BER). The NER pathway is one of the pathways responsible for the removal of DNA adducts produced by cytotoxic drugs such as cisplatin and nitrogen mustards (Chaney and Sancar 1996). Drug resistant cancer cells promote DNA replication to nullifying the cytotoxic effects (Selvakumaran, Pisarcik et al. 2003). BER removes damaged base pairs and induce DNA repair via endonucleases. This action may lead to resistance to oxidizing (e.g. H₂O₂) and alkylating agents such as cyclophosphamide and nitrogen mustards (Kelley, Kow et al. 2003). The mismatch repair (MMR) pathway corrects single base mispairs incorporated by cytotoxic drug exposures. A deficient MMR system can confer therapy resistance as cells fail to recognise DNA damage and continue to proliferate. Approximately 25% of sporadic breast cancers show a deficient MMR system (Fedier, Schwarz et al. 2001)

1.9.3 Chemotherapy-Induced Apoptosis and Drug Resistance:

Apoptosis induced cell death, is one of the key mechanisms of action of chemotherapeutic agents (Kaufmann and Earnshaw 2000). It is postulated, that defects in the pathways involved in apoptosis may result in drug resistance (Reed 1999). *In-vitro* studies have shown that two protein

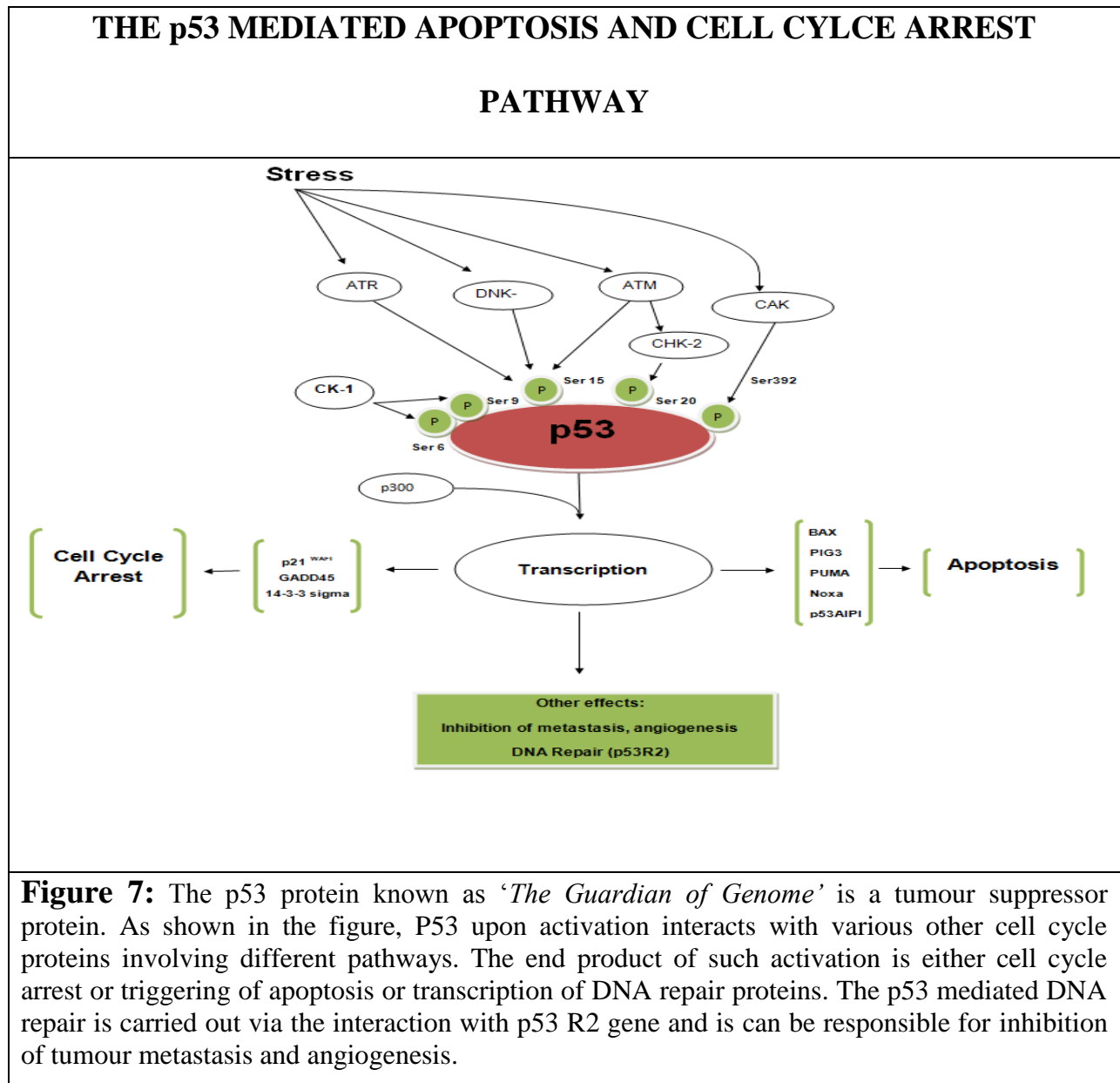
families: the p53, Bax and Bcl-2 are involved in the initiation of apoptosis. In breast cancers, loss of p53 is found to confer resistance to DNA-damaging agents such as doxorubicin. The Bcl-2 apoptotic protein also plays an important role in MDR. The relative amounts of the two proteins determine whether apoptosis can be triggered as imbalances in the ratios of anti- and pro-apoptotic Bcl-2 family members may be associated with therapy resistance.

1.9.3.1 P53 Protein and Chemoresistance:

The TP53 gene known as the '*guardian of genome*' is located on the short arm of chromosome 17 and encodes p53 tumour suppressor protein. Normally, low concentrations of the p53 protein reside in the cell in an inactive state due to its association with its negative regulator murine double minute-2 protein (mdm2). A normal physiological activation of p53 occurs in response to cellular stress, e.g. DNA damage, and induces the transcription of genes involved in cell cycle control and apoptosis (May and May 1999; Vogelstein, Lane et al. 2000). In a normal adult cell, p53 protein binds to mdm2 to remain in an inactive state. In the event of DNA damage, p53-mdm2 complex disassociates and release the active p53 to induce cell cycle arrest at the G₁ checkpoint. The active p53 then seek to repair the damage DNA by either promoting or repressing the expression of target genes (e.g. p53R2 gene, ribonucleotide reductase gene, DNA polymerases). In the event of repair not possible, p53 directs the cell towards apoptosis by inhibiting cyclin dependent kinase complex activity through p21 protein (Figure 7). This mechanism is implicated in anthracycline chemo sensitivity in breast cancer treatment (Osborne, Wilson et al. 2004).

The p53 status in breast cancer plays an important role in tumour responsiveness to anti-neoplastic agents. This action, mediated via p53 dependent change in the Bcl-2/Bax ratio occurs

through increased expression of Bax and reduced expression of the Bcl-2 protein. Therefore, loss of normal p53 function can potentially result in resistance to chemotherapeutic agents due to loss of apoptotic properties. Further, the prognostic value of p53 in providing information on tumour response following systemic chemotherapy is found to increase when combined with ER, PR, HER2, Bcl-2 and Bax expressions (Zheng, Lu et al. 2001; Yamashita, Nishio et al. 2004).



1.9.4 Alteration of Molecular Pathways & Drug Resistance:

1.9.4.1 PIP3/AkT-mTOR Pathway:

Activation of Phosphatidylinositol-3kinase (PI3K) is reported to occur in breast, ovarian, pancreatic and oesophageal cancers (Zhou, Liao et al. 2001). PI3K phosphorylates inositol lipids at the 3-position of the inositol ring to generate the 3-phosphoinositides PtdIns-3-P, PtdIns-3,4-P2, and PtdIns-3,4,5-P3. Akt, also known as protein kinase B (PKB), is a major target of PI3K and belongs to subfamily of serine/threonine protein kinases with three identified member proteins: Akt/AKT1/PKB, AKT2/PKB, and AKT3/PKB. Activation of AkT occurs via PDK1 through phosphatidylinositol-3kinase (PIP3) after ligands binds to the receptors at the cell membrane. This activation depends on the integrity of the PH domain, which binds to PI3K products, and on the phosphorylation of Thr308 in the activation loop and Ser473 in the C-terminal activation domain by PDK1 (Cheng, Jiang et al. 2002). The activity of Akt is negatively regulated by *PTEN*, a tumour suppressor gene. *PTEN* encodes a dual-specificity protein and lipid phosphatase that reduces intracellular levels of PtdIns-3,4-P2 and PtdIns-3,4,5-P3 in cells by converting them to PtdIns-4-P1 and PtdIns-4,5-P2 respectively, thereby inhibiting the PI3K/Akt signaling pathway. Activation of AkT, results in different downstream cellular processes such as cell survival, cell proliferation and cell migration via the inhibition of pro-apoptotic proteins BAD and activation of GSK3 β protein and Forkhead protein transcription factor (Figure 8). The phosphatidylinositol-3kinase/(AkT) pathway has been implicated in acquired therapeutic resistance in breast cancer, through evasion of cell death (West and Dennis 2011). In breast cancers, Akt activation is found to correlate with HER-2/neu over expressions; Akt-induced signalling is suggested to increase drug-induced apoptosis resistance in cells over expressing HER-2/Neu via Mdm2 phosphorylation (Zhou, Liao et al. 2001).

REPRESENTATION OF PIP3/Akt-mTOR PATHWAY IN BREAST CHEMOTHERAPY RESISTANCE

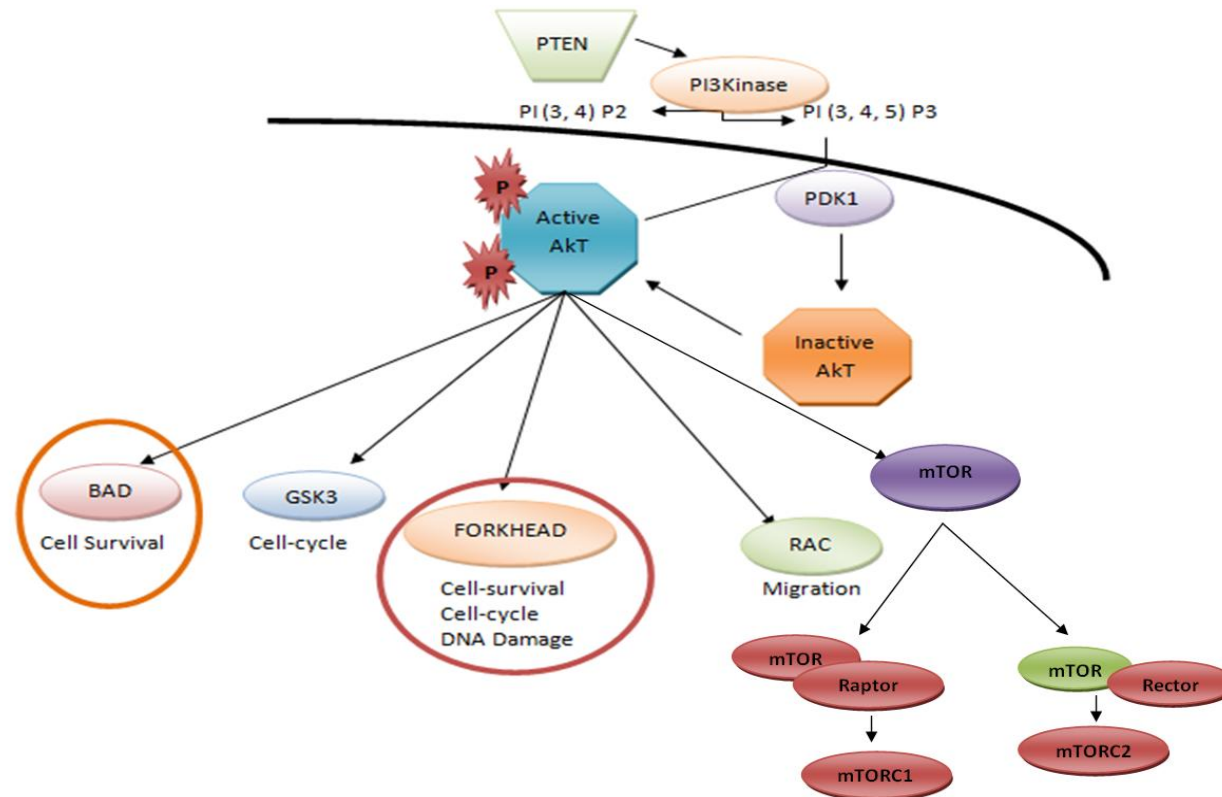


Figure 8: A general sketch of the PKB/AKT pathway. PIP3 is activated by PI3K and recruits AKT to the cell membrane via activation of PDK1. AKT activation stimulates cell cycle progression, survival, metabolism and migration through phosphorylation of many physiological substrates. Acquired chemotherapy resistance in breast cancer occurs through cytotoxic drugs mediated activation of PIP3/AKT inhibition of apoptosis via downregulation of BAD protein.

1.9.4.2 Role of Integrins in Chemoresistance:

Integrins mediate cell to cell interactions and cell attachments to the extracellular matrix (ECM). In addition to the above described roles, ligation of integrins with ECM ligands induces a variety of intracellular signals and regulates several cellular responses including migration, differentiation, proliferation and programmed cell death (Frisch and Francis 1994; Hood and Cheresh 2002). Integrins are composed of α and β chain heterodimers which are activated upon by ligand binding. Focal adhesion kinase (FAK), Integrin-Linked and Src kinases are example integrins which upon binding form clusters on the cell surface called focal adhesions. These focal adhesions, then acts as a structural link between the ECM and the intracellular actin cytoskeleton for the mediation of signal transductions to the intracellular signalling pathways. It has been hypothesised that the integrin-ECM interactions causes chemotherapy resistance by activating the downstream signalling survival pathways such as PIP3/AKT and MAPK/ERK (Figure 9) in a complex and tissue specific mannerisms (Mitra and Schlaepfer 2006). The role of integrins in breast cancer chemotherapy resistance was first reported by Aoudjit F and Vuori K *et al*; using MDA-MB-231 and MDA-MB-435 breast cancer cell lines (Aoudjit and Vuori 2001). In this study, ligation of $\beta 1$ integrins by their extracellular matrix ligands was found to inhibit the release of cytochrome c from mitochondria, preventing apoptosis induction in response to paclitaxel and vincristine therapies. The above $\beta 1$ mediated protection was found to be dependent on the activation of the PI3-kinase/AkT pathway. Further, in the same study, other integrins such as laminin-1-binding integrin $\alpha 6\beta 1$ and fibronectin were also found to exert protective effects against the drug-induced apoptosis via activation of PI3-kinase/AkT mechanism and via down regulation of pro-apoptotic Bad protein.

THE INTEGRIN-PIP3/AKT MEDIATED THERAPY RESISTANCE AXIS

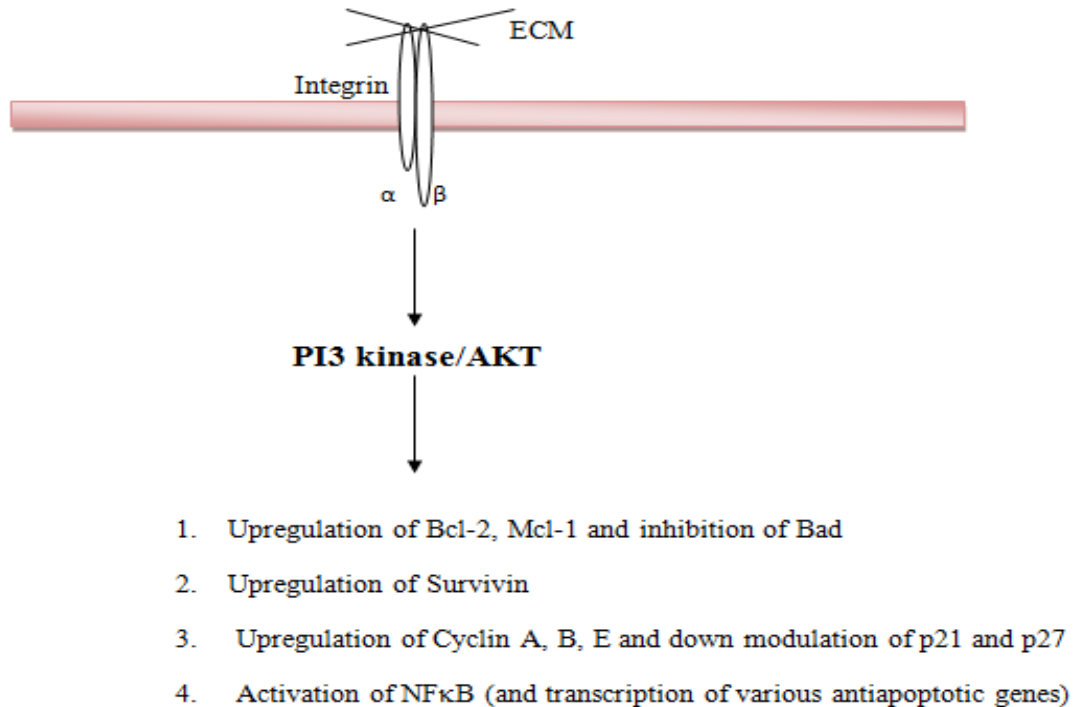


Figure 9: The PIP3-kinase/AKT pathway in integrin-mediated drug resistance. Integrin/ECM interactions lead to the activation of PIP3-kinase/AKT, which then regulates various downstream targets including proteins of Bcl-2 family, cyclins and NFκB. Further, activation of the transcription factor NFκB, increase the expression of several anti-apoptotic proteins and lead to chemoresistance (adapted from Chemotherapy Research and Practice Volume 2012, Article ID 283181).

1.9.4.3 The Role of 14-3-3 Mediated Pathway in Chemoresistance:

14-3-3 proteins are a family of highly conserved proteins that are involved in a wide range of cellular processes. Recent evidence indicates that some of these proteins have oncogenic activity and that aberrant expression of 14-3-3 promotes tumourigenesis in lung, prostate, ovarian and pancreatic tissues (Radhakrishnan, Putnam et al. 2011). The number of proteins in the 14-3-3 family varies with species. However, in mammals, seven isoforms have been identified namely

beta/alpha, gamma, eta, sigma, epsilon, theta/tau and zeta/delta and they function by binding to other proteins predominantly through phosphorylated serine residues. Translational studies have identified 14-3-3 gamma isoform as a downstream negatively regulated p53 target protein and that loss of p53 function leads to over expression of 14-3-3 gamma isoform promoting genomic instability in lung cancer (Riley, Sontag et al. 2008; Radhakrishnan, Putnam et al. 2011). The above mechanism mainly implicated in lung tumourigenesis and chemoresistance. Further, 14-3-3 sigma and eta isoforms are known to play a key role in cell cycle arrest and has a role in cell death interacting via Mdm4, Chk2 and Cdc25c motif loop (Bustos 2012). Therefore, down regulation of these protein isoforms or up regulation of 14-3-3 gamma isoform result in cell survival evading cell death from the inactivation of p53 pathway in response to chemotherapy induced DNA damage (section 1.9.3.1). Also, 14-3-3 proteins are downstream effectors of the PIP3/AkT pathway and have a role in mediating cell survival, proliferation and cell regulation by evading apoptosis (section 1.9.4.1). The above outlined mechanisms in combination and/or binding of 14-3-3 proteins with disordered ligand partners (e.g. proteins involved in regulation of the cytoskeleton; GTPase function; membrane signalling; phases of the cell cycle- apoptosis) have been postulated to cause chemoresistance with 14-3-3 family of proteins.

1.10 PROTEOMICS FOR BIOMARKER DISCOVERY:

The discovery of biomarkers up until the late 1980s was very much limited to a handful of proteins. However, in the last decade, technological advancements in protein separation (e.g. sub-bio fractionisation), identification (e.g. mass spectrometry) and enrichment methods have lead to the discovery of hundreds of new biomarkers for a range of purposes. Early studies utilised cell line models to make novel biomarker discoveries. However, more recently, the use of biological samples (e.g. plasma, urine, cerebrospinal fluid, tumour interstitial fluid, and

tumour tissues) have gained momentum with both proteomic and non-proteomic based approaches ((Olsson, Zetterberg et al. ; Shao, Wang et al. ; Sun, Yang et al. ; Pitteri and Hanash 2007).

The aim of this section is to provide an overview of proteomic workflow for biomarker discovery and to discuss the challenges of using different clinical samples with proteomics. A literature search was conducted on pubmed using the term “challenges of clinical samples with proteomics” and 22 articles published in human studies in last 10 years were selected and reviewed.

1.11 BIOMARKER:

The official National Institutes of Health definition of a biomarker is a substance that is objectively measured and evaluated as an indicator of normal biologic processes, pathogenic processes or pharmacologic responses to a therapeutic intervention (Diamandis 2010). A biomarker can therefore be a mutated gene signature, altered mRNA or a differentially expressed protein which can be studied under three “omic” categories of genomics, transcriptomics, and proteomics.

1.11.1 Proteomics Vs. Other Omic Studies:

Omic' technologies include genomics, transcriptomics, proteomics and metabolomics all of which have a significant potential in generating novel biomarkers of exposure, susceptibility and response. However, for this review, the discussion as to why proteomics should be preferred over other omic studies for the cancer biomarker discoveries will be largely limited to comparing proteomics to genomics and transcriptomics studies only.

Proteome study in contrast to genome or mRNA has an inherent advantage for it may allow the identification of genomic and transcriptomic modifications, being that the identified proteins are itself the biological endpoints. Genomic studies involve analysing a change in the genome structure as a marker of response; this usually is a change in the DNA sequence. Genome based research in the last decade has transformed with the availability of information on gene sequencing and development of high-density DNA microarrays. (Lipshutz, Fodor et al. 1999; Shou, Qian et al. 2006). However, genomics compared to the other two '*omic*' studies, due the static nature of human genome and very few mutations altering its functional status may have a limited role in cancer biomarker studies. Firstly, genomic studies are dependent on classification methods for assessment of differential gene expressions (Moler, Chow et al. 2000). Discrepancies are known to exist between high differential gene expressions and the accuracy of their classification methods limiting the role of genomics for biomarker studies (Xiong, Fang et al. 2001). Further, the gene functioning is affected by alternative splicing; the mRNA transcripts of a single gene can undergo hundreds of alternative splicing events adding or deleting functional domains, changing affinities, and/or altering mRNA stability. This produce variable transcripts making genome based study alone less specific (Gardina, Clark et al. 2006). Furthermore, find a limited role in large population based studies genomics find a limited role due to the lack of comprehensive analytical techniques to evaluate all splice variations, individual patient differences and tissue complexities (Furey et al.; 2001).

The transcriptome by definition is a subset of genes transcribed in an organism that link the genome, proteome and the cellular phenotype. With the advent of the DNA microarrays platform in transcriptomics, measuring the mRNA expression levels is now possible (Leder, Merila et al. 2009). In a normal cell state, besides the post-translational modifications, frequency of mRNA

expressions determines the cell protein content. In cancer cells, excessive mRNA turnover occurs causing a mismatch between the peak mRNA expressions and protein translations. This difference up to as high as 20 folds between the cell protein content and mRNA expressions limits protein expressions analysis from a quantitative mRNA data using transcriptomics studies (Gygi, Rochon et al. 1999).

In contrast to genomic and transcriptomic studies, studying proteome has an inherent advantage for it allows identification of all genomics and transcriptomics modifications, being that the identified protein is itself the biological endpoint. Also, studying proteins allows researchers to translate the findings into immunohistochemistry and thus readily translated into clinical practice in histopathology labs.

1.12 PROTEOMICS:

A global analysis of protein expression, interaction and functional status can be studied under proteomics. Proteins via their post-translation modifications acquire stability and functional variability (Johann, McGuigan et al. 2004) and therefore give an accurate reflection of cell functionality and response. Currently, proteomic technology has been used in two main areas of cancer research: early diagnosis and treatment (included prediction of response to treatment and targeting novel cancer agents) (Chuthapisith, Layfield et al. 2007). Whilst many proteomic techniques exist, studying differential protein expressions using current proteomic methods can be grouped into gel based and gel free mass spectrometry (MS) methods and micro-array based methods.

1.13 Workflow of Proteomic Discovery Pathway:

The proteomic based biomarker discovery pipeline mainly consists of four stages; discovery stage, data mining stage, confirmation stage and validation stage. In the *discovery stage* proteins are identified using *MS-dependent* or *MS-free* proteomic methods. The *Data mining stage* involves using a software programme such as *Ingenuity Pathway Analysis* (IPA) for mapping differentially expressed proteins (DEPs) to molecular pathways to understand the relationships between proteins and mechanisms of tumourogenesis and therapy resistance. The *Confirmatory stage* involves confirming the differential expression of identified proteins using an immunoblotting technique. Following confirmation, in the *Validation stage*, putative biomarkers are validated to assess their clinical relevance using archival series of pre-treatment clinical samples in a tissue based-immuno-histo-chemistry (IHC) approach or non-tissue based Enzyme Linked Immno Sorbent Assay (ELISA) approach. The proteomic biomarker discovery pipeline described above is illustrated in the Figure 10.

THE WORKFLOW OF BIOMARKER DISCOVERY PATHWAY

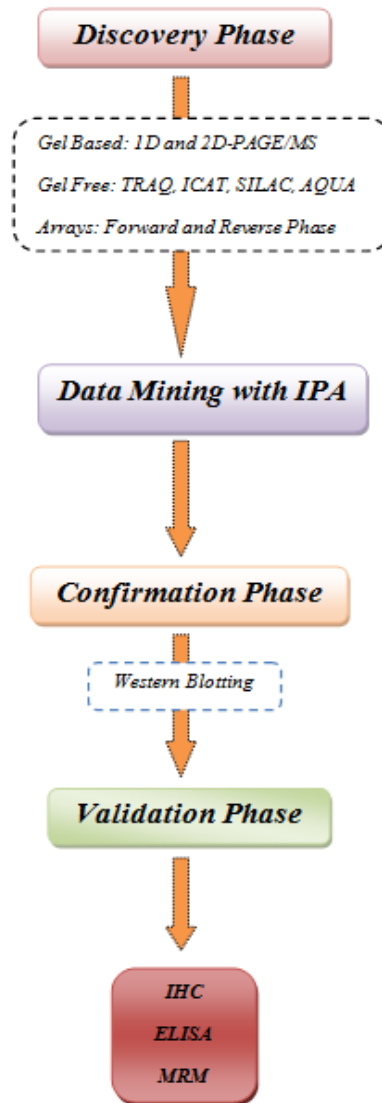


Figure 10: shows the proteomic biomarker discovery pipeline. **1D/2D-PAGE/MS:** One and two dimensional polyacramide gel electrophoresis/Mass Spectrometry; **iTRAQ:** iso-baric tag for absolute and relative quantification; **SILAC:** Stable isotope labelling amino acid; **ICAT:** Isotope-coded affinity tagging; **AQUA:** Absolute quantification; **IPA:** Ingenuity Pathway Analysis; **IHC:** Immunohistochemistry; **ELISA:** Enzyme linked immuno sorbent assay; **MRM:** Multi chain reaction.

1.13.1 Proteomic Discovery Phase:

This is the first stage in the proteomic biomarker workflow and involves protein separation using gel-based (1D-PAGE, 2D-PAGE and 2D-DIGE) or gel-free techniques (i-TRAQ, ICAT and SILAC) followed by protein identification using mass spectrometry (MS) (Zong, Zhang et al. 2007). However, protein identification and analysis of differential expressions can also be achieved using another approach which does not involve use of mass spectrometry called microarray. This method is usually preferred if proteins fail to generate a sufficient number of peptides with mass spectrometry assisted techniques to gain a significant identification, or if the specific form of protein is not represented in the database. Microarray-based proteomic methods can be employed in a forward (antibody immobilised) or reverse (protein lysate immobilised) phase and offers a range of methods that compliment traditional mass spectrometry-based proteomic methods. However, none of the approaches when used on their own can fully analyse the whole proteome in a single experiment, therefore using them in combination increases the chances of wider proteome coverage.

1.13.1.1 MS-Assisted Gel Based Methods:

This is a low-throughput method in which using principles of electrophoresis, proteins are separated in polyacramide gel based on molecular weight and iso-electric point following extraction from the sample in a suitable buffer (e.g. Laemmli buffer) prior to gel loading. The one-dimensional (1D-PAGE) method separates proteins based on molecular weight in a vertical plane; separated proteins are then visualized as bands of different molecular weights and identified using a ladder of molecular marker proteins from co-electrophoresis. In the two-dimensional method, protein separation takes place in the horizontal and vertical planes based on

the proteins iso-electric point and molecular weights. The first dimension horizontal separation is to the iso-electric point based on the net protein charge along an immobilized pH gradient (IPG) strip in electric field (Gorg, Weiss et al. 2004). Following electrophoresis, proteins from the IPG strip are separated as individual spots on the polyacramide gel which are then visualized by gel staining using either silver stain or coomassie blue stain. Using software analysis (e.g. RegStatGel) the pattern of gel spots between samples (treatment sensitive and resistant) are studied for differential expression. A two-fold differential expression is taken as significant (Zhu, Rawe et al. 2008) and protein spots showing this change are then cut and digested into their peptide from for identification using MS.

1.13.1.2 Limitations of Gel based MS based Proteomic Methods:

In the past, global analyses of protein expression have usually been carried out using 2D-PAGE, a well-established but notoriously difficult analytical method. Though unrivalled in its ability to resolve thousands of individual proteins, 2D-PAGE demands considerable effort and skill for reproducibility. Even in the most experienced hands, the above technique encounters difficulties at identifying membrane-bound proteins the targets of several important drugs. Further, more than 15% of a cell's proteins with this technique may never be identified because of the proteins hydrophobicity. The 2D-PAGE technique also has limitations at detecting low abundance, or rarely expressed proteins, a group thought to carry out several critical functions in the cell. Therefore, other complementary proteomic techniques such as microarrays (forward or reverse phase) and/or gel free MS methods (iTRAQ, ICAT, SILAC and AQUA) are usually employed alongside 2D-PAGE/MS in order to achieve a more thorough interrogation of the cell proteome.

1.13.1.3 MS based-Gel Free Methods:

“Gel-free,” MS-based, proteomics techniques has emerged as the methods of choice for quantitatively comparing proteins levels among biological proteomes, since they are more sensitive and reproducible than 2D-PAGE-based methods (Haqqani, Kelly et al. 2008). Protein identification from these methods is based on high-throughput ‘*shotgun*’ analysis of peptides from a complex liquid mixture using high performance liquid chromatography (Chen and Yates 2007). Currently, the MS-based methods utilize mainly stable isotope labels (e.g., ICAT, iTRAQ) or “Label-free” methods to identify differentially expressed proteins in two or more samples.

However, despite its superiority over gel-based methods, limitations of the application of shotgun proteomics exist and include mainly issues of data analysis. Generally, a single multidimensional protein identification technology used to identify proteins with shotgun proteomics method generates $\geq 70,000$ spectra in a single experiment. For a complete quantitative profiling of proteins, multiple MS runs may be required. As a result, the rapid expansion of protein databases, searching this many spectra can pose an enormous computational load making real protein identifications versus the false discoveries a challenging and time consuming task (Wu and MacCoss 2002). Therefore, due the above limitations, a less complex but a high-throughput complimentary method such as microarrays that allows screening of multiple proteins in a single experiment in a short period of time remains an attractive and favoured approach in proteomic translational research. Hence, for this research project, considering the limitations of above mentioned proteomic approaches and researcher’s (TH) time constraints, a simpler proteomic approach such as antibody microarray was preferred over more complex and time consuming gel-based OR gel-free MS methods.

1.13.1.4 MS-free Approach: Forward Phase Antibody Microarray Technique

Microarrays provide a high-throughput proteomic method that allows screening of multiple proteins in the forward-phase approach. However, microarrays with antigen immobilised in a reverse-phase can screen only one protein at a given time. In the forward-phase approach, protein lysate is screened using multiple immobilised antibodies spotted onto a nitrocellulose coated microscope slide. This method is good to compare protein expressions of two samples (e.g. therapy sensitive vs therapy resistance) as it allows comparing differential protein expressions between the samples as fold changes (Smith, Watson et al. 2006). Following protein extraction and quantification, proteins from two samples are labelled with different fluorescent dyes. The treatment sensitive sample is labelled with Cy3 fluorescent dye and treatment-resistant sample with Cy5 dye. Labelled samples are then incubated with the nitrocellulose slide containing immobilized antibodies. There is a range of commercially available microarray kits available covering up to 700 antibodies per slide. Differential protein expressions are detected by studying the fluorescent signal intensity of the antigen-antibody binding complexes for each sample at the wavelength corresponding to dye label (Figure 11). Protein detection using the forward-phase microarray method can be used complementarily with the MS based approaches to enhance the credibility of discovered biomarkers.

THE FORWARD-PHASE ANTIBODY MICROARRAY WORKFLOW TECHNIQUE

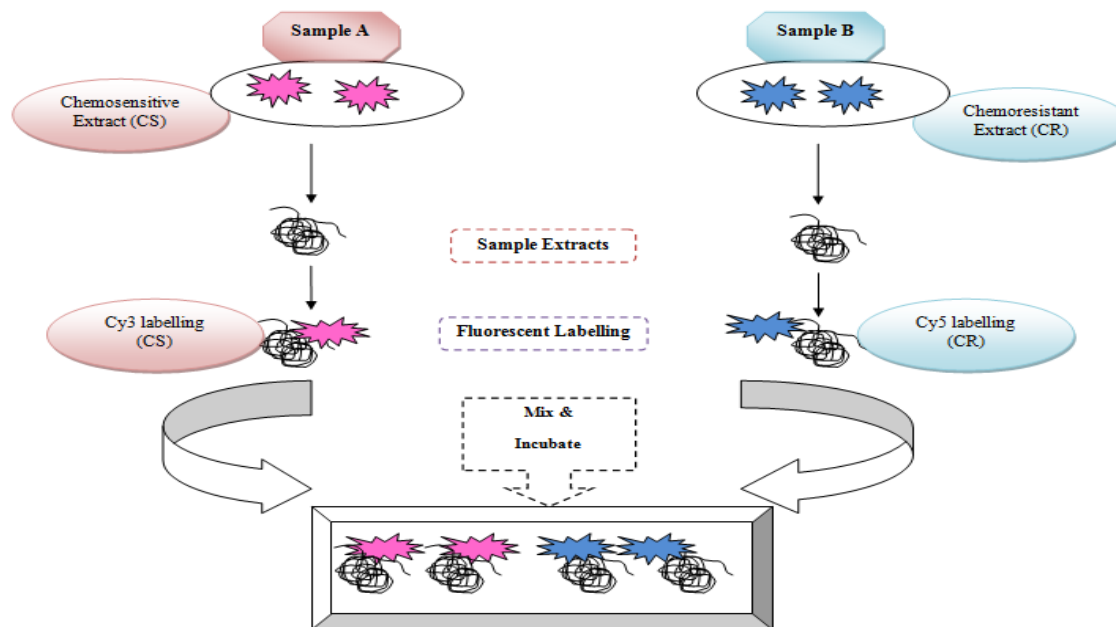


Figure 11: A graphical illustration of forward-phase antibody microarray technique. Each microarray kit contains a pre-coated antibody slide covering up to 700 antibodies. Sample A is a chemo-sensitive sample extract which is labelled with Cy3 fluorescent dye. Sample B is chemo-resistant extract which is labelled with Cy5 fluorescent dye. Both the samples are mixed and incubated with a nitrocellulose slide containing up to 700 immobilised antibodies. Differential expressions are analysed by studying the fluorescent signals of antigen-antibody complexes for each samples at the wavelength corresponding to the dye label.

1.14 Clinical Samples in Proteomic Cancer Research:

Cancer biomarker studies in the past heavily depended on cell line models for novel discoveries. However, more recently, different biological samples such as plasma, serum, urine, CSF, tumour interstitial fluid, circulating tumour cells, and fresh tumour samples have all been used in biomarker discovery research. Using cell lines models and clinical samples have their own advantages and disadvantages; however, clinical samples are more preferable over cell lines because of their ability to reflect the true tumour environment and attached clinical and pathological data with them. However, despite this advantage, a more routine use of clinical samples in cancer biomarker studies remain largely restricted due to the issues of tissue heterogeneity and a lack of guidance on standardized methods for sample collection, transfer and storage (Dihazi and Muller 2007; Ericsson and Nister 2011).

1.14.1.1 Tumour Samples Proteomics:

Translational studies have used different clinical samples with various '*omic*' platforms to study therapy responses (Hodgkinson et al. 2012), classify tumours and to investigate tumour biology (Zepeda-Castilla, Recinos-Money et al. 2008). Biomarker studies of the early years used formalin fixed paraffin embedded (FFPE) tissues with gene expression profiling for making novel discoveries. Since then, using smaller amount of protein with high resolution MS, global analysis of clinical samples with proteomic methods has been achieved (Zepeda-Castilla, Recinos-Money et al. 2008). More recently proteomic studies have used tumour samples with MS to monitor and assess responses to cytotoxic therapies (Bauer 2010). Our research group have recently published a pilot study using post-treatment resected fresh breast tumour samples for the first time with proteomics (antibody microarray and 2D-PAGE-MALDI/TOF/TOF) to

discover biomarkers of anthracycline-taxane breast chemotherapy resistance (Hodgkinson et al. 2012). Clinical tissues commonly employed for biomarker research include both fresh and frozen-formalin fixed samples and are by nature complex and heterogeneous. Therefore, utilising them for biomarker discovery studies involves overcoming the obstacles of tissue heterogeneity. In order to recapitulate the *in-vivo* molecular interactions that drive disease at the micro-environment level, analysis of sub-populations of cells from the heterogeneous microecology is required. However, a selective seclusion and utilisation of tumour cells from a heterogeneous tumour environment can be a challenge. Laser Capture Micro-Dissection (LCM) is one technique that isolates histologically pure cancer cells using laser-assisted micro-dissection from complex heterogeneous tissues and micro-environments (Braakman, Luiders et al. ; Braakman 2011). Since its advent, genomic and proteomic biomarker studies have witnessed an important step forward. Using comparative proteomics (2D-PAGE/MS and LC-MS/MS) with LCM on isolated breast cancer cells, proteins of breast cancer metastasis and prognosis have been identified (Braakman, Luiders et al. ; Braakman 2011). However, protein yield from cancer cells using the LCM technique can be usually low. Further, staining methods used in the identification of cancer cells with LCM, can pose hindrance with the downstream analysis proteomic technique employed. Therefore, for the above reasons, LCM method for isolation of breast tumour cells was not considered for this project. A brief overview of the benefits and limitations using different tissue for proteomic biomarker discovery are shown in the Table 6.

Table 6:**Limitations and Benefits of using tissue samples for biomarker discovery**

<i>Clinical Tissue</i>	<i>Benefits</i>	<i>Limitations</i>
Fresh tissue; biopsy samples	Pre-treatment sample High tumour percentage Good sample quality May be helpful for predictive biomarker discovery	Requires ethic approval Requires patient consent Optimization of techniques of protein extraction and quantification Sample size variations
Formalin fixed paraffin embedded tissues (FFPE)	Multiple FFPE cores can be assembled in a single block and used in tissue microarrays- MS analysis to collate large information for further proteomic analysis Helpful for predictive biomarker discoveries	Issues of protein solubilisation Optimization of techniques of protein extraction Protein modifications from formaldehyde fixation limiting antigen detection Ethical and consent issues
Fresh tissue; resected samples	Helpful in assessing therapy responses Provides markers of therapy monitoring Provides prognostic markers of disease	Tissue heterogeneity Variable sample quality and amount Optimization of techniques of protein extraction and identification Background variations with structural proteins

1.15 PROJECT AIMS & OBJECTIVES:

The primary aim of this research project is to expand the list of identified putative biomarkers of neo-adjuvant chemotherapy resistance in luminal (ER+) breast cancers using further fresh tumour samples and an antibody microarray proteomic approach. Selected proteins from the panel will be taken forward for pilot clinical validations using a pre-treatment archival samples series to confirm their clinical relevance. Further, this project also aims to optimise a new antibody microarray protocol which will enable the use low sample volumes ($\leq 1\text{ml}$) for future microarray based proteomic work.

The secondary aim of my project is to undertake immuno-validations of the breast neoadjuvant chemotherapy resistance DEPs discovered by Dr. Victoria Hodgkinson (PhD) using comparative (AbMA and 2D-PAGE-MS/TOF) proteomics in a larger archival series (Hodgkinson 2012). Further, utilising a few clinical samples excluded from the current study, protein extraction and quantification methods using smaller tissue volumes will be optimised for the future proteomic work involving core biopsy samples.

CHAPTER II

MATERIALS AND METHODS

Chapter 2.

2.1 INTRODUCTION:

The majority of thesis will focus on application of the antibody microarray proteomic technique with fresh tumour samples for the analysis of resistance of breast tumours to anthracycline-taxane chemotherapy. Further, principles and details of the antibody microarray technique with *full/standard, half-labelling and modified half-labelling protocols* including description of *Ingenuity Pathway Analysis* for data mining will be discussed in detail. Also, protein confirmations and clinical validations using immunoblotting and immunohistochemistry techniques will be outlined and discussed in detail.

All chemicals used in the research study were of the highest quality and purchased from *Sigma-Aldrich* unless otherwise stated. The contamination of samples for proteomic analyses was minimized by wearing a lab coat, nitrile gloves and a visor where appropriate. Furthermore, preparation of clinical samples for experiments was carried out under strict aseptic conditions.

2.2 STUDY DESIGN:

The pilot breast cancer research study originally approved by the South Humber Local Research Ethics Committee (ref 07/Q1105/43) in 2007 was conducted in two stages by two independent researchers Dr. Victoria Hodgkinson (VH) (PhD) and Dr. Tasadooq Hussain (TH) (MD student and author of this thesis). For the initial part of the study, VH collected a total of n=38 post-treatment fresh tumour samples and analysed n=8 samples in four pairs using a comparative proteomic approach (Antibody Microarray and 2D-PAGE/MS experiments) to identify predictive putative biomarkers of anthracycline-taxane neoadjuvant resistance (Hodgkinson et

al.2012). In the second stage of the project, a further fresh set of n=6 samples in three pairs were analysed by TH using a newly optimised '*Half-labelling Antibody Microarray Protocol*'. An outline of the study design is depicted in Figure 12. Initially, patients who matched the requirements of the study were identified by the clinicians in the Breast Unit at Castle Hill Hospital. They were informed of the research study, and if patients wished to participate they were provided with an information sheet and a signed record of consent was taken. This may have been towards the end of the chemotherapy treatment, prior to surgery. During surgical resection of the residual tumour, breast surgeons took a small sample of macroscopic tumour, which was immediately stabilised by snap-freezing in liquid nitrogen. Tumour samples provided by the surgeon varied in size from 2 mm³ to 2 cm³. Tumour samples were then stored at minus 80° C until required. After allowing time for histopathological tests and reports to be completed, patient notes were accessed by a clinician involved in the study, and relevant data was recorded. This included details regarding the type of tumour, the molecular subtype of the tumour, the chemotherapy administered tumour sizes pre- and post-treatment from DCE-MRI and US scans, as well as the pathology reports from both the core biopsy specimen taken upon diagnosis and the tumour resection.

A FLOWCHART OF THE STUDY DESIGN

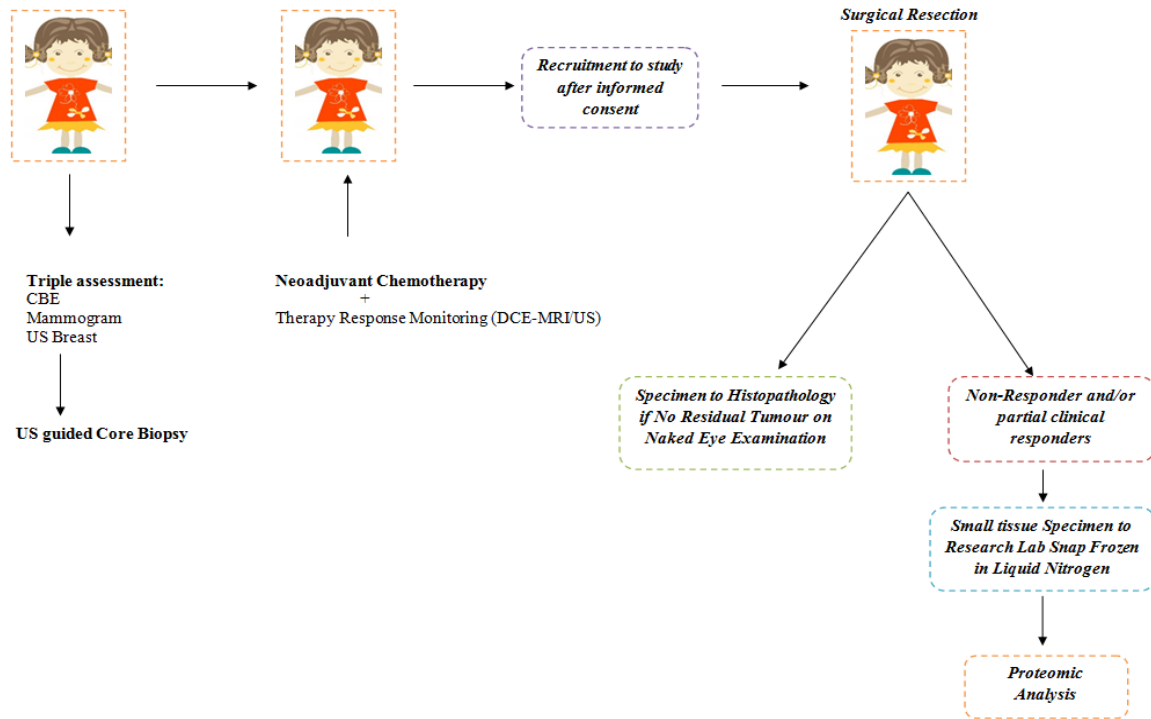


Figure 12: The flow chart depicts different stages patient journey from the time of initial clinic presentation with breast lump to the point of surgical resection. Patient recruitment for this study took place after completing the NACT and before surgical resection. Only samples from tumours that were non-responders and/or deemed to have a partial clinical response were collected and used for proteomic analysis.

2.3 SAMPLE COLLECTION AND PATIENT SELECTION:

The study included patients receiving neoadjuvant chemotherapy for locally advanced breast cancer at Hull and East Riding Hospitals NHS Trust, Hull from 2007 to 2011 (5 years). Both VH and TH were jointly involved in the sample collection and storage process. A total of 50 post-treatment fresh breast tumour samples were collected as per the ethical approval. The clinico-pathological details of all n=50 samples and the determined therapy responses for each tumour

are outlined in the Appendix 1 of the thesis. Of the n=50 total samples collected for both studies, a total of n=38 tumour samples were collected initially by Victoria Hodgkinson (VH) during her PhD study period (2008-2010). Of the 38 samples, four samples were excluded from the VH study and used for preliminary optimisations. The remaining 34 samples were pooled and carried forward for the proteomic analysis. Of the available n=38 samples, only n=8 samples were initially used by VH for the combined antibody microarray and 2D-PAGE/MS analysis grouping them into 4 pairs of chemosensitive and chemoresistant. A consort chart as shown in the Figure 13 outlines how clinical samples were collected (n=38), pooled and used for pilot proteomic analysis (n=8) and optimisation experiments (n=4) in the VH project.

A further n= 12 samples were collected by TH between May to July 2011 to bring the final number to n=50 before stopping the sample collection. This last set of samples (n=12) were not included in the initial VH pilot study and kept frozen at – 80 degrees centigrade for a later use. The clinical data for these 12 samples was completed by TH in January 2012. The second consort chart shown in Figure 14 outlines the final number of samples collected (n=50), the number of samples that were available for proteomic analysis in both the studies (n=26) and the total number of samples that were excluded from both the studies (n=24).

The third consort chart as shown in the Figure 15 outlines the samples that were used (n=6) in this project for further four antibody microarray experiments and the sample pair that was used for western blot analysis. All 6 tumour samples selected for this study and the VH pilot study were all ductal ER+ clinical variant of intrinsic Luminal A molecular subtype. This molecular subtype was selected for proteomic analysis due to its poor sensitivity to anthracycline-taxane neoadjuvant chemotherapy (sections 1.8.1, 1.8.2 and 1.8.3).

2.3.1 Response Evaluation From Clinical Samples:

For the project samples, therapy responses were determined using RECIST criteria (section 1.5.1.3) with the help of an Oncologist (Dr. Vijay Agarwal) and samples were paired according to therapy regimens, therapy responses and tissue availabilities. Responses were categorised into chemosensitive (Responders) and chemoresistant (Non-responders). Tumours were classed as chemosensitive (Responders) if following neoadjuvant chemotherapy a $\geq 30\%$ reduction in the tumour size was noted at the final histology from the baseline measurements at the pre-treatment breast MR and/or if no residual tumour was found at the final resection histology. Tumours that progressed following neoadjuvant treatment ($\geq 20\%$ increase in tumour size from baseline breast-MR measurement) and/or showed no change in the tumour size from the baseline (stable disease) were termed as chemoresistant (Non-responders). The above method, to assess tumour responses comparing the pre-treatment MR tumour measurement to the final histology residual tumour size and not the post-treatment MR tumour measurement was a novel approach undertaken for the first time with the VH samples (Hodgkinson et al. 2012). Assessing therapy response this way, eliminated any bias at accurate estimation of a therapy response that could occur as a result of tumour fragmentation following taxane therapy on the post-treatment MR (Denis, Desbiez-Bourcier et al. 2004). To maintain uniformity between the two studies (VH and TH), the same therapy assessment strategy and cut-off criteria as described above by our research group were used for the response evaluation of tumour samples analysed in this project.

All patients in the study received neo-adjuvant chemotherapy regimen consisting of 4 cycles of EC [epirubicin (90 mg/m²) + cyclophosphamide (600 mg/m²)] and 4 cycles of docetaxel (100 mg/m²), given at 3-weekly intervals in the order of EC followed by Docetaxel. Following the treatment, depending on the patient response, either resection of residual tumour or mastectomy

was carried out. The consort chart in Figure 15 and Table 7 outlines all the 6 clinical samples used for the antibody microarray analysis in this project. The clinical data of analysed samples (8 from VH work; 5 from this study) with their neoadjuvant therapy responses is listed in Table 8 and 9 with the full list of all 50 patients listed in the Appendix 1 of this thesis.

Table 7: Samples Selected for the Antibody Microarray Analysis

<i>Sample Pairs</i>	<i>Clinical Response</i>	
	Chemosensitive	Chemoresistant
Pair 1	#16B	#1B
Pair 2	#38	#15B
Pair 3	#12B	#1

2.3.2 Sample Collection at Surgery:

At the time of surgery, patients were approached for the sample donation and an informed consent was obtained from the willing donors. Samples were taken by the operating surgeon (usually a breast consultant) and collected in a micro-centrifuge tube to be snap frozen in liquid nitrogen and stored at minus 80°C until required. The pieces of solid tumour provided ranged between 1 to 3 and the size between 2 mm³ to > 2 cm³ and the number of pieces of solid tumour provided (in separate microcentrifuge tubes) by the surgeon ranged from 1 to 3.

At the time of consent, patients were asked for the permission to access their case notes for relevant clinical information which included chemotherapy details, radiological and pathological results and reports for determination of response and molecular typing (ER/PR/HER2 status).

AN OUTLINE OF SAMPLE COLLECTION AND UTILISATION FROM VH-PILOT PROJECT

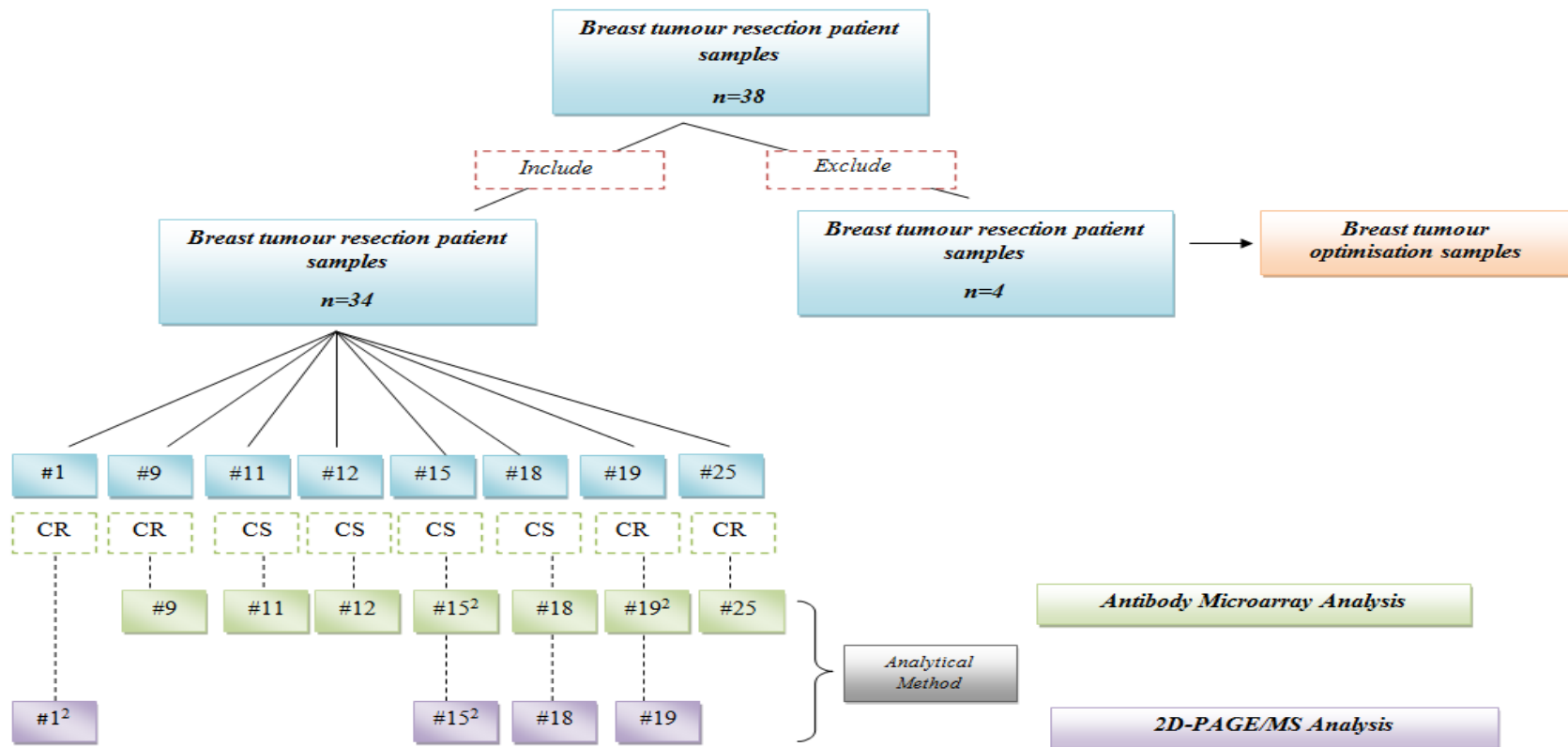


Figure 13: The consort chart outlines the project breast sample collection and utilisation for the VH pilot project. A total of 38 samples were collected initially of which 34 were taken for proteomic analysis and 4 for initial optimisation work. Of the 34 samples, 8 samples were paired and analysed using combined antibody microarray (green colour) and 2D-PAGE/MS approaches (purple colour). For samples which were included in more than one experiment (²) is shown.

FLOW CHART OUTLINING THE SAMPLE COLLECTION, UTILISATIONS & EXCLUSIONS

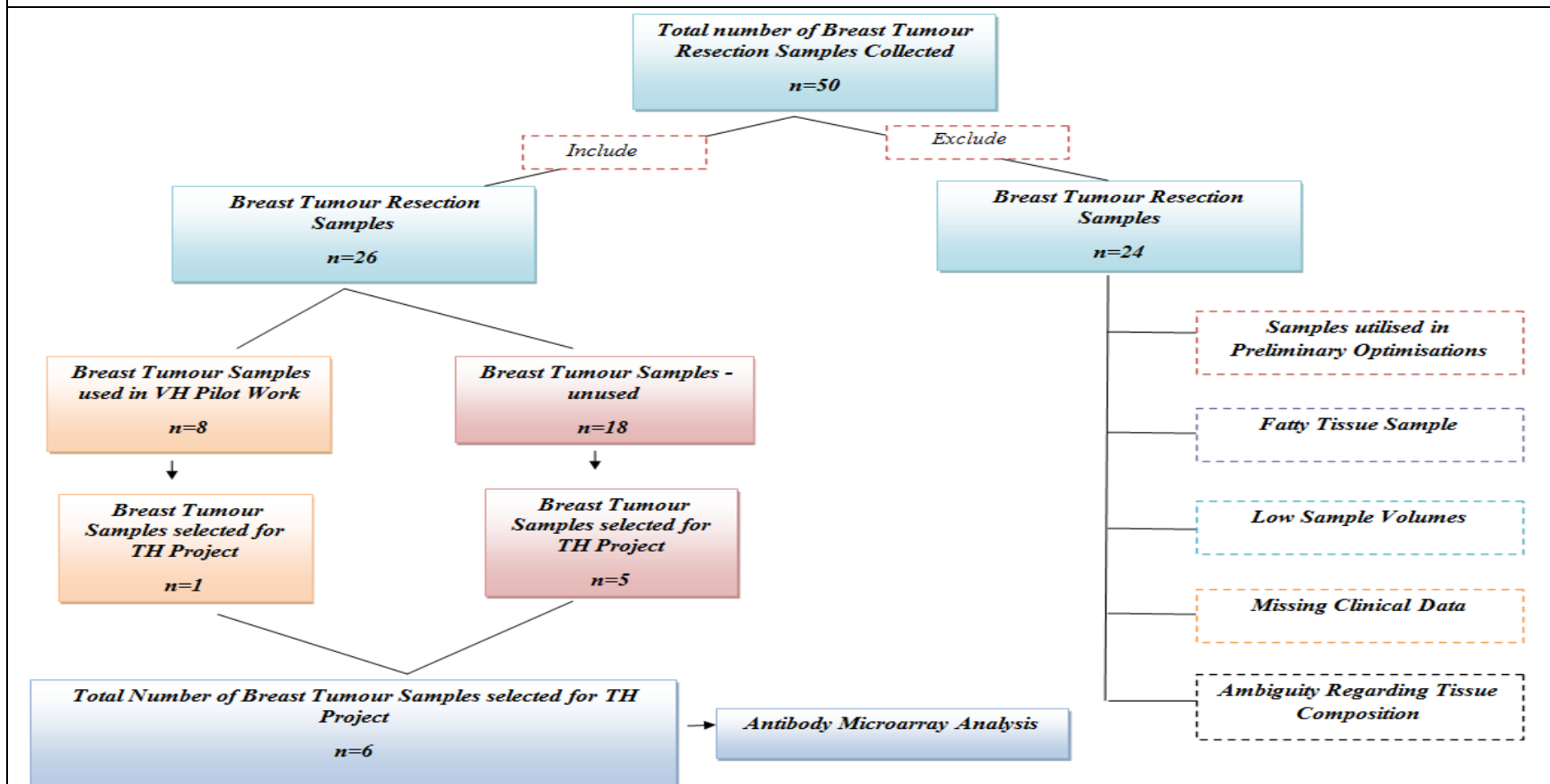


Figure 14: The consort chart outlines the utilisation of n=50 samples collected for the breast cancer project. From the 50 samples collected, only 26 were taken forward for proteomic analysis and the rest were excluded for the reasons outlined above. For the current project, 6 samples were selected from the pool of 26 available and used for the antibody microarray experiments. Of the 6 samples used, 1/6 sample was selected from the VH 8 sample cohort and the rest (n=5) were all unutilised samples.

AN OUTLINE OF CURRENT RESEARCH PROJECT & METHODS

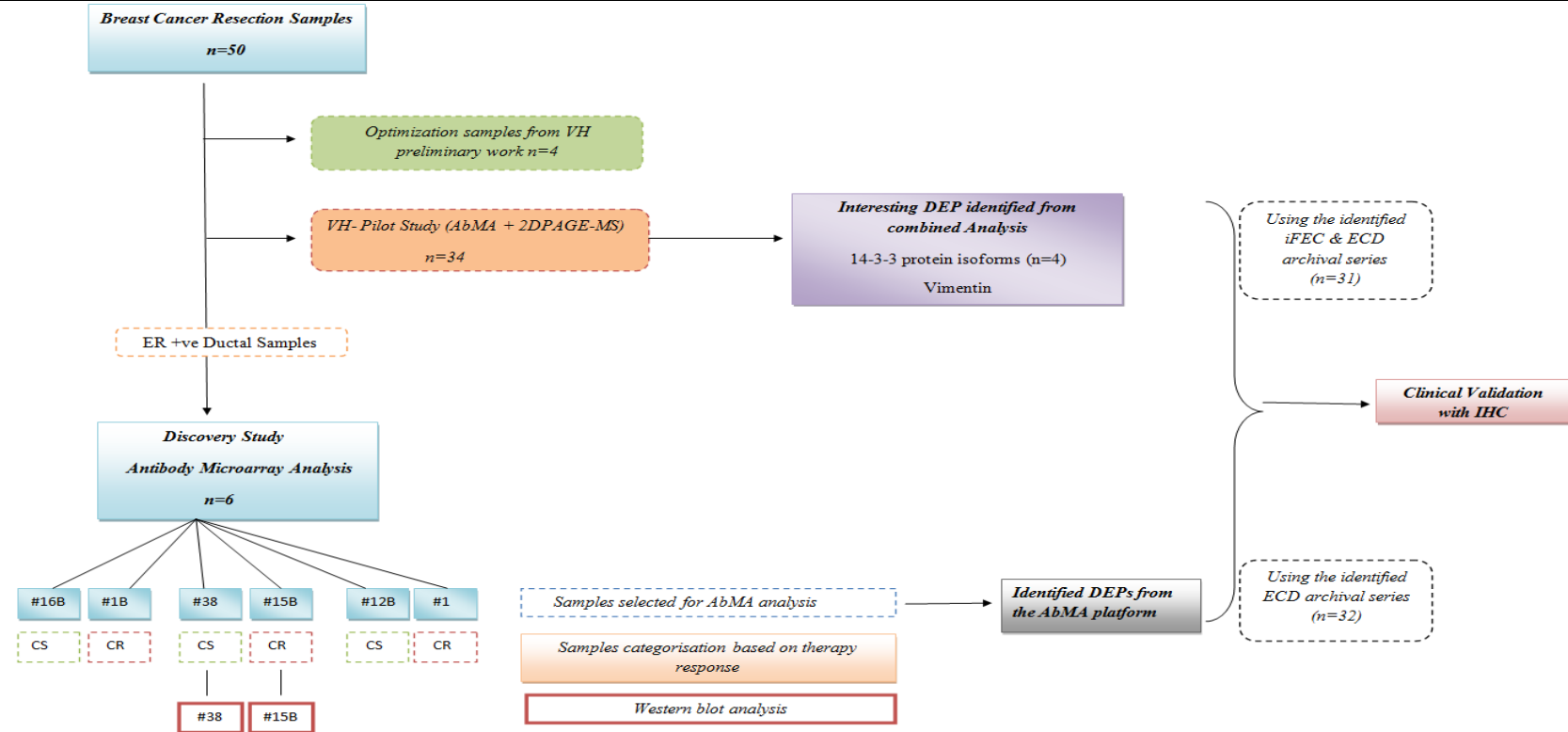


Figure 15: The consort chart outlines the current research project. From the total of 50 breast samples collected, 26 samples were eligible for proteomic analysis. VH pilot study used 8/26 samples. For this study, 6 samples in 3 pairs (light blue colour) were selected and used for the antibody microarray experiments. Samples were paired as chemosensitive (CS) or chemoresistant (CR) based on using RECIST criteria (light orange colour). All 6 samples were ER+ (luminal) ductal sub-type. Only one pair (#38^{CS} vs. #15B^{CR}; red colour) out of three was successfully confirmed on western blot. In the second part of the project, 14-3-3 isoforms identified in VH pilot study and the new DEPs identified in the current study were selected for immuno validations using two archival iFEC & ECD pre-treatment core biopsy sample series.

CLINICAL AND THERAPY RESPONSE DATA OF SAMPLES USED IN THE CURRENT PROJECT

Sample Number	Histology	Receptor Status	Chemotherapy Regimen	Therapy Response
#16B	Ductal	ER + and PR, HER2 -	EC x 4; D x 1	CS
#1B	Ductal	ER + and PR, HER2 -	EC x 4; D x 2	CR
#38	Ductal	ER, PR + and HER2-	EC x 4; D x 4	CS
#15B	Ductal	ER, PR + and HER2 -	EC x 4; D x 4	CR
#12B	Ductal	ER, PR + and HER2-	EC x 4; D x 4	CS
#1	Ductal	ER+ and PR, HER2 -	EC x 4; D x 4	CR

Table 8: Table listing clinical tumour samples (n=6), showing the breast carcinoma types, the receptor status (ER/PR/HER2), and therapy administered, represented by EC: epirubicin + cyclophosphamide, D: docetaxel with the number of cycles. Response was classified as chemo-sensitive (CS) or chemo-resistant (CR) based on RECEIST criteria if the tumour regressed by $\geq 30\%$ from the baseline or showed no response and/or increased by $\geq 20\%$ from the baseline at pre-treatment MRI

CLINICAL AND THERAPY RESPONSE DATA OF SAMPLES USED IN VH-PILOT SERIES

Sample Number	Histology	Receptor Status	Chemotherapy Regimen	Therapy Response
#9	Ductal	ER, PR and HER2 +	EC x 4	CR
#11	Ductal	ER, PR+ and HER2 -	EC x 4; D x 4	CS
#12	Ductal	ER, PR + and HER2-	EC x 4; D x 2*	CS
#15	Ductal	ER, PR + and HER2 -	EC x 4; D x 4	CS
#18	Ductal	ER, PR + and HER2-	EC x 4; D x 2	CS
#1	Ductal	ER+ and PR, HER2 -	EC x 4; D x 4	CR
#19	Ductal	ER+, PR and HER2-	EC x 2	CR
#25	Ductal	ER,PR and HER2+	EC x 4; D x 4*	CR

Table 9: Table listing clinical tumour samples (n=8), showing the breast carcinoma types, the receptor status (ER/PR/HER2) and therapy administered, represented by EC: epirubicin + cyclophosphamide, D: docetaxel with the number of cycles. Reduced doses are indicated* (also see Appendix A) Response was classified as chemo-sensitive (CS) or chemo-resistant (CR) based on RECEIST criteria if the tumour regressed by $\geq 30\%$ from the baseline or showed no response and/or increased by $\geq 20\%$ from the baseline at pre-treatment MRI

2.3.3 Archival Series Pre-treatment Core Biopsy Patient Selection:

2.3.3.1 : MRI-iFEC Archival Series:

The clinical validations of 14-3-3 protein isoforms and Vimentin protein from VH pilot work was carried out using a pre-treatment core biopsy archival series (n=35) previously identified and characterised (Garimella et al. 2007) and a small pre-treatment core biopsy samples series (n=32) collected from the patients selected for this study.

Ethical approval had previously been granted for the archival series entitled '*monitoring the effects of chemotherapy in breast cancer patients using magnetic resonance imaging and molecular markers*' from the Hull and East Riding Research Ethics Committee (ref 03/00/038).

All patients in this cohort were recruited between 2000 and 2002 from the Hull and East Riding NHS trust, and had histologically-proven breast cancer with a primary tumour of ≥ 3 cm. In total, 35 archival tissue samples were obtained from 36 locally advanced breast cancers (one patient had bilateral breast cancer). These comprised 75% ER-positive tumours and 69% PR-positive tumours. Patient consent was obtained to allow access to pre-treatment core biopsy samples and to perform serial DCE-MRI scans (pre-treatment, after 2nd cycle of chemotherapy, and post-treatment) so that tumour response to therapy could be monitored. Patients were treated with 6 cycles of 5-fluorouracil (200 mg/m²), epirubicin (60 mg/m²) and cyclophosphamide (600 mg/m²) (infusional FEC), administered at 3-weekly intervals. Tumour response was assessed after the 2nd cycle using DCE-MRI scans. Patients who showed a response continued with the full course of treatment, and where no response was observed, chemotherapy was terminated. Following this, definitive surgery was performed to remove residual tumour.

In order to avoid any confusion and a mix up with the other series used in the validation work, this series will be referred as '*MRI-iFEC*' series.

2.3.3.2 EC-D Archival Series:

The second series used for clinical validations included pre-treatment core biopsies of patients recruited (n=50) for this study and the VH study. All the patients in this series were treated with Epirubicin, Cyclophosphamide and Docetaxel in the doses and regimens as described in the section 2.3.1. Therefore, this series was referred as the '*EC-D*' series. For this series, the tumour response was assessed on pre-treatment DCE-MRI scans and final histology using RECIST criteria described in the section 1.5.1.3. Patient clinical data was collected from hospital computer records and patient notes by the author of this thesis (TH) and Miss Dalia ElFadl (previous breast research fellow). Therapy responses were assessed by Dr. Vijay Agarwal (Oncologist). Patients who showed a response at the 2nd DCE-MRI scan on treatment continued with the full course of treatment, and where no response was observed, chemotherapy was terminated and definitive surgery was performed to remove residual tumour. The clinico-pathological status of tumour samples collected for the study are summarised in the Table 10.

EC-D SERIES SAMPLE CLINICO-PATHOLOGICAL STATUS

Receptor Status	Numbers (n=50)	Percentage
ER+	37/50	74%
PR+	13/50	26%
Histology		
Ductal	42/50	84%
Lobular	8/50	16%
Response Data		
CR	19/50	38%
CS	28/50	56%
SD	1/50	2%
PD	2/50	4%

Table 10: The clinico-pathological characteristics of tumour samples collected for the study showed the majority of tumours were ER+ (74%) ductal (84%) type. The therapy response data as determined using the RECIST criteria showed majority of the tumours were CS (56%) and 38% of tumours showed chemoresistance to anthracycline-taxane therapy.

CR=Chemoresistant CS=Chemosensitive PD=Progressive disease SD= Stable disease

2.4 SAMPLE PREPARATION FOR MICROARRAY ANALYSIS:

2.4.1 Introduction:

Sample preparation in proteomics is an important step, as complimentary proteomic studies have discovered this process to be end-application specific and size dependant (Gromov, Celis et al. 2008). Tissue preparation for proteomic studies is carried out in a two step process, tissue breaking down and homogenisation. The process of tissue homogenisation is an important step and has to be carried out in correct lysis buffer for subsequent protein extraction. Although, surgical excision provides large tissue samples allowing classical tissue homogenisation with mechanical methods (tissue ruptor, sonicator, grinding in liquid nitrogen and cryostat sectioning), optimal methods of homogenisation and protein extraction with smaller tissue samples (e.g. core biopsy) are yet to be fully established (Gromov, Celis et al. 2008). Furthermore, preparation of lysis buffer for tissue suspension is decided based on the end-application (array or 2D-PAGE/MS) due to reagent compatibilities as no single ideal solubilisation buffer exists for all proteomic applications (Gorg, Weiss et al. 2004; Weiss and Gorg 2008).

2.5 Protein Extraction Methodology:

The technique of protein extraction with mechanical homogenisation using breast tumour samples was earlier optimised by VH (for the pilot work). Findings from VH experimental preliminary optimisation studies showed a poor correlation between tumour size (by eye), or mass (g) and protein yield (mg/ml). This was mostly due to a high amount of tissue heterogeneity between tumour samples (Hodgkinson, D et al. 2012). Therefore, all the breast tumour samples used in

this project even though appeared approximately the same size by naked eye examination were weighed before suspending into the lysis buffer.

The breast tumour samples used in this project were first resuspended in antibody microarray extraction/labelling buffer (Sigma-Aldrich) and mechanically homogenised using a hand held tissue ruptor. Polypropylene microcentrifuge tubes were used in the tissue extraction to prevent any retention of protein/peptide on the glass surface. Initially, a 10 ml of antibody extraction solution was prepared by adding 100 μ l of Phosphatase Inhibitor Cocktail, 50 μ l of Protease Inhibitor Cocktail and 1.2 μ l of Benzonase Working Solution. This solution was called as Buffer 'A' and kept on ice until required. The addition of Protease and Phosphatase inhibitors helps maintain the protein composition by inhibiting their breakdown in the sample; benzonase removes nucleic acid present in the sample. The next few steps from this stage were carried out in a Class II Tissue Culture Hood, using a sterile technique. Breast tumour sample was removed from -80° C freezer and weighed after defrosting. To avoid protein degradation sample was kept on ice when not handled. Individual tumour samples were transferred in a sterile Petri dish on ice and cut into pieces using a sterile scalpel knife and washed with cold PBS solution to remove any residual blood clots adhered to the tumour tissue. Four times w/v of Buffer A was then added to the tissue in a universal tube and the tissue was mechanically homogenised on ice using a hand-held homogeniser called Tissue Ruptor (#9001273, Qiagen)

The hand-held homogeniser has been used commonly for homogenising plant and animal tissues (Burden Sept 2008). It consists of an outer stationary tube (stator) and an inner turning shaft (rotor) connected to a motor. The working action involves applying tangential shearing force the tissues when the shaft is running at 10,000-20,000 rpm. To avoid cross-contamination between the samples, we used a disposable shaft (#990890, Qiagen) between each experiment. Each

sample was homogenised individually three times, conducting each homogenising action strictly for 30 s with a 30 s rest in between. Resting the samples prevented protein denaturisation from the heat generated by the Tissue Ruptor at high speeds. After homogenisation, samples were centrifuged for 10 s at 10,000 x *g* in a microcentrifuge tube to remove any fat contained in the sample (Figure 16).

SAMPLE PREPARATION AND PROTEIN EXTRACTION METHOD






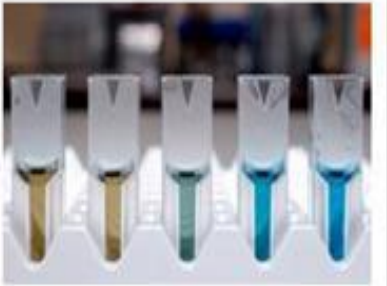
		
<p>Tissue was weighed to determine the amount of Buffer A required</p>	<p>Tissue was dissected into small pieces and washed in ice-cold PBS</p>	<p>Tissue was transferred into 4 volumes (w/v) of Buffer A and homogenised on ice using a TissueRuptor (Qiagen)</p>
		
<p>Tissue sample was centrifuged at 10 000 x g in a microcentrifuge tube. The supernatant was retained and the fat layer was discarded</p>	<p>Centrifugation was repeated to clarify the sample, until no further fat could be removed</p>	<p>The protein concentration of the sample was determined using the Bradford Assay (#B6916, Sigma Aldrich). The sample was then diluted to 1 mg/ml</p>

Figure 16: Sample preparation and protein extraction from clinical tissue samples for antibody microarray analysis. The steps involved in the extraction of protein for clinical samples include weighing the tissue first followed by tissue slicing Buffer A suspension. The samples are then mechanically homogenised individually and centrifuged repeatedly to obtain a clear supernatant which is then used in the Bradford Assay for protein quantification.

2.5.1 Mechanical Homogenisation for Small Sample Volumes:

Tissue Ruptor can be used for homogenising samples varying in sizes from less than 1 ml up to 40 L. However, this method may not be ideal for smaller tissue samples (e.g. core biopsy sample). This is due to an increased risk of protein denaturation and tissue entrapment reported from an earlier study (Burden Sept 2008). Therefore, for smaller tissue volume alternative methods of homogenisation are recommended to avoid excessive tissue loss and protein breakdown. These methods includes: Cryo-Grinding, Vortex-Bead Beating and Sonication methods (Burden Sept 2008). Of the above three methods, we employed Sonication for homogenisation of smaller size breast tumour sections for the pilot protein extraction and quantification optimisation experiments using low tissue volumes.

The initial sample processing for the Sonicator method was carried out similar to the Tissue Ruptor method as described in the section 2.5 A Water-Bath Sonicator (Scientific Laboratories, serial #030172) was used for the homogenisation. Firstly, tumour samples were suspended in micro centrifuges with four times w/v of Buffer A; micro centrifuges where then suspended in a Water-Bath Sonicator (Scientific Laboratories, serial #030172) and sonicated for a total of 5 min for 3 times. In between each sonication process, samples were rested for 5 min on ice to avoid protein denaturation from the heat generated. Finally, samples were centrifuged for 10 s at 10,000 x g in a microcentrifuge tube in order to remove any fat contained in the sample which collects as a supernatant layer at the top of the micro centrifuge. This layer is carefully pipetted out and the solution containing the tissue lysate is transferred into a fresh microcentrifuge tube. The samples are then placed on an end-over-end rotator set at a slow speed in a cold room at 4° C for overnight or at least 16 hours. At the end of the mixing period, samples are centrifuged at 13,000 x g for 5 min keeping them in the cold room. Samples after this point are ready for the

protein quantification using one of the four spectroscopic protein assay method (e.g. Bradford assay). For our samples, protein quantification was carried out using Bradford Protein Quantification Assay as it is compatible with the reagents used in antibody microarray analysis.

2.6 BRADFORD PROTEIN QUANTIFICATION METHOD:

The Bradford protein assay is a spectroscopic analytical procedure used to measure the concentration of protein in a solution. The Bradford Reagent (Kit #128K4340, Sigma Aldrich) consists of Brilliant Blue G dye in phosphoric acid and methanol (Table 11). The dye exists in three forms: cationic (red), neutral (green), and anionic (blue) under acidic conditions, the dye is predominantly in the doubly protonated red cationic form ($A_{\text{max}} = 470 \text{ nm}$). However, when the dye binds to protein, it is converted to a stable unprotonated blue form ($A_{\text{max}} = 595 \text{ nm}$) which is then detected at 595 nm in the assay using a spectrophotometer or microplate reader (Sedmak and Grossberg 1977). This shift in the absorbance spectrum ($A_{\text{max}} = 470 \text{ nm}$ to 595 nm) occurs as a result of dye-protein complex and is therefore proportional to the amount of protein present in the sample. The colour development in Bradford assay is associated with the presence of certain basic amino acids (primarily arginine, lysine and histidine) in the protein. Van der Waals forces and hydrophobic interactions also participate in the binding of the dye to the protein. The number of Coomassie dye ligands bound to each protein molecule is approximately proportional to the number of positive charges found on the protein. Free amino acids, peptides and low molecular weight proteins do not produce colour with coomassie dye reagents. In general, the mass of a peptide or protein must be at least 3000 daltons to be assayed with this reagent.

BRADFORD ASSAY COOMASSIE PLUS REAGENT CONTENTS

Bradford Assay Reagent Content List: (950ml)

Coomassie G-250 dye

Methanol

Phosphoric acid

Solubilising agents in water

Table 11: Bradford assay reagent consists of Brilliant blue G dye in phosphoric acid and methanol. In the acidic state the dye remain stable in red cationic form ($A_{\max} = 470 \text{ nm}$). However, when binded to protein in the sample, the dye convert to stable unprotonated blue anionic form ($A_{\max} = 595 \text{ nm}$). The colour development in the assay remains proportional to the amount of protein in the sample.

2.6.1 Determination of Protein Concentration:

The protein concentration of the tumour sample is determined by comparison to that of a series of protein standards known to reproducibly exhibit a linear absorbance profile in this assay. Although different protein standards can be used, the two most commonly employed protein standards are the Bovine Serum Albumin (BSA) and Bovine Serum Globulin (BSG). For this project quantification experiments, we chose Bovine Serum Albumin as our standard as it is the most widely used protein with a greater dye-protein colour developing property with majority of the commercially available assay reagents.

Eight BSA protein standards were prepared, ranging from concentrations of 0.1 to 1.4 mg/ml diluted in Buffer A in microcentrifuge tubes. A 5 μl volume of each standard concentration in

duplicates was placed in separate wells in a 96-well plate. Tissue extracts of unknown protein concentration at a similar volume of 5 μ l were also placed into separate wells in the 96-well in undiluted and diluted concentrations (e.g. 1:5, 1:10 and 1:20). Bradford Reagent was mixed gently and brought to the room temperature and 250 μ l was added to each protein standard and each sample concentration. The 96-well plate was then mixed for 30 s on the spectrophotometer (Multiscan MS plate reader, Labsystems) and incubated at room temperature for 5 min. Absorbance was subsequently measured at 595 nm.

2.6.2 Plotting BSA Standard Protein Curve:

The unknown protein concentration in the sample is determined by plotting a BSA protein standard curve against the absorbance at 595 nm (Figure 17). The protein concentration of the tissue extracts is then calculated using the equation of the line $y = mx + c$; protein concentration x is determined from the equation as $x = (y - c) / m$. The 'y' in the equation represents the protein concentrations values obtained at 595nm from the undiluted (neat) and diluted samples before any corrections for dilutions are applied. Figure 20 is an example of BSA standard curve at 595nm absorbance. The equation for the line of best fit is shown R^2 as a correlation between protein concentrations in the standards and absorbance at 595nm. A R^2 value of 1 or near 1 represents a strong correlation.

THE BSA PROTEIN STANDARD CURVE

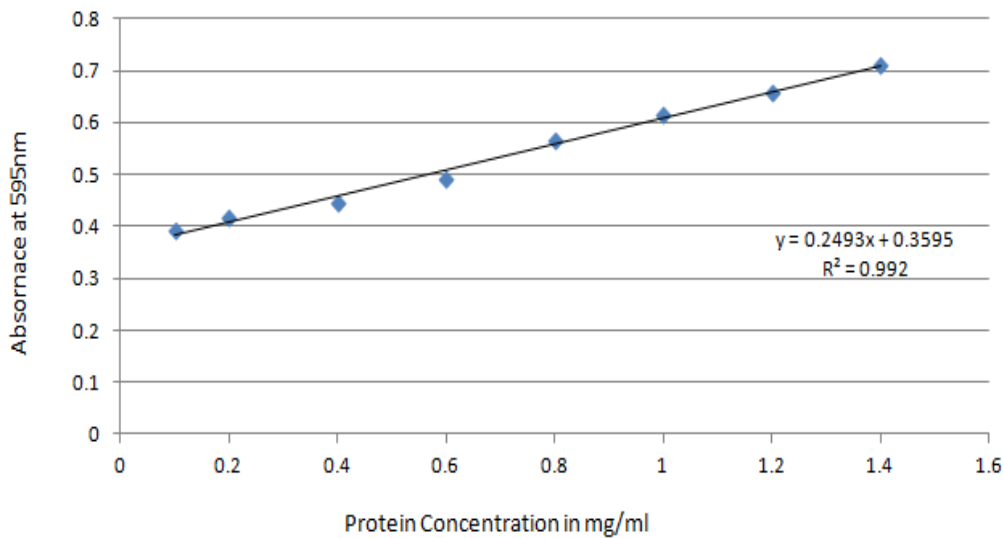


Figure 17: is an example of how protein standards curve for BSA at concentrations 0.1 to 1.4 mg/ml measured at 595nm absorbance looks like. The equation of the line $y=mx + c$ is represented in this example by $y = 0.2493x + 0.3595$, x in the equation represent the protein concentration to be determined and is calculated from the equation $x = (y - 0.3595) / 0.2493$ where y is the protein concentration value obtained from the neat sample and before correction for the dilution. R^2 from the equation represent correlation between protein concentrations in the standards and absorbance at 595nm. A R^2 value of 1 or near 1 represents a strong correlation which is an indirect indication that similar standard volumes were pipetted into each well.

2.7 ANTIBODY MICROARRAY:

2.7.1 Panorama[®] Antibody Microarray-XPRESS Profiler 725 Kit:

For this research project, the Panorama[®] Antibody Microarray-XPRESS Profiler 725 Kit (SIGMA-ALDRICH) was exploited in order to study the differential protein expression between chemosensitive and chemoresistance breast cancers. The Panorama[®] Antibody Microarray-XPRESS Profiler 725 contains 725 different antibodies each spotted in duplicate on a nitrocellulose-glass slide (Figure 18). These antibodies represent families of proteins known to be involved in a variety of different biological pathways (Cell signalling, Apoptosis, P53 family of proteins and Transcriptional factors). The Panorama[®] Antibody Microarray XPRESS Profiler kit has been previously exploited in many proteomic studies to assess differential protein expressions for various tumours (e.g. breast and colorectal) and cell line studies and has been found to be a useful proteomic method providing a large amount of high quality data for analysis (Celis, Moreira et al. 2005; Kopf, Shnitzer et al. 2005; Madoz-Gurpide, Canamero et al. 2007).

The differential protein expressions by this method are detected when proteins binds to their corresponding antibodies spotted on the slide. Each slide contains 725 antibodies spotted in 32 sub-arrays each containing duplicate spots of 23 antibodies, as well as duplicate positive control spots for Cy3 and Cy5 (monoclonal antibody that recognises Cy3 and Cy5), and 11 negative controls (Appendix 2). The differential protein expressions with Panorama[®] Antibody Microarray are analysed by labelling each sample (chemosensitive and resistant) with a different Cyanine Dye™ (Cy™ 3 or Cy5). Fluorescent signal intensity for each sample is then recorded individually at the wavelength corresponding to the dye label of the sample and compared. The fluorescence intensity detected on the array with each antibody depends on this binding affinity;

therefore, signal intensity comparison can be performed only within the same antigen/antibody system and not between different antibodies.

The Panorama[®] Antibody Microarray- XPRESS Profiler 725 is an accurate and robust protein expression profiling technique which is easy to learn and perform. Usually a single experiment can be completed within a day. Antibodies spotted on the slide are in high density to ensure strong signals. The proprietary treatment of the slide coating minimizes background staining, thereby, maximising the signal-to-noise ratio for accurate analysis (Kopf, Shnitzer et al. 2005).

THE PANORAMA XPRESS PROFILER 725-KIT

A



B

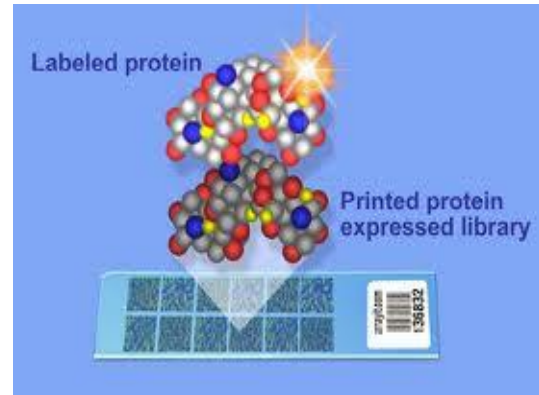


Figure 18: The picture A on the above shows an unscanned antibody microarray slide. Each slide comes with multiple printed spots each representing one antibody. On the Panorama XPRESS Profiler 725 array slide there are 725 printed antibody spots. The picture B on the right hand side shows a representation of the antibody microarray slide with printed protein library and labelled proteins together. The labelled protein samples are added to the slide and incubated before scanning.

2.8 ANTIBODY MICROARRAY EXPERIMENT PROTOCOL:

Following Bradford protein quantification, protein concentrations from the breast tumour samples were determined as described in the section 2.6.1. Only those samples that had protein concentrations $\geq 1\text{mg/ml}$ were selected for antibody microarray analysis. This was keeping in line with the SIGMA recommendations of using the Panorama[®] Antibody Microarray-XPRESS Profiler-725 kit with a minimum protein concentration of 1mg/ml for array analyses.

For all the six samples used in the project, the protein concentrations were determined and found to be $\geq 1\text{mg/ml}$ required protein concentration for microarray analysis. Therefore, all 6 samples were eligible for the microarray analysis. Individual sample concentrations found at the Bradford Protein Assay from our research samples will be discussed in the detail in the results chapter of the thesis.

The antibody microarray experiment protocol will be discussed under 4 main headings:

1. Sample Dilution and Protein Labelling
2. Determination of dye/protein molar ratio
3. Microarray slide incubation
4. Slide scanning and Data analysis

2.8.1 Sample Dilution and Protein Labelling:

In the standard microarray protocol, sample dilution with Buffer A is carried out to bring the final volume to an ml at 1mg/ml sample concentration. Protein labelling using the above dilution is termed as '*Full-Labelling Microarray Protocol*'. A second protocol using 0.5 ml of final sample volume at 1mg/ml protein concentration termed as '*Half-Labelling Microarray Protocol*' has been optimised in this research project for the first time. The optimisation details of the

'Half-Labeling Microarray Protocol' will be discussed in the subsequent sections of this chapter. With the optimisation of the new protocol, researcher will now be able to use low sample volumes (0.5 ml) at 1mg/ml protein concentration technically advancing the antibody microarray proteomic research.

2.8.1.1 Standard or Full-Labeling Microarray Protocol:

Extracts with protein concentrations >1.0 mg/mL were used for fluorescent labeling. The range of concentrations used in this study was 1.0 to 8 mg/ml. A dual fluorescent-labeling assay analogous to that exploited in cDNA microarray experiments was used. Extracts were labelled separately using Cy3 or Cy5 dyes (GE Healthcare). Each protein sample (1 mL) was added directly to one vial of either Cy3 or Cy5 and mixed thoroughly by inversion. The labeling reaction was allowed to proceed for 30 minutes at room temperature in the dark. During this period, samples were mixed every 10 minutes. Labelled samples were purified from free excess Cy dye using the Sigma-Spin columns supplied with the antibody microarray kit. The columns were centrifuged for 2 minutes at 4,000 rpm before 150 μ L of labelled protein sample were pipetted onto the centre of the column. A further centrifugation at 4,000 rpm was done for 4 minutes. The eluate was retained, and protein concentration was estimated using the Bradford assay as described in section 2.6.1. Labelled protein was stored at -20°C until hybridization. For the purpose of this study, chemosensitive sample was labelled with Cy3 and chemoresistant sample was labelled with Cy5 (Figure 19).

WORKFLOW OF THE FULL-LABELLING MICROARRAY PROTOCOL

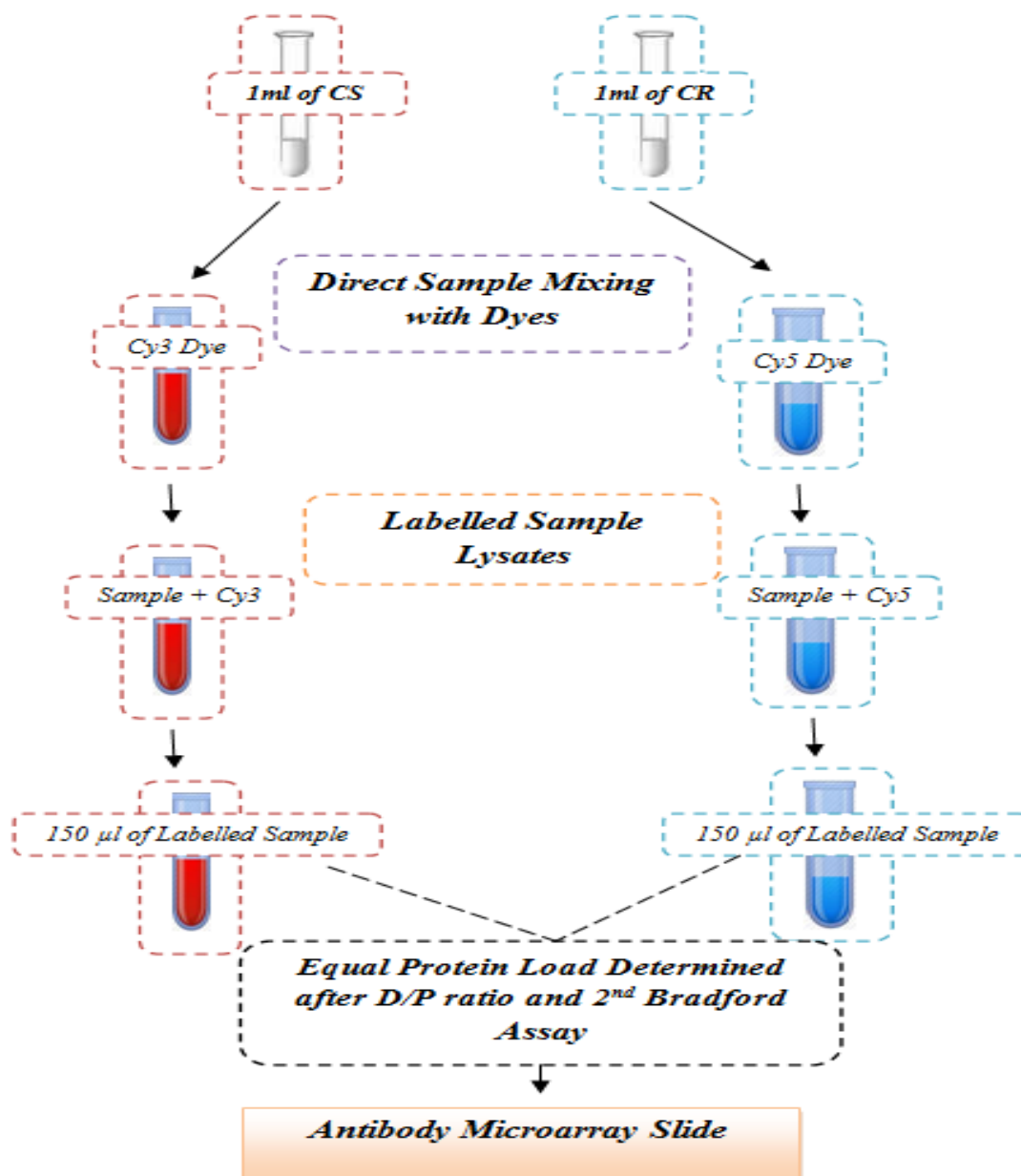


Figure 19: The workflow of the full-labelling Microarray Protocol is shown above. At first, one ml of sample (CS and CR) volume at 1mg/ml concentration is directly mixed with dyes. The labelled protein lysates are then loaded onto spin-columns at 150 µl volume and D/P ratios determined. Finally an equal amount of protein load is calculated and the samples are loaded onto the array slide.

2.8.1.2 Determination of Dye/Protein Molar Ratio (D/P Ratio):

The Dye to Protein Molar Ratio (D: P ratio) is determined by measuring the absorbance of the Cy3-labelled and Cy5-labelled protein samples at 552 nm and 650 nm respectively after diluting the samples to 1:150 (15 μ l of labelled sample + 135 μ l of Buffer A) and blanking the UV spectrometer machine with Buffer A or water and using the calculations supplied with the microarray kit. As specified in the microarray kit, to use the labelled samples in a microarray experiment, D/P ratio of ≥ 2 is required. A lower ratio (≤ 2), doesn't stop the array assay being carried forward; however, at this ratio a higher than normal background interference should be expected at the slide scanning stage. After this step, antibody microarray slides are washed by a brief submersion in PBS. The Cy3 and Cy5 labelled sample pairs are added at equal protein concentrations to 5 mL of Array Incubation buffer (antibody microarray kit component). The resulting solution is mixed by inversion and added to a well of the quadriPERM Cell Culture Vessel supplied with the antibody microarray kit. The antibody microarray slide is added to the well containing the labelled samples. The Vessel is protected from exposure to light with aluminium foil and incubated on an orbital shaker (30 rpm) at room temperature for 45 minutes. Subsequently, 5 mL of wash buffer (antibody microarray kit component) is added to the remaining wells of the Vessel and the slide is washed on an orbital shaker for 5 minutes in each well. The wash buffer is decanted from well 4 and replaced with 5 mL of proteomics grade water (Bio-Rad, Hemel Hempstead, United Kingdom) for a final wash for 2 minutes. The hybridized antibody microarray slide is removed from the well and air dried in the dark. After this step, the microarray slide is scanned for final analysis.

2.8.1.3 Slide Hybridization, Fold Change Cut-off & Quality Control:

The hybridized antibody microarray slide is scanned using a GenePix Personal 4100A Microarray Scanner (Axon Instruments, Union City, CA) with 532 and 635 nm lasers (Figure 20). Primary analysis is done with the GenePix Pro (version 4.1) software package (Axon Instruments). Images of scanned antibody microarrays are gridded and linked to a protein print list. Absent spots are flagged automatically by GenePix Pro; however, all spots are manually reviewed. Further analysis is done using Acuity (version 4.0) software (Axon Instruments) for the identification of differentially expressed proteins. Microarrays are normalized based on the Lowess method due to a slight skew in data distribution. The log ratios of Cy5 to Cy3 are determined for each spot to estimate the relative concentrations of each protein in the two independently dye labelled samples of each experiment. Unreliable data is removed from analyses by applying quality control criteria. Such criteria were set to include only those spots with a small percentage (<3%) of saturated pixels, spots that were not flagged as absent, spots with relatively uniform intensity and uniform background, and those spots that were detectable above background levels. Proteins showing a ≥ 1.8 fold differences in expression in 90% of individual microarrays are deemed significant.

In microarray analysis, as indicated by previous studies, a fold change of ≥ 1.3 to ≥ 1.8 has been considered significant to represent differential protein expression (Ghobrial, McCormick et al. 2005; Smith, Qutob et al. 2009). Previously, our research group, using a total of 13 independent antibody microarray experiments encompassing a range of oncology-related research on human tissue, cells or cell lines from 5 distinct sample groups set a fold change of ≥ 1.8 and a substance match of $\geq 90\%$ to represent a significant differential expression and a high quality microarray experiment (Hodgkinson, ElFadl et al. 2011). Therefore, this cut-off and substance match criteria

was taken as a standard reference to analyse data obtained from the six microarray experiments performed in this project. However, using the same sample set, if multiple experiments are performed, differentially expressed protein data showing a fold changes ≥ 1.5 but ≤ 1.8 is considered as supporting evidence and proteins are taken to the next stage (confirmation and validation) only if the value of ≥ 1.8 is reached in at least one experiment.

SCANNED IMAGES OF THE PANORAMA-XPRESS PROFILER-725

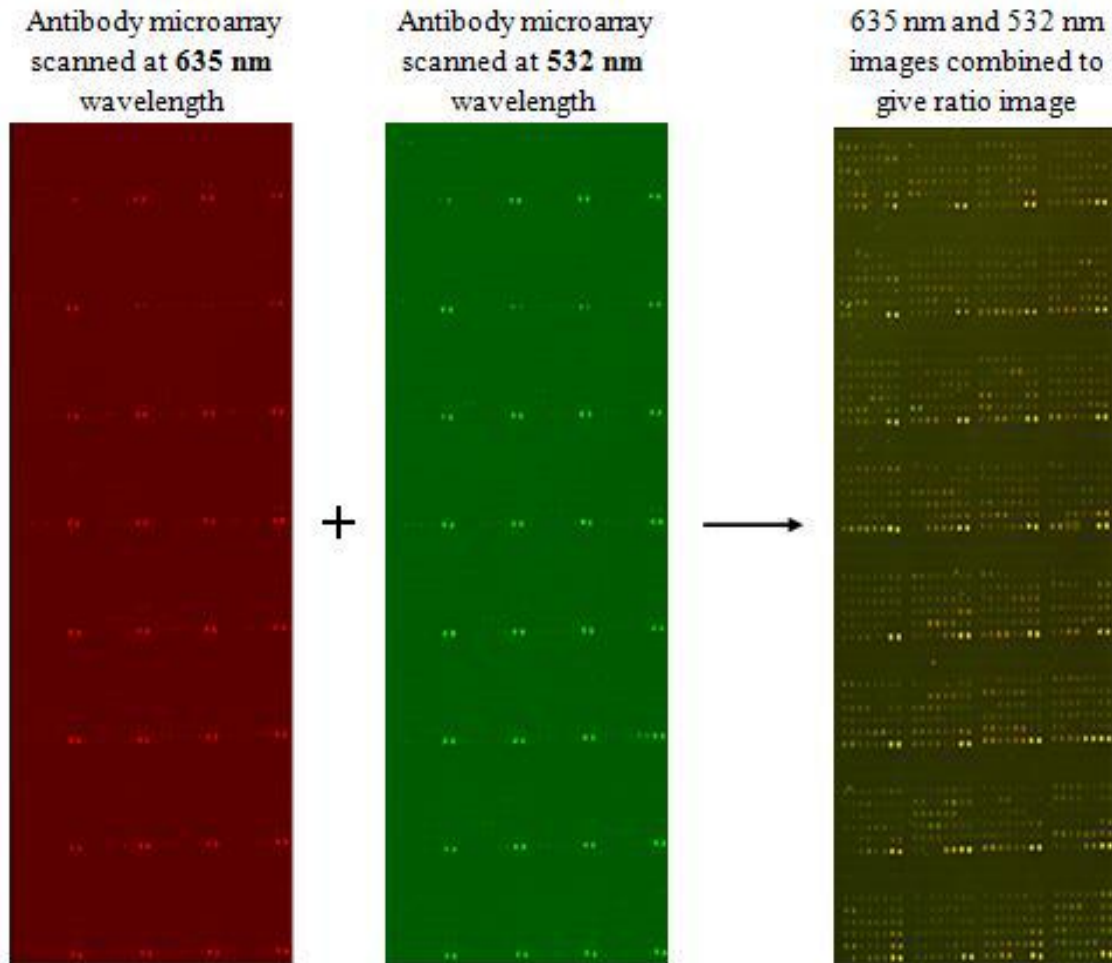


Figure 20: shows a scanned image of the Panorama[®] Antibody Microarray- XPRESS Profiler 725 slide; each slide contains 725 antibodies spotted in 32 sub-arrays each containing duplicate spots of 23 antibodies, as well as duplicate positive control spots for Cy3 and Cy5 (green spots). The above image displayed is a hybridised slide image when the array slide is scanned at two different wavelengths (532nm and 653nm). From the above image the relative intensity of two dyes can be determined for each antibody. If the difference in the relative intensity of each dye is >1.8 fold, this represent a significant fold change for a differential protein expression of that particular protein. (Courtesy V.C.Hodgkison, PhD thesis)

2.9 OPTIMISATION OF HALF-LABELLING PROTOCOL:

2.9.1 Introduction:

For the first time, tumour lysates in this research project were analysed using **0.5 ml** of sample volume with Panorama-XPRESS Profiler Antibody Microarray Kit. Previous to this study, all breast tumour samples used in the VH pilot study were analysed using the '*Standard/Full- Labelling Protocol*'. Optimisation of this new protocol for microarray analysis is therefore, a technical advancement from the previously used and only available protocol to-date for the microarray analysis.

2.9.2 Half-Labeling Microarray Protocol:

In this protocol, the sample dilution with Buffer A is carried out to bring the final volume to **0.5 ml** at 1mg/ml sample concentration.

2.9.3 Protein Labelling for the Half-Protocol:

Similar to the '*Standard/Full-Labeling Microarray Protocol*', protein lysates in the '*Half-labelling Microarray protocol*' are also labelled with fluorescent dyes (Cy3 and Cy5). However, as in this protocol, only a **0.5ml** of the final sample volume is used for the experiment, cyanine dyes supplied to be used for a ml of sample volume require a prior dilution with a non-aqueous based solution (e.g. DMSO) prior to mixing with the protein lysate. The above step is the first modification to the standard/full labelling protocol.

1st Modification from the Standard Protocol:

Firstly, the cyanine dyes (Cy3 and Cy5) are diluted in 50 µl of freshly prepared Dimethyl-Sulfoxide (DMSO) solution instead of directly mixing the **0.5 ml** of sample lysates. A 25 µl of the dye-DMSO volume is then mixed with the respective sample lysate and the final volume is brought to 525 µl for each sample (Figure 21). The above modification was carried out to allow utilising only half the dye volumes for protein labelling with this protocol. Following consultations with the GE Healthcare Consortia and SIGMA, issues of poor dye solubilisation with aqueous based solutions were ironed out and freshly prepared DMSO solution was used for the dye dilution.

2nd Modification from the Standard Protocol:

At this step, instead of adding 150 µl of labelled sample volume onto the Sigma spin-columns as in the standard protocol, 300 µl of labelled sample is added to the spin-columns to have a maximum protein (150 µg) available to load onto the microarray slide at the final step. Similar to the standard protocol, second protein quantification is undertaken using labelled samples and the protein concentrations are checked before going ahead with the experiment.

2.9.3.1 D/P Ratio, Slide Hybridisation & Quality Control:

Before hybridization, the dye-to-protein molar ratio was determined following the calculations supplied with the antibody microarray kit. Only samples with a dye-to protein molar ratio >2 were applied to the antibody microarray as recommended in the antibody microarray kit protocol. Antibody microarray slides were washed by a brief submersion in PBS and the slide incubation, scanning and application of quality control was performed as described in sections 2.8.1.3 and 2.8.1.3

WORKFLOW OF THE HALF-LABELLING MICROARRAY PROTOCOL

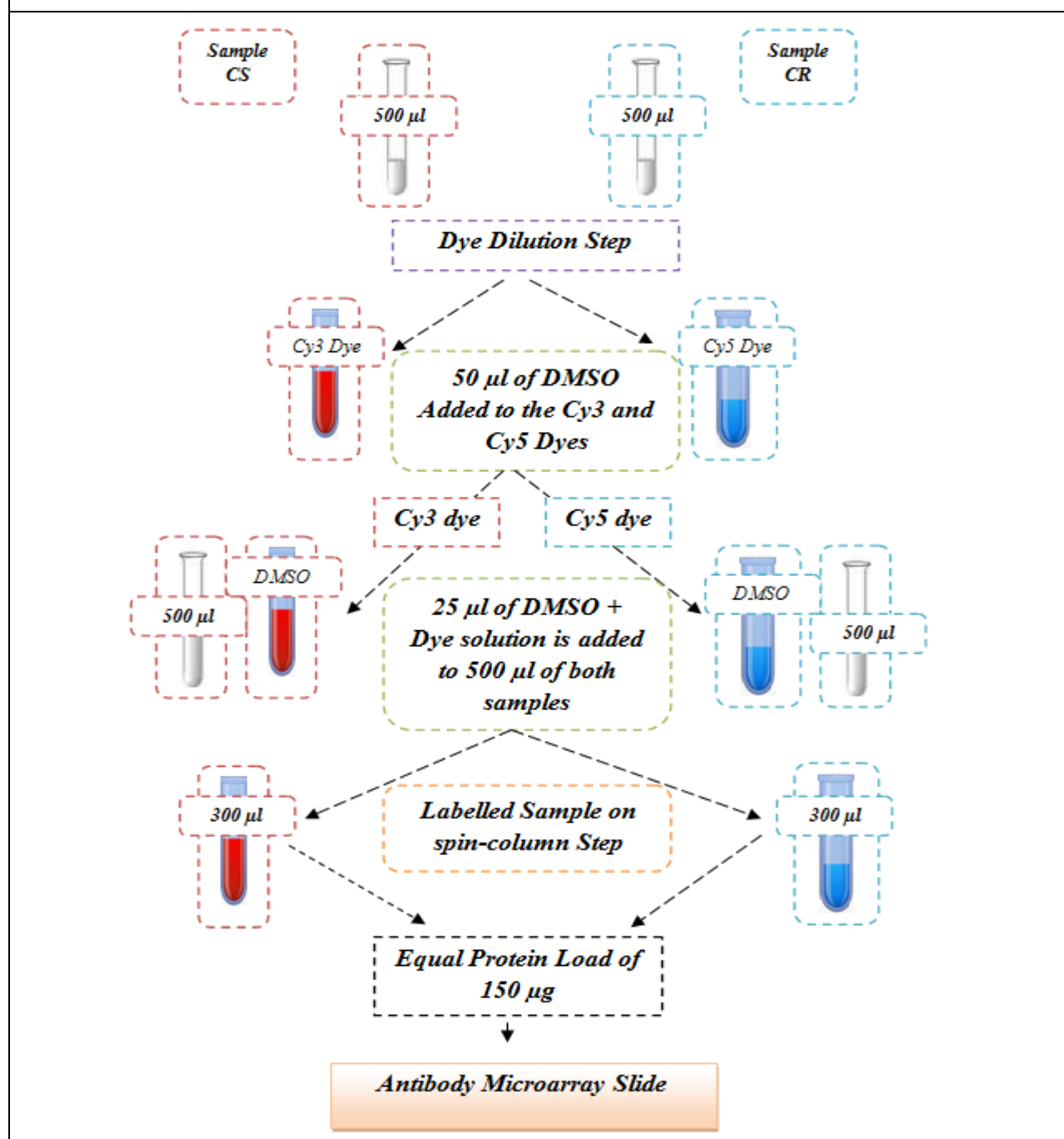


Figure 21: The workflow of Half Labelling Microarray Protocol. As shown in the figure 0.5 ml of both the samples (CS and CR) are not mixed directly with cyanine dyes but after DMSO dilution. Secondly, a total of 300 µl of sample and not 150 µl as in standard protocol is loaded onto spin-columns for protein quantification and to determine D/P ratios.

2.10 DATA MINING:

2.10.1 Introduction:

The DEPs identified and selected from the antibody microarray experiments are carried forward to the confirmation phase. However, selection of DEPs that will go the next stage from the bigger cohort of identified DEPs has to be performed in a logical and meaningful way. A useful tool to aid the prioritization of proteins, which are to be carried forward, is software (e.g. Array Unlock and Ingenuity Pathway Analysis) which analyses and interprets the data using knowledge bases (Jimenez-Marin, Collado-Romero et al. 2009). For our samples array data analysis we used Ingenuity Pathway Analysis (IPA) (Ingenuity Systems Inc., USA). Protein lists were uploaded into IPA software, where they were mapped against the Ingenuity Knowledge Base, to highlight direct relationships between candidate proteins using networks and canonical pathways. The top five canonical pathways to which maximum DEPs are matched along with other pathways to which DEPs are matched in decreasing order highlights and prioritizes the proteins of most interest. DEPs associated with pathways (e.g. apoptosis inhibiting, DNA repair inhibition) aid understanding and presenting potential hypotheses (Chemoresistant in our samples), giving researchers' informative direction for downstream confirmation.

2.10.2 Ingenuity Pathway Analysis:

The data generated by antibody microarray analysis was analysed using IPA (Ingenuity Systems, www.ingenuity.com). Each set of data, containing a list of gene symbols, which had been checked against the IPI and NCBI databases, was uploaded into IPA software online. The Ingenuity Knowledge Base is the core facility and repository behind IPA, holding all the biological and chemical information, functional annotations and model relationships for genes,

proteins, complexes, disease states, cells, tissues etc in a well-structured and accessible manner. The Ingenuity Knowledge Base is a comprehensive database containing manually reviewed, accurate information. Within the Ingenuity Knowledge Base there are four types of information, including both experimental- and literature-based 104 sources, which is all manually reviewed: (1) Ingenuity® Expert Findings, which contains experimentally-demonstrated information; (2) Ingenuity® Expert Assist Findings, from recently published journal abstracts; (3) Ingenuity® Expert Knowledge, containing signalling and metabolic pathway information, which is curated from a team of Ingenuity experts ; (4) Ingenuity® Supported Third Party Information, which is selected from a range of specific sources and databases including Entrez Gene, Gene Ontology and RefSeq.

For network generation, each gene was mapped to the corresponding gene within the Ingenuity Knowledge Base, and an ‘annotated dataset’ was generated. Genes which were successfully mapped into the Ingenuity Knowledge Base were called ‘network eligible’ molecules, and were subsequently overlaid onto a global molecular network developed from the information contained within the Ingenuity Knowledge Base. During analysis of data, networks of ‘network eligible’ molecules were then algorithmically generated based on their connectivity. The general settings allowed the maximum number of ‘molecules per network’ and ‘networks per analysis’ to be included, to highlight direct relationships between human molecules which had been reported in both tissues and cell lines.

Canonical pathway analysis of the dataset involved the identification of pathways within the IPA library of canonical pathways that were most significant to the dataset. All molecules mapped within the dataset were considered for canonical pathway analysis. The significance of the association between the dataset and the canonical pathway was measured by two factors; 1) A

ratio of the number of molecules within the dataset that can be mapped into a pathway, divided by the total number of molecules involved in that pathway, 2) Fisher's exact test was performed to determine the probability that the association between the dataset and the canonical pathway identified had occurred by chance, which was displayed as a p-value.

2.11 IMMUNOBLOTTING:

Before taking any interesting DEPs forward to the validation stage, their presence is confirmed using a second independent technique such as immunoblotting.

2.11.1 Western Blotting:

The western blot (sometimes called the protein immunoblot) is a widely accepted analytical technique used to detect specific proteins in the given sample of tissue homogenate or extract. It uses gel electrophoresis to separate native proteins which are then transferred to a membrane (typically nitrocellulose), where they are probed with antibodies specific to the target protein.

2.11.2 Protein Extraction and Quantification:

The samples (cell line lysates or tissue extracts) used for Western blot ideally should have their protein extraction and quantification carried out using Western blot extraction and quantification methodology. However, breast tumour samples from this study for Western blotting had protein extraction and quantification using antibody extraction/labelling buffer and Bradford quantification assay as described in the sections 2.5 and 2.6.1. The tissue protein extracts were then diluted into a Western extraction sample buffer containing 4ml of DH_2O , 1ml of 0.5M TRIS: HCL at pH 6.8, 0.8 ml glycerol, 1.6ml of 10% SDS and 200 μl of 0.05% bromophenol blue. To every 190 μl of extraction sample buffer a further 10 μl of 5% β mercaptoethanol is

added to allow a full denaturation of the proteins. Sample extracts are used at 10 µg and 20 µg protein concentrations to achieve a final dilution volume of 25 µl with sample extraction buffer.

2.11.3 One-Dimensional Electrophoresis:

After diluting the protein extracts with WB extraction buffer, proteins in the extracts were then denatured by heating at 95°C in a thermocycler for 5 min. They were then placed on ice to prevent reversal of protein denaturation, vortexed and centrifuged at maximum speed (~12,000 *x* g) for 30 s. Twenty microlitre of extract was then loaded into appropriate wells in a 12% Precise Protein Gel (Thermo Scientific) with Tris-HEPES-SDS running buffer, alongside 10 µl of Precision Plus Protein Western C Standard (#161-0376, Bio-Rad), as a marker of molecular weight. The gel was run at a constant voltage of 140V for 40 min.

2.11.4 Transfer of Proteins to Nitrocellulose Membrane:

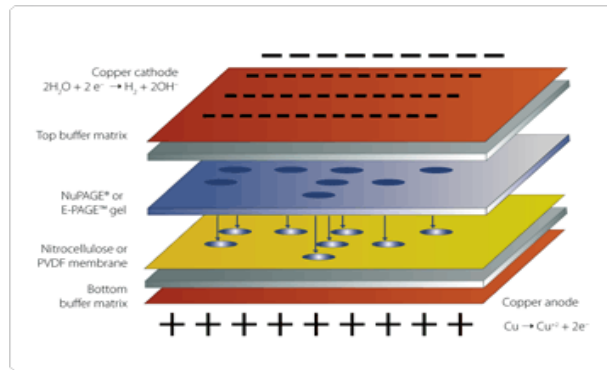
Proteins that had been separated by molecular weight were transferred onto a nitrocellulose membrane using the iBlot dry transfer system (Invitrogen) with 'iBlot gel transfer stacks, nitrocellulose' (Serial#793403, Invitrogen) (Figure 22). Whilst using the stack, firstly, the 'bottom' disposable transfer stacks containing membranes were placed in the machine following which, gels were placed on top of the membrane in the required orientation. Filter paper soaked with dH₂O was then placed on top of the gels and air bubbles were removed using a roller. The 'top' disposable pack containing the cathode was placed on top of the membrane followed by a sponge containing an electrode. The standard transfer, as recommended by the manufacturer was used, which ran for 7 min, and transferred the proteins from the gel onto the nitrocellulose membrane.

THE i-BLOT DRY TRANSFER SYSTEM FOR IMMUNOBLOTTING

A



B



C

Figure 22: Invitrogen i-blot dry transfer system is shown in figure A and B. Figure C illustrates the stack arrangement for the transfer system. The anode (red) stack is placed at the bottom, above this there is a layer of PVDF membrane. The 1D-PAGE containing proteins spots is placed above the anode to allow protein transfer onto the PVDF membrane below. Finally, a cathode stack with the shiny surface facing front is placed over the gel with a filter paper in between the two layers.

2.11.5 Blocking Non-specific Binding Sites on Membrane:

Once the proteins had been transferred onto the membrane, the free binding sites on the membrane were blocked by incubating the membrane with 'blocking solution' (5% low-fat milk powder (Marvel), diluted in TBS-Tween20) in a Nalgene staining box on an orbital shaker for 1 hour at *RT* or 16 hours at 4° C. This was necessary to prevent unwanted binding of antibodies to the membrane when probing for a specific protein.

2.11.6 Adding Primary and Secondary Antibodies:

The primary antibody to the protein of interest was optimised and diluted to its optimum concentration in blocking solution. It was incubated with the membrane for 2 hours at *RT* on an orbital shaker. Following this, the membrane was washed 3 times with TBS-Tween20 (5 min per wash) on an orbital shaker, to remove any unbound antibody. The membrane was then incubated with a HRP-conjugated secondary antibody to the animal the primary antibody was raised in. This was diluted to its optimum concentration in blocking solution and incubated with the membrane for 1 hour at *RT* on an orbital shaker. For visualisation of the Precision Plus Protein Western C Standard molecular weight marker, 1 µl of Precision Protein StrepTactin-HRP conjugate (#161-0381, Bio-Rad) was also added to the blocking solution containing secondary antibody. Three washes of 5 min each with TBS-Tween20 were carried out on an orbital shaker.

2.11.7 Loading Control:

Loading control is added to the membrane to test for accurate loading of extract proteins into the gel, thus allowing fair comparisons to be made between samples. For this, proteins which should be present in all cells at equal concentrations called 'housekeeping proteins' (example β actin, α tubulin or GAPDH) are used.

2.11.8 Protein Detection:

Protein detection is carried out by incubating the membrane with equal amounts of Supersignal West Pico Stable Peroxide Solution and Supersignal West Pico Luminol Enhancer Solution from the Supersignal West Pico Chemiluminescent Substrate Kit (#34078, Thermo Scientific) for 5 min with frequent gentle manual agitation in the dark. The membrane is then developed by placing it between transparent plastic sheets in an intensifying cassette with CL-XPosure Film (#34090; Lot# 85140102; Thermo Scientific) and gentle manual agitation in 250 ml each of GBX Developer (#, Sigma Aldrich) until bands appeared. This is followed by 30 s incubation in 250 ml 5% Acetic Acid and then 250 ml GBX Fixer (Lot#061M1859), with gentle manual agitation in a plastic tray. The developed films were then allowed to air-dry before scanning and densitometry

2.11.9 Densitometry:

Densitometry was used to quantify the density of bands on films, representing expression of a particular protein in the chosen protein extract. The film was scanned using a GS-800 Calibrated Densitometer (Bio-Rad) and Quantity One software (Bio-Rad) was used to normalise the protein of interest against the loading control (Beta-actin). The normalised optical density of the target bands was then given allowing for the target protein expression to be compared between both the chemosensitive and chemoresistant samples. This then allowed for the optical density of the target band to be recorded and the subsequent fold-change to be calculated.

2.12 IMMUNOHISTOCHEMISTRY

Immuno-histochemistry (IHC) technique is a combination of immunological, histological and biochemical methods for the identification of specific tissue components. It is one of the most common techniques used for the validation of proteins confirmed on immunoblotting. The visualization and localization of the cellular components is achieved by means of a specific antigen/ antibody reaction using a labelled antibody.

2.12.1 Archival Samples used in Pilot Clinical Validations:

As described before in the section 2.3.3, two different archival pre-treatment series (MRI-iFEC and EC-D) were selected for clinical validations. The IHC validations for the 14-3-3 protein isoforms (alpha/beta, zeta/delta and epsilon isoform) were carried out using the MRI-iFEC series and rest of the other proteins (14-3-3 theta/tau, Vimentin, Akt1, FAK) were validated using the EC-D series (Figure 23).

2.12.2 Blocking and Antigen Retrieval Methods:

The principles of the IHC procedure can be studied under the following headings:

Blocking phase:

In this phase, the endogenous RBC peroxidase, biotin activity and the background specific (from diffused proteins) and non-specific binding is blocked by using methanol with hydrogen peroxide and a blocking serum (e.g. R.T.U.Horse serum).

Antigen retrieval phase:

The aim of this step is to release proteins or expose antigenic sites by using heat (steamer, pressure cooker, or microwave) in Heat Induced Epitope Release (HIER) method or using an enzyme in the Protein Induced Epitope Release (PIER) method.

SELECTED PROTEINS FOR IMMUNOHISTOCHEMICAL VALIDATIONS & THE USED ARCHIVAL SERIES

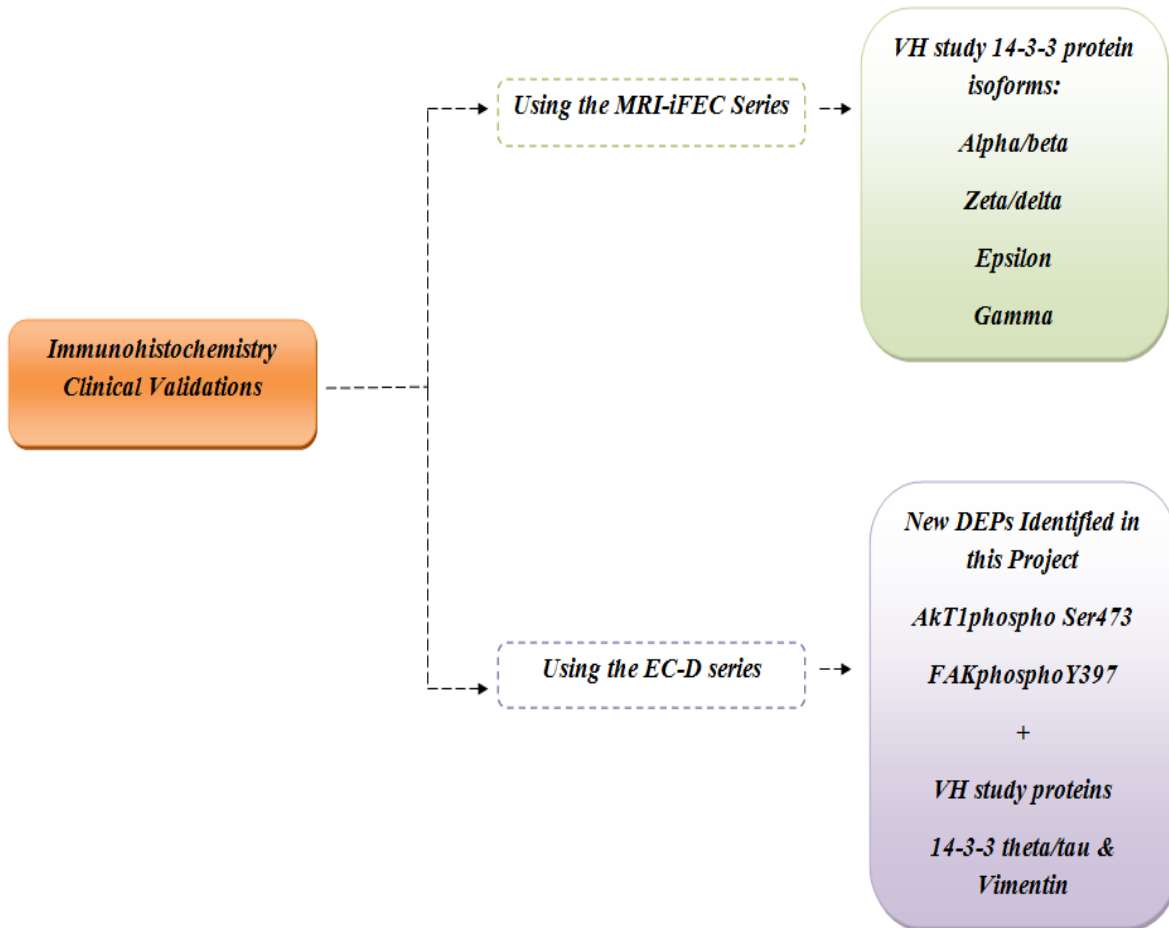


Figure 23: shows the proteins selected for the immuno-histochemical validations using MRI-iFEC and EC-D series. In total four 14-3-3 isoforms were validated using the MRI-iFEC series and two new proteins and two proteins (14-3-3 theta/tau and Vimentin) from VH study were validated using the EC-D series.

2.12.2.1 Cutting Tissue Sections:

The formalin-fixed, paraffin-embedded tissues are sectioned into slices as thin as 4 to 5 μ m with a microtome. These sections are then mounted onto glass slides that are coated with an adhesive. After mounting, the sections are dried in an oven or microwave in preparation for deparaffinization.

2.12.2.2 De-waxing and rehydration:

In this step the tissue sections are first de-waxed by incubating in warm (~50 °C) HistoClear II (#HS-200, National Diagnostics) for 10 min. This step is followed by two further 10 s incubations (with a gentle shaking of the rack) in separate solutions of HistoClear II (#HS-200, National Diagnostics). Sections are then rehydrated by incubating for 10 s in three separate 100% ethanol solutions shaking the rack gently at each step. The sections were then rinsed in running tap water for 1 min.

2.12.2.3 Blocking of endogenous peroxidase:

The endogenous peroxidase activity of red blood cells is blocked by incubating the tissue sections with 400 ml of methanol containing 30% hydrogen peroxide for a period of 20 min.

2.12.2.4 Antigenic site retrieval:

Antigenic site retrieval is achieved by applying the principles of the HIER method; slides are boiled in a stainless steel pressure cooker at 15 psi pressure with 1500 ml of distilled water and 15 ml of Vector Antigen Unmasking Solution (1:100) (#H-3300, Vector Laboratories) at a full pressure of 3 min. Slides are then transferred into a pot containing Tris Buffer Saline (TBS).

2.12.2.5 Blocking of non-specific binding sites:

For this step, the slides are arranged serially onto a sequenza system (Shandon, Basingstoke, UK) using cover plates. An accurate slide assembly ensures that there are no air bubbles between the slides and the cover plate using TBS-washes. Non-specific binding sites within sections are blocked by incubating slides with 100µl (3 drops) of pre-diluted blocking serum (normal horse serum) from Quick Kit (Vector #PK-7800) for 10 min. At the end of 10 min incubation, a 2 x 5 min TBS rinses are performed and slides as slides are prepared for antigen detection.

2.12.2.6 Antigen detection:

For this step, a diluted antigen-specific primary antibody, a secondary antibody and conjugated streptavidin-peroxidase complex is used. The blocking solution (TBS + 1.5% blocking serum) and the diluted primary antibody solution (TBS + 1.5% blocking serum + primary antibody) are prepared and applied to the slides sparing the negative of the primary antibody solution. Slides are then incubated for 2 hrs at room temperature and rinsed with 2 x 5 min TBS thereafter. Finally, slides are incubated with 100µl (3 drops) of pre-diluted biotinylated pan-specific universal secondary antibody from Quick Kit (Vector #PK-7800) for 20 min before incubating slides with 100µl (3 drops) of conjugated streptavidin-peroxidase complex reagent (Vector #PK-7800) for 10 min.

2.12.2.7 Antibody Visualisation:

Antibody visualisation is achieved using 0.02% diaminobenzidine (DAB) in 400 ml of TBS containing 0.125% hydrogen peroxide (30% w/w solution). DAB is commonly employed in enzyme-mediated immuno detection as a substrate for the Horse Radish Peroxidase (HRP) enzyme. Slides when incubated with the DAB solution (DAB + H₂O₂) develop a brown-coloured

polymeric oxidation product which stains the tissue sections. DAB staining can then be visualized directly by bright-field light microscopy. The underlying chemical process in the colour development involves oxidation of hydrogen peroxide (H_2O_2) by HRP enzyme and formation of free oxygen radical which then oxidizes diaminobenzidine to a complex polymeric compound. The incubation time with DAB is strictly controlled to 30 min or else DAB starts precipitating on to the tissues.



2.12.2.8 Colour Enhancement, counterstaining and differentiation:

The contrast of the staining is enhanced by incubating slides in 0.5% copper sulphate in 0.9% sodium chloride solution for 5 min. Sections are counterstained by incubating with filtered Harris' Haematoxylin (#HHS32, Sigma Aldrich) gently shaking the rack for 20 s. Excess haematoxylin is removed by washing the slides in running tap water and the differentiation of the counterstaining is produced by incubating slides in acid alcohol (70% alcohol, 1% HCl (conc)) with gentle shaking for 10 s. Slides are then washed in running tap water and prepared for mounting following rehydration.

2.12.2.9 Rehydration, clearing and mounting:

In this final step, tissue sections are rehydrated by taking slides through 100% ethanol solutions three times with gentle rack shaking for 10 s in each solution. Sections are finally dipped into three clearing HistoClear II (#HS-200, National Diagnostics) solutions with gentle rack shaking

for 10 s in each solution. All slides are then mounted onto cover-slips using Histomount (#HS-103, National Diagnostics) and left to dry overnight.

2.12.2.10 Scoring of immunostained tissue sections:

The scoring system was developed by Victoria Hodgkinson (PhD) for the breast cancer proteomic-pilot study. Slides were scored after observation of all slides across the sample series based on the percentage of stained tumour cells and the intensity of tumour cell staining. For the cytoplasmic staining, slides were scored '*positive*' if > 50% tumour cell coverage was found showing a moderate to strong intensity staining. If the staining was noted in less than 50% tumour cells in weak or weak-moderate intensity slides were scored '*negative*.' For the nuclear membrane staining, slides were scored '*positive*' if in a single cluster > 20% tumour cells were found to be stained. If the cell staining in the cluster was found to be involving < 20% of tumour cells the slides were scored '*negative*.' Similarly, for the cell membrane staining, a 50% of membrane staining in at least 50% of tumour cells was scored '*positive*'. If the staining involved <50% of membrane and/or <50% of cells the slides were scored '*negative*.' (Tables: 12, 13 and 14). The scoring was performed by two observers (VH and TH) independently, after consultation with a consultant histopathologist (Dr. Ann Campbell). In the event of disagreement between the two observers, we decided to involve a third observer (Dr. Ann Campbell) to score the slides in order to minimize the inter-observer variability.

For the immuno validation work in this project, the tissue staining noted with the breast cores (*EC-D* series) using AkT Phospho Ser473, Vimentin and FAK phosphoY397 protein antibodies and with 14-3-3 protein family (beta/alpha, zeta/delta and epsilon) antibodies using the MRI-iFEC series was similar in location and intensity to the one described by our research group

previously (Hodgkinson et al. 2012). Therefore, the same scoring method and scores were used for the six proteins assessed in the pilot validation work from this research study.

Table 12: IHC scoring system for the cytoplasmic staining

Chemoresistance Breast cancer study (MRI-iFEC series)

Antibody:

Antibody dilution: |

Detection method: Streptavidin-Avidin-Biotin Method

Scoring system: for cytoplasmic staining:

% Coverage within tumour area	>50%	>50%	>50%	>50%
Symbol	-	-/+	+	++
Intensity	Weak	Weak-moderate	Moderate	Strong
Score	Negative		Positive	

Table 13: IHC scoring system for the cell membrane staining

Chemoresistance Breast cancer study (MRI-iFEC series)

Antibody (name, cat #, supplier):

Antibody dilution:

Detection method: R.T.U. VectaStain (PK-7800, Vector) (secondary and complex double-time incubations)

Scoring system: for cell membrane staining:

Staining in $\geq 50\%$ of tumour cells	Staining in $< 50\%$ of tumour cells
Positive	Negative

Table 14: IHC scoring system for the Nuclear membrane staining

Chemoresistance Breast cancer study (MRI-iFEC series)

Antibody:

Antibody dilution:

Detection method: Streptavidin- Avidin-Biotin Method

Scoring system: for nuclear membrane staining:

Staining in $\geq 20\%$ of <u>clusters</u> of tumour cells	Staining in $< 20\%$ of tumour cell clusters
Positive	Negative

2.12.2.11 Statistical Correlation of IHC scoring:

The statistical significance between histological scores and responses to breast cancer chemotherapy (chemosensitivity or chemoresistance) was assessed using a two-tailed Fishers exact test. A P value of ≤ 0.05 was considered significant. Statistical calculations were performed using the online software programme (GraphPad 116 software Inc (USA) at <http://www.graphpad.com/quickcalcs/contingency1.cfm>). The clinical response data and IHC scores were entered in a 2 x2 contingency table as shown below in Figure 24.

FISCHERS EXACT TEST CONTINGENCY TABLE		
	<i>Positive</i>	<i>Negative</i>
<i>Chemo-sensitive</i>	<i>x</i>	<i>x</i>
<i>Chemo-resistance</i>	<i>x</i>	<i>x</i>

Figure 24: shows a 2 x 2 contingency table for Fischer’s exact test. The values (*x*) is entered for the number of patients that show a chemo-sensitive or chemo-resistant response against a positive or a negative IHC score for a particular staining localization.

CHAPTER III

RESULTS

Hussain T; Scaife L; Hodgkinson V; Agarwal V; Mahapatra T; Kneeshaw P; McManus P; Lind M; Cawkwell L Proteomic Identification of Putative Markers of Chemotherapy Resistance; *EJSO; Volume 39, Issue 5 , Page 480-81, May 2013*. Poster presentation at ABS Conference and AGM; Manchester 2013.

Chapter 3.

3.1 INTRODUCTION:

This chapter will cover the results of protein extraction/quantification and antibody microarray experiments carried out using chemoresistant and chemosensitive sample pairs. The six samples (3 pairs of chemosensitive and chemoresistant) used in this project were selected after matching them on the basis of the chemotherapy regimens, number of chemotherapy cycles, immunohistochemical receptor (ER, PR and HER2) status, chemotherapy responses and tissue availability (section 2.3). Protein extraction and quantification from the selected sample pairs was carried out using the protein extraction and quantification techniques as described in sections 2.5 and 2.6.1. The information on the sample weights and the dilution volumes of the extraction/labelling buffer (4 times weight/volume) used for the suspension of research samples is provided in the Table 15 below. The technique of recording sample weights, volume dilutions, mechanical homogenisation and protein quantification has already been illustrated in Figure 19 and described in the section 2.4.

Table 15: Project samples Recorded Weights and Dilution Volumes for Protein Extraction

Number	Sample Number	Wt in grams	Buffer volume at 4 w/v in millilitres
1	#16B	0.115	0.46
2	#1B	0.306	1.224
3	#38	0.446	1.784
4	#15B	0.337	1.348
5	#12B	0.392	1.568
6	#1	0.209	0.836

3.1.1 Results from the Bradford Quantification Assay:

Using protein lysates from the above listed 6 research samples, protein quantification experiments was carried out with the Bradford assay (section 2.6.1. A total of two quantification experiments were carried out using the same sample lysates independently by TH and VH (post-doc) to accurately analysis the samples and eliminate any confounding bias (e.g. individual pipetting errors) influencing the experiment findings. The individual Bradford quantification results from two experiments (TH and VH) using all 6 research samples are listed in Tables 16 and 17. The final protein concentrations for all 6 samples were decided by taking an average reading of TH and VH protein concentrations. The results of the combined average protein

concentrations (TH + VH) for all 6 samples are listed in the Table 18. For the microarray analysis, the calculations of individual sample dilutions were based on the combined average quantification values from the TH and VH data.

Table 16: Final Protein Concentrations for 6 Clinical Samples: TH analysis

Sample #	Sample	Absorbance	Protein concentration (x)	Correct for dilution	Average	Final Concentration (mg/ml)
#16B/CS	1(1:5)	0.167	0.794117647	3.970588235	4.105219553	4.345484673
	1 (1:5)	0.18	0.847970174	4.23985087		
	1(1:10)	0.096	0.5	5	4.585749793	
	1 (1:10)	0.076	0.417149959	4.171499586		
#1B/CR	2(neat)	0.169	0.802402651	0.802402651	0.783761392	1.19400718
	2 (neat)	0.16	0.765120133	0.765120133		
	2 (1:5)	0.029	0.222452361	1.112261806	1.153686827	
	2(1:5)	0.033	0.23902237	1.195111848		
	2(1:10)	0.013	0.156172328	1.561723281	1.644573322	
	2(1:10)	0.017	0.172742336	1.727423364		
#38/CS	3(1:5)	0.109	0.553852527	2.769262635	2.531068766	3.071665286
	3(1:5)	0.086	0.458574979	2.292874896		
	3(1:10)	0.048	0.301159901	3.011599006	3.612261806	
	3(1:10)	0.077	0.421292461	4.212924606		
#15B/CR	4(neat)	0.256	1.162800331	1.162800331	1.218724109	1.874067937
	4(neat)	0.283	1.274647887	1.274647887		
	4(1:5)	0.069	0.388152444	1.94076222	1.951118476	
	4(1:5)	0.07	0.392294946	1.961474731		
	4(1:10)	0.05	0.309444905	3.094449047	2.452361226	
	4(1:10)	0.019	0.181027341	1.810273405		
#12B/CS	5(1:5)	0.144	0.698840099	3.494200497	3.483844242	3.931234466
	5(1:5)	0.143	0.694697597	3.473487987		
	5(1:10)	0.079	0.429577465	4.295774648	4.37862469	
	5(1:10)	0.083	0.446147473	4.461474731		
#1/CR	6(1:5)	0.317	1.415492958	7.077464789	7.004971003	8.177299089
	6(1:5)	0.31	1.386495443	6.932477216		
	6(1:10)	0.199	0.926677713	9.266777133	9.349627175	
	6(1:10)	0.203	0.943247722	9.432477216		

Table 17: Final Protein Concentrations for 6 Clinical Samples: VH analysis

Sample	Absorbance	Protein concentration (x)	Correct for dilution	Average Protein concentration (mg/ml)	Samples #
1 (1:5)	0.255	0.916963996	4.584819981	4.517515407	#16B/CS
1 (1:5)	0.261	0.93642556	4.682127798		
1: (1:10)	0.111	0.449886474	4.498864742		
1: (1:10)	0.105	0.430424911	4.304249108		
2 (neat)	0.277	0.988323062	0.988323062	1.333198184	#1B/CR
2 (neat)	0.273	0.975348686	0.975348686		
2 (1:2)	0.133	0.52124554	1.04249108		
2 (1:2)	0.12	0.479078819	0.958157639		
2 (1:5)	0.055	0.268245216	1.341226078		
2 (1:5)	0.058	0.277975997	1.389879987		
2 (1:10)	0.04	0.219591307	2.195913072		
2 (1:10)	0.027	0.177424586	1.774245864		
3 (1:5)	0.171	0.644502108	3.222510542	3.386312034	#38/CS
3 (1:5)	0.164	0.621796951	3.108984755		
3 (1:10)	0.085	0.365553033	3.655530328		
3 (1:10)	0.082	0.355822251	3.558222511		
4 (1:2)	0.193	0.715861174	1.431722348	1.782246729	#15B/CR
4 (1:2)	0.192	0.71261758	1.425235161		
4 (1:5)	0.08	0.349335063	1.746675316		
4 (1:5)	0.075	0.333117094	1.665585469		
4 (1:10)	0.049	0.248783652	2.487836523		
4 (1:10)	0.032	0.193642556	1.93642556		
5 (1:5)	0.175	0.657476484	3.28738242	3.491728836	#12B/CS
5 (1:5)	0.172	0.647745702	3.238728511		
5 (1:10)	0.081	0.352578657	3.525786572		
5 (1:10)	0.093	0.391501784	3.91501784		
6 (1:10)	0.219	0.800194616	8.001946156	7.969510217	#1/CR
6 (1:10)	0.217	0.793707428	7.937074278		

Table 18: TH/VH Combined Average Protein Concentrations

Samples #	TH Average (protein conc. mg/ml)	VH Average (protein conc. mg/ml)	Averages of TH and VH (protein conc. mg/ml)
#16B	4.34548	4.51751	4.4314977
#1B	1.194	1.333	1.2635991
#38	3.07166	3.38631	3.228986
#15B	1.87406	1.78224	1.8281534
#12B	3.93123	3.49172	3.7114794
#1	8.177299	7.96951	8.0734046

3.2 HALF PROTOCOL OPTIMISATION EXPERIMENTS USING BREAST TUMOUR SAMPLES:

3.2.1 Introduction:

In this section of thesis, three “*Half-labelling Microarray Protocol*” optimisation experiments using breast tumour lysates are highlighted and discussed. The initial results from the first two failed optimisation experiments using the new protocol and a third experiment that passed the quality-control are provided and discussed in detail.

As mentioned above, the ‘*Half-labelling Microarray Protocol*’ was optimised in three experiments using breast tumour lysates. The sample lysates used in the three optimisation experiments were chosen randomly from the 6 study samples. The three optimisation experiments were called experiment # 1, #1b and #2b. The sample pairs used for experiments #1 and #1b were sample #16 (chemosensitive) vs #1B (chemoresistant). For experiment #2b, sample #38 (chemosensitive) vs 15B (chemoresistant) were used. All the three optimisation experiments were carried out using protocol as described in the section 2.9.

3.3 EXPERIMENT # 1: SAMPLE #16B (CS) vs. #1B (CR)

Protocol Used: ‘Half-Labeling Microarray Protocol’

Kit: SIGMA-Panorama XPRESS-725 Profiler Kit

Catalogue #089K4791 (2009 Stock Kit)

3.3.1 Introduction:

This was the first experiment in the series using samples #16B (CS) and #1B (CR). The sample receptor status, therapy response summary along with the final protein concentrations and volume dilution summaries are provided in Tables 19 and 20 below:

Table 19: The Summary of Samples Characteristics and Therapy Response

Samples	Receptor Status	NACT	Response
#16B(CS)	ER +; PR & HER 2-	EC X4; D X 1	PR
#1B(CR)	ER +; PR & HER2-	EC X4; D X2	PD

Table 30: Final Sample and Dilution Buffer Volumes (µl) for Sample #16B vs #1B

Samples	Final Bradford Conc. (mg/ml)	Final Sample volumes in µl	Final Buffer A volumes in µl
#16B (CS)	4.431977	112.8287	387.1713
#1B (CR)	1.263599	395.6951	104.3049

3.3.2 Sample Dilutions and Protein Labelling:

The samples at final concentrations were diluted with Buffer A to bring the final volume up to 500 µl. The chemosensitive (CS) sample #16B was labelled with Cy3 (pink colour) and the chemoresistant (CR) sample #1B with Cy5 (blue colour) fluorescent dyes after diluting cyanine dyes with 50 µl of **aqueous solution Buffer A**. The steps following from this stage were as described in sections 2.9.2 and 2.9.3. The results from the protein concentrations on the 2nd Bradford assay are listed below in the Table 21.

Table 41: Results from 2nd Bradford Quantification using Labelled Samples

Sample	Absorbance	Protein Concentration (mg/ml)	Average
#16B Cy3; CS	0.165	0.765473527	
#16B Cy3; CS	0.179	0.817673378	0.791573
#1B Cy5; CR	0.18	0.821401939	
#1B Cy5; CR	0.174	0.799030574	0.810216

3.3.3 D/P Ratio, Slide Hybridisation & Quality Control:

The dye-protein molar ratio for the experiment was calculated as described in section 2.8.1.2 and the values obtained for Cy3 and Cy5 in this experiment were Cy 3; #16B; CS = 3.37 and Cy 5; #1B; CR = 4.13. As the ratio obtained for both Cy3 and Cy5 was ≥ 2 , the experiment was taken forward and an optimal protein load for each of the sample was calculated from the left over sample volume. For this experiment, a protein load of **80 μg** (sample volume of 101.6 μl for #16B and 98.73 μl for #1B) each sample was decided. The slide was then incubated with equal volume of sample lysates and scanned for the final data analysis (Figure 25). The quality control percentage for the experiment was determined following manual slide arrangement and substance match percentage values of 84 % (TH) and 85% (VH) were obtained at two independent analyses at two different times. From the above % match results, the experiment was classed as 'Failed' and the experiment data was not taken forward for the data mining stage.

EXPERIMENT #1 (SAMPLE #16B vs #1B) FLOW CHART

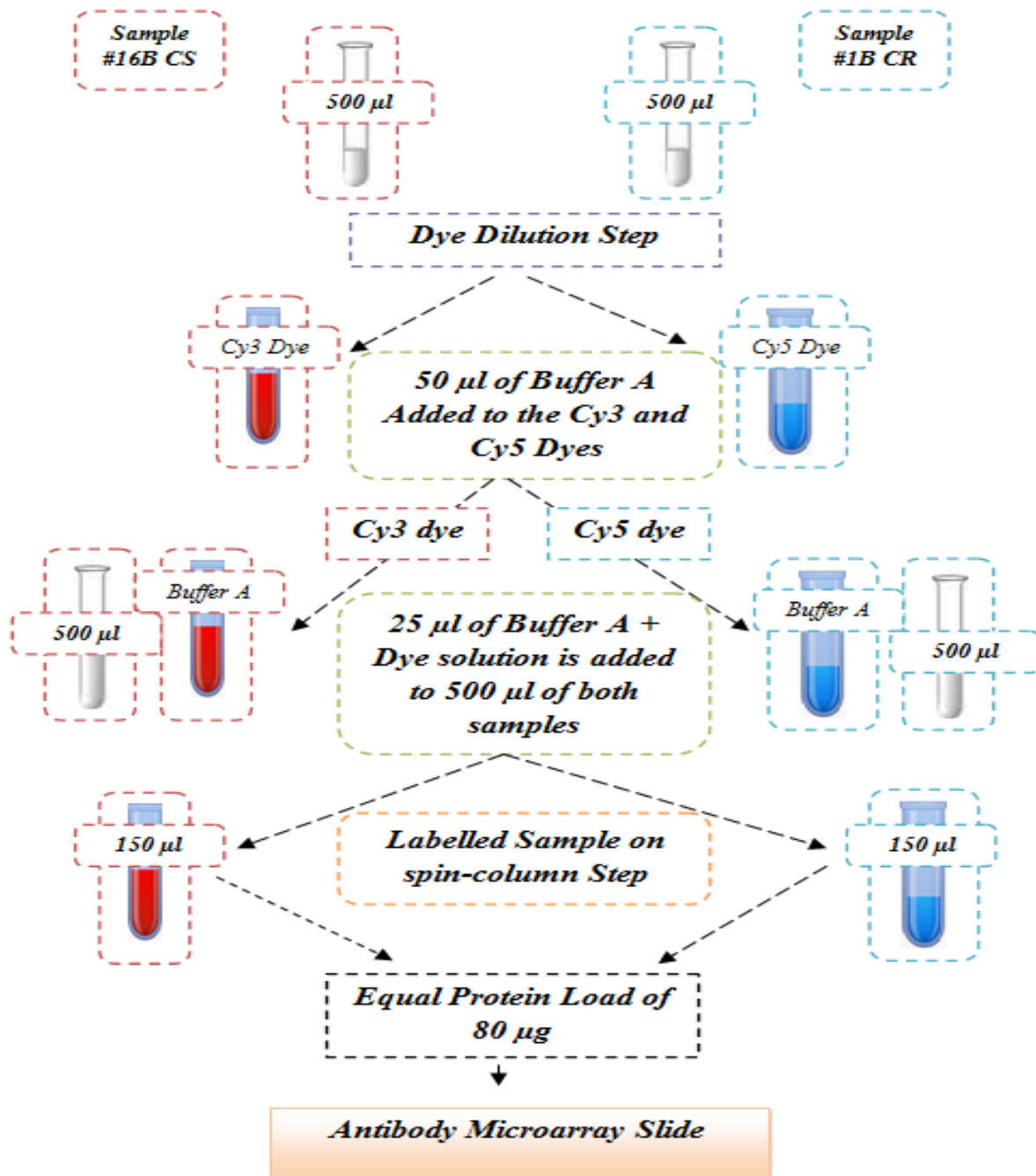


Figure 25: The flowchart for the 'Half-labelling Microarray Protocol' is as shown above. Prior to sample labelling with the dyes, the dyes are diluted with 50 µl of Buffer A. A 25 µl of the dye-Buffer A solution is then added to samples to reduce the volume of dye used for the low sample volume in this protocol.

3.3.4 Discussion:

The experiment #1 was analysed and the possible reasons of the failure were determined. Discussions were carried out with SIGMA and the GE Healthcare Consortia and the steps that were different in the '*Half labelling Microarray Protocol*' (e.g. the dye dilution step and the spin column protein load) were re-analysed. Abnormal spot morphologies (oval shape instead of the round) and an excessive background interference (Figure 26) noted at the time of slide analysis were explored as potential factors that may have contributed to the failure. Adequacy of protein load onto the array slide with low sample volumes and the slide validity were some of the issues that were discussed with SIGMA.

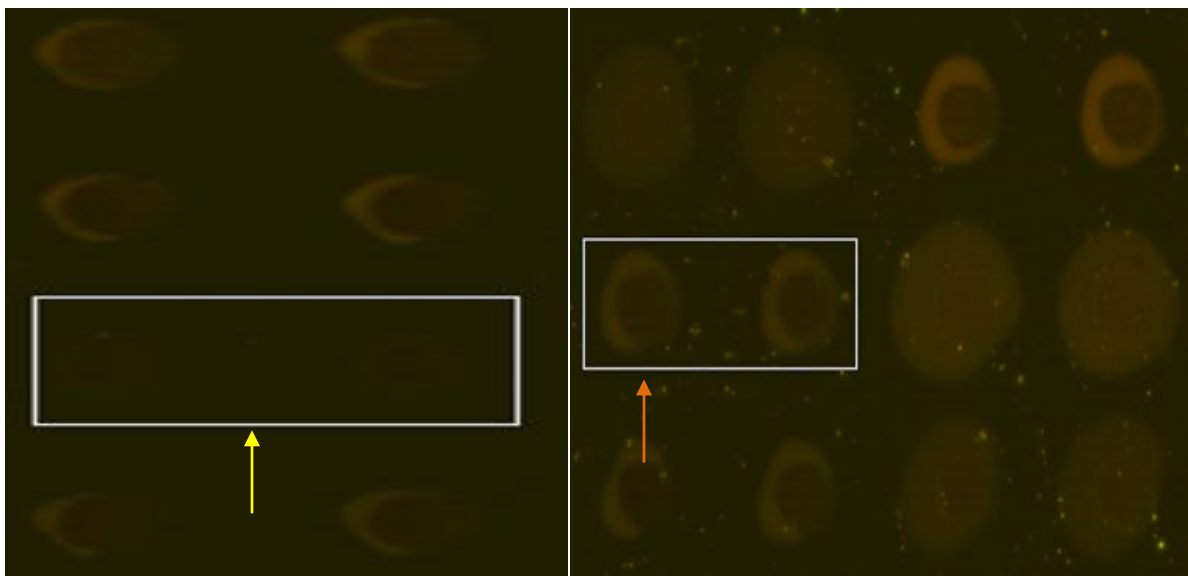
Finally, it was concluded that all the above factors had potential to fail the experiment in combination and/or individually. Also, during discussions with SIGMA, it was discovered that the Panorama- XPRESS Profiler 725 kit used in this experiment was released from the SIGMA's 2009 stock (slide validity up to one year only). Following the discovery, our research group decided to repeat the experiment using the labelled lysates of the same sample pair and a new kit without making any alterations to the '*Half labelling Microarray Protocol*'. The repeat experiment was called experiment #1b.

SPOT MORPHOLOGIES FROM THE FAILED MICROARRAY SLIDE

(EXPT #1)

A

B



C

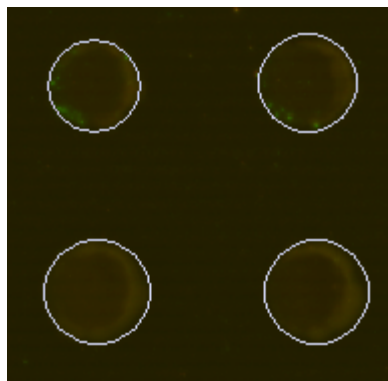


Figure 26: The morphology of the spots from the failed slide of the AbMA experiment #1 is shown. In the figure A, the spots are not visible due an excessive background staining (yellow arrow). In figure B, the visible spots are oval in shape (orange arrow) instead of the normal round morphology. The normal rounded spots are illustrated in figure C for comparison.

3.4 EXPERIMENT #1b: LABELLED Cy 3 #16B (CS) vs. Cy 5 #1B (CR)

Protocol Used: 'Half-Labeling Microarray Protocol'

Kit: SIGMA-Panorama XPRESS-725 Profiler Kit

Catalogue #071M4826 (2012 Stock Kit)

In this experiment, the labelled Cy3 (CS) 16B and Cy5 (CR) 1B samples extracts from the previous experiment #1 were used. At the start of the experiment, 150 µl of each of the labelled sample was added onto the SIGMA spin-columns and the unbound dye was removed by centrifugation. After this, a 2nd Bradford protein quantification was performed using 10 µl of each of the labelled sample and the results from the quantification are highlighted in Table 22.

Table 52: Results from 2nd Bradford Quantification using Labelled Samples

Sample	Absorbance	Protein Concentration (mg/ml)	Average
#16B Cy3; CS	0.222	1.014989293	
#16B Cy3; CS	0.232	1.057815846	1.057816
#16B Cy3; CS	0.244	1.109207709	
#16B Cy3; CS	0.230	1.049250535	
#1B Cy5; CR	0.251	1.139186296	
#1B Cy5; CR	0.247	1.122055675	
#1B Cy5; CR	0.256	1.160599572	1.147752
#1B Cy5; CR	0.258	1.169164882	

3.4.1 D/P ratio, Slide Hybridisation & Quality Control:

The D/P ratios for each of the labelled sample were as follows: for Cy3 #16B was 2.432 and for Cy5 #1B: 3.0534. Based on the above calculation, a protein load of 100 µg for both samples was determined to go onto the array slide (Figure 27). The slide was then incubated and finally scanned for the data analysis. A substance match percentage of 82% was obtained on TH and 81% on VH analysis. This experiment too failed to pass the quality control of $\geq 90\%$ substance match and the data was not taken forward for interpretation.

3.4.2 Discussion:

The possible reasons for the experiment failure were discussed with SIGMA and the GE Healthcare consortia again. The microarray slide used in this experiment was a new replacement kit issued by SIGMA. Following discussions, issues of inadequate protein load on to the array slide and dye solubilisation compatibility with aqueous based solution (e.g. Buffer A) came to light. Therefore, a few alterations to the existing '*Half-labelling Microarray Protocol*' were considered. In order to achieve a maximum protein load of 150 µg onto the array slide, the protein load on the SIGMA spin columns increased from 150 µl to 300 µl. Second, the dye solubilisations were carried out using an organic solvent (e.g. dimethyl-sulphoxide; DMSO), under basic pH conditions, at room temperature instead of an aqueous based solution (AbMA extraction/labelling buffer; Buffer A). With the above modifications, a third optimisation experiment using a new sample pair #38 (CS) and #15B (CR) was carried out. This experiment was called experiment #2b.

LABELLED Cy 3 #16B (CS) vs. Cy 5 #1B (CR) FLOW CHART

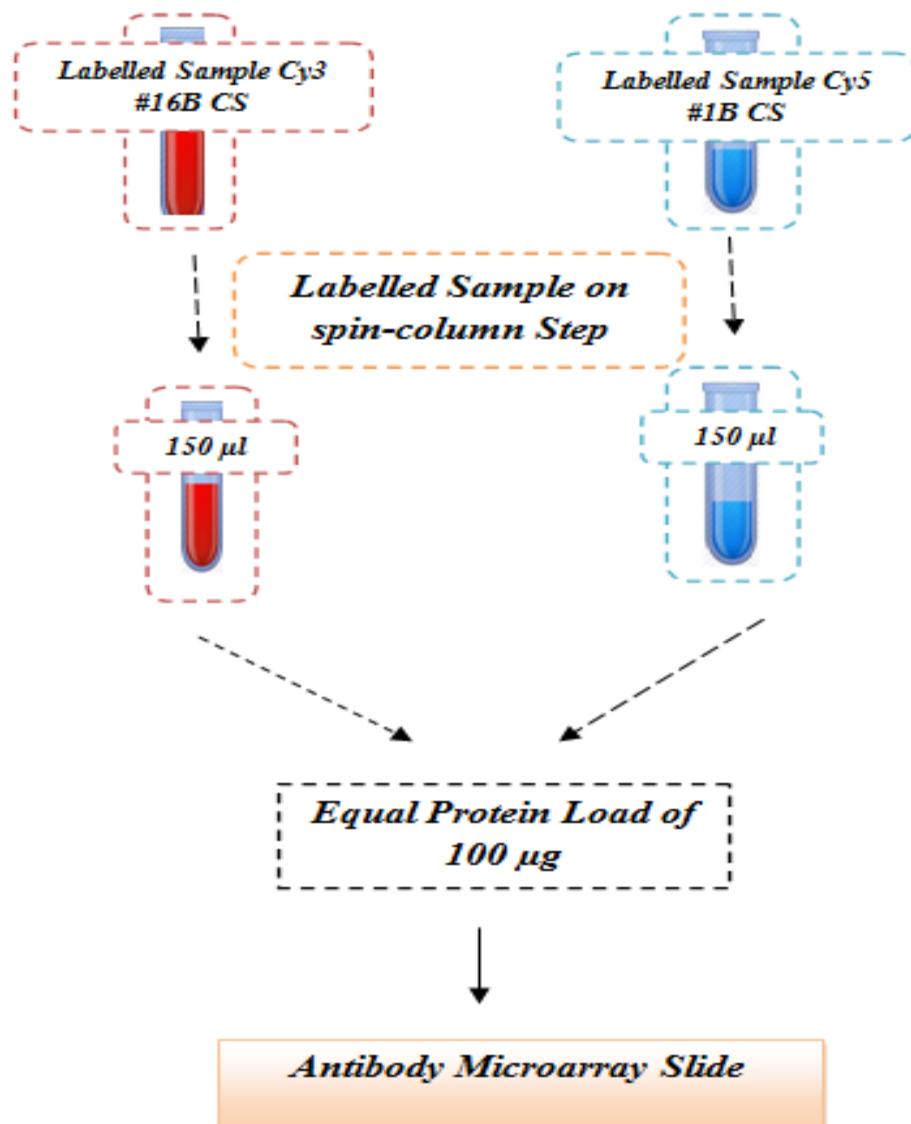


Figure 27: The flowchart for the 'Half-labelling Microarray Protocol' is as shown above. Labelled Cy3#16B and Cy5#1B were used. A volume of 150 µl was loaded onto Sigma spin-columns and a maximum 100 µg protein load was determined for each of the samples to load onto the array slide.

3.5 EXPERIMENT 2b: SAMPLE #38 (CS) vs. #15B (CR)

Protocol Used: ‘Half-Labeling Microarray Protocol’ (With modifications)

Kit: SIGMA-Panorama XPRESS-725 Profiler Kit

Catalogue #071M4826 (2012 Stock Kit)

3.5.1 Introduction:

For this optimisation experiment, three modifications were carried out to the ‘Half labelling Microarray Protocol’ as listed below:

1. A 50 µl of freshly prepared DMSO was used instead of Buffer A for the dye solubilisation
2. A 300 µl of labelled samples were loaded on to the SIGMA spin columns instead of 150 µl
3. A maximum protein load of 150 µg was added on to the array slide

The sample details, response summary along with the final protein concentrations and Buffer A sample dilution volumes are provided in the Table 23 and 24 respectively.

Table 63: Summary of Samples Characteristics and Therapy Response

Sample	Receptor Status	NACT	Response
#38(CS)	ER + PR + HER2-	EC X4; D X 4	PR
#15B(CR)	ER + PR + HER2-	EC X4; D X4	SD

Table 74: Final Sample and Dilution Buffer Volumes (µl) for Sample #38 vs #15B

Samples	Final Bradford Conc. (mg/ml)	Final Sample volumes in µl	Final Buffer A volumes in µl
#38 (CS)	3.228	154.8474	345.1526
#15B (CR)	1.825	273.50	226.50

3.5.2 Protein labelling and Dye Solubilisation:

In this experiment, cyanine dyes were diluted in a freshly prepared 50 µl of DMSO solution. The rest of the steps in the protocol were as described in sections 2.9.2 and 2.9.3. A total of 300 µl of each of the labelled sample was loaded on to the SIGMA spin columns (Figure 28). A 2nd Bradford assay was carried out using 10 µl of each labelled sample in duplicates (Table 25).

Table 85: Results from 2nd Bradford Quantification using Labelled Samples

Sample	Absorbance	Protein Concentration (mg/ml)	Average
#38 Cy3; CS	0.215	0.82122905	
#38 Cy3; CS	0.214	0.81794282	0.8195859
#15B Cy5; CR	0.235	0.886953664	
#15B Cy5; CR	0.233	0.880381203	0.8836674

EXPERIMENT 2b SAMPLE #38 vs #15B FLOWCHART

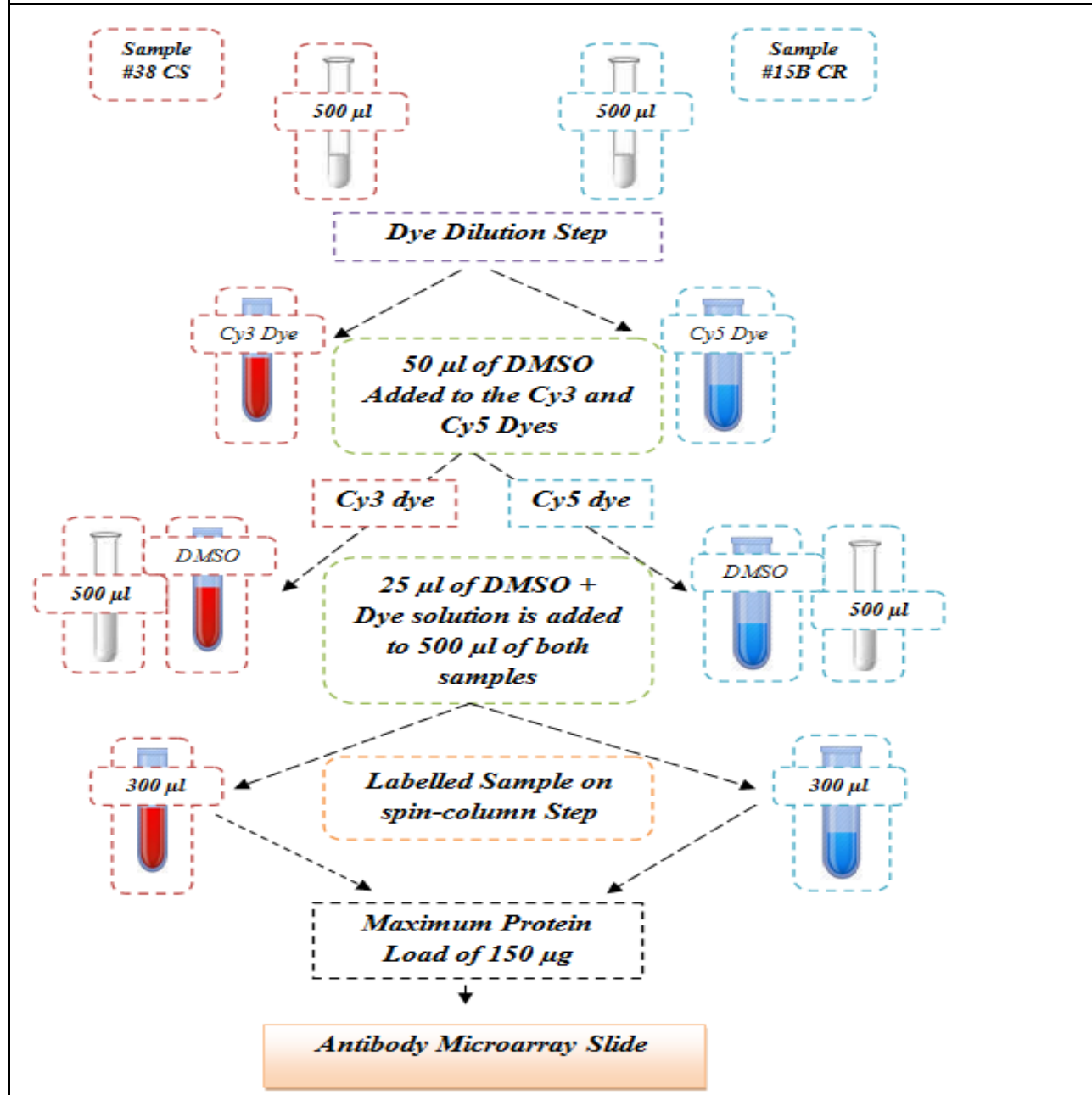


Figure 28: The flowchart for the 'Half-labelling Microarray Protocol' with modifications is as shown above. Prior to sample labelling with the dyes, the dyes are diluted with 50 µl of DMSO instead of Buffer A solution. A 25 µl of the dye-DMSO solution is then added to each of the samples to reduce the volume of dye used for the low sample volume in this protocol. A volume of 300 µl is loaded onto spin-columns and a maximum protein load of 150 µg onto the array slide.

3.5.3 D/P Ratio, Slide Hybridisation & Quality Control:

The D/P ratio for ty3 and Cy5 samples was determined as 4.32 and 4.09 respectively and a maximum protein load of 183.0 µg (150 µl) for Cy3 #38 and 169.7 µg (150 µl) for Cy5 #15B was added onto the array slide. The slide was incubated and scanned. For the above experiment, a substance match percentages of 91% on TH and 92% on VH analysis were obtained and the experiment was classed as 'Pass Quality-Control. The data obtained from this experiment was then carried forward for the final analysis. After optimising the protocol with success, the '*Half-labelling Microarray Protocol*' with modifications was used for two other experiments involving samples #12B (CS) vs #1 (CR) and the first sample pair of sample # 16B (CS) vs. 1B (CR) that failed the quality control in experiment#1 and #1b earlier.

Whilst the above experiments were optimised, a single microarray experiment was carried out using the standard '*Full-labelling Microarray Protocol*' with samples #38 (CS) and #15B (CR) to explore any quantification errors that may have caused previous two failures. As the standard protocol was previously used with the breast tumour samples in the VH pilot study, a pass quality control at sample protein concentration was considered to vindicate the possibility of such an error. This experiment was called experiment #2.

3.6 EXPERIMENT #2: SAMPLE #38 (CS) vs #15B (CR)

Protocol Used: ‘*Full-Labeling Microarray Protocol*’

Kit: SIGMA-Panorama XPRESS-725 Profiler Kit

Catalogue #089K4791 (2012 Stock Kit)

This experiment was carried out using SIGMA’s standard *Full-labeling Microarray Protocol* prior to the optimization of the ‘*Half-labeling Microarray Protocol*’. The sample pair selected for this experiment was #38 (CS) and #1B (CR) used earlier in the ‘*Half-labeling Microarray Protocol*’ optimisation experiment # 2b. The above pair was selected as it had a higher volume of lysate to carry out two experiments with ease. Further, using the same sample pairs with two different protocols (*half and full*) data comparison across two experiments could be performed to confirm the robustness of the optimised new protocol.

The volume of protein and Buffer A solution for this experiment was calculated using the formula as described in the section 2.8.1. The final sample and buffer volumes calculated for this experiment are shown in the Table 26.

3.6.1 Protein Labelling for Samples:

Following the protocol labelling as described in the section 2.8.1.1, the 1100 µl volume of sample lysate was directly mixed with cyanine dyes. A 150 µl volume of labelled protein was loaded on to the spin-columns and unbound dye removed. A 2nd Bradford quantification was performed using 10 µl of each of the sample in duplicates (Table 27).

Table 96: The Final Sample and Dilution Buffer A Volumes (µl) for Sample #38 vs #15B

Samples	Final Bradford Conc. (mg/ml)	Final Sample volumes in µl	Final Buffer A volumes in µl
#38 (CS)	3.386	324.86	775.14
#15B (CR)	1.782	617.3	482.71

Table 27: Results from 2nd Bradford Quantification using Labelled Samples

Sample	Absorbance	Protein Concentration (mg/ml)	Average
#38 Cy3; CS	0.209	0.81294964	
#38 Cy3; CS	0.198	0.778542383	0.795746
#15B Cy5; CR	0.257	0.963090397	
#15B Cy5; CR	0.254	0.9537066	0.9583985

3.6.2 D/P Ratio & Quality Control:

The D/P ratios determined for Cy3 and Cy5 in this experiment were as follows: Cy3 #38 (CS): 3.78 and Cy5 #15B (CR): 3.39. Slide was incubated with a maximum protein load of 80 μg and scanned for analysis (Figure 29). For the above experiment, substance match percentages of 93% and 93% were obtained independently by TH and VH. The data generated from this experiment carried forward for the final analysis.

EXPERIMENT #2: SAMPLE #38 (CS) vs #15B (CR) FLOW CHART

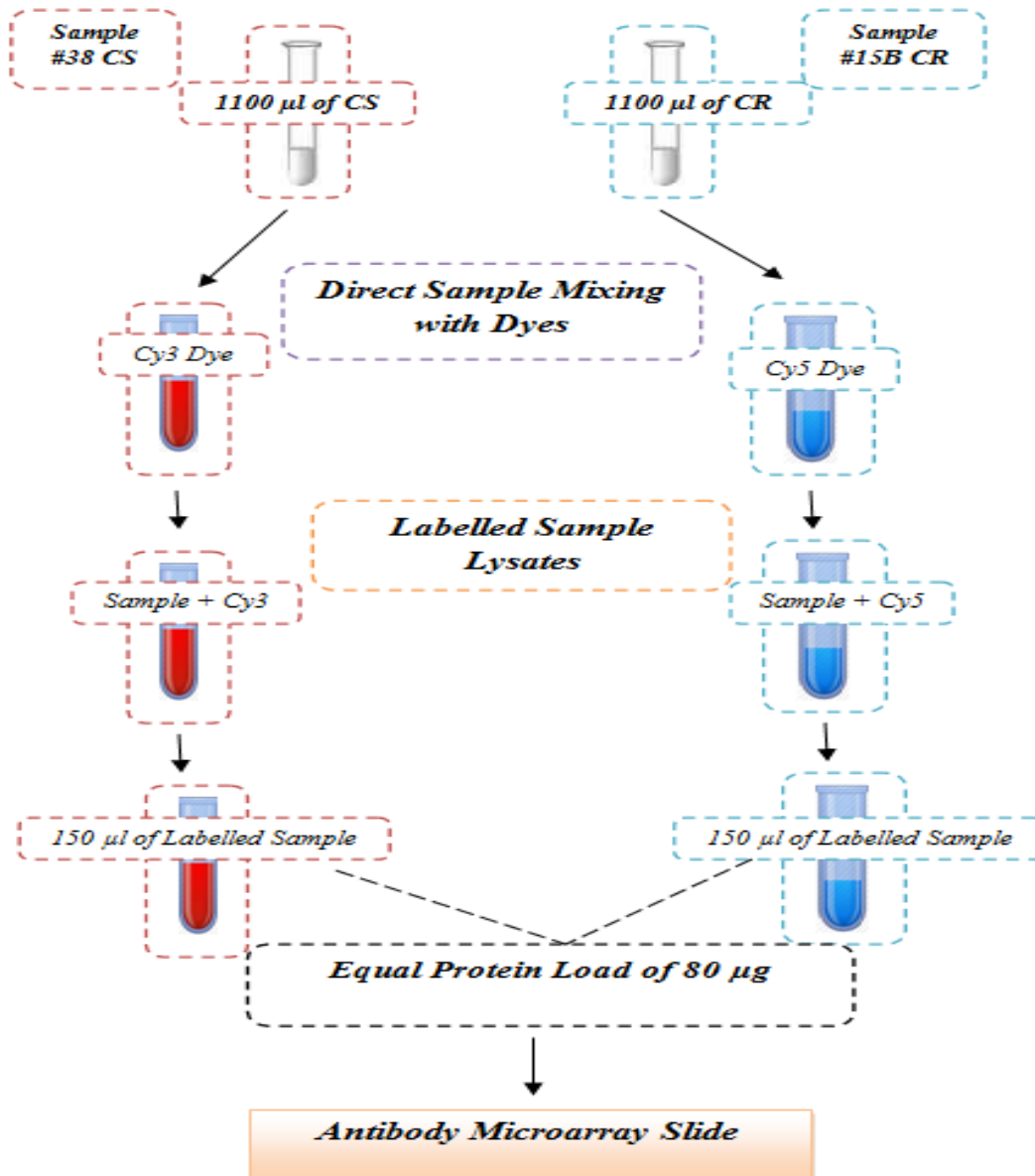


Figure 29: The 'Full-labelling Microarray Protocol' for experiment #2 is shown above. An 1100 µl of each of the sample volume was directly added to cyanine dyes and 150 µ of the labelled protein is the loaded into the spin-columns. A maximum protein of 80 µg was loaded onto the array slide.

3.7 EXPERIMENT 1c: SAMPLE 16B (CS) vs. 1B (CR)

Protocol Used: ‘*Modified-Half-Labeling Microarray Protocol*’

Kit: SIGMA-Panorama XPRESS-725 Profiler Kit

Catalogue #071M4826 (2012 Stock Kit)

This experiment was carried out using the first pair of samples #16B and 1B that earlier failed the two optimisation experiments (#1 and #1b). The sample dilution for this experiment was carried out using fresh lysates. The details of the volume dilutions used in this experiment are highlighted in the Table 28 below:

Samples	Final Bradford Conc. (mg/ml)	Final Sample volumes in μl	Final Buffer A volumes in μl
#16B (CS)	4.431977	112.84	387.15
#1B (CR)	1.263599	395.5	104.5

3.7.1 Protein labelling and Dye Solubilisation:

For this experiment, cyanine dyes were first diluted in a freshly prepared 50 μ l of DMSO (Lot #RNBB8134) solution. A total of 300 μ l of each of the labelled sample is then loaded on to the SIGMA spin columns and unbound dye removed. A 2nd Bradford assay was then carried out using 10 μ l of each labelled sample in duplicates (Table 29).

Table 29: Results from 2nd Bradford Quantification using Labelled Samples

Sample	Absorbance	Protein Concentration (mg/ml)	Average
#16B Cy3; CS	0.202	1.054961089	
#16B Cy3; CS	0.203	1.059824903	1.057393
#1B Cy5; CR	0.227	1.17655642	
#1B Cy5; CR	0.192	1.006322957	1.09144

3.7.2 D/P Ratio and Quality Control:

The D/P ratios determined for Cy 3 # 16B and Cy 5 #1B in this experiment were as follows: Cy3 #16B (CS): 2.92 and Cy5 #1B (CR): 1.8. The D/P ratio for Cy5 #1B came out ≤ 2 ; however, we decided to go ahead with the experiment following SIGMA's recommendation on a D/ P ratio ≤ 2 . A maximum protein load of 141.9 μg for Cy3 #16B and 137.4 μg for Cy5 #1B was determined and added onto the array slide. The slide was incubated and scanned. For the above experiment, a substance match percentage of 96% was obtained by TH and the data was taken forward for the final analysis. The workflow of the above experiment is illustrated in the Figure 30 below.

EXPERIMENT 1c WITH SAMPLE #16B vs #38B AND MODIFIED-HALF LABELLING MICROARRAY PROTOCOL

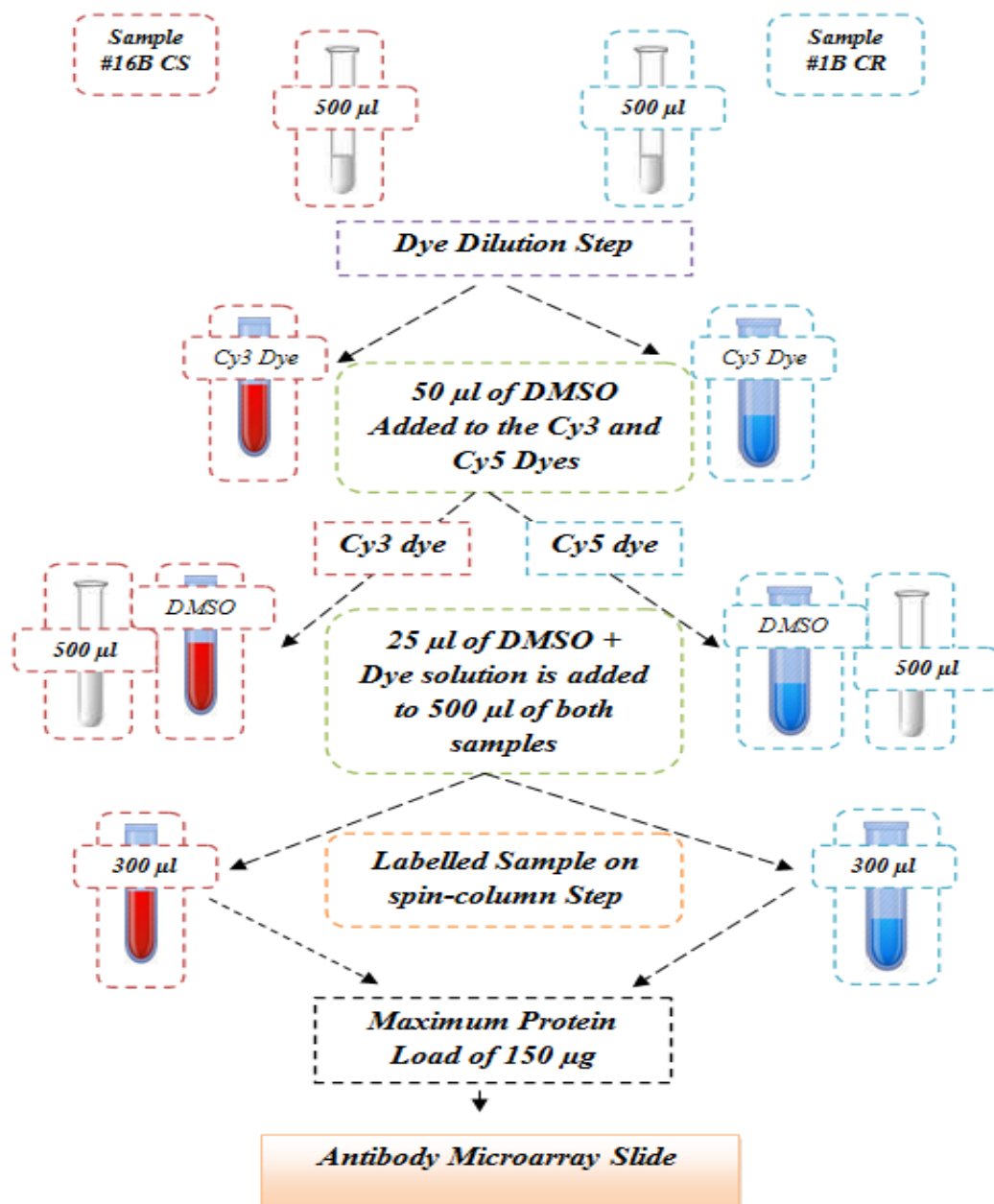


Figure 30: Repeat experiment 1c using sample #38B and #15B with the ‘Modified-Half-labelling Microarray Protocol’ is shown above.

3.8 EXPERIMENT #3: SAMPLE #12B (CS) vs. #1 (CR)

Protocol Used: ‘*Modified-Half-Labeling Microarray Protocol*’

Kit: SIGMA-Panorama XPRESS-725 Profiler Kit

Catalogue #071M4826 (2012 Stock Kit)

This experiment was carried out using the ‘*Half-labelling Microarray Protocol*’. The average Bradford quantification results for the samples are as highlighted in Table 30.

Table 100: Final Sample and Dilution Buffer A Volumes (µl) for Sample #12B vs #1

Samples	Final Bradford Conc. (mg/ml)	Final Sample volumes in µl	Final Buffer A volumes in µl
#12B (CS)	3.71145	134.7	365.3
#1 (CR)	8.07335	61.9	438.1

3.8.1 Protein labelling and Dye Solubilisation:

In this experiment, cyanine dyes were diluted in a freshly prepared 50 µl of DMSO (LOT#RNBB8134) solution. A total of 300 µl of each of the labelled sample is then loaded on to the SIGMA spin-columns. A 2nd Bradford assay was carried out using 10 µl of each labelled sample in duplicates (Table 31).

Table 31: Results from 2nd Bradford Quantification using Labelled Samples

Sample	Absorbance	Protein Concentration (mg/ml)	Average
#12B Cy3; CS	0.174	0.7939352641	
#12B Cy3; CS	0.182	0.766609881	0.752981
#1 Cy5; CR	0.295	1.151618399	
#1 Cy5; CR	0.292	1.141396934	1.146508

3.8.2 D/P Ratio and Quality Control:

The D: P ratios determined for Cy3 and Cy5 were as follows: Cy3 #38 (CS): 4.29 and Cy5 #15B (CR): 2.9. A maximum protein load of 199.46 µg was added for Cy3 #12B and 130.8 µg for Cy5 #1 onto the array slide and the slide was scanned. For the above experiment, a substance match percentage of 91% was obtained by TH and the data generated from the experiment was carried forward for the final analysis. In the Table 32 a brief summary of all the experiments (optimisations and research) with sample pairs, slide analysis percentage match data and quality-control data is provided.

Table 32: A Summary of Optimisation and Research Experimental Protocols and Quality-Control Data

OPTIMISATIONS EXPERIMENTS						
Experiment Number	Sample pair	Protocol Used	Substance Match Percentages		Quality Control	
			TH	VH	Pass	Fail
#1	#16B (CS) vs 38B (CR)	Half-Labeling	84%	85%	No	Yes
#1b	Cy3 #16B vs Cy5 #15B	Half-Labeling	82%	81%	No	Yes
#2b	#38 (CS) vs 15B (CR)	Modified-Half-Labeling	91%	92%	Yes	No
RESEACRH EXPERIMENTS						
Experiment Number	Sample pair	Protocol Used	Substance Match Percentages		Quality Control	
			TH	VH	Pass	Fail
#1c	#16B(CS) vs 38B (CR)	Modified-Half-Labeling	96%	Not done	Yes	No
#2	#38(CS) vs 15B (CR)	Full-Labeling	93%	93%	Yes	No
#3	#12B (CS)vs #1 (CR)	Modified-Half-Labeling	91%	Not done	Yes	No

3.9 MICROARRAY DATA ANALYSIS:

The data from the experiment was analysed and protein fold changes were calculated to determine a significant fold-change cut-off value as described in the section 2.8.1.3. Using the equation $y = \log_2 x$ and $x = 2^y$ where 'x' is the fold change and 'y' is the Log base 2 ratios of Cy3 and Cy5 the protein fold changes were determined. A fold change of >1.8 (log ratios above ~ 0.85) was considered significant for differential expression and represented in bold (section 2.8.1.3). Fold change values between 1.50 and 1.79 were recorded as supporting data and represented in italics. Fold change values <1.5 were not considered eligible for interpretation and recorded in the data set as '---'. Lastly, proteins that failed the quality control due to a substance match of $\geq 90\%$ in the data set were represented as \otimes .

In the Table 33 from the discovery phase of the study, the combined DEP data from all four antibody microarray experiments that passed the quality control is listed in the above described format. Table 34 lists the total number of discovered DEPs from all four antibody microarray experiments, with the total number of DEPs that had a significant (≥ 1.8) fold change values in atleast one experiment out four, 2/4 and 3/4 experiments respectively.

Table 33: Antibody Microarray Data: Current Study (4 Experiments)

Significant expression fold change (> 1.8) is indicated in bold. For proteins which show < 1.8-fold change in expression, supporting data from other experiments is shown upward of 1.5-fold. Values considered to be not significant (---) and antibody spots which did not pass the analysis criteria for experimental quality control (⊗) are also indicated.

Protein	ID	Fold change			
		#1c Repeat 16B vs 1B	#2 38 vs 15B	#2b 38 vs 15B	#3 12B vs 1
14 3 3	T5942	3.15	<i>1.54</i>	⊗	5.28
ARC	A8344	---	---	---	1.89
aSynuclein	S3062	---	---	---	---
BclxL	B9429	2.57	<i>1.71</i>	---	1.99
Calbindin D 28K	C7354	5.27	---	---	⊗
Casein Kinase 2b	C3617	---	---	---	⊗
Cathepsin D	C0715	<i>1.76</i>	---	---	⊗
CDK5	C6118	1.92	---	---	---
Csk	C7863	---	---	---	2.44
CUGBP1	C5112	2.24	⊗	---	---
Cytokeratin peptide 4	C5176	2.51	---	---	---
Dimethyl Histone H3 dimeLys 9	D5567	---	---	---	---
DR3	D3563	---	---	---	---
DR4	D3813	---	---	<i>1.79</i>	2.76
Dystrophin	D8043	1.88	---	---	---
E2F6	E1532	2.74	---	⊗	1.96
FAKpTyr577	F8926	1.98	2.05	---	⊗
FANCD2	F0305	1.95	1.86	---	2.05
G9a Methyl Transferase	G6919	⊗	1.99	---	2.3
GRANZYME B	G1044	---	1.82	---	---
HDAC2	H3159	<i>1.79</i>	---	---	---
HDAC6	H2287	1.88	---	---	---

Histone H3 pSer 10	H6409	---	1.5	---	---
ILK	I1907	2.06	2.05	⊗	---
LIM Kinase 1	L2290	---	1.81	---	---
MAP Kinase Activated Protein Kinase 2	M3550	---	---	---	---
MAP Kinase ERK1	M7927	---	---	---	---
MAP1	M4278	---	---	---	---
MAP1 Light chain	M6783	⊗	⊗	⊗	⊗
MDMX	M0445	1.8	---	---	1.51
MeCP2	M9317	---	1.86	---	---
Mint2	M3319	4.03	⊗	---	⊗
MSK1	M5437	---	---	---	3.42
Myosin Light Chain Kinase	M7905	---	---	---	---
Neurofilament 68	N5139	---	---	---	---
NFkB	N8523	1.87	⊗	---	⊗
p19INK4d	P4354	2.53	1.61	---	2.14
P38 MAP Kinase Non Activated	M8432	---	---	1.61	---
Pan cytokeratin	C2931	2.1	2.79	1.65	2.17
Pinin	P0084	1.76	---	---	2.26
PKB pSer473	P4112	1.72	---	---	⊗
PRMT2	P0748	3.56	2.91	---	---
Protein Kinase Ba	P1601	---	---	---	1.69
Protein Kinase C PKC	P5704	---	⊗	---	---
Rab7	R8779	1.74	⊗	⊗	2.16
RNaseL	R3529	---	---	---	2.25
SHPTP2	S3056	---	---	---	⊗
SNX6	S6324	---	---	⊗	5.33
SynCAM	S4945	1.97	⊗	---	⊗
Tau pSer199 202	T6819	1.98	⊗	⊗	⊗

Transforming Growth factor beta pan	T9429	3.2	1.59	---	⊗
TWEAK receptor	T9700	2.76	1.66	---	---
Tyrosine hydroxylase	T2928	---	---	---	---
Ubiquitin C terminal Hydroxylase	U5258	⊗	---	---	---
ZAP70	Z0627	---	---	1.87	---
Zyxin	Z0377	2.15	---	---	---

Table 114: Total Number of DEPs Identified from the Discover Phase: Current Study

	<i>Number</i>
Total Number of DEPs from the Antibody Microarray Discovery Phase	55
Total Number of DEPs from the Discovery Data showing a Significant Fold Change of ≥ 1.8	36
Total Number of DEPs with ≥ 1.8 Fold Change in atleast 1/4 experiments	25
Total Number of DEPs with ≥ 1.8 Fold Change in atleast 2/4 experiments	9
Total Number of DEPs with ≥ 1.8 Fold Change in atleast 3/4 experiments	2

3.9.1 Discussion:

From the discovery stage of this project, a total of 55 DEPs were discovered across four antibody microarray experiments. Of these, a total of 36 DEPs showed a significant fold change of ≥ 1.8 . A total of 25/36 DEPs were found in at least one experiment (Table 35), 9/36 DEPs in at least two experiments (Table 36) and 2/36 DEPs in at least three experiments (Table 37). Comparing the data from the sample pair #38 (CS) vs #15B (CR) which was analysed using both full (expt. #2) and half (expt. #2b) labelling protocols, a total of 15 DEPs and 4 DEPs were discovered in each of experiment respectively. Of the 15 DEPs from experiment # 2 using the standard labelling protocol, only 9/15 DEPs were found to show significant (≥ 1.8) protein expressions. In contrast, only 2/4 identified DEPs in experiment #2b from the half labelling protocol showed a significant (≥ 1.8) fold change (Table 38).

Table 35: List of Significantly Expressed DEPs : One out of Four Discovery Microarray Experiments

Proteins	Number of Experiments (n=4)	Significant fold change (≥ 1.8)
ARC	1/4	Yes
Calbindin D 28K	1/4	Yes
CDK5	1/4	Yes
CSK	1/4	Yes
CUGBP	1/4	Yes
Cytokeratin Peptide	1/4	Yes
Dystrophin	1/4	Yes
GRANZYME B	1/4	Yes
HDAC6	1/4	Yes
Pinin	1/4	Yes
Rab 2	1/4	Yes
RNaSeL	1/4	Yes
SNX	1/4	Yes
SynCAM	1/4	Yes
LIM Kinase	1/4	Yes
MDMX	1/4	Yes
MeCP2	1/4	Yes
Mint2	1/4	Yes
MSK1	1/4	Yes
NFkB	1/4	Yes
Tau pSer199202	1/4	Yes
TGF β Pan	1/4	Yes
TWEAK Receptor	1/4	Yes
ZAP 70	1/4	Yes
Zyxin	1/4	Yes

Table 36: List of Significantly Expressed DEPs : Two out of Four Discovery Microarray Experiments

Proteins (n=9)	Number of Experiments (n=4)	Significant fold change (≥ 1.8)
14-3-3	2/4	Yes
BcL-XL	2/4	Yes
DR4	2/4	Yes
E2F6	2/4	Yes
FAKpTyr577	2/4	Yes
G9a Methyl transferase	2/4	Yes
ILK	2/4	Yes
P19INK4d	2/4	Yes
PRMT2	2/4	Yes

Table 37: List of Significantly Expressed DEPs : Three out of Four Discovery Microarray Experiments

Proteins (n=2)	Number of Experiments (n=4)	Significant fold change (≥ 1.8)
FANCD2	3/4	Yes
Pancytokeratin	3/4	Yes

**Table 38: List of Significantly Expressed DEPs : Full Labelling vs. Half Labelling Protocols
Sample #38B (CS) vs. #15B (CR)**

Proteins with Significant Fold Change (≥ 1.8)	Sample pair	Proteins with Significant Fold Change (≥ 1.8)
<i>Full-Labelling Protocol</i>	#38 (CS) vs. #15B (CR)	<i>Half-Labelling Protocol</i>
FAKpTyr577		DR4
FANCD2		ZAP70
G9a MethylTransferase		
GRANZYME B		
ILK		
Lim Kinase 1		
MeCP2		
Pancytokeratin		
PRMT2		

3.9.2 Data Analysis : Combined Approach

3.9.2.1 Combined Antibody Microarray Experiment Data:

For the next stage of the project, the DEP data from the current study (4 x AbMA experiments) was combined with the antibody microarray data (5 x AbMA experiments) from the VH study (Table 39) and analysed using IPA software in the data mining phase.

A total of 89 DEPs were discovered from the combined 9 experiments (Table 40). Of these, 8/89 DEPs were found in two experiments, 5/89 in four experiments, 1/89 in four experiments, 1/89 in five experiments and 1/89 in six experiments (Table 41 and 42). In the VH study, all five antibody microarray experiments were carried out using fresh breast tumour samples (Table 9) and the '*Standard/Full-labelling Microarray Protocol*'. In the data mining phase (details to follow in next chapter) of the 89 DEPs identified using the combined analysis, only 72/89 DEPs were successfully matched onto IPA for the initial analysis.

3.9.2.2 Combined 2D-PAGE/MS & Antibody Microarray Data:

A further expansion of the list of DEPs identified at the discovery stage for IPA analysis was performed by combining the DEP data from the three 2D-PAGE/MS experiments (Table 43) of the VH study with the DEP data from the nine combined antibody microarray experiments (Table 44). The combined data from 12 discovery experiments was then re-analysed with IPA. The aim of this combined analysis was to match DEPs onto new molecular pathways involved in breast chemotherapy resistance and/or to increase the number of DEP matches onto the previously identified molecular pathways from the VH study.

Table 39: Antibody Microarray DEP Data: VH Study (5 Experiments)

Significant expression fold change (> 1.8) is indicated in bold. For proteins which show < 1.8-fold change in expression, supporting data from other experiments is shown upward of 1.5-fold. Values considered to be not significant (---) and antibody spots which did not pass the analysis criteria for experimental quality control (⊗) are also indicated.

IPA SYMBOL	ID	1 11 vs 19 Fold Changes	2 15 vs 9 Fold Changes	3 15 vs 19 Fold Changes	4 12 vs 25 Fold Changes	5 18 vs 25 Fold Changes
ZYX	Z0377	-7.797	-2.01	-2.21	-2.02	-2.63
MAPK12	S0315	-1.04	-3.76	⊗	1.07	-1.46
TPM1	T2780	-1.02	-2.67	-1.08	⊗	-1.09
YWHAQ	T5942	-1.54	-1.9	-2.29	-2.55	-1.52
CASP13	C8854	-1.28	-1.19	-2.69	-1.47	-1.08
MYD88	M9934	-1.28	-1.17	-2.08	-2.18	-1.09
TNFSF10	T9191	-1.17	-1.05	-1.83	-1.62	1.11
H3F3A	H9286	-1.09	-1.07	-1.27	-2.21	-1.03
EGF	E2520	1.01	-1.06	-1.39	-2.13	-1.17
UNC13A	M6194	-1.23	-1.14	-1.11	-2.08	-1.09
TBP	T1827	-1.45	-1.39	-1.19	-2.08	-1.37
ANXA5	A8604	-1.03	-1.27	-1.21	-2.02	-1.09
LIMS1	P9371	-1.35	-1.26	-1.51	-1.9	-1.38
PNN	P0084	⊗	2.54	2.39	1.53	1.48
RALA	R8529	1.37	CNM	3.7	⊗	1.18
PRKCB	P3203	3.256	1.16	1.29	1.7	1.24
BCL2L1	B9429	1.09	2.26	1.49	1.57	2.62
STK17A	D1314	1.03	2.18	1.05	1.22	1.37
BID	B3183	-1.05	2.16	1.55	1.97	1.96
H3F3A	D5567	2.135	-1.1	1.03	-1.11	1.03

AKT1	P1601	2.099	-1.01	-1.3	-1.1	-1.07
RIPK1	R8274	2.071	1.34	1.2	2.56	1.45
MAPT	T5530	1.63	⊗	2.04	⊗	1.17
ACAN	C8035	1.56	1.19	2	1.3	1.12
DSC1	D1286	1.07	1.06	1.92	1.45	-1.11
RELN	R4904	1.95	⊗	1.19	⊗	1.43
MKI67	P6834	1.921	1.22	1.26	1.41	1.01
RPS6KB1	S4047	1.08	1.25	1.22	2.44	1.1
RPS6KA1	R5145	1.04	1.21	1.15	2.33	1.07
PTK2	F8926	1.06	⊗	1.01	2.2	-1.08
MYC	C3956	1.32	1.23	1.15	2.17	1.02
MECP2	M9317	1.38	1.22	1.1	2.17	1.15
SIRT1	S5313	1.39	1.32	1.12	2.08	1.44
PRKCB	P3078	1.23	1.22	1.2	2.06	1.47
CHUK	I6139	1.61	1.31	1.15	2.03	1.4
SMARCB1	H9912	1.38	1.42	1.1	2.03	1.33
CETN1	C7736	1.51	1.47	1.17	1.9	1.44
TNPO1	T0825	1.13	1.28	1.16	1.84	1.26
SP1	S9809	1.39	1.35	1.08	1.82	1.08

Table 120: Combined Antibody Microarray DEP Data : Current Study + VH Study (9 Experiments)

Significant expression fold change (> 1.8) is indicated in bold. For proteins which show < 1.8-fold change in expression, supporting data from other experiments is shown upward of 1.5-fold. Values considered to be not significant (---) and antibody spots which did not pass the analysis criteria for experimental quality control (⊗) are also indicated.

Protein Name	Gene Name	#1 (11vs19)	#2 (15vs9)	#3 (15vs19)	#4 (12vs25)	#5 (18vs25)	#6 (16Bvs1B)	#7 (38vs15B)	#8 (38vs15B)	#9 (12Bvs1)
14-3-3	YWHAQ	-1.54	-1.90	-2.29	-2.55	-1.52	-3.15	-1.54	⊗	-5.28
Acetyl Histone H3 AcLys9	H3F3A	---	---	---	-2.21	---	---	---	---	---
Annexin V	ANXA5	---	---	---	-2.02	---	---	⊗	---	---
ARC	NOL3	---	---	---	---	---	---	---	---	1.89
aSynuclein	SNCA	---	---	---	---	---	---	---	---	---
BclxL	BCL2L1	---	2.26	---	1.57	2.62	2.57	1.71	---	1.99
BID	BID	---	2.16	1.55	1.97	1.96	---	---	1.69	---
Calbindin D 28K	CALB1	---	---	---	---	---	-5.27	---	---	⊗
Casein Kinase 2b	CASP13	---	---	---	---	---	---	---	---	⊗
Caspase 13	CASP13	---	---	-2.69	---	---	---	---	---	---
Cathepsin D	CTSD	---	---	---	---	---	-1.76	---	---	⊗
CDK5	CDK5	---	---	---	---	---	-1.92	---	---	---
Centrin	CETN1	1.51	---	---	1.90	---	---	---	---	---
Chondroitin sulfate	ACAN	1.56	---	2.00	---	---	---	---	---	---
cMyc	MYC	---	---	---	2.17	---	---	---	---	---
Csk	CSK	---	---	---	---	---	---	---	---	2.44
CUGBP1	CUGBP1	---	---	---	---	---	-2.24	⊗	---	---
Cytokeratin peptide 4	KRT4	---	---	---	---	---	-2.51	---	---	---
Desmosomal protein	DSC1	---	---	1.92	---	---	---	---	---	---
Dimethyl Histone H3	H3F3A	2.14	---	---	---	---	---	---	---	---
DR3	TNFRSF25	---	---	---	---	---	---	---	---	---

DR4	TNFRSF10A	---	---	---	---	---	---	---	1.79	2.76
DRAK1	STK17A	---	2.18	---	---	---	---	---	---	---
Dystrophin	DMD	---	---	---	---	---	1.88	---	---	---
E2F6	E2F6	---	---	---	---	---	-2.74	---	⊗	-1.96
Epidermal Growth Factor	EGF	---	---	---	-2.13	---	---	---	---	⊗
FAK pTyr577	PTK2	---	---	<i>1.51</i>	---	-1.95	---	---	---	⊗
FAKpTyr397	PTK2	---	⊗	---	2.20	---	-1.98	-2.05	---	⊗
FANCD2	FANCD2	---	---	---	---	---	1.95	1.86	---	2.05
G9a Methyl Transferase	EHMT2	⊗	⊗	---	---	---	⊗	-1.99	---	-2.3
GRANZYME B	GZMB	---	---	---	---	---	---	1.82	---	---
HDAC2	HDAC2	---	---	---	---	---	<i>1.79</i>	---	---	---
HDAC4	HDAC4	---	---	---	---	-1.89	---	---	---	---
HDAC6	HDAC6	---	---	---	---	---	1.88	---	---	---
Histone H3 pSer 10	H3F3A	---	---	---	---	---	---	<i>1.5</i>	---	---
hSNF5 INI1	SMARCB1	---	---	---	2.03	---	---	---	⊗	---
IKKa	CHUK	<i>1.61</i>	---	---	2.03	---	---	---	⊗	---
ILK	ILK						2.06	2.05	⊗	---
Ki-67	MKI67	1.92	---	---	---	---	---	---	---	---
LIM Kinase 1	LIMK1						---	-1.81	---	---
MAP Kinase Activated Protein Kinase 2	MAPKAPK2	---	---	---	---	---	---	---	---	---
MAP Kinase ERK1	No Human	---	---	---	---	---	---	---	---	---
MAP1	No Human	---	---	---	---	---	---	---	---	---
MAP1 Light chain	No Human	---	---	---	---	---	⊗	⊗	⊗	⊗
MDMX	MDM4	---	---	---	---	---	1.8	---	---	<i>1.51</i>
MeCP2	MECP2	---	---	---	2.17	---	---	1.86	---	---
Mint2	APBA2	---	---	---	---	---	-4.03	⊗	---	⊗
MSK1	RPSK6KA5	---	---	---	---	---	---	---	---	3.42
MyD88	MYD88	---	---	-2.08	-2.18	---	---	-1.52	---	-1.64
Munc13 1	UNC13A	---	---	---	-2.08	---	---	---	---	---

Myosin Light Chain Kinase	MYLK	---	---	---	---	---	---	---	---	---
Neurofilament 68	NEFL	---	---	---	---	---	---	---	---	---
NFkB	NFKB1	---	---	---	---	---	-1.87	⊗	---	⊗
p19INK4d	CDKN2D	---	---	---	---	---	2.53	-1.61	---	-2.14
P38 MAP Kinase Non Activated	MAPK14	---	---	---	---	---	---	---	1.61	---
Pan cytokeratin	No gene name	---	---				2.1	2.79	1.65	2.17
PINCH 1	LIMS1	---	---	-1.51	-1.90	---	---	---	---	
Pinin	PNN	⊗	2.54	2.39	1.53	---	1.76	---	---	2.26
PKB pSer473	AKT1	---	---	---	---	---	-1.72	---	---	⊗
PRMT2	PRMT2	---	---	---	---	---	-3.56	-2.91	---	---
Protein Kinase Ba	AKT1	2.10	---	---	---	---	---	---	---	1.69
Protein Kinase C PKC	PRKCB	---	---	---	---	---	---	⊗	---	---
Protein Kinase Cb1	PRKCB	---	---	---	2.06	---	---	⊗	---	---
Protein Kinase Cb2	PRKCB	3.20	---	---	1.70	---	⊗	1.53	---	⊗
Rab7	RAB7A	---	---	---	---		-1.74	⊗	⊗	-2.16
RALAR	RALA	---	⊗	3.70	⊗	---	---	---	---	⊗
Reelin	RELN	1.95	⊗	---	⊗	---	---	1.76	---	---
RIP	RIPK1	2.07	---	---	2.56	---	---	1.65	---	1.54
RNaseL	RNASEL	---	---	---	---	---	---	---	---	-2.25
ROCK1	ROCK1	---	---	---	---	---	---	---	1.96	---
Rsk1	RPS6A1	---	---	---	2.33	---	---	---	---	---
S6 Kinase	RPS6KB1	---	---	---	2.44	---	---	---	---	---
SAPK3	MAPK12	---	---	---	---	---	⊗	⊗	---	⊗
SHPTP2	PTPN11	---	-3.76	⊗	---	---	---	---	---	⊗
Sir2	SIRT1	---	---	---	2.08	---	---	1.71	---	---
SNX6	SNX6	---		---	---	---	---	---	⊗	5.33
Sp1	SP1	---	---	---	1.82	---	---	---	---	---
SynCAM	no human	---	---	---		---	-1.97	⊗	---	⊗
Tau	MAPT	1.63	⊗	2.04	⊗	---	⊗	⊗	⊗	⊗
Tau pSer199 202	MAPT	---	---	---	---	---	-1.98	⊗	⊗	⊗

TBP	TBP	---	---	---	-2.08	---	---	---	⊗	---
TRAIL	TNFSF10	---	---	-1.83	-1.62	---	---	---	⊗	---
Transforming Growth factor beta pan	TGFB1	---	---	---	---	---	-3.2	-1.59	---	⊗
Transportin 1	TNPO1	---	---	---	1.84	---	---	---	---	---
Tropomyosin	TPM1	---	-2.67	---	⊗	---	---	---	---	---
TWEAK receptor	TNFRSF12A	---			---	---	-2.76	-1.66	---	---
Tyrosine hydroxylase	TH	---		---	---	---	---	---	---	---
Ubiquitin C terminal Hydroxylase L1	UCHL1	---	---	---	---	---	⊗	---	---	---
ZAP70	ZAP70						---	---	-1.87	---
Zyxin	ZYX	-7.80	-2.01	-2.21	-2.02	-2.63	-2.15	---	---	---

Table 41: Total Number of DEPs Identified from Combined TH +VH Microarray Analysis

	<i>Number</i>
Total Number of Combined DEPs from the Discovery Phase (TH and VH AbmA)	89
Total Number of DEPs from the Discovery Data showing a Significant Fold Change of ≥ 1.8	74
Total Number of DEPs with ≥ 1.8 Fold Change in at least 2/9 experiments	8
Total Number of DEPs with ≥ 1.8 Fold Change in at least 3/9 experiments	5
Total Number of DEPs with ≥ 1.8 Fold Change in at least 4/9 experiments	1
Total Number of DEPs with ≥ 1.8 Fold Change in at least 5/9 experiments	1
Total Number of DEPs with ≥ 1.8 Fold Change in at least 6/9 experiments	1

Table 4132: DEPs Identified in ≥ 2 Experiments from the Combined Microarray Data: TH & VH Studies

DEPs in 2 or more experiments (n=16)	DEPs identified in experiments (2/9)	DEPs identified in experiments (3/9)	DEPs identified in experiments (4/9)	DEPs identified in experiments (5/9)	DEPs identified in experiments (6/9)
Bcl-XL			√		
BID		√			
DR4	√				
E2F6	√				
FAKpTyR577		√			
FANCD2		√			
ILK	√				
MeCP2	√				
MyD88	√				
P1911INK4d	√				
PRMT2	√				
Pancytokeratin		√			
Pinin		√			
RIP	√				
14-3-3				√	
Zyxin					√
Total	8	5	1	1	1

Table 43: The DEP Data from 2D-PAGE/MS Experiments (n=3) : VH Study

A total of three comparative 2D-PAGE MALDI-TOF/TOF experiments were performed by VH to identify differentially expressed proteins (DEPs) associated with chemotherapy resistance. The table lists (alphabetically by gene symbol, from the IPI database) those DEPs identified in at least two experiments (n=57), showing ≥ 2 -fold change in expression, along with the direction of change (\downarrow / \uparrow). Protein identifications with 1 peptide match are indicated (1). Where a protein is not identified as a DEP, --- is shown, to represent status unknown.

Protein	Gene Symbol	#15cs v #19cr	#15cs v #1cr	#18cs v #1cr
Activator of 90 kDa heat shock protein ATPase homolog 1	<i>AHSA1</i>	\uparrow_1	\uparrow	---
Annexin A3	<i>ANXA3</i>	---	\uparrow	\uparrow
Serum amyloid P-component	<i>APCS</i>	\downarrow	\downarrow	\downarrow_1
Apolipoprotein A1	<i>APOA1</i>	\downarrow	\downarrow	\downarrow_1
Adenine phosphoribosyltransferase	<i>APRT</i>	\uparrow_1	---	\uparrow_1
Rho GDP-dissociation inhibitor 1	<i>ARHGDI1</i>	---	\uparrow	\uparrow
Rho GDP-dissociation inhibitor 2	<i>ARHGDI2</i>	\uparrow	\uparrow	\uparrow_1
ATP synthase subunit beta, mitochondrial	<i>ATP5B</i>	\uparrow	---	\uparrow_1
Barrier-to-autointegration factor	<i>BANF1</i>	---	\uparrow	\uparrow_1
Macrophage-capping protein	<i>CAPG</i>	---	\uparrow	\uparrow
Isoform 2 of F-actin-capping protein subunit beta	<i>CAPZB</i>	\uparrow	\uparrow	\uparrow_1
T-complex protein 1 subunit beta	<i>CCT2</i>	\downarrow_1	\uparrow	---
Creatine kinase B-type	<i>CKB</i>	\downarrow	\downarrow	\downarrow
Chloride intracellular channel protein 1	<i>CLIC1</i>	\uparrow	\uparrow	\uparrow_1
Coactosin-like protein	<i>COTL1</i>	---	\uparrow_1	\uparrow
Cellular retinoic acid-binding protein 2	<i>CRABP2</i>	\uparrow_1	\uparrow	\uparrow
Isoform 1 of Eukaryotic translation initiation factor 5A-1	<i>EIF5A</i>	---	\uparrow	\uparrow
Ferritin light chain	<i>FTL</i>	\downarrow	\downarrow_1	\uparrow

Glycerol-3-phosphate dehydrogenase [NAD+] cytoplasmic	<i>GPD1</i>	↓	↓	---
Glutathione S-transferase omega-1	<i>GSTO1</i>	---	↑	↑
Glutathione S-transferase P	<i>GSTP1</i>	↓	↑	↑
HEBP2 protein (fragment)	<i>HEBP2</i>	---	↑	↑
highly similar to Heat-shock protein beta-6	<i>HSPB6</i>	↓	↓	---
Keratin, type I cytoskeletal 19	<i>KRT19</i>	↑	↑/↓	↑ ₁
Keratin, type II cytoskeletal 8*	<i>KRT8</i>	↑	↓	---
Isoform 1 of Acyl-protein thioesterase 1	<i>LYPLA1</i>	↑ ₁	↑ ₁	---
Microtubule-associated protein RP/EB family member 1	<i>MAPRE1</i>	---	↑	↑
Microfibril-associated glycoprotein 4	<i>MFAP4</i>	↓	↓ ₁	---
Myosin regulatory light chain 12B	<i>MYL12B</i>	↑	↑	↑
Isoform 1 of Nucleoside diphosphate kinase A	<i>NME1</i>	↑	↑	↑
Protein disulfide-isomerase	<i>P4HB</i>	↑	---	↑
Platelet-activating factor acetylhydrolase IB subunit beta	<i>PAFAH1B2</i>	---	↑ ₁	↑
Prohibitin	<i>PHB</i>	---	↑	↑ ₁
Inorganic pyrophosphatase	<i>PPA1</i>	---	↑	↑
Peroxiredoxin 3 isoform b	<i>PRDX3</i>	↑	↑	↑
Proteasome subunit alpha type-1(isoform long)	<i>PSMA1</i>	---	↑	↑ ₁
Proteasome subunit beta type-3	<i>PSMB3</i>	---	↑	↑
Proteasome activator complex subunit 1	<i>PSME1</i>	↑	↑	↑
Proteasome activator subunit 2	<i>PSME2</i>	---	↑	↑
Histone-binding protein RBBP4	<i>RBBP4</i>	---	↑	↑
Ribonuclease inhibitor	<i>RNH1</i>	↑	↑	↑
RPSA 40S ribosomal protein SA	<i>RPSAP15</i>	↑	↑	↑
Protein SEC13 homolog	<i>SEC13</i>	↑ ₁	↑	↑
Isoform 3 of Alpha-1-antitrypsin	<i>SERPINA1</i>	↓	↓ ₁	---
Stathmin	<i>STMN1</i>	↑	↑ ₁	↑

Tubulin-specific chaperone A	<i>TBCA</i>	↑ ₁	↑ ₁	↑ ₁
Isoform 2 of Tropomyosin alpha-1 chain	<i>TPM1</i>	↓	↑	↑
Isoform 2 of Tropomyosin alpha-3 chain	<i>TPM3</i>	↑	↑	↑
Isoform 2 of Tropomyosin alpha-4 chain	<i>TPM4</i>	---	↑	↑
Tumor protein, translationally-controlled 1	<i>TPT1</i>	↑	↑ ₁	↑
Transthyretin	<i>TTR</i>	---	↓	↓ ₁
Vimentin	<i>VIM</i>	↓	↓	↑
14-3-3 protein beta/alpha	<i>YWHAB</i>	---	↑	↑
14-3-3 protein epsilon	<i>YWHAE</i>	↑	↑	↑ ₁
14-3-3 protein gamma	<i>YWHAG</i>	---	↑	↑
14-3-3 protein theta/tau	<i>YWHAQ</i>	↑	↑	↑
14-3-3 protein zeta/delta	<i>YWHAZ</i>	↑	↑	↑

Table 144: Combined DEP Data from 2D-PAGE/MS + Microarray Experiments for IPA Analysis

A total of 3 x 2D-PAGE/MS and 9 x Combined Microarray experiments were performed using breast tumour samples in two proteomic studies (VH and TH). The combined DEP data shown below was used for IPA analysis. A total of 122 DEPs were identified from the combined approach (57 from 2D-PAGE/MS and 65 from AbMA experiments).

Protein Name	Gene Name
14-3- 3	YWHAQ
14-3-3 protein epsilon	YWHAE
14-3-3 protein gamma	YWHAH
14-3-3 protein theta	YWHAQ
14-3-3 protein zeta/delta	YWHAZ
Activator of 90 kDa heat shock protein ATPase homolog 1	AHSA1
Adenine phosphoribosyltransferase	APRT
Annexin A3	ANXA3
Annexin V	ANXA5
Apolipoprotein A1	APOA1
ARC	NOL3
ATP synthase subunit beta, mitochondrial	ATP5B
Barrier-to-autointegration factor	BANF1
BclxL	BCL2L1
BID	BID
Calbindin D 28K	CALB1
CDK5	CDK5
Cellular retinoic acid-binding protein 2	CRABP2
Centrin	CETN1
Chloride intracellular channel protein 1	CLIC1
Chondroitin sulfate	ACAN
cMyc	MYC
Coactosin-like protein	COTL1
Creatine kinase B-type	CKB

Csk	CSK
CUGBP1	CUGBP1
Cytokeratin peptide 4	KRT4
Desmosomal protein	DSC1
Dimethyl Histone H3/Acetyl Histone H3 AcLys9	H3F3A
DR4	TNFRSF10A
DRAK1	STK17A
Dystrophin	DMD
E2F6	E2F6
Epidermal Growth Factor	EGF
FAKpTyr577	PTK2
FANCD2	FANCD2
Ferritin light chain	FTL
G9a Methyl Transferase	EHMT2
Glutathione S-transferase omega-1	GSTO1
Glutathione S-transferase P	GSTP1
Glycerol-3-phosphate dehydrogenase [NAD+], cytoplasmic	GPD1
GRANZYME B	GZMB
HDAC4	HDAC4
HDAC6	HDAC6
HEBP2 protein (fragment)	HEBP2
highly similar to Heat-shock protein beta-6	HSPB6
Histone-binding protein RBBP4	RBBP4
hSNF5 INI1	SMARCB1
IKKa	CHUK
ILK	ILK
Inorganic pyrophosphatase	PPA1
Isoform 1 of Acyl-protein thioesterase 1	LYPLA1
Isoform 1 of Alpha-1-antitrypsin	SERPINA1
Isoform 1 of Eukaryotic translation initiation factor 5A-1	EIF5A
Isoform 1 of Nucleoside diphosphate kinase A	NME1
Isoform 2 of F-actin-capping protein subunit beta	CAPZB
Isoform 2 of Tropomyosin alpha-3 chain	TPM3

Isoform 2 of Tropomyosin alpha-4 chain	TPM4
Isoform 3 of Tropomyosin alpha-1 chain	TPM1
Isoform Long of 14-3-3 protein beta/alpha	YWHAB
Isoform Long of Proteasome subunit alpha type-1	PSMA1
Keratin, type I cytoskeletal 19	KRT19
Keratin, type II cytoskeletal 8	KRT8
Ki-67	MKI67
LIM Kinase 1	LIMK1
Macrophage-capping protein	CAPG
MDMX	MDM4
MeCP2	MECP2
Microfibril-associated glycoprotein 4	MFAP4
Microtubule-associated protein RP/EB family member 1	MAPRE1
Mint2	APBA2
MSK1	RPS6KA5
Munc13 1	UNC13A
MyD88	MYD88
Myosin regulatory light chain 12B	MYL12B
NFkB	NFKB1
p19INK4d	CDKN2D
peroxiredoxin 3 isoform b	PRDX3
PINCH 1	LIMS1
Pinin	PNN
Platelet-activating factor acetylhydrolase IB subunit beta	PAFAH1B2
PRMT2	PRMT2
Prohibitin	PHB
Proteasome activator complex subunit 1	PSME1
Proteasome activator subunit 2	PSME2
Proteasome subunit beta type-3	PSMB3
Protein disulfide-isomerase	P4HB
Protein Kinase Ba	AKT1
Protein Kinase Cb2/Protein Kinase Cb1	PRKCB
Protein SEC13 homolog	SEC13

Rab7	RAB7A
RALAR	RALA
Reelin	RELN
Rho GDP-dissociation inhibitor 1	ARHGDI1
Rho GDP-dissociation inhibitor 2	ARHGDI2
Ribonuclease inhibitor	RNH1
RIP	RIPK1
RNaseL	RNASEL
ROCK1	ROCK1
RPSA 40S ribosomal protein SA	RPSAP15
Rsk1	RPS6KA1
S6 Kinase	RPS6KB1
SAPK3	MAPK12
Serum amyloid P-component	APCS
Sir2	SIRT1
SNX6	SNX6
Sp1	SP1
Stathmin	STMN1
Tau pSer199 202	MAPT
TBP	TBP
T-complex protein 1 subunit beta	CCT2
TRAIL	TNFSF10
Transforming Growth factor beta pan	TGFB1
Transportin 1	TNPO1
Transthyretin	TTR
Tropomyosin	TPM1
Tubulin-specific chaperone A	TBCA
Tumor protein, translationally-controlled 1	TPT1
TWEAK receptor	TNFRSF12A
Vimentin	VIM
ZAP70	ZAP70
Zyxin	ZYX

3.10 PILOT OPTIMISATION EXPERIMENTS USING SMALL TUMOUR SAMPLES:

3.10.1 Introduction:

Keeping with the secondary aims of the current study, smaller breast tissue samples that were excluded from the study were used in pilot experiments to optimise protein extraction and quantification methods. The aim of this exercise was to optimise a protocol that will facilitate using smaller size breast core biopsy samples for future proteomic experiments.

3.10.2 Experiment Protocol:

For this pilot experiment, breast tumour samples were cut into small tissue sizes and the samples were weighed (Table 48) before suspending them into 4 w/v antibody microarray extraction/labelling buffer. All samples were then mechanically homogenised using a water sonicator bath as described in the section 2.5.1 and left on the end-over-end rotator overnight at 4°C. Protein quantification was carried out using Bradford assay at 1:2 and 1:5 dilutions. Results from the quantification for each sample are displayed below in the Table 46.

Table 45: Pilot Series Samples: Recorded Tissue Weights and Dilution Volumes

Sample #	Weight in grams	Dilution Volume in μl (4w/v)
1	0.0779	311.6
2	0.0605	242
3	0.0644	257.6
4	0.0311	124.4

Table 46: Bradford Quantification Results: AbMA Extraction Buffer & Water Sonicator Method							
sample	Absorbance	Protein concentration (x)	Correct for dilution	Average	Final concentrations (mg/ml)	Weight of Sample (g)	Conc. in mg/ml at 1ml dilution
1(neat)	0.802	2.93	2.927360775	2.932549291	5.01	0.0779	1.67
1(neat)	0.805	2.937737807	2.937737807				
1(1:2)	0.573	2.135247319	4.270494639	4.457281218			
1(1:2)	0.627	2.322033898	4.644067797				
1(1:5)	0.263	1.062953995	5.314769976	5.565548253			
1(1:5)	0.292	1.163265306	5.816326531				
2(neat)	0.761	2.785541335	2.785541335	2.73884469	4.65167762	0.0605	1.163
2(neat)	0.734	2.692148046	2.692148046				
2(1:2)	0.542	2.028017987	4.056035974	4.101003113			
2(1:2)	0.555	2.072985126	4.145970253				
2(1:5)	0.25	1.017986856	5.089934279	5.202352127			
2(1:5)	0.263	1.062953995	5.314769976				
3(neat)	0.719	2.640262885	2.640262885	2.557246627	4.270321688	0.0644	1.06
3(neat)	0.671	2.47423037	2.47423037				
3(1:2)	0.553	2.066067105	4.13213421	4.090626081			
3(1:2)	0.541	2.024558976	4.049117952				
3(1:5)	0.203	0.855413352	4.277066759	4.450017295			
3(1:5)	0.223	0.924593566	4.622967831				
4(neat)	0.737	2.702525078	2.702525078	2.683500519	3.332670356	0.0311	0.41
4(neat)	0.726	2.66447596	2.66447596				
4(1:2)	0.452	1.716707022	3.433414044	2.604462124			
4(1:2)	0.469	1.775510204	1.775510204				
4(1:5)	0.197	0.834659287	4.173296437	4.060878589			
4(1:5)	0.184	0.789692148	3.94846074				

3.10.3 Discussion:

In the above experiment, the feasibility of protein extraction using smaller size tissue samples and protein quantification to 1mg/ml concentration was explored. The protein concentrations of different size breast tissue samples were recorded and analysed to a 1ml of sample volume. Results from the Bradford assay (Table 49) showed that protein concentrations varied according to the sample size. The protein yields for samples #1 to #3 (weight range: 0.0779 -0.0644) were found to be ≥ 1 mg/ml. Sample #4 (weight 0.0311g) yielded a protein concentration of ≤ 1 mg/ml. Therefore, from the above study findings, it was hypothesised that it may be feasible to extract proteins using the antibody extraction/labelling buffer with sample weight ≥ 0.05 g using the water sonicator method for microarray analysis.

If the above results can be replicated, the next step would involve determining the number of core biopsies (14 gauge hand-held biopsy gun) that can be safely obtained from patients to yield the required protein concentration (1mg/ml) for microarray analysis. In a recent two-phase randomised controlled study, using different size biopsy guns, breast cores obtained from cadaver breast tissues and parenchymal models showed the mean specimen volume of breast tissue obtained using a 14 gauge biopsy gun can be about 14.9 mm³ (Krebs, Berg et al. 1996). Another study investigating the quantity and quality of tissue harvested from breast biopsy using 14, 16 and 18-gauge concluded, that both the quantity and quality of breast biopsy specimens was maximum with only 14-gauge biopsy needles with atleast six passes in each lesion (14-gauge, 13.14 mm²; 16-gauge, 9.6 mm²; 18-gauge, 6.41 mm²; $p < .05$) (Helbich, Rudas et al. 1998). However, in both these studies, tissue volume and surface areas and not the tissue weights were taken as the reference points to report the study findings.

Therefore, hypothesising from the above experiment (protein concentrations matches to tissue weights), if the weight to surface area and/or volume correlations are to be performed, an approximate assumption is that 3 to 4 breast cores may be needed to yield the required protein concentration of 1mg/ml to run a microarray experiment. However, researchers should be mindful that the recommended biopsy numbers have to be reasonable for patients' compliance and safety, and should also be agreeable to ethics committee for approval prior to the moving towards core biopsy sample collection from patients.

CHAPTER IV

DATA MINING

Aim:

The aim of this chapter is to discuss the data mining process using the combined antibody microarray and 2D-PAGE/MS experimental data with Ingenuity Software Analysis.

Hussain T; Scaife L; Hodgkinson V; Agarwal V; Mahapatra T; Kneeshaw P; McManus P; Lind M; Cawkwell L. A Comparative Proteomic Approach to identify putative biomarkers of chemotherapy resistance in breast cancer. Abstract, 2013 ASCO Annual Meeting, Chicago, IL.

Chapter 4.

4.1 INTRODUCTION:

In the last decade, the use of proteomic approaches in cancer research for the identification of novel biomarkers of disease diagnosis, prognosis and therapy resistance has gained popularity. Although proteomics has great potential in providing deeper understanding of the role of individual proteins and protein networks in disease and in unveiling the underlying disease mechanisms, challenges arise in transforming the large-scale experimental data into biomedical knowledge for clinical practice. Therefore, in order to understand how proteins relate to, or interact with each other in a biological context, enhanced interpretation of the generated data through the use of data mining tools is essential. The overall goal is to extract useful information that leads to the identification of protein biomarker candidates. However, data mining have limitations in that the pathways and/or protein families may not be able to find all identified proteins at the discovery stage.

4.1.1 Data Mining Approaches:

There are several widely-used bioinformatics software systems available to perform bioinformatics analysis and interpret the analysis result. Examples of some of the commonly used software programmes include R/Bioconductor, GALAXY, DAVID, KEGG, Panther, Gene Set Enrichment Analysis, PPI spider, Reactome and Ingenuity Pathway Analysis (IPA) (Satoh 2012). IPA contains a library of approximately 3,000,000 biological and chemical interactions and functional annotations in Ingenuity knowledge base). Each molecular pathway in knowledge base is manually curated by expert biologists and has definite scientific evidence. By uploading

the list of Gene IDs and expression values into the Core Analysis tool, the network-generation algorithm identifies focused genes integrated in a global molecular network which can then be selected for further investigation. IPA also calculates the score p-value that reflects the statistical significance of association between the genes and the networks by the Fisher's exact test.

4.1.2 DEP selections for IPA Analysis:

As described in the section 4.2, a combined approach was used to analyse the DEP data. Differentially expressed proteins of breast chemotherapy resistance previously identified by our research group (Hodgkinson et al, 2012) were combined with the DEP data from the current study (4 x AbMA experiments) for IPA analysis. Identified DEPs with ≥ 1.8 fold-changes in expression from the combined 9 antibody microarray experiments and ≥ 2 fold-changes in expression from the 2D-PAGE/MS studies were considered for IPA analysis. A total of 65 DEPs from the combined nine antibody microarray experiments and 57 DEPs from 2D-PAGE/MS experiments (n=122 DEPs) were found eligible for IPA analysis. Further, a literature review for proteins associated with breast chemotherapy resistance, showed 57 proteins to be involved with resistance to various cytotoxic agents (e.g. Doxorubicin, Paclitaxel, Etoposide and Mitoxantrone) in MCF-7 cell lines (Hodgkinson et al, 2010). Of the 57 implicated proteins, 14-3-3 epsilon, cytokeratin-19, HSP27, Sorcin and Stathmin were reported to be involved with anthracycline-taxane (Doxorubicin and/or Paclitaxel) resistance and confirmed on immunoblotting (Chuthapisith et al. 2007). Of these 5 proteins, 2 proteins (14-3-3 epsilon and Stathmin) were also found in the 2D-PAGE/MS pilot studies (Hodgkinson et al 2012). Therefore, a total of additional three proteins leaving the two duplicates found in 2D-PAGE/MS data were selected and added 122 DEPs and a total of 125 DEPs were loaded onto IPA for analysis (Table 47; Figure 31 and 32).

4.1.2.1 Combined Antibody Microarray IPA Analysis:

The IPA analysis was carried out in two stages; at first 72 DEPs identified from the combined antibody microarray data was analysed with their gene names. This analysis was called ‘Analysis #1’. In this analysis, a total of 65 DEPs from the original 72 loaded were mapped onto Ingenuity Knowledge Base Pathway Network. The final results from this analysis are presented in the next section of this thesis.

4.1.2.2 Combined 2D-PAGE/MS & Antibody Microarray IPA Analysis:

A further second analysis (Analysis #2), involving DEPs from the combined nine antibody microarray, three 2D-PAGE/MS experiments and three literature proteins was carried out by loading a total of 125 DEPs onto IPA as highlighted in the Figure 34. Of these, only 124 DEPs were successfully mapped onto Ingenuity Knowledge Base Pathway Network. The final results from this analysis are also presented in the following next sections of this thesis.

Table 47: Ingenuity Pathway Analysis: Data Selection & Proteomic Method

Samples	Method	DEPs
Breast Tumour Samples(TH)		
#16B ^{CS} vs #1B ^{CR} ; Half Protocol	AbMA	Appendix 3
#38 ^{CS} vs #15B ^{CR} ; Full & Half Protocols	AbMA	Appendix 4
#12B ^{CS} vs #1 ^{CR} ; Half Protocol	AbMA	Appendix 5
Breast Tumour Samples(VH)		
#11 ^{CS} vs #19 ^{CR} ; Full Protocol	AbMA	Table 43 (Hodgkinson et al.; Journal of Proteomics, Vol 75, Issue 4, 2012)
#15 ^{CS} vs #9 ^{CR} ; Full Protocol	AbMA	Table 43 (Hodgkinson et al.; Journal of Proteomics, Vol 75, Issue 4, 2012)
#15 ^{CS} vs #19 ^{CR} ; Full Protocol	AbMA	Table 43 (Hodgkinson et al.; Journal of Proteomics, Vol 75, Issue 4, 2012)
#12 ^{CS} vs #25 ^{CR} ; Full Protocol	AbMA	Table 43 (Hodgkinson et al.; Journal of Proteomics, Vol 75, Issue 4, 2012)
#18 ^{CS} vs #25 ^{CR} ; Full Protocol	AbMA	Table 43 (Hodgkinson et al.; Journal of Proteomics, Vol 75, Issue 4, 2012)
Breast Tumour Samples(VH)		
#15 ^{CS} vs #19 ^{CR}	2DMS	Table 47 (Hodgkinson et al.; Journal of Proteomics, Vol 75, Issue 9, 2012)
#15 ^{CS} vs #1 ^{CR}	2DMS	Table 47 (Hodgkinson et al.; Journal of Proteomics, Vol 75, Issue 9, 2012)
#18 ^{CS} vs #1 ^{CR}	2DMS	Table 47 (Hodgkinson et al.; Journal of Proteomics, Vol 75, Issue 9, 2012)
Literature (2D-PAGE/MS Duplicates*)		
*14-3-3 epsilon	2DMS	Chuthapisith et al.; Intl. J Oncol, 30(2007)
Sorcini	2DMS	Chuthapisith et al.; Intl. J Oncol, 30(2007)
HSP27	2DMS	Z. Fu, C. Fenselau; J.Proteome Res 4(2005)
*Stathmin	2DMS	Chuthapisith et al.; Intl. J Oncol, 30(2007)
Cytokeratin 19	2DMS	Chuthapisith et al.; Intl. J Oncol, 30(2007)

FLOWCHART SHOWING DEP NUMBERS ELIGIBLE FOR A COMBINED IPA ANALYSIS

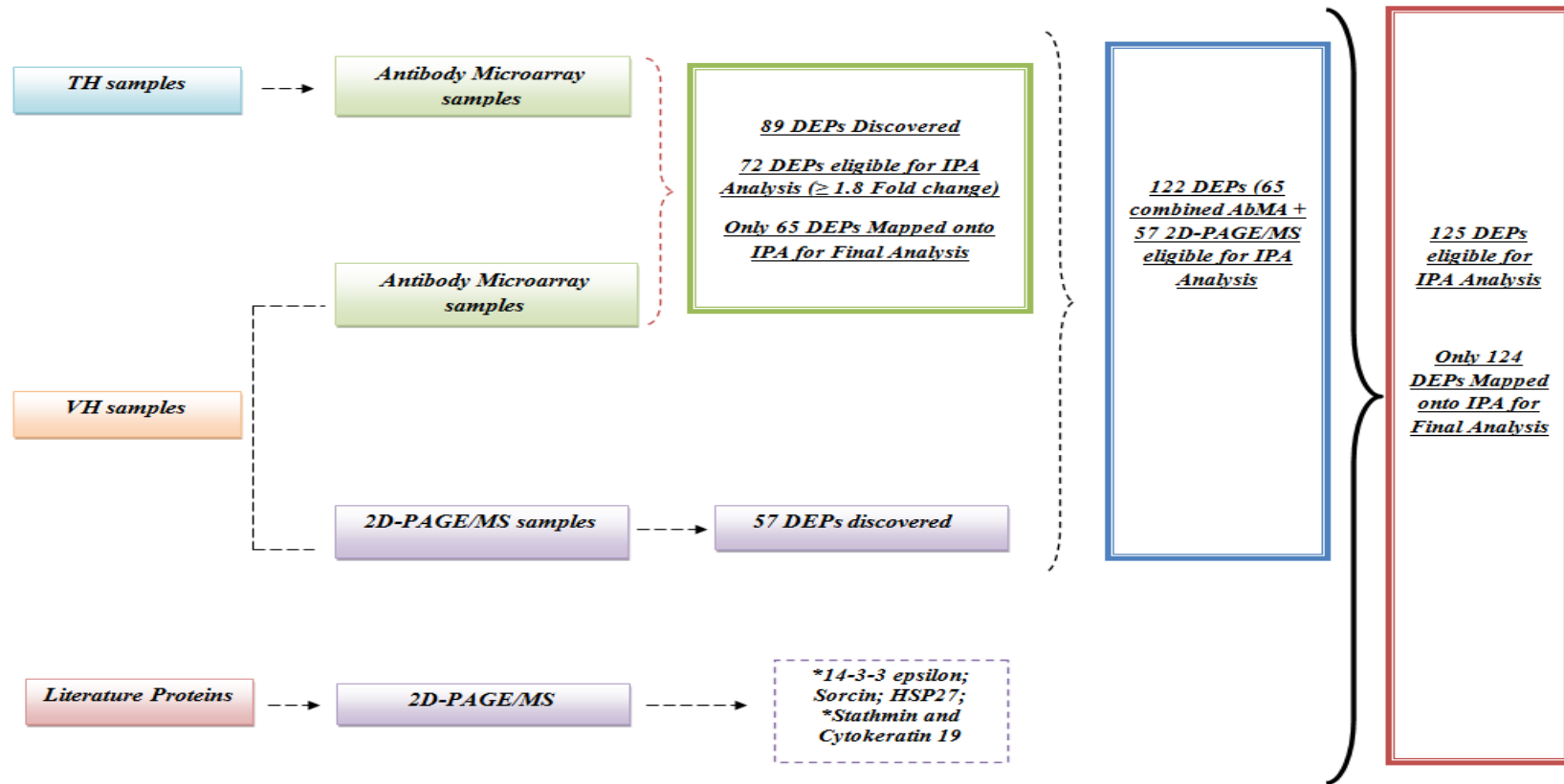


Figure 31: Flowchart showing number of DEPs that were eligible for combined IPA analysis. A total of 89 DEPs were discovered from combined 9 AbMA experiments; of these only 72 DEPs were eligible for IPA analysis after exclusions and 65/72 DEPs were matched onto IPA for analysis. From the combined 2D-PAGE/MS data, a total of 122 DEPs were found eligible for IPA loading; 3 literature proteins (* protein duplicates from 2D-PAGE/MS) were added onto this list a total of 125 DEPs were loaded onto IPA.

FLOWCHART SHOWING SOURCE OF DEP DATA FOR COMBINED IPA ANALYSIS

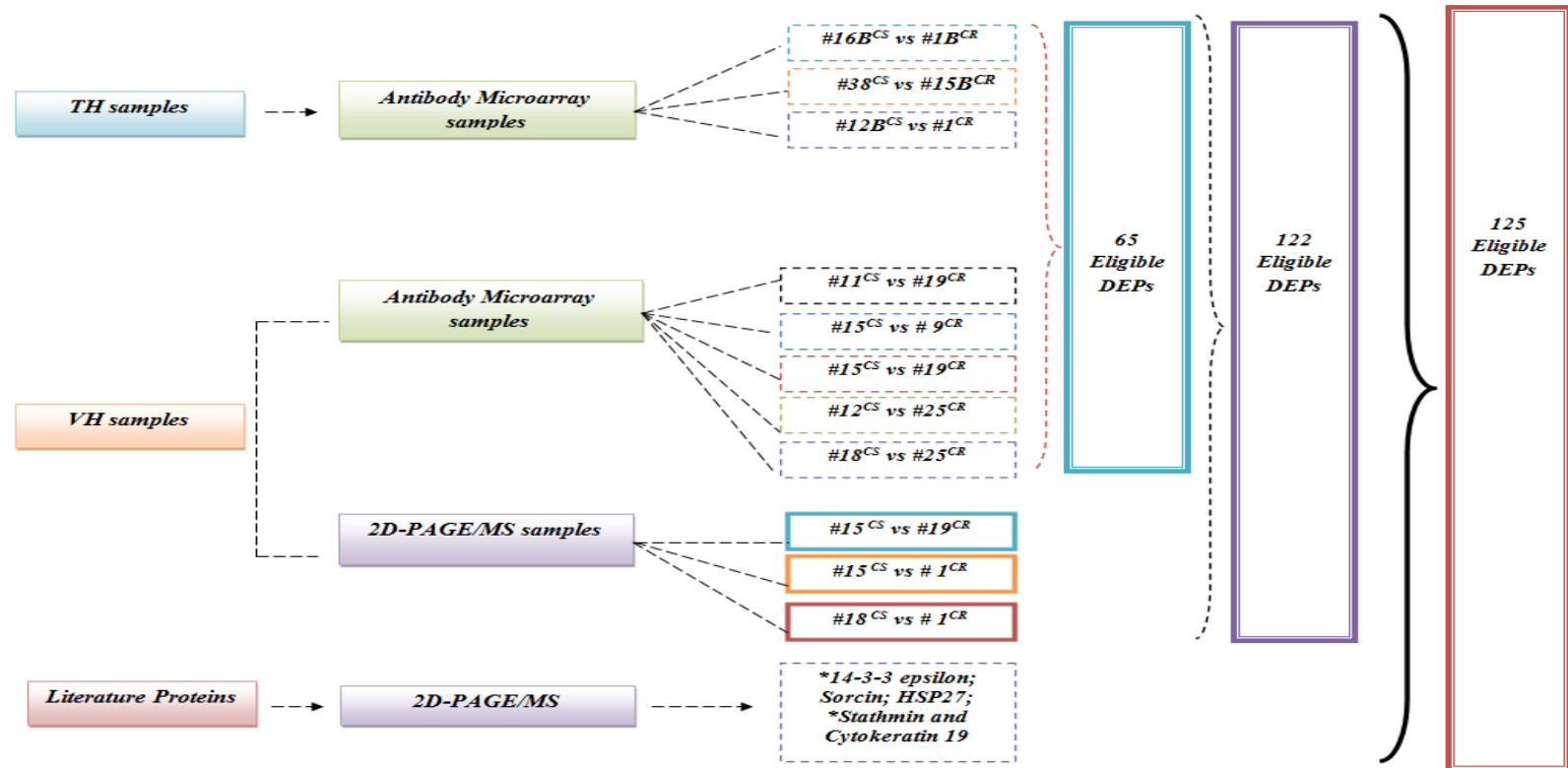


Figure 32: Flowchart showing the source of DEPs for combined IPA analysis is shown. DEPs from the current study and the VH pilot work along with the 5 literature proteins from the Mcf-7 cell line work were analysed with IPA. A total of 125 DEPs (65 from combined AbMA 9 experiments + 57 from 2D-PAGE/MS + 3 additional literature proteins) were loaded onto IPA of which 124 were successfully mapped onto IPA for final analysis. * Protein duplicates from 2D-PAGE/MS data

4.2 RESULTS:

4.2.1 Combined Antibody Microarray (9 experiments) Data Mining Results:

As described in the section 4.1.2 and Figures 34 and 35, a total of 89 DEPs were discovered from combined nine antibody microarray experiments. Of these only 72/89 DEPs were eligible for IPA analysis and 17/89 DEPs were excluded if found only once in each of the nine experiments and/or had missing gene names. A total of 72 DEPs with their gene names were loaded onto IPA (Appendix 6) and the protein genes were matched onto the pathway network of Ingenuity Knowledge Base (Analysis #1, section 4.1.2.1). A total of 65/72 molecules in the dataset were matched and a list of 269 canonical pathways was generated. The top three canonical networks identified from the data were ‘Cell Death and Survival’, ‘Renal Necrosis/Cell Death’ and ‘Cell-To-Cell Signalling and Interaction’ pathways. In total the three pathways between them contained 56 focus molecules with a network score of 115. Further, IPA also identifies top five canonical pathways from the protein matches and included ‘CML signalling’ with 11 DEPs, ‘IL-8 signalling’ with 11 DEPs, ‘ERK5 with 6 DEPs, ‘Molecular Mechanisms of Cancer’ with 13 DEPs and ‘Pancreatic signalling’ pathways with 6 DEPs respectively. Other 5 canonical pathways were selected if they included atleast 4 proteins from the combined analysis #1 data set and included 14-3-3 mediated signalling (6 DEPs), apoptosis signalling (6 DEPs), death receptor signalling (6 DEPs), PI3K/AKT signalling (8 DEPs) and PTEN signalling (8 DEPs). A list of top five canonical pathways and five other selected pathways with the number of matched DEPs is highlighted in the Table 48.

Table 48: Canonical Pathways and Protein Matches Identified on IPA with Combined Analysis # 1 Data

The table shows the top 5 and 5 other most relevant canonical pathways identified by IPA (n=10). The 5 pathways were selected if they had atleast 4 molecules from the data. The molecules (gene identifiers) associated with each of the canonical pathways are listed in a decreasing order, along with the number of canonical pathways (-) each of them appeared in. For each canonical pathway, the number of matched molecules from the data is also shown at the end.

Gene Identifier	IPA Identified Canonical Pathways									
	CML signalling	ERK5 Signalling	IL8 Signalling	Molecular Mechanisms of Cancer	Pancreatic Signalling	14-3-3 mediated	PIP3/ AKT	PTEN	Apoptosis Signalling	Death Receptor Signalling
NFKB1 ⁽⁹⁾	√		√	√	√	√	√	√	√	√
AKT1 ⁽⁸⁾	√	√	√	√	√	√	√	√		
BCL2L1 ⁽⁷⁾	√		√	√	√		√	√	√	
CHUK ⁽⁵⁾	√		√				√	√	√	
MAPK12 ⁽⁴⁾			√	√			√	√		
RPS6KB1 ⁽⁴⁾		√	√				√	√		
BID ⁽³⁾				√					√	√
EGF ⁽³⁾		√	√		√					
E2F6 ⁽³⁾	√			√	√					
MYC ⁽³⁾	√	√		√						
PTK2 ⁽³⁾			√	√				√		
RPS6KA1 ⁽³⁾	√					√			√	
CDKN2D ⁽²⁾				√						√
ILK ⁽²⁾							√	√		
PRKCB ⁽²⁾			√	√						

RALA ⁽²⁾				√	√					
ROCK ⁽²⁾			√						√	
TGFB1 ⁽²⁾	√			√						
TNFSF10 ⁽²⁾						√				√
YWHAQ ⁽²⁾		√				√				
FANCD2 ⁽¹⁾				√						
HDAC4 ⁽¹⁾	√									
HDAC6 ⁽¹⁾	√									
LIMK1 ⁽¹⁾			√							
LIMS1 ⁽¹⁾							√			
MAPT ⁽¹⁾						√				
RIPK1 ⁽¹⁾										√
RPS6KA5 ⁽¹⁾		√								
TNFRSF10A ⁽¹⁾										√
# Molecules	11	6	11	13	6	6	8	8	6	6

4.2.2 Combined Antibody Microarray & 2D-PAGE/MS Data Mining Results:

A total of 125 proteins with their gene names (65 from combined AbMA experiments + 57 from 2D-PAGE/MS experiments + 3 literature proteins; (Figure 35) (Appendix 7) were loaded onto IPA in this analysis (Analysis #2, section 4.1.2.2). Of these, a total of 124 DEPs were mapped on to the Ingenuity Knowledge Base and a list of 286 canonical pathways was generated. Some of the pathways identified in this combined analysis (analysis #2) overlapped with the pathways identified in the analysis #1. Looking at the enormity of the generated data output (286 pathways) from this analysis, only 9 pathways out of 286 were selected for analysing chemoresistance. Of these, 5 pathways were the top 5 canonical pathways given by IPA and the other four were manually selected. The criteria to pathway selection were defined and included, pathways which had 4 or more DEPs mapped onto them from the data set and/or had a highest number of DEP matches onto a single discrete pathways and/or if a pathway(s) had been previously reported with chemotherapy resistance in cancers and/or if pathway dysregulation can be associated with chemoresistance. The 9 selected pathways with the matched DEPs are highlighted in the Table 49. Further, Table 50 highlights the 6 most relevant pathways selected from the original 9 pathways with their DEPs matches. These 6 pathways included PIP3/AKT signalling pathway with 13 DEPs matches, 14-3-3 mediated pathway with 11 DEPs, ERK/MAPK signalling pathway with 10 DEPs, P70S6K pathway with 12 DEPs, Cell Cycle: G2/M DNA Damage Checkpoint Regulation pathway with 6 DEPs and Death receptor signalling pathway with 6 DEPs respectively. Each pathway with DEPs from across the combined data (analysis #2, section 4.2.2) is illustrated in Figures 33 to 38.

Table 49: IPA Identified Canonical Pathways and Protein Matches with Combined Analysis # 2 Data

The table shows the top 5 and 4 other most relevant canonical pathways identified by IPA (n=9), that contain at least 4 molecules from the data. The molecules (gene identifiers) associated with each of the canonical pathways are listed, along with the number of canonical pathways (-) each of them appeared in decreasing order. For each canonical pathway, the number of matched molecules from the data is also shown at the end.

*YWHAZ (14-3-3 zeta/delta); *YWHAQ (14-3-3 theta/tau);*YWHAG (14-3-3 gamma);*YWHAB(14-3-3 epsilon);*YWHAE(14-3-3 epsilon)

Gene Identifier	IPA Identified Canonical Pathways								
	PIP3/AKT Signalling	ERK 5 Signalling	14-3-3 Mediated Signalling	Acute Phase Response Signalling	Myc Apoptosis Signalling	Death Receptor Signalling	P70S6K Signalling	Cell Cycle: G2/M DNA Damage Checkpoint Regulation	ERK/MAPK Signalling
*YWHAZ ⁽⁷⁾	√	√	√		√		√	√	√
*YWHAQ ⁽⁷⁾	√	√	√		√		√	√	√
*YWHAG ⁽⁷⁾	√	√	√		√		√	√	√
*YWHAB ⁽⁷⁾	√	√	√		√		√	√	√
*YWHAE ⁽⁷⁾	√	√	√		√		√	√	
AKT1 ⁽⁶⁾	√	√	√	√	√		√		
RPS6KA1 ⁽⁴⁾		√	√				√		√
CHUK ⁽³⁾	√			√		√			
PRKCB ⁽³⁾			√				√		√
NFKB1 ⁽³⁾	√			√		√			
MYC ⁽³⁾		√			√				√
MAPK12 ⁽³⁾			√	√	√				
RPS6KB1 ⁽³⁾	√	√					√		
RIPK1 ⁽²⁾				√		√	√		

VIM ⁽³⁾			√	√			√		
BID ⁽²⁾					√	√			
H3F3A/H3F3B ⁽²⁾	√								√
RPS6KA5 ⁽²⁾		√							√
MAPT ⁽²⁾			√				√		
TTR ⁽¹⁾					√				
TNFSF10 ⁽¹⁾						√			
TNFRSF10A ⁽¹⁾						√			
SERPINA1 ⁽¹⁾				√					
PTK2 ⁽¹⁾									√
MYD88 ⁽¹⁾				√					
MDM4 ⁽¹⁾								√	
LIMS1 ⁽¹⁾	√								
ILK ⁽¹⁾	√								
FTL ⁽¹⁾				√					
EGF ⁽¹⁾				√					
CRABP2 ⁽¹⁾				√					
BCL2L1 ⁽¹⁾	√								
APOA1 ⁽¹⁾				√					
APCS ⁽¹⁾				√					
#Molecules	13	10	11	13	10	6	12	6	10

Table 50: Relevant Pathways Selected from the Combined Analysis # 2 Data

Canonical Pathway	Number of Mapped DEPs
PIP3/AKT Signalling	13
14-3-3 Mediated	11
P70S6K Signalling	12
ERK/MAPK Signalling	10
Cell Cycle: G2/M DNA Damage Check point Regulation	6
Death Receptor Signalling	6

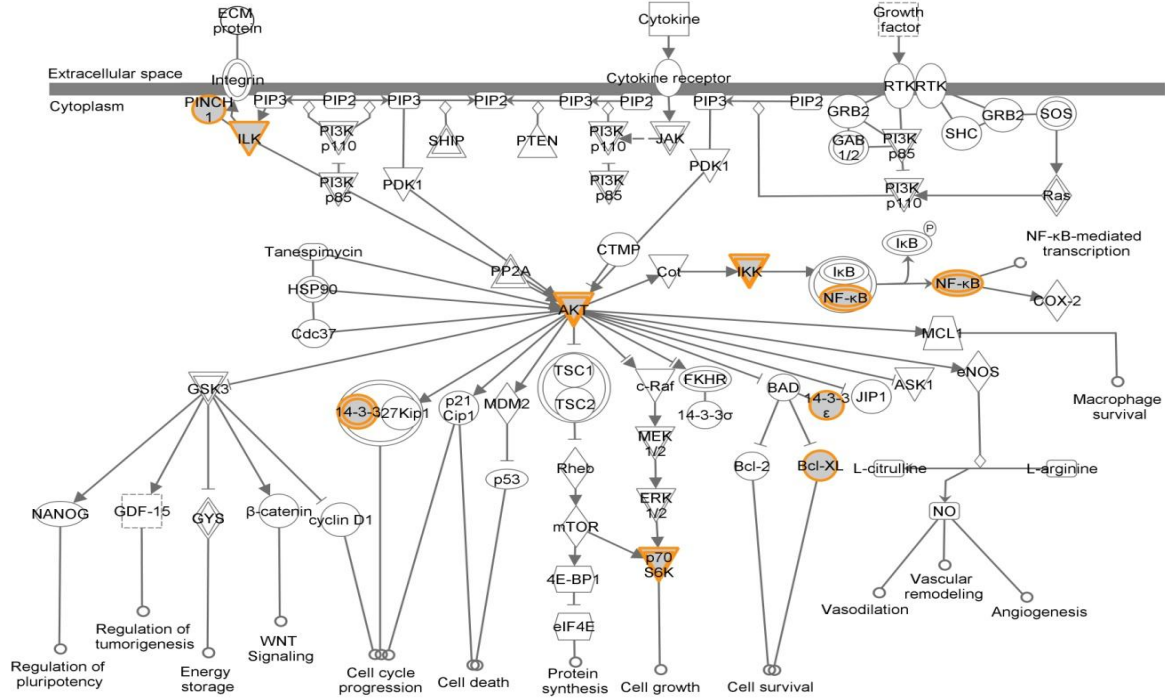
4.2.3 Confirmed DEPs from the Combined Data: VH Study

Previously, our research group confirmed a total of three DEPs on immunoblotting from the combined AbMA + 2D-PAGE/MS data in the VH study. Details of the three confirmed DEPs with their used antibody dilutions and antibody details are listed in the Table 51 below.

Table 151: Previously Confirmed DEPs on Immunoblotting:

<i>Protein</i>	<i>Antibody Dilution</i>	<i>Antibody Cat #</i>
14-3-3 (beta, eta, tau and sigma)	1:1000	ab9063 (AbCAM)
BID	1:200	ab32060 (AbCAM)
BcL-XL	1:400	ab23270(AbCAM)

PI3K/AKT Signaling



© 2000-2013 Ingenuity Systems, Inc. All rights reserved.

● Breast AbMA
● Breast 2DMS

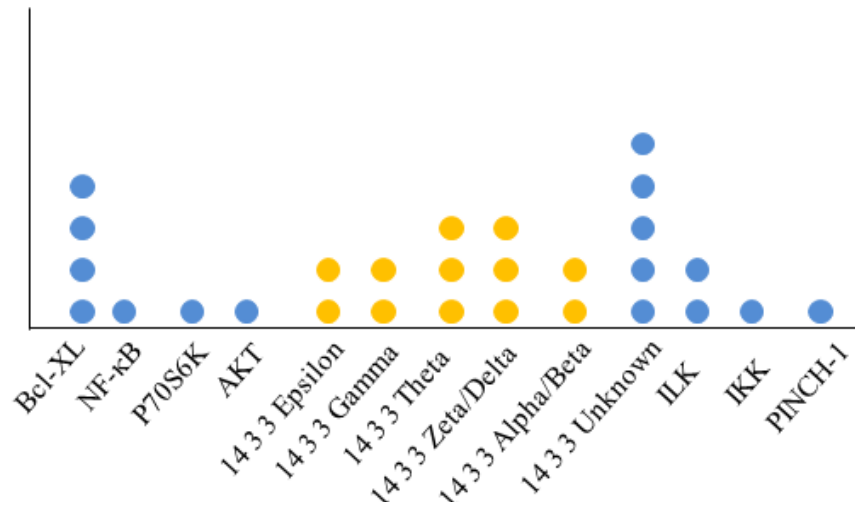
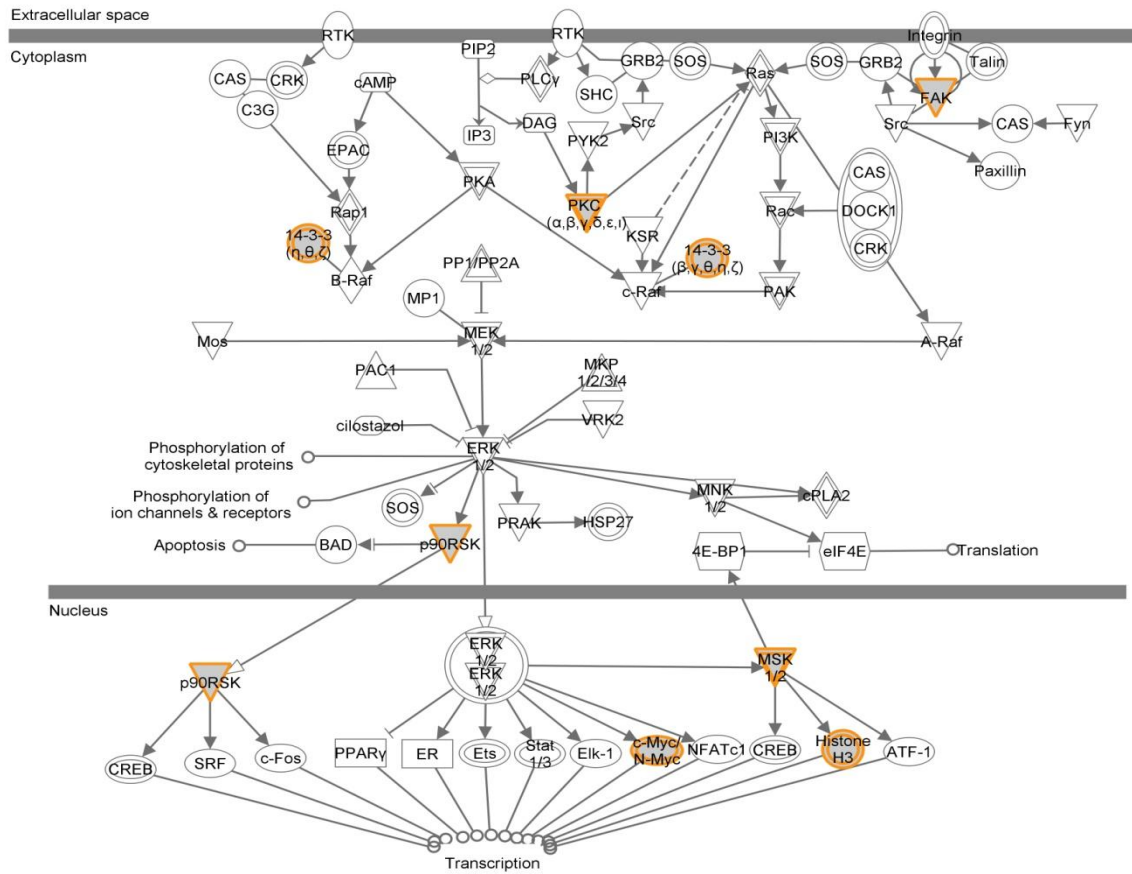


Figure 33: A total of 13 DEPs were mapped onto the PI3K AKT signalling pathway. Of these 13, 8 proteins were identified more than once. As seen in the figure above, the total number of DEPs highlighted in the pathway are different to the total numbers actually mapped onto the pathway (bar chart); this variability is because each pathway is created manually after searching literature listing the proteins and their isoforms either under a single gene name or omitting inclusion of some proteins or their isoforms due to paucity of evidence in defining their roles in the pathway development.

ERK/MAPK Signaling



© 2000-2013 Ingenuity Systems, Inc. All rights reserved.

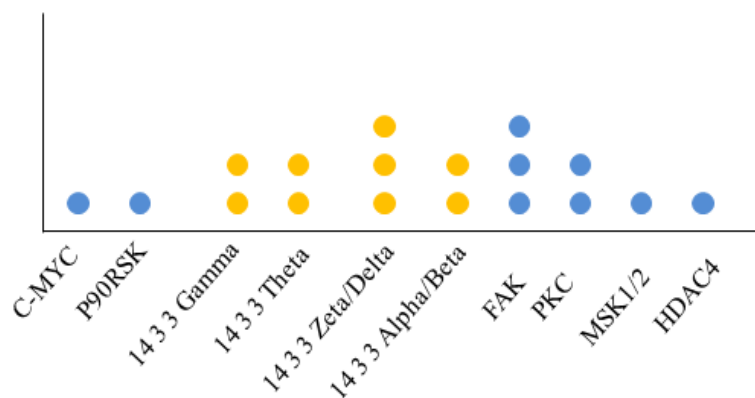
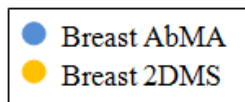
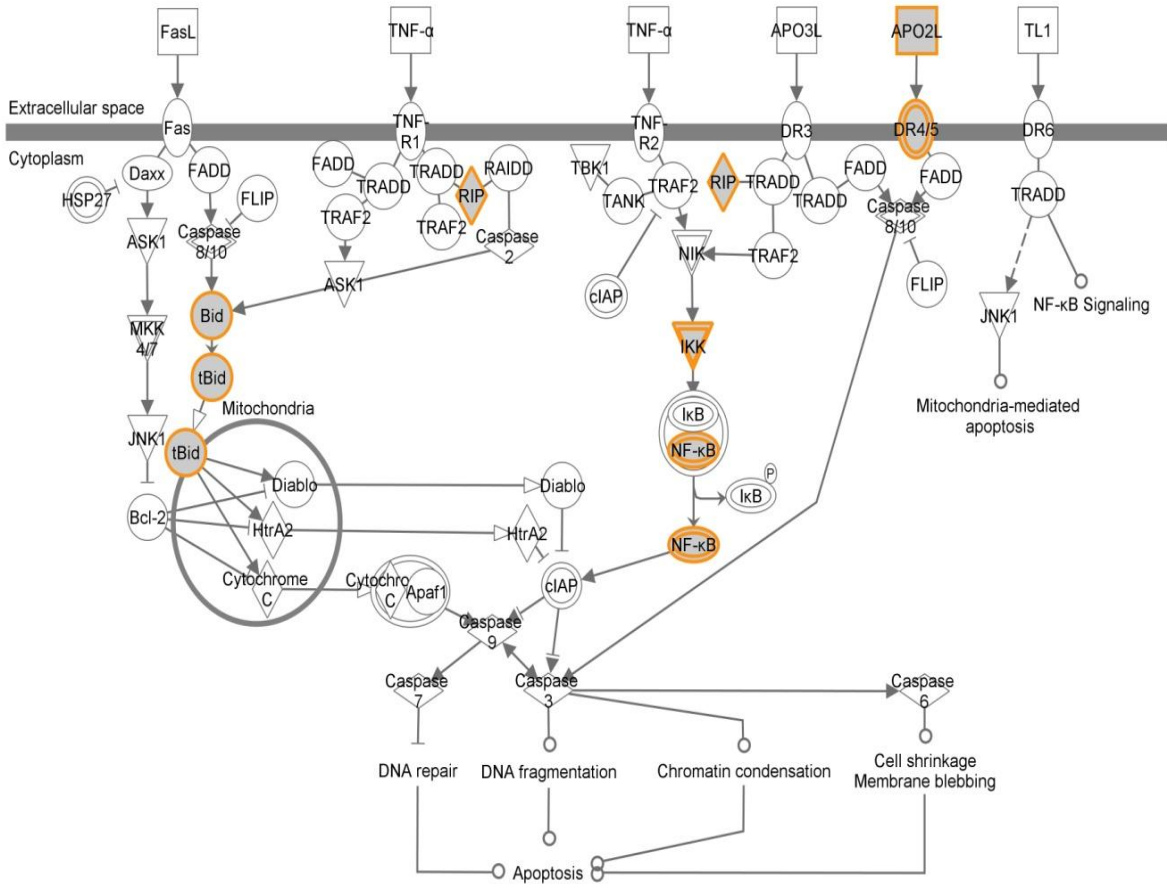


Figure 34: A total of 10 DEPs were mapped onto the ERK MAPK Signaling pathway as indicated above. Of these 10, 6 proteins were identified more than once.

Death Receptor Signaling



© 2000-2013 Ingenuity Systems, Inc. All rights reserved.

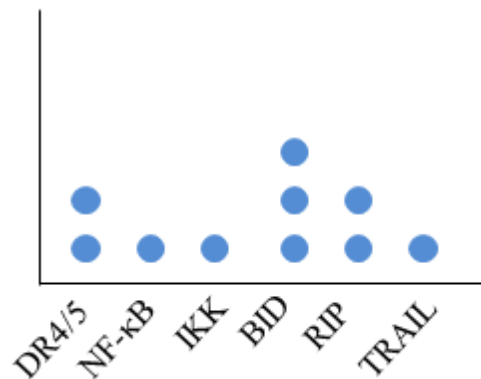
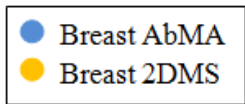
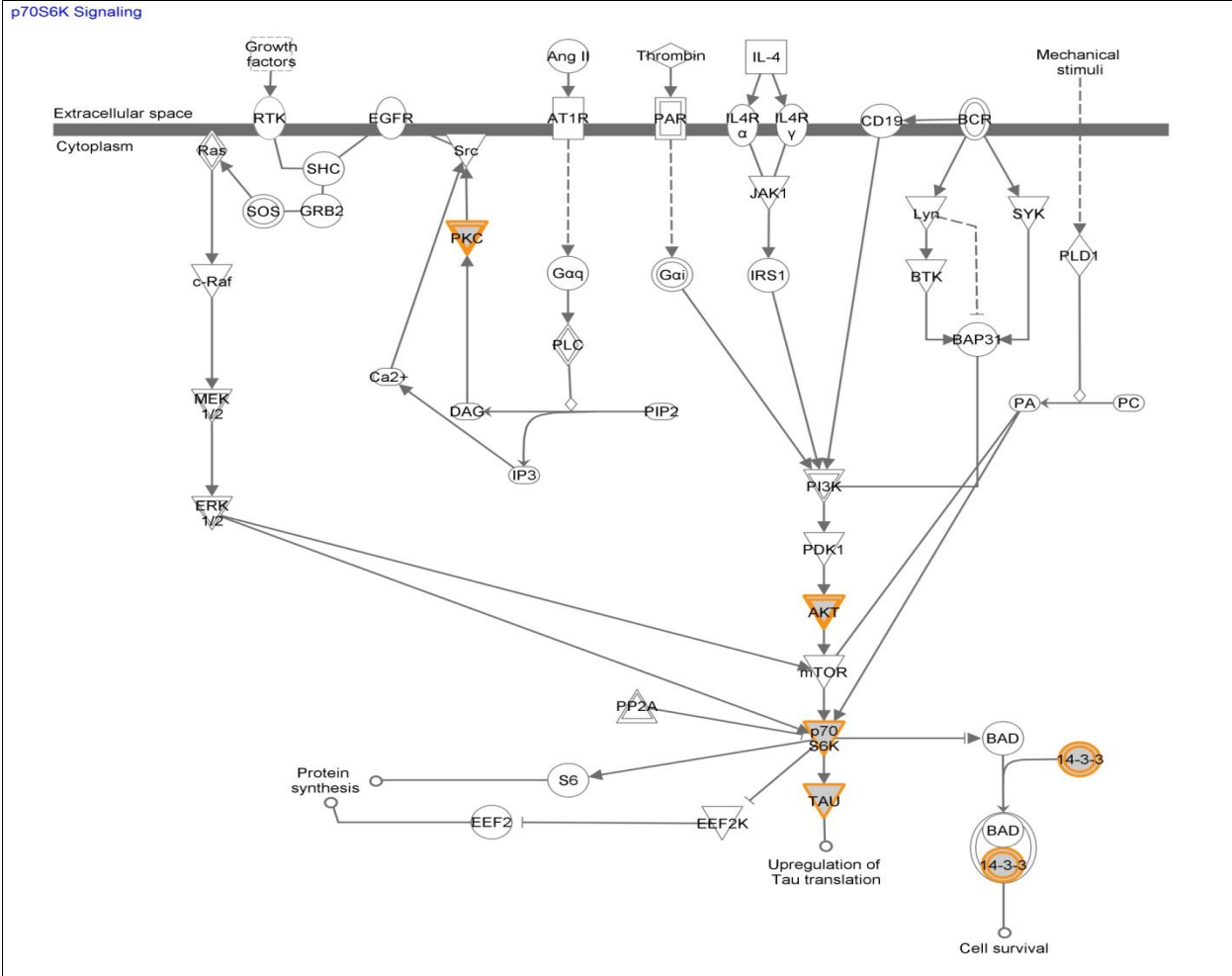


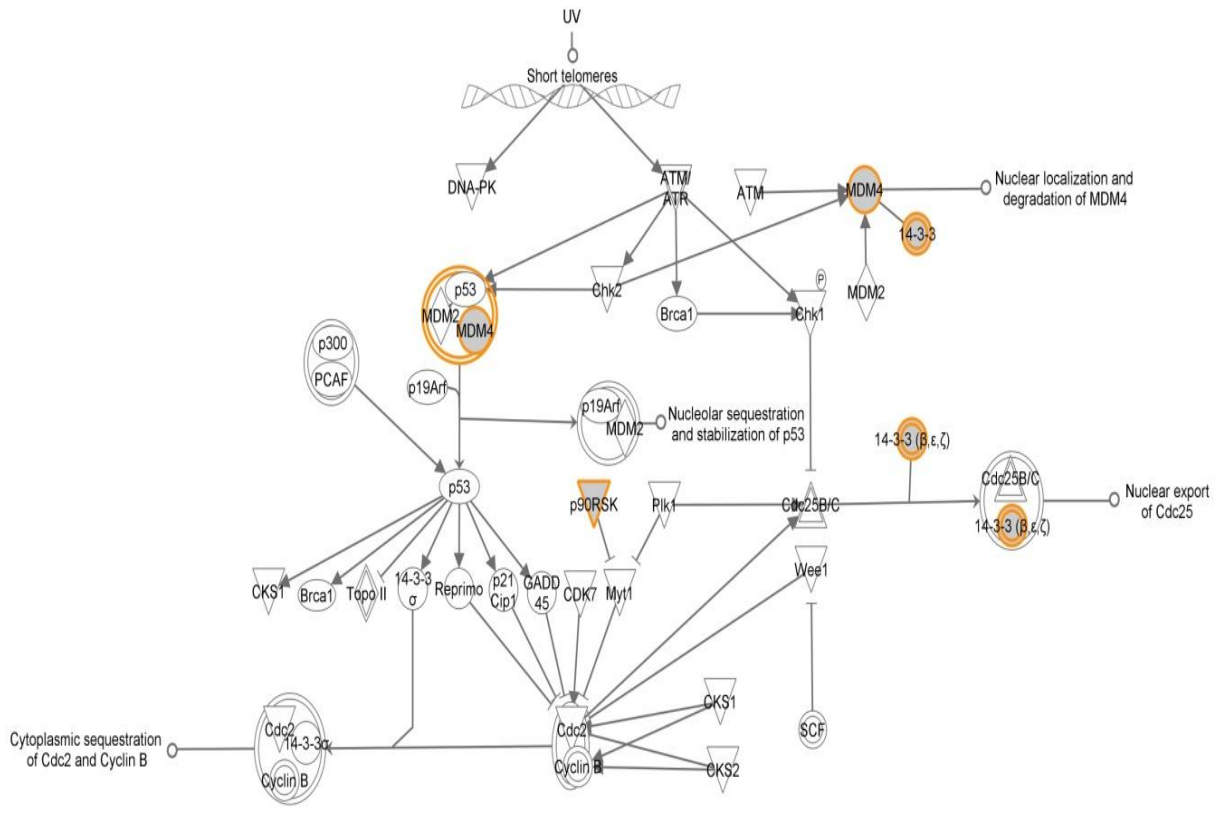
Figure 35: A total of 6 DEPs were mapped onto the Death Receptor Signaling pathway as indicated above. Of these 6, 3 proteins were identified more than once.



● Breast AbMA
● Breast 2DMS



Figure 36: A total of 9 DEPs were mapped onto the P70S6K Signalling pathway as indicated above. Of these 9, 7 proteins were identified more than once.



© 2000-2013 Ingenuity Systems, Inc. All rights reserved.

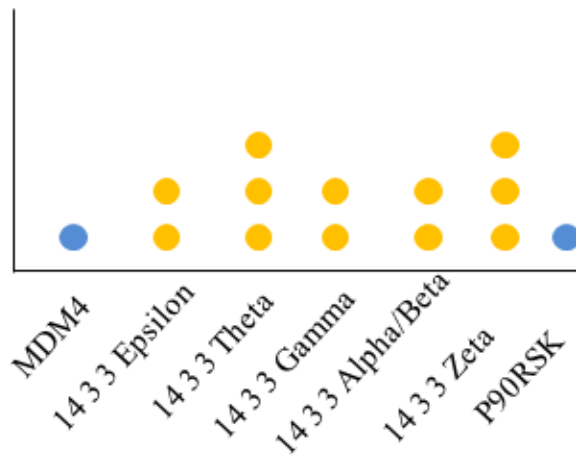
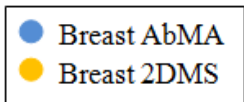
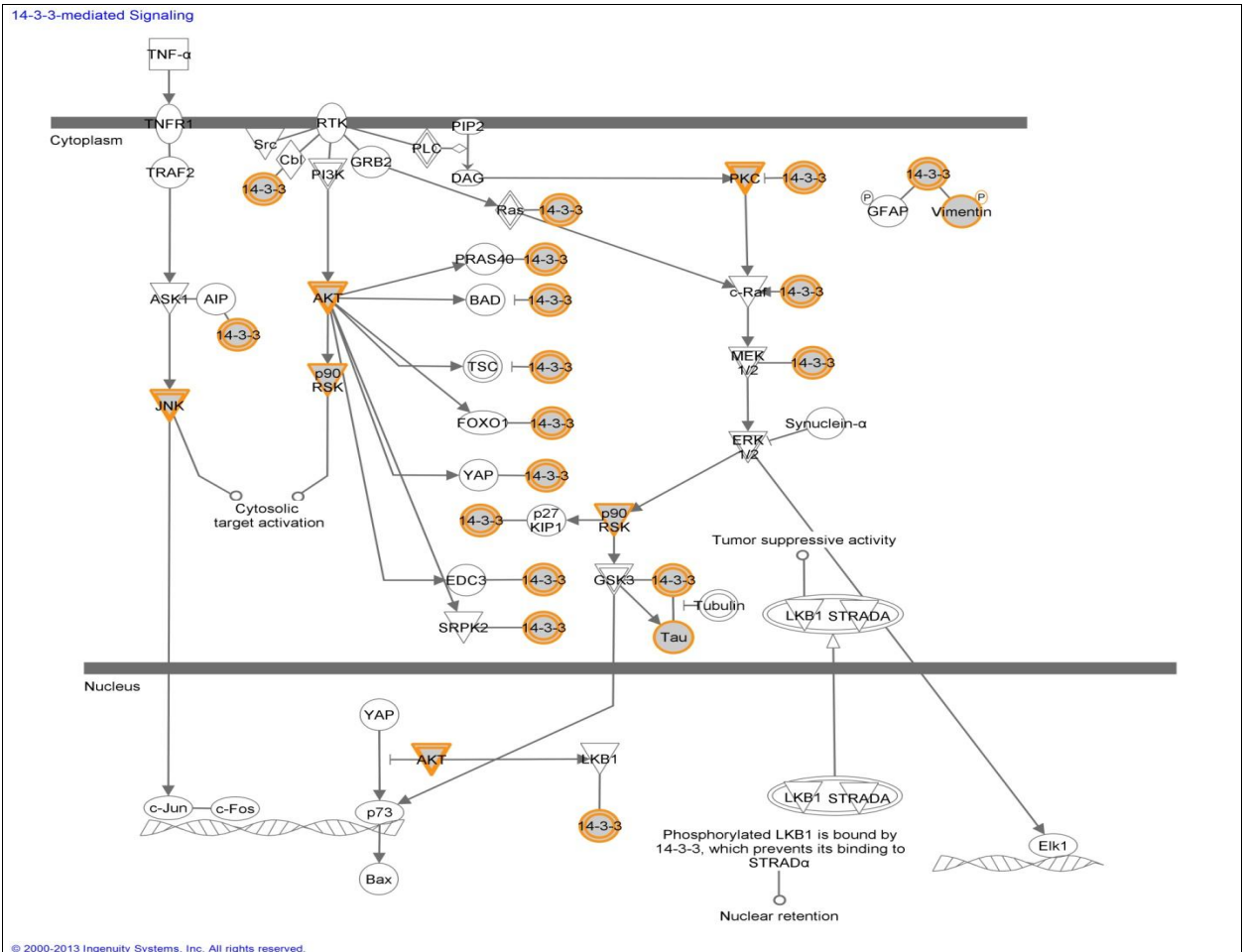


Figure 37: A total of 7 DEPs were mapped onto the Cell Cycle: G2M DNA Damage Checkpoint Regulation pathway as indicated above. Of these 7, 5 proteins were identified more than once.



● Breast AbMA
● Breast 2DMS



Figure 38: A total of 11 DEPs were mapped onto the 14-3-3 mediated signalling pathway as indicated above. Of these 11, 8 proteins were identified more than once.

4.3 DISCUSSION:

As discussed in the section 4.1.2 our research group had previously identified 14-3-3 theta/tau, BcL-XL and BID as putative biomarkers of breast chemotherapy resistance using fresh tumour samples in a pilot study (Hodgkinson et al. 2012). All three proteins, 14-3-3 theta/tau (*YWHAQ*), BcL-XL (*BCL2L1*) and BID (*BID*) were successfully confirmed on immunoblotting (refer Table 55 for details) and 14-3-3 theta/tau and truncated form of BID were successfully validated using the MRI-iFEC series.

From this project, leading from our previous work, a further three additional proteins, Akt1 (*PKCB*), Vimentin (*VIM*) and Focal Adhesion Kinase (FAKY397) (*PTK2*) were selected from the combined IPA analysis #2 data. Of the three selected proteins, vimentin was identified from all three 2D-PAGE/MS experiments from the VH study (Table 43) and was mapped onto 14-3-3 mediated signalling pathway from the selected 6/9 pathways (Figure 40) and overall onto 3/9 analysed pathways, Akt1 was identified from 1/9 combined microarray data (Table 40) and mapped onto PIP3/AKT signalling (Figure 33) and p70S6K signalling (Figure 36) and 14-3-3 mediated signalling (Figure 40) pathways from the selected 6 pathways but overall onto 6/9 pathways analysed. The FAKY397 protein was identified from 3/9 combined microarray data (Table 40) and was mapped only onto ERK/MAPK signalling pathway (Figure 36) from the overall 9 pathways analysed.

Also, from the combined analysis #2, previously identified and confirmed proteins (14-3-3 pan, BID and BcL-XL) and the five isoforms of 14-3-3 family namely, 14-3-3 theta/tau (*YWHAQ*), 14-3-3 zeta/delta (*YWHAZ*), 14-3-3 gamma (*YWHAG*), 14-3-3 epsilon (*YWHAE*) and 14-3-3 beta/alpha (*YWHAB*) were also analysed. Of the five 14-3-3 protein isoforms, theta/tau

(*YWHAQ*) was found in 3/3 2D-PAGE/MS (Table 43) and 3/9 combined antibody microarray experiments (Table 40) and mapped onto seven IPA pathways (Table 49), 14-3-3 zeta/delta (*YWHAZ*) in 3/3 2D-PAGE/MS experiments (Table 46) and mapped onto seven IPA pathways (Table 49), 14-3-3 gamma (*YWHAG*) in 2/3 2D-PAGE/MS experiments (Table 47) and mapped onto seven IPA pathways (Table 52), 14-3-3 epsilon (*YWHAE*) in 3/3 2D-PAGE/MS experiments and mapped onto six IPA pathways (Table 49) and 14-3-3 beta/alpha (*YWHAB*) in 2/3 2D-PAGE/MS experiments (Table 43) and mapped onto seven IPA pathways (Table 52). Similarly, BcL-XL (*BCL2L1*) was identified in 4/9 combined antibody microarray data (Table 46) and mapped onto only PIP3/AKT signalling pathway (Figure 35), BID (*BID*) was identified in 3/9 combined antibody microarray data (Table 43) and mapped only onto Death Receptor Signalling pathway (Figure 35) from the selected 6/9 pathways and overall onto two pathways from the nine analysed.

4.4 DEPs For Confirmations and Validations: Current Study

From the combined data mining stage in this current study, majority of molecular pathways that were identified were keeping in line with the expected pathways of chemotherapy resistance (sections 1.9.4.1, 1.9.4.2 and 1.9.3.1). However, despite using a combined approach, not all molecular pathways involved in chemoresistance may have been identified. This mainly due to the limitations of discovery techniques (section 1.13.1.2 and 1.13.1.3) and the data mining approaches (section 4.1.14.1.1). Therefore, working within the above limitations, so far, three proteins (Akt1, FAK, and Vimentin) have passed through the discovery pipeline, where their differential expression was first recognised during discovery-phase experiments. The above three proteins will now be taken to the next stages of confirmations and clinical validations.

Further, three other isoforms of the 14-3-3 protein (epsilon, beta/alpha, zeta/delta) previously identified but not validated will be clinically validated. The 14-3-3 theta/tau isoform previously validated using the MRI-iFEC series (section 2.3.3.1) will now undergo further validations using the *EC-D* series (section 2.3.3.2) in a combined approach. The aim of this combined analysis (MRI-iFEC + *EC-D*) was to validate 14-3-3 theta/tau in a large patient cohort for a more extensive downstream analysis.

CHAPTER V

CONFIRMATION AND CLINICAL VALIDATION

Aim:

To carry forward prioritised DEPs from the data mining phase for confirmation and clinical validation

Hussain T; Scaife L; Hodgkinson V; Agarwal V; Mahapatra T; Kneeshaw P; McManus L P; Lind J M ; Drew P; Cawkwell L. Proteomic identification of predictive biomarkers of neo-adjuvant chemotherapy resistance in breast Cancer: a possible role of Akt-1, FAKY397, 14-3-3 theta/tau, tBID ? ***BASO ~ACS Conference, Oral Presentation in the Roland Raven Paper Prize Session November 2013***

Chapter 5.

5.1 INTRODUCTION:

As discussed in the section 4.4, three protein candidates (AKT1 phosphoser473, FAK phosphoY397 and Vimentin) from this current study were selected for confirmation using western blotting. Pilot validations of the selected three proteins and 4 isoforms of 14-3-3 protein (theta/tau, beta/alpha, zeta/delta, and epsilon) previously identified by our research group was carried out using immunohistochemistry. Western blotting was performed using the technique as described in section 2.11.1. The details of primary antibodies optimised for the western experiments are listed in Table 52 below.

Table 52: Details of the primary antibodies used for Western Blotting

<i>Antibody</i>	<i>Concentration</i>	<i>Blocking agent</i>	<i>Incubation period</i>	<i>Antibody details</i>
Vimentin	1:15,000	5% non-fat milk	2hrs	Rabbit polyclonal (#ab92547, Abcam)
AKT1 phospho Ser473	<i>Not fully optimised</i>	5% BSA	-	Rabbit polyclonal (#ab66138, Abcam) Rabbit Monoclonal (#3787S, Cell Signaling Technology)
FAK phosphoY397	<i>Not fully optimised</i>	1% and 5% BSA	-	Rabbit polyclonal (#ab4803, Abcam)

5.1.1 Optimisations of Primary Phospho-Antibodies:

Primary antibody optimisation experiments for phospho-antibodies: AKT1 phosphoSer473 and FAK phosphoY397 for immunoblotting were unsuccessful. A total of 6 optimisation experiments were carried out for AKT1 phosphoSer473 antibody using MCF-7 and Daudi cell lines after blocking non-specific membrane sites with 5% milk and 5% bovine serum albumin (BSA) and using i-blot (semi-dry) membrane transfer technique. The AKT1 phosphoSer473 antibody used for the optimisation experiments was purchased from Cell Signaling Technology (Lot#3787S) and AbCAM (Lot#66138) and was rabbit monoclonal (Cell Signaling Technology) and rabbit polyclonal (AbCAM) respectively. The details of the AKT1 phosphoSer473 antibody, optimisation dilutions, incubations times and membrane blocks are listed in the Table 53 below.

For FAK phosphoY397 antibody, a total of 4 optimisation experiments were carried out using MCF-7 and Daudi cell lines after blocking non-specific membrane sites with 5% milk and 1% bovine serum albumin (BSA) using i-blot (semi-dry) membrane transfer technique. The FAK phosphoY397 antibody used for the optimisation experiments was purchased from AbCAM (Lot#4803) and was rabbit polyclonal. The details of the FAK phosphoY397 antibody, optimisation dilutions, incubations times and membrane blocks are listed in the Table 54 below.

The secondary antibody (Santa Cruz Lot #D0312) used in all optimisation experiments (both AKT1 and FAK) was raised in the same animal (rabbit) as the primary. The duration of TBS-Tween washes was increased from two 3 x 5 min (a total 30 min) before and after secondary incubations from the standard protocol as described in the section 2.11.62.11.6 to a total of two 3 x 10 min (a total 60 min) washes to avoid excessive background staining from non-specific binding.

Table 53: AkT1 phosphoSer473 Primary Antibody Immunoblotting Optimisation Experiments

<i>Antibody</i>	<i>Supplier</i>	<i>Dilutions</i>	<i>Primary Incubation Time</i>		<i>Block</i>	<i>TBS-Tween Washes</i>
AkT1 phosphoSer473 (Molecular Wt. 56 kDa)	Cell Signaling Technology (Lot#3787S)	1:1000 (Expt #1 & 2)	2 hrs	Overnight at 4°C	5% Milk 1hr	3 x 5 min twice before and after secondary (Total of 30 min)
		1:500 (Expt #3 & 4)	√	√		
	AbCAM (Lot#66138)	1:5000 (Expt #5 & #6)	√	x	5% Milk 1hr	3 x 10 min twice before and after secondary
			√	x	5% BSA 1hr	(Total of 60 min)

Table 54: FAK phosphoY397 Primary Antibody Immunoblotting Optimisation Experiments

<i>Antibody</i>	<i>Supplier</i>	<i>Dilutions</i>	<i>Primary Incubation Time</i>		<i>Block</i>	<i>TBS-Tween Washes</i>
FAKphosphoY397 (Molecular Wt. 125 kDa)	AbCAM (Lot#4803)	1:1000 (Expt #1 & 2)	2 hrs	Overnight at 4°C	5% Milk 1hr	3 x 10 min twice before and after secondary (Total of 60 min)
		1:1000 (Expt #3 & 4)	√	√		1% BSA 2hr

5.1.2 Reasons for Failed Optimisations:

The possible reasons for the optimisations failure can be broadly studied under two main categories:

- Absence of band detection
- High background staining

5.1.2.1 Reasons for No Band Detection:

Table 5165:

The primary antibody and the secondary antibody are not compatible

Not enough primary or secondary antibody is bound to the protein of interest

Cross-reaction between blocking agent and primary or secondary antibody.

The primary antibody does not recognize the protein in the species being tested.

The protein of interest is not abundantly present in the tissue

Poor transfer of protein to membrane.

Excessive washing of the membrane

Too much blocking does not allow the visualization of protein of interest

Over-use of the primary antibody

5.1.2.2 Reasons for High Background Staining:

Table 56:

Blocking of non-specific binding might be absent or insufficient

The primary antibody concentration may be too high.

Incubation temperature may be too high.

The secondary antibody may be binding non-specifically or reacting with the blocking reagent

Washing of unbound antibodies may be insufficient.

Membrane choice may give high background

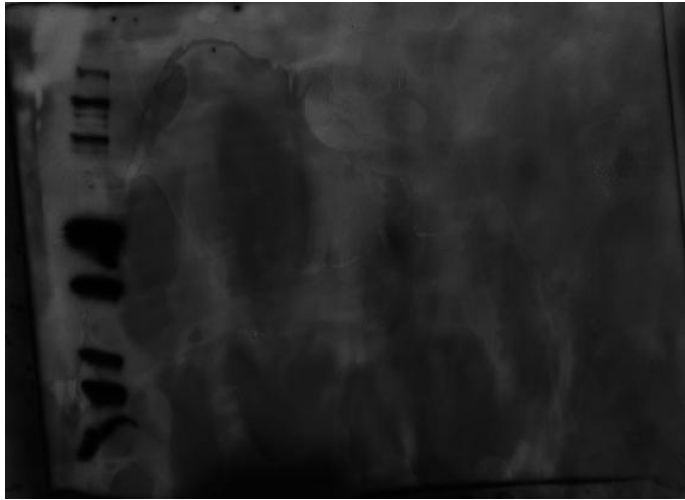
The membrane has dried out.

5.1.2.3 Trouble shooting with Optimisation Experiments:

With both the phospho-antibodies from the ten optimisation experiments (6 x Akt1; 4 x FAK), a high background staining and absence of protein specific bands was noted (Figure 39 and 40). For the above reasons the antibody optimisations failed. Exact reasons for the failures were not fully determined, however, they were assumed to be related to the protein transfer technique as described in the section 2.11.4 and/or combination of any of the above factors listed in sections 5.1.2.1 and 5.1.2.2. The above two issues were discussed with AbCAM and experiments #5 and #6 for Akt1 and #3 and #4 for FAK were repeated with a few modifications to the standard protocol (e.g. longer TBS-Tween washes, using different BSA concentrations, and longer periods of non-specific blocking). However, non-specific staining was still visibly persistent with no detection of protein specific bands. A further attempt at optimisations was given up due to time limitation. Learning from the experience, the author suggests that any future western experiments involving phospho-antibodies should have protein extractions done in a western specific buffer, protein separation done using 8% gels (instead of 12 % used) and protein transfer performed using wet-transfer technique.

SCANNED WESTERN BLOT IMAGE OF Akt1 phosphoSer473 ANTIBODY

A



B

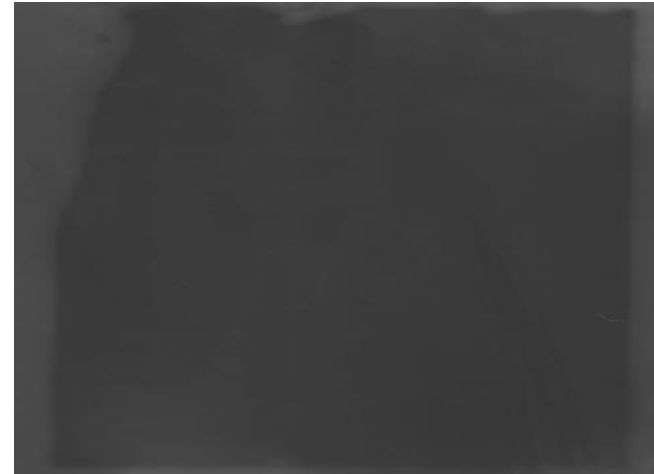
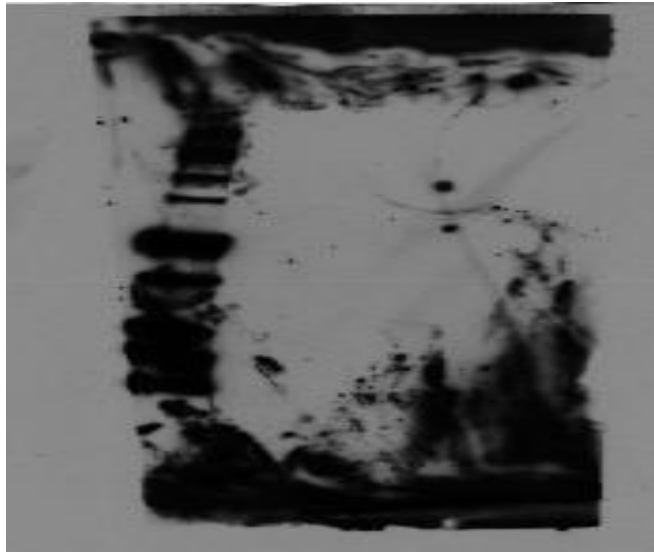


Figure 39: The scanned western blot images of Akt1 Phosphoser473 antibody. Figure A represents membrane image at 1:5000 dilution (Cell signaling #3787S) with 2 hr primary incubation using 5% milk block. Figure B represents membrane with 5% BSA block at 1:5000 dilution with 60 min washes. In both images, protein bands were not detected with excessive background staining noted.

SCANNED WESTERN BLOT IMAGE OF FAK phosphoY397 ANTIBODY

A



B

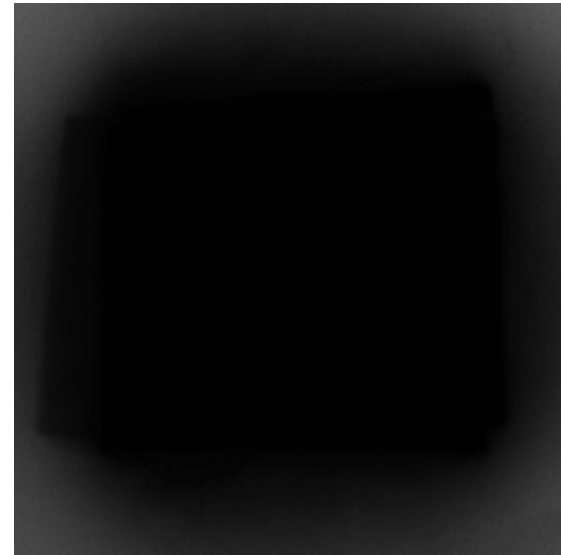
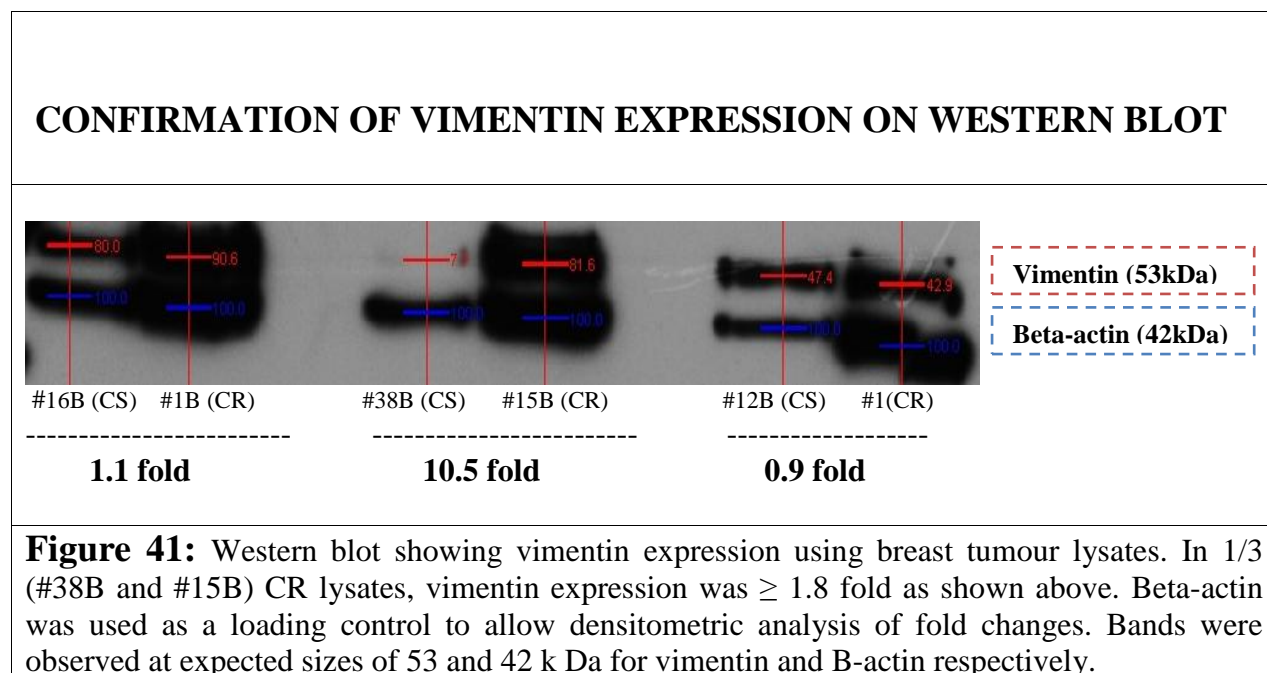


Figure 40: The scanned western blot images of FAK PhosphoY397 antibody. Figure A represents membrane image at 1:5000 dilution (abcam#4803) with 2 hr primary incubation using 5% milk block and 60 min washes. Figure B represents membrane with 1% BSA block at 1:5000 dilution and 60 min washes. In both images, protein bands were not detected with excessive background staining noted.

5.2 RESULTS:

Vimentin (*VIM*) was selected for downstream analysis and taken forward to the next stages of confirmation and validations in the biomarker discovery pipeline. The optimised antibody dilution used for this protein for immunoblotting is listed in the Table 55. Western blot for this protein was performed using breast tumour lysates; protein extractions from the tumour samples was performed using protein extraction technique as described in the section 2.5 using antibody microarray extraction labelling buffer. Immunoblotting for the experiment was performed using the technique as described in the section 2.11.1. Vimentin expressions were confirmed on immunoblotting in both chemosensitive and chemoresistant tumour lysates. However, protein expressions in only 1/3 chemoresistant samples (#38B and #15B) was found to show a ≥ 1.8 fold change (Figure 41).



5.3 IMMUNOHISTOCHEMISTRY:

5.3.1 Introduction:

As described in the section 4.4 of the thesis, three proteins from the current study and four isoforms of 14-3-3 protein from the VH study will be taken forward for clinical validations .A total 7 proteins will be validated using two different archival series described in the section 2.3.3. Immunohistochemistry technique used for the experiments will be as described in the section 2.122.12 of the thesis. The details of primary antibodies and the detection methods for each antibody are given in the Table 57 below.

Table 57: Primary Antibodies used for Immunohistochemical Staining

<i>Antibody</i>	<i>Archival Series</i>	<i>Dilution</i>	<i>Antibody Details</i>	<i>Detection Method</i>
14-3-3 theta/tau	ECD series	1:100	#ab64991, Abcam	Streptavidin-avidin-biotin method
14-3-3 beta/alpha	i-FEC series	1:50	#ab32560, Abcam	Streptavidin-avidin-biotin method
14-3-3 zeta	i-FEC series	1:25	#ab51129, Abcam	Streptavidin-avidin-biotin method
14-3-3 epsilon	i-FEC series	1:100	#ab43057, Abcam	Streptavidin-avidin-biotin method
AkT1 phospho Ser 473	ECD series	1:50	#ab66138, Abcam	Streptavidin-avidin-biotin method
Vimentin	ECD series	1:50	#ab92547, Abcam	Streptavidin-avidin-biotin method
FAK phosphoY397	ECD series	1:50	#ab4803, Abcam	Streptavidin-avidin-biotin method

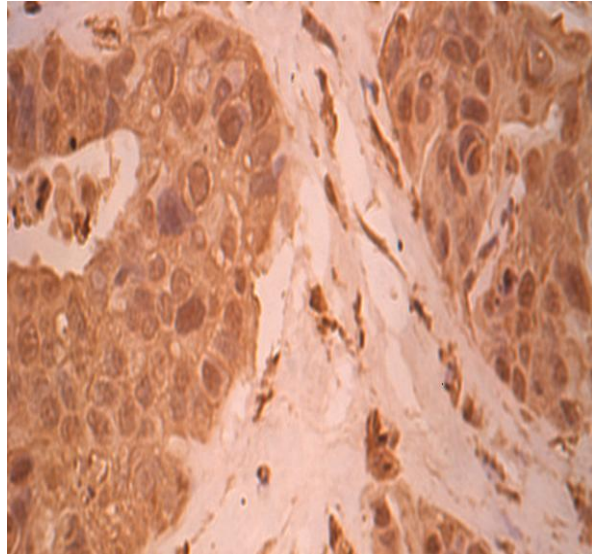
5.4 CLINICAL VALIDATION OF VIMENTIN PROTEIN:

Clinical studies have shown vimentin has a role in breast chemotherapy resistance on immunoblotting. Therefore, in order to confirm the expression of vimentin in clinical samples and validate protein expressions with chemoresistance, a pilot immunohistochemical study using 21 chemosensitive and 8 chemoresistant FFPE samples from patients treated with 4 cycles of epirubicin-cyclophosphamide and 4 cycles of docetaxel (*EC-D* series; section 2.3.3.2) was performed. Slide staining was assessed and scored independently by 2 assessors (TH and Veronica M O'Donnell) with any discrepancies adjudicated by a consultant breast pathologist (Dr. Ann Campbell). Following observation of all the slides, two slides were selected as reference controls that showed strong and weak antibody staining for the experiment. The staining assessments for the rest of the slides were adjudicated against the reference controls and the above routine was followed across all the seven immunohistochemical studies.

After slide assessments, it was observed that when present, strong positive staining was predominantly nuclear, with occasional cytoplasm and cell membrane staining observed (Figure 42). Intensity of nuclear staining was called positive (strong staining) if staining was noted in $\geq 20\%$ of clusters of tumour cells and negative (weak/no staining) if staining was weak or absent in $\leq 20\%$ of clusters of tumour cells. In total 7/21 (33.3%) chemosensitive samples demonstrated an increase expression of vimentin in the invasive carcinoma compared to 3/8 (37.5%) from the chemoresistant group. However, the decrease expression of vimentin was not significantly associated in the chemoresistant group ($p=1.00$; Fishers exact test) (Table 58).

IHC Analysis of Vimentin Expression Using the EC-D series

A



B

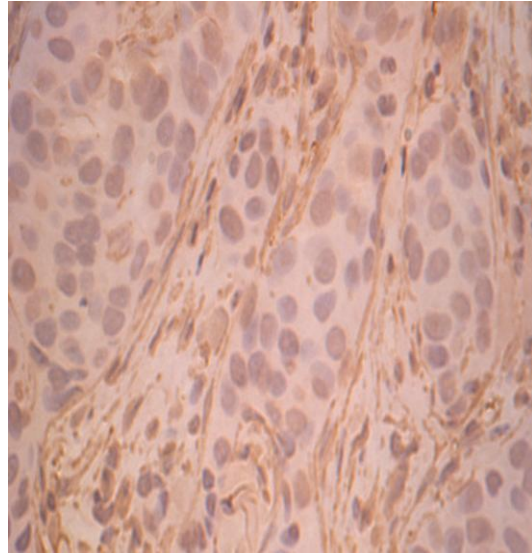


Figure 42: Immunohistochemical analysis of vimentin expression in invasive breast carcinoma cells. The Figure A shows the slide that was assessed as positive for nuclear staining with moderate cytoplasm positivity in at least 20% of invasive carcinoma cells. The Figure B shows weak nuclear and cytoplasm staining which was recorded as negative (reference control).

ECD series; Vimentin (ab92547, Abcam) at 1:50 dilution

Cell membrane staining			
	Positive	Negative	Total
Responder	2	19	21
Non-responder	0	8	8
<i>Total</i>	2	27	29
P = 1.00			

Cytoplasmic staining			
	Positive	Negative	Total
Responder	2	19	21
Non-responder	0	8	8
<i>Total</i>	2	27	29
P = 1.00			

Nuclear staining			
	Positive	Negative	Total
Responder	7	14	21
Non-responder	3	5	8
<i>Total</i>	10	19	29
P = 1.00			

Table 58: IHC scoring assessment results for vimentin staining using the EC-D series. Brown staining was predominantly nuclear with occasional cytoplasm and cell membrane staining observed. However, decreased expression of vimentin in the nucleus and cytoplasm was not significantly associated in the chemoresistant group ($p=1.00$; Fishers exact test).

5.5 CLINICAL VALIDATION OF AKT1 PhosphoSer473 PROTEIN:

The role of Akt1 in chemotherapy resistance in general and breast chemotherapy resistance in specific has been already discussed in the section 1.9.4.1 of the thesis. For clinical validation of this protein, a serine phosphorylated form of Akt1 was selected because of its previously reported association with anthracyclines (e.g. Doxorubicin) chemotherapy resistance (Li, Lu et al. 2005). Further, the serine473 phosphorylated form in the same study was also found to be associated with chemoresistance to other drugs such as paclitaxel, 5-fluorouracil and gemcitabine. Therefore, in order to explore the role of Akt1 phosphoser473 in mediating resistance to anthracycline-taxane chemotherapy, using the *EC-D* series, 19 chemosensitive and 12 chemoresistant FFPE samples from 30 patients were analysed in a small pilot immunohistochemical study.

Following the assessments of slides, it was observed that when present, strong positive staining was predominantly cytoplasmic and nuclear, with occasional cell membrane staining observed (Figure 43). Intensity of cytoplasmic staining was called as positive (strong/moderate staining) if staining was noted in $\geq 50\%$ of clusters of tumour cells and negative (weak/weak-moderate staining) if staining was weak or weak-moderate in $\geq 50\%$ of clusters of tumour cells. In total 8/12 (66.6%) chemoresistant samples demonstrated an increase expression of Akt1 Phospho Ser473 in the invasive carcinoma compared to 5/19 (26.3%) from the chemosensitive group. The increase expression of Akt1 PhosphoSer473 was significantly associated in the chemoresistant group ($p=0.05$; Fishers exact test). Intensity of nuclear staining was called as positive (strong staining) if staining was noted in $\geq 20\%$ of clusters of tumour cells and negative (weak staining) if staining was weak in $\leq 20\%$ of clusters of tumour cells. In total 6/12 (50%) chemoresistant

samples demonstrated an increase expression of Akt1 PhosphoSer473 in the invasive carcinoma compared to 0/21 (0%) from the chemosensitive group. The increase expression of Akt1 phosphoSer473 was significantly associated in the chemoresistant group ($p=0.0001$; Fishers exact test) (Table 59).

IHC Analysis of Akt1 PhosphoSer473 Expression Using the EC-D series

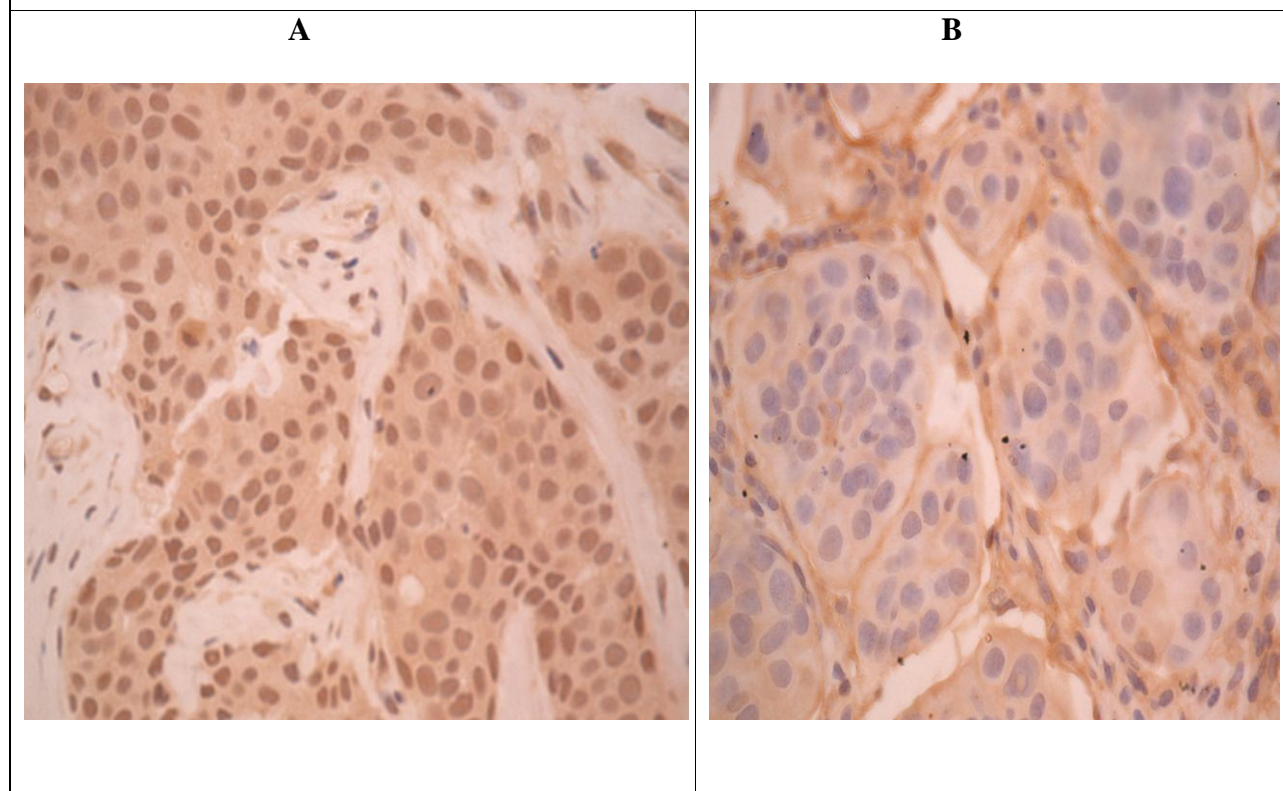


Figure 43: Immunohistochemical analysis of Akt1 PhosphoSer473 expression in invasive breast carcinoma cells Figure A shows, positive nuclear staining of Akt1 PhosphoSer473 with moderate cytoplasm positivity in at least 20% of invasive carcinoma cells. Figure B shows weak staining for the protein recorded as negative (reference control).

ECD series; Akt1 PhosphoSer473 (ab66138, Abcam) at 1:50 dilution

Cytoplasmic staining			
	Positive	Negative	Total
Responder	5	14	19
Non-responder	8	4	12
<i>Total</i>	13	18	31
P = 0.05			

Nuclear staining			
	Positive	Negative	Total
Responder	0	21	21
Non-responder	6	1	7
<i>Total</i>	6	22	28
P = 0.0001			

†

Cell membrane staining			
	Positive	Negative	Total
Responder	4	17	21
Non-responder	1	6	7
<i>Total</i>	5	23	28
P = 1.00			

Table 59: IHC scoring for Akt1 PhosphoSer473 using the ECD series. Brown staining was predominantly cytoplasmic & nuclear with occasional cell membrane staining observed. An increased expression of Akt1 PhosphoSer473 in nuclear membrane and cytoplasm was significantly associated in the chemoresistant group ($p=0.05$ and 0.0001 ; Fishers exact test).

5.6 CLINICAL VALIDATION OF FAK PospHoY397 PROTEIN:

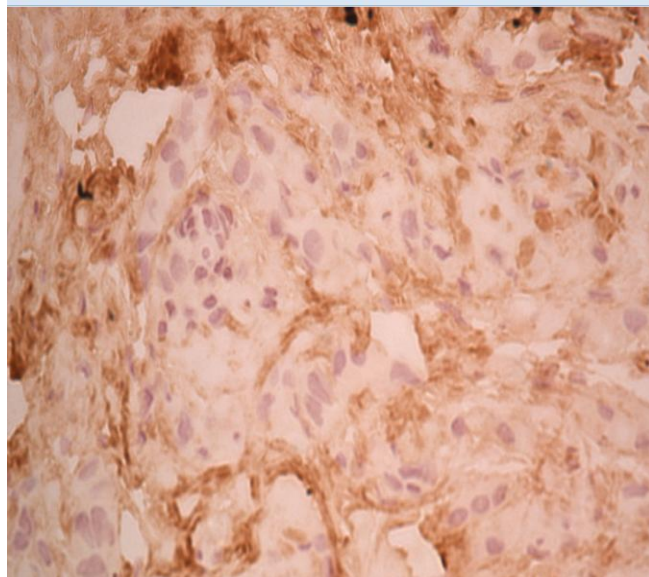
As discussed in the section 1.9.4.2, Focal Adhesion Kinase (FAK) is an integrin involved in integrin-mediated cell signalling and overexpressed in a variety of solid tumours. In breast cancer, expression of FAK protein compared to normal breast tissue has been shown to be specifically unregulated (Watermann, Gabriel et al. 2005). The role of integrins in breast cancer chemotherapy resistance specific to taxanes was first reported by Aoudjit F and Vuori K using breast cell lines (Aoudjit and Vuori 2001). Since then, integrins have also been linked with chemoresistance to 5FU in breast and colonic cancers (Chen, Wang et al. 2009). It has been reported, knock down of FAK using antisense oligonucleotides increases the sensitivity of breast cancer cells to chemotherapeutic agents (Satoh, Surmacz et al. 2003). This finding supports the pivotal role FAK plays in neoplastic signal transduction thereby showing potential to be a biomarker for malignant transformation and chemoresistance. Therefore, in order to assess the differential expression of FAK phosphoY397 in the clinical context of breast chemoresistance, a small pilot immunohistochemical study using 20 chemosensitive and 9 chemoresistant samples from the *EC-D* series was undertaken.

Following the assessments of slides, it was observed that when present, strong positive staining was predominantly cytoplasmic and nuclear, with occasional cell membrane staining observed (Figure 44). Intensity of cytoplasmic staining was called positive (strong/moderate staining) if staining was noted in $\geq 50\%$ of clusters of tumour cells and negative (weak/weak-moderate staining) if staining was weak or weak-moderate in $\geq 50\%$ of clusters of tumour cells. In total 6/9 (66.6%) chemoresistant samples demonstrated an increase expression of FAK phosphoY397 in the invasive carcinoma compared to 5/20 (25%) from the chemosensitive group. The increase expression of FAK phosphoY397 was significantly associated in chemoresistant group ($p=0.04$;

Fishers exact test). In total 2/9 (22.2%) chemoresistant samples demonstrated an increase nuclear expression of FAK phosphoY397 in the invasive carcinoma compared to 9/20 (45%) from the chemosensitive group. The increase expression of FAK phosphoY397 was not significantly associated in the chemoresistant group ($p=0.41$; Fishers exact test) (Table 60).

IHC Analysis of FAK PhosphoY397 Expression Using the EC-D series

A



B

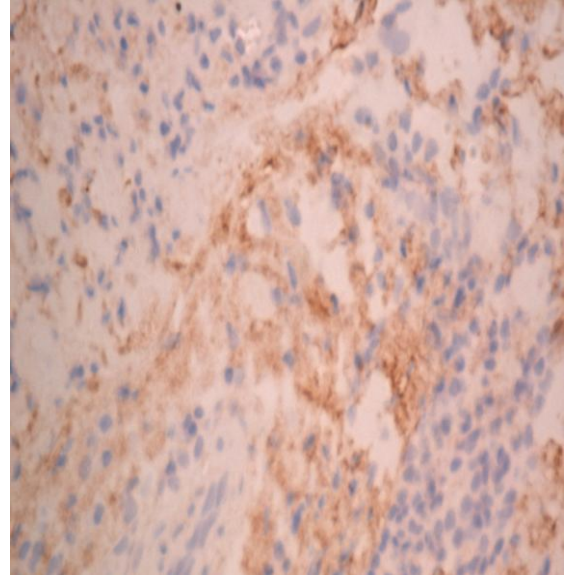


Figure 44: Immunohistochemical analysis of FAK phosphoY397 expression in invasive breast carcinoma cells. Figure A shows positive cytoplasmic staining recorded when seen in at least $\geq 50\%$ of invasive carcinoma cells. Figure B shows weak staining recorded as negative (reference control).

ECD series; FAK Phospho Y397(ab4803, Abcam) at 1:50 dilution

Cytoplasmic staining			
	Positive	Negative	Total
Responder	5	15	20
Non-responder	6	3	9
<i>Total</i>	11	18	29
P = 0.04			

Nuclear staining			
	Positive	Negative	Total
Responder	9	11	20
Non-responder	2	7	9
<i>Total</i>	11	18	29
P = 0.41			

Table 6170: IHC scoring for FAK phosphoY397 using the ECD series. Brown staining was predominantly cytoplasmic & nuclear with occasional cell membrane staining observed. An increased expression of FAK phosphoY397 in the cytoplasm was significantly associated in the chemoresistant group ($p=0.04$; Fishers exact test).

5.7 CLINICAL VALIDATION OF 14-3-3 theta/tau ISOFORM:

As described in the section 4.2.3 of this thesis, previously pilot immuno validations were carried out for the 14-3-3 theta/tau isoform using a small pilot series of pre-treatment archival samples (MRI-iFEC series; section 2.3.3.1) (Hodgkinson et al. 2012). From that study, (Hodgkinson, D et al. 2012) following assessment of slides, a positive staining of 14-3-3 theta/tau was recorded when strong nuclear membrane positivity was seen in at least 20% of invasive carcinoma cells (Figure 47 (A: 1)). Positive staining was seen in 8/9 (88%) chemotherapy resistant (CR) samples,

compared with 9/22 (40%) of chemotherapy-sensitive (CS) samples ($p=0.020$, Fisher's exact test).

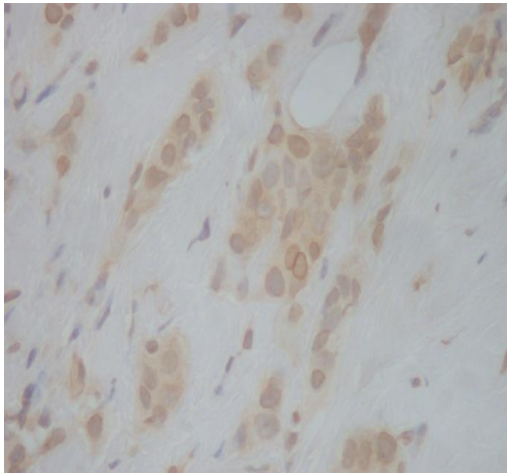
In order to fully assess the role of 14-3-3 theta/tau in chemoresistance, clinical validations in a larger sample cohort was required. Therefore, this protein isoform was included for further clinical validations using the *EC-D* series. A combined data analysis from both the studies (VH + current study) was then carried out to assess the expression of this protein isoform with chemoresistance.

Following assessments of slides in this study, strong cytoplasm and nuclear membrane positivity (Figure 45 (A: 2)) was seen in 3/6 (50%) of the chemoresistant group compared to 13/17(76.4%) from the chemosensitive group ($p=0.315$; Fishers exact test) (Table 61). On the combined analysis (MRI-iFEC + EC-D series), an overall cytoplasm and nuclear membrane positivity was seen in 11/15 (73.3%) of the chemoresistant group compared to 22/39 (56.4%) from the chemosensitive group ($p=0.35$; Fishers exact test) (Table 62).

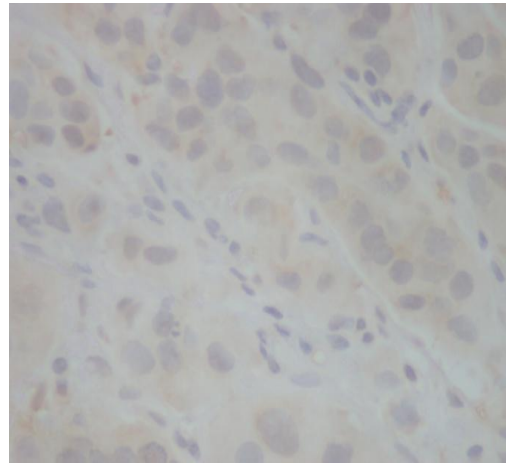
In conclusion, no significant association with chemoresistance was found with this protein isoform from the combined analysis.

IHC Analysis of 14-3-3 theta/tau Expressions: MRI-iFEC and EC-D series

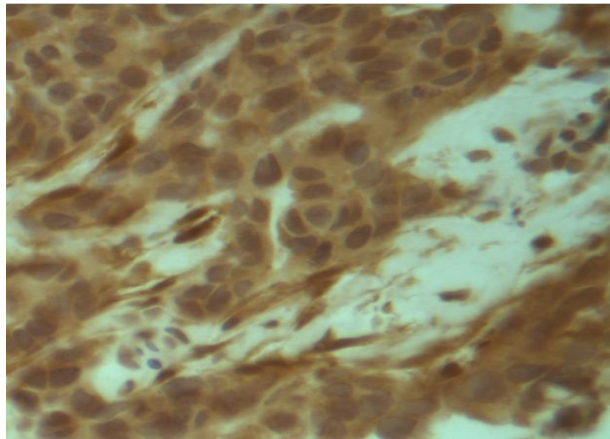
A:1



B:1



A:2



B:2

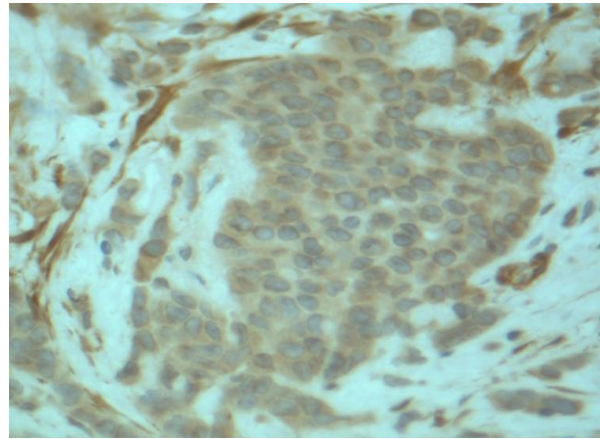


Figure 45: Immunohistochemical analysis of 14-3-3 theta/tau expression in invasive breast carcinoma cells. Figure A1 and A2 shows positive cytoplasmic staining in > 50% of cells and strong nuclear membrane positivity in at least 20% of invasive carcinoma cells. Figure B1 and B2 show weak staining which was recorded as negative (reference control).

ECD series; 14-3-3 theta/tau (ab64991, Abcam) at 1:100 dilution

Cell membrane staining			
	Positive	Negative	Total
Responder	4	13	17
Non-responder	1	5	6
<i>Total</i>	5	18	23

P = 1.00

Cytoplasmic staining			
	Positive	Negative	Total
Responder	15	2	17
Non-responder	4	2	6
<i>Total</i>	19	4	23

P = 0.2705

Nuclear membrane staining			
	Positive	Negative	Total
Responder	13	4	17
Non-responder	3	3	6
<i>Total</i>	16	7	23

P = 0.3185

Table 61: IHC scoring for 14-3-3 theta/tau using the ECD series. Brown staining was predominantly nuclear with occasional cytoplasm and cell membrane staining observed. However, an increased expression of 14-3-3 theta/tau in the nucleus and cytoplasm was not significantly associated in the chemoresistant group ($p=0.31$; Fishers exact test).

MRI-iFEC + ECD series; 14-3-3 theta/tau (ab64991, Abcam) at 1:100 dilution

Nuclear membrane staining			
	Positive	Negative	Total
Responder	22	17	39
Non-responder	11	4	15
<i>Total</i>	33	21	54

P = 0.35

Table 62: IHC scoring for 14-3-3 theta/tau from the combined analysis. Brown staining was predominantly nuclear with occasional cytoplasm and cell membrane staining observed. However, an increased expression of 14-3-3 theta/tau in the nucleus and cytoplasm was not significantly associated in chemoresistant group ($p=0.35$; Fishers exact test).

5.8 CLINICAL VALIDATION OF 14-3-3 epsilon ISOFORM:

The above protein isoform was found in all three 2D-PAGE/MS experiments in the VH study (Table 46). The up-regulations of four 14-3-3 isoforms (14-3-3 eta, 14-3-3 beta/alpha, 14-3-3 theta/tau, and 14-3-3 sigma) were confirmed using an antibody which recognised all four 14-3-3 isoforms previously by our research group (Hodgkinson et al. 2012). The 14-3-3 epsilon isoform was independently confirmed using epsilon specific antibody on the western blot in the same study. Therefore, this isoform was now selected for clinical validation using archival 8 chemoresistant and 18 chemosensitive FFPE samples from the MRI-iFEC series. Following assessments of slides, a strong cytoplasm and cell membrane positivity was seen in 3/8 (37.5%) of the chemoresistant group compared to 7/18 (38.8%) from the chemosensitive group ($p=1.00$; Fishers exact test) (Table 63).

MRI-iFEC series; 14-3-3 epsilon (ab43057, Abcam) at 1:100 dilution

Cell membrane staining			
	Positive	Negative	Total
Responder	5	13	18
Non-responder	2	6	8
<i>Total</i>	7	19	26
P = 1.0000			

Cytoplasmic staining			
	Positive	Negative	Total
Responder	7	11	18
Non-responder	3	5	8
<i>Total</i>	10	16	26
P = 1.0000			

Table 63: IHC scoring for 14-3-3 epsilon using the MRI-iFEC series. Brown staining was predominantly in cytoplasm with occasional cell membrane staining observed. However, an increased expression of 14-3-3 epsilon in cytoplasm was not significantly associated in the chemoresistant group ($p=0.31$; Fishers exact test).

5.9 CLINICAL VALIDATION OF 14-3-3 beta/alpha ISOFORM:

The above protein isoform was found in three 2D-PAGE/MS experiments in the VH study (Table 46) and confirmed on the western blot using a pan 14-3-3 antibody (Hodgkinson et al. 2012). This isoform was now selected for clinical validation using archival 8 chemoresistant and 18 chemosensitive FFPE samples from the MRI-iFEC series. Following slide assessments, a strong cell membrane and cytoplasm positivity was seen in 8/9 (88.8%) of the chemoresistant group compared to 10/18 (55.5%) from the chemosensitive group ($p=0.19$; Fishers exact test) (Table 64).

MRI-iFEC series; 14-3-3 beta/alpha (ab32560, Abcam) at 1:50 dilution

Cytoplasmic staining			
	Positive	Negative	Total
Responder	7	11	18
Non-responder	5	4	9
Total	12	15	27
P = 0.4479			

Nuclear membrane staining			
	Positive	Negative	Total
Responder	3	15	18
Non-responder	0	9	9
Total	3	24	27
P = 0.5292			

Cell membrane staining			
	Positive	Negative	Total
Responder	10	8	18
Non-responder	8	1	9
Total	18	9	27
P = 0.1925			

Table 64: IHC scoring for 14-3-3 alpha/beta using MRI-iFEC series. Brown staining was predominantly in cell membrane with occasional cytoplasmic staining observed. However, an increased expression of 14-3-3 beta/alpha in cytoplasmic membrane was not significantly associated in the chemoresistant group ($p=0.19$; Fishers exact test).

5.10 CLINICAL VALIDATION OF 14-3-3 zeta/delta ISOFORM:

The above protein isoform was found in two 2D-PAGE/MS experiments in the VH study (Table 46) but was not confirmed on western blotting. Therefore, this isoform was now selected for clinical validation using archival 8 chemoresistant and 18 chemosensitive FFPE samples from the MRI-iFEC series. Following slide assessments, a strong cytoplasmic and membrane positivity was seen in 4/9 (44.4%) of the chemoresistant group compared to 15/21 (71.4%) from the chemosensitive group ($p=0.22$; Fishers exact test) (Table 65).

MRI-iFEC series; 14-3-3 zeta/delta (ab51129, Abcam) at 1:25 dilution

Cell membrane staining			
	Positive	Negative	Total
Responder	7	14	21
Non-responder	1	8	9
<i>Total</i>	8	22	30
P = 0.3742			

Cytoplasmic staining			
	Positive	Negative	Total
Responder	15	6	21
Non-responder	4	5	9
<i>Total</i>	19	11	30
P = 0.2252			

Table 185: IHC scoring for 14-3-3 zeta isoform using the MRI-iFEC series. Brown staining was predominantly in cytoplasm with occasional cell membrane staining observed. However, an increased expression of 14-3-3 zeta in cytoplasm was not significantly associated in the chemoresistant group ($p=0.22$; Fishers exact test).

5.11 DISCUSSION:

5.11.1 Role of 14-3-3 in Breast Chemoresistance:

Our research group identified five isoforms (epsilon, theta/tau, beta/alpha, zeta/delta and gamma) of 14-3-3 protein from three 2D-PAGE/MS experiments using fresh breast tumour samples. Of these, only the 14-3-3 theta/tau (*YWHAQ*) isoform was taken through all stages of biomarker discovery pipeline and successfully validated (Hodgkinson, D et al. 2012). The immunohistochemical analysis of 14-3-3 theta/tau from our previous study showed a statistically significant association between high expression of 14-3-3 theta/tau within the nuclear membrane and chemoresistance ($p=0.02$). Therefore in this project, this protein isoform was selected for a more extensive downstream analysis using the *EC-D* series. The aim of the analysis was to combine the IHC data from both the MRI-iFEC and the *EC-D* series in order to assess the protein expression in a larger patient cohort. However, IHC result from the combined immunohistochemical analysis of 54 patients' combined series (MRI-iFEC + *EC-D*) did not reach a statistical significance for the protein expression with chemoresistant samples.

Analysing the above findings for the possible reasons of failure to achieve a clinical significance indicate a multifactorial trail. Some of these include, study under-power, higher number of responders than non-responders in the combined analysis, slide ambiguities from low and/or absent tissue staining, inter-observer variability in slide assessments and scoring and the use of two different chemotherapy regimens (FEC vs *EC-D*). Furthermore, the IHC assessments for the other isoforms (epsilon, beta/alpha, and zeta/delta) also failed to achieve any statistical significance which could well be again secondary to the combination of any of the above listed factors. Therefore, in order to fully assess the significance this protein expression in breast

chemotherapy resistance, future screening should involve a larger patient cohort in a well designed study with equal numbers for responders and non-responders and patients with similar chemotherapy regimens.

The 14-3-3 protein has seven mammalian isoforms which are all reported to associate with proteins involved in critical processes including cell cycle regulation, intracellular signalling and apoptosis (Tzivion, Gupta et al. 2006). Overall, studies have shown that 14-3-3 proteins promote cell survival by inhibition of apoptosis (Masters, Subramanian et al. 2002) and have been widely associated with cancer and response to therapeutic agents (section 1.9.4.3). The association between doxorubicin and paclitaxel chemotherapy resistance in breast cancer and expression of 14-3-3 proteins has been shown previously using MCF-7 breast cancer cell lines (Liu, Liu et al. 2006; Chuthapisith 2007). Furthermore, 14-3-3 theta/tau (*YWHAQ*) has been also found involved with tamoxifen resistance via inhibition of tamoxifen-induced apoptosis in breast cancer cells (Wang, Liu et al. 2010). Also, the 14-3-3 theta/tau (*YWHAQ*) isoform is shown to be associated with response to chemotherapeutic agents, where single nucleotide polymorphisms affect the gene encoding of *YWHAQ* (Vazquez, Grochola et al. 2010). Therefore, aberrations within the 14-3-3 proteins may present an array of mechanisms by which resistance to chemotherapeutic agents may arise, warranting a wider research into their role as the putative biomarkers of breast chemotherapy resistance.

5.11.2 Role of Vimentin in Breast Chemoresistance:

The above protein was found in three 2D-PAGE/MS experiments, mapped onto 3/9 molecular pathways on analysis #2 (section 4.1.2.2) and therefore selected for downstream analysis in this project. Vimentin is a member of the intermediate filament family. Along with microtubules and

actin microfilaments, vimentin is an integral component of the cell cytoskeleton. In cancer, altered vimentin level is associated with a dedifferentiated phenotype, increased motility, invasiveness, and poor clinical prognosis (Kokkinos, Wafai et al. 2007).

The protein expression was confirmed on western blotting with a ≥ 1.8 fold change noted in only 1/3 analysed chemoresistant samples (section 5.2). On IHC, vimentin expressions were largely nuclear with some moderate cytoplasmic staining. However, these expressions failed to achieve a statistical significance in the chemoresistant tumours. Vimentin (*VIM*) expression has recently been documented in tumour cells of infiltrating human breast carcinomas ((He, Whelan et al. 2011). The development of breast chemotherapy resistance and cancer invasiveness by losing the expression of epithelial marker and acquisition of vimentin expression was first shown by Sommers *et al.*; using Adriamycin and Vinblastine-resistant human breast cell lines (Sommers, Heckford et al. 1992). The mechanism of chemoresistance with vimentin however, remains poorly understood; although two different biological theories: direct histogenetic derivation from myoepithelial cells and epithelial–mesenchymal transition (EMT) reflecting the end-stage of breast cancer dedifferentiation have been postulated to explain a potential link between the development of chemoresistant phenotype and vimentin expression by immunohistochemical analysis (Korsching, Packeisen et al. 2005). Using a Molecular Evolution Assay, increased expression of the epithelial marker E-cadherin and the mesenchymal marker vimentin have been found associated with in-vitro resistance to doxorubicin in breast cancer cells (Kopp, Oak et al. 2012). Further, in-vitro studies involving breast cell lines (MCF-7) transfected with transcription-inhibitor Snail gene (Snail gene), showed an increased correlation of vimentin expression with EMT and multidrug resistance via Breast Cancer Resistant Protein (BCRP) (Chen, Wang et al. 2010). In another recent study, a higher level of vimentin expression

alongside an increased alteration in expression levels of genes (e.g. slug) related to epithelial-mesenchymal transition (EMT) has been shown to cause chemoresistance to paclitaxel, docetaxel, and doxorubicin (Iseri, Kars et al. 2011). Acquired resistance to breast chemotherapy in relation to vimentin can also be explained by the alteration to death receptor signaling pathway that promote epithelial-to-mesenchymal transition (Antoon, Lai et al. 2012). Therefore, from the above evidence, the role of vimentin in the EMT transition and development of multidrug resistance becomes clear. Targeting EMT transcription factors and studying the downstream molecular targets of vimentin therefore may serve as novel strategies to curb both metastasis and the associated drug resistance. From this study, down-regulation of vimentin was observed with chemoresistance on IHC, however, without achieving a statistical significance. Based on the above finding, a further exploration of loss of vimentin expression with chemoresistance in ER+ breast tumours need to be explored.

Although vimentin is an aggressive marker for breast cancer growth, up-regulation of the protein has been reported to be associated with favourable responses to Taxotere/Carboplatin/Herceptin neoadjuvant chemotherapy in triple negatives and HER2+ breast cancer subtypes (He, Whelan et al. 2011). The above evidence, suggest down-regulation of the Vimentin protein may therefore be associated with chemoresistance. In the ER+ breast tumours, association of vimentin down-regulation with chemoresistance has been recently reported following Taxotere, Epirubicin and Cyclophosphamide neoadjuvant chemotherapy (Yi, Peng et al. 2013). However, this trend was not demonstrated for vimentin in 2/3 chemoresistant ER+ breast tumours on immunoblotting from the current study, although previously, vimentin was found down-regulated in all three 2D-PAGE/MS experiments by our research group (Hodgkinson et al. 2012).

However, selection of vimentin as biomarker of chemotherapy resistance requires a careful consideration as this protein is included in the “Top15” human repeatedly identified differentially expressed proteins (RIDEPs) list (Petрак, Ivanek et al. 2008). The RIDEP phenomenon in proteomics experiments has been recently reported (Mariman 2009) and is hypothesised to occur involving proteins that may be involved in the cellular stress response. Therefore, these proteins if selected would require careful validation for further downstream analysis.

5.11.3 Role of Akt1 in Breast Chemoresistance:

Akt protein (*PKB*) was found in one experiment from the combined antibody microarray analysis, and mapped onto 8/10 molecular pathways on IPA analysis #1 (Table 51) and onto 6/9 in analysis #2 (Table 52). In this study, expression of Akt1 phosphoser473 in breast cancer cells was confirmed on IHC and a significant correlation was noted between higher nuclear expressions in the chemoresistant tumours (Figure 43). The role of PIP3/Akt pathway in chemoresistance has been discussed in the section 1.9.4.1 of this thesis. Many studies in the past have revealed a prognostic and/or predictive role of Akt phosphorylation not just in breast cancers but also other cancers such as prostate and non-small cell lung cancer (Lin, Hsieh et al. 2005; Al-Bazz, Brown et al. 2009). Lin *et al*; using breast cancer cells (MDA-MB-468 and MCF-7) and Kinexus phosphorylated protein screening assays showed a greater than 70% correlation between invasive breast carcinomas ($p < 0.05$) and phosphorylated forms of PDK-1, AKT, p70S6K, and EGFR (Lin, Hsieh et al. 2005). In sharp contrast, phosphorylation of the same proteins was nearly undetectable or was at low levels in normal mammary tissues in the same assay. The above findings clarify the role of phosphorylated Akt in the breast malignant phenotype. The activation of phospho-Akt in breast cancer was further demonstrated by Al-Bazz

et al. using western blot analysis of the breast tumour lysates with phospho-Ser473 antibody. Findings from the study showed phospho-Akt was expressed in 88% of primary breast tumours with the highest frequency in invasive ductal carcinoma (NOS) (Al-Bazz, Brown et al. 2009). In the same study, expression of activated (phosphorylated) form of Akt (Ser473) was also found to be significantly related to oestrogen receptor status ($p=0.014$) but showed a poor correlation to the disease recurrence and patient survival. Furthermore, phosphorylation of Akt1 at Ser473 and not Thr 308 results in cell survival, proliferation and tumour progression has been shown by a transfection study of MDA-MB 468 breast cell line with the human kinome siRNA library. Findings from the study showed, choline-kinase can significantly up-regulate the Akt1 activity. A reduction in Ser473 phosphorylation of Akt1 with choline-kinase inhibitors was noted to cause tumour regressions in rat xenograft models (Chua, Gallego-Ortega et al. 2009). Using tissue microarrays, examination of FOXO3a and phosphorylated-Akt (P-Akt) expression in breast cancer tissue showed chemotherapy resistance and tumour progression in invasive ductal breast carcinoma linked to an uncoupling of the Akt-FOXO3a signaling axis (Chen, Gomes et al. 2010). In these breast cancers activated Akt fails to inactivate and re-localize FOXO3a to the cytoplasm, and nuclear-targeted FOXO3a does not induce cell death or cell cycle arrest. Also, phosphorylated Akt1 has been also shown to cause chemoresistance to cisplatin in breast cancer cells from the activation of its downstream mediators, (e.g., glycogen synthase kinase-3 beta (GSK-3 β) and forkhead in human rhabdomyosarcoma (FKHR) via the CCR9-CCL25 signaling axis (Johnson-Holiday, Singh et al. 2011).

However, before considering taking forward Akt1 for clinical assays as the biomarker of breast chemoresistance, further confirmations of the protein up-regulation in chemoresistant tumours with a complimentary technique may be required. In conclusion, Akt1 phosphoSer473 should

now undergo rigorous confirmations with complimentary techniques alongside extensive clinical validations using a larger cohort of pre-treatment archival sample series.

5.11.4 Role of FAK in Breast Chemoresistance:

The above protein was found in three combined antibody microarray experiments and mapped onto 1/9 in combined IPA analysis #2 (Table 52). The role of integrins in general and FAK in specific with regards to breast chemotherapy resistance have been discussed earlier in the section 1.9.4.2 of the thesis. Focal adhesion kinase (FAK) is a protein of 125 kDa that localizes to focal adhesions and activates tyrosine phosphorylation in response to integrin clustering. Tyrosine 397 is an autophosphorylation site of FAK, which is a critical component in downstream signaling and important for the anti-apoptotic activity of FAK and activation of Akt pathways (Lorch, Thomas et al. 2007). Activation of FAK leads to stimulation of the MAP kinase cascade and of PKB/Akt/NF- κ B cell signalling cascade and induce PI3K/Akt dependent anti-apoptosis (Yamamoto, Sonoda et al. 2003). The role of FAK phospho Y397 protein in tumour survival and the effects of its inhibition and reversal of anti-apoptosis have been further clarified in a recent *in-vitro* study using a small molecule inhibitor called ‘*Y11*’ (Golubovskaya, Figel et al. 2012). In this study, ‘*Y11*’ molecule was found to significantly and specifically decrease FAK autophosphorylation at Y397 site thereby effecting the viability and clonogenicity of breast BT474 cancer cells and increased detachment and apoptosis *in-vitro*. Further, constitutive activation of FAK and/or Laminin induced phosphorylation of FAK protein has been reported to cause intrinsic chemoresistance to gemcitabine (Huanwen, Zhiyong et al. 2009). Studies aimed at identifying the cause of chemo-resistance from activation of FAK protein revealed; constitutively FAK remains active in both the chemo-sensitive and chemo-resistant cell lines. However, inhibition of phosphorylation of Y397 by chemotherapeutic agents (e.g. cisplatin) is

found to confer the benefits of chemo-sensitivity by reversing its affects of anti-apoptosis (Villedieu, Deslandes et al. 2006).

The effects of FAK inhibition on chemo-resistance has also been studied *in-vitro* and *in-vivo* using the FAK inhibitor TAE226, alone and in combination with docetaxel, in taxane-sensitive (SKOV3ip1 and HeyA8) and taxane-resistant (HeyA8-MDR) ovarian cancer cell lines (Halder, Lin et al. 2007). *In-vitro*, TAE226 was found to inhibit the phosphorylation of FAK at both Y397 and Y861 sites thus inhibiting cell growth in a time- and dose-dependent manner, and enhancing docetaxel-mediated growth inhibition by 10 and 20-fold in the taxane-sensitive and taxane-resistant cell lines, respectively. *In-vivo*, FAK inhibition by TAE226 significantly reduced tumour burden in the HeyA8, SKOV3ip1, and HeyA8-MDR models (46-64%) with the greatest efficacy observed with concomitant administration of TAE226 and docetaxel in all three models. Alternatively, FAK activity can also be modified by transient, constitutive or conditional expression of inhibitory splice variants of FAK, FAK-related non-kinase (FRNK), or the Focal Adhesion Targeting (FAT) domain (Jones, Machado et al. 2001; van Nimwegen, Verkoeijen et al. 2005). Overexpression of these mutant variants is shown to either induce tumour cell killing by itself, or enhance the susceptibility to cell death to various anticancer drugs (e.g. Doxorubicin) *in-vitro* (Heidkamp, Bayer et al. 2002; Tsutsumi, Kasaoka et al. 2008).

In our study, FAK phosphoY397 expressions were confirmed on IHC only and a significant correlation was noted between higher cytoplasmic expressions in the chemoresistant tumours (Figure 46). However, limitations to protein assessments on IHC exists and include absence of a widely accepted single scoring system, site of staining, embedding medium (HistoGel™ or agarose), density of cells and thickness of cut sections (Atkins, Reiffen et al. 2004). All these factors alone or in combination can potentially influence the statistical correlations of protein

expressions determined using the technique. Therefore, due to above reasons, before concluding on the role of this protein in chemoresistance, rigorous confirmations are required.

5.11.5 Study Limitations:

This thesis has involved the analysis of novel biomarkers of anthracycline-taxane neoadjuvant breast chemotherapy using fresh tumour samples. So far, in the current study, two proteins (Akt1 and FAK) have come through the discovery and validation phases of the proteomic discovery pipeline, where their differential expression first recognised during discovery-phase experiments, and their expressions validated in clinical samples in small pilot series (Akt1 vs FAK; nuclear vs cytoplasm; $p=0.05$ vs $p=0.04$). These proteins are in addition to the two proteins (14-3-3 theta/tau, tBID) discovered and validated previously by our research group (Hodgkinson et al. 2012). However, 14-3-3 theta/tau protein previously validated using a pilot archival series (iFEC) in the VH study failed to show a significant association with chemoresistance in the combined (iFEC and *EC-D* series) IHC analysis. The possible reason to this, as elucidated in the section 5.11.1 include having a smaller patient series for the immuno validations (under-power study) AND/OR having a higher ratio of responders to non-responders in the combined analysis AND/OR potential bias introduced from the inter-observer variability as the slides were assessed by two different researchers at two different time points AND/OR using archival series from patients treated with two different chemotherapy regimens (iFEC vs *EC-D*). Further, the immuno validations of 14-3-3 beta/alpha, zeta/delta and epsilon protein isoforms also failed to attain statistical significance with chemoresistance for the above same reasons and also because researchers (TH and VH) undertaking the pathological assessments were not fully blinded to the treatment outcomes. Thus, future immuno work with these proteins

should involve a larger archival patient series treated with similar chemotherapy regimens with assessors fully blinded to treatment outcomes.

Using a comparative approach (AbMA + 2D-PAGE/MS) and a combined data analysis (9 x AbMA + 3 x 2D-PAGE/MS experiments) in two studies, a total of only 8 proteins (14-3-3 theta/tau, epsilon, beta/alpha, gamma, zeta/delta vimentin, Akt1 and FAK) have been identified as putative markers of chemoresistance. The reasons to such a low number of identified DEPs include technical limitations of proteomic methods, tumour heterogeneity and paucity of complete information on the molecular pathways on IPA. In both the studies (TH and VH), the two proteomic methods (2D-PAGE/MS and antibody microarray) that were used to analyse breast tumour samples are known to have limitation at providing a full proteome coverage on their own in a single experiment. With the conventional gel-based methods, gel variability, limitations at detecting low-abundant, membrane bound proteins and background variations with structural proteins all preclude a thorough proteome interrogation. With the antibody microarray, only 725 pre-coated antibodies cannot provide whole proteome coverage. Therefore, possibilities exist that a few other proteins of clinical relevance to therapy resistance may have been missed despite adopting a complimentary approach.

Both the cancer studies (TH & VH projects) used fresh tumour samples for proteomic analysis. Clinical tissues by nature are complex and heterogeneous. Utilising them for biomarker discovery studies can be a potential confounder. The reasons to this include difficulties of recapitulating the *in-vivo* molecular interactions and analysis of sub-populations of cells from the heterogeneous microecology. Laser Capture Micro-Dissection (LCM) is one technique that isolates histologically pure cancer cells using laser-assisted micro-dissection from complex heterogeneous tissues and micro-environments. However, the most critical limitation of

performing LCM, on any sample type, prior to proteomic analysis is sample loss, and the ability to retain sufficient sample for downstream applications (Craven, Totty et al. 2002).

As discussed in the section 2.10.2 of the thesis, molecular information stored in the Ingenuity Knowledge Base is manually curated and up-dated in a timely fashion from the published literature, pilot experimental data involving human cancer research studies and archival databases. Possibilities exist that a particular pathway(s) identified but not reported previously may therefore have been missed. This pathway(s) may be relevant to chemoresistance and has a potential to be overlooked. The above limitation has to be always kept in mind when using IPA for data mining purposes. Analysing data using a combination of different analytic methods may help overcome the above limitation. However, for this research, as only IPA was used for analysing the DEP data, author acknowledges this being one of the limitations of the study.

The clinical response data for the tumour samples used in the study was reported using the RECIST criteria (section 2.3.1). Tumours showing a $\geq 30\%$ reduction in tumour size post-treatment (at final histology) and/or complete disappearance at the final histology were called responders. However, a more robust method of representing therapy responses involves plotting a water fall plot assessing therapy response at different time points. A waterfall plot is an ordered chart where each tumour is symbolized by a vertical bar, which represents the maximum change with respect to a reference evaluation obtained during a specific period. For this study research samples, plotting a waterfall graph required assessing variations in the sum of the longest diameters of tumours on imaging (MR or US scan) whilst on therapy (e.g. 0, 3 and 6 months). However, assessing therapy responses by the above method for the study samples was difficult. This because imaging technique used in the therapy monitoring lacked uniformity in application coupled with missed patient attendances at times. Further, it was also discovered that there was

paucity of some important radiological information (e.g. tumour size not mentioned) from the 3 month scan reports which made difficult assessing therapy responses across different time points. A combination of all the above factors made assessments of therapy responses via waterfall graph method restrictive and challenging. Therefore, author acknowledges this as one other limitation of the study.

CHAPTER VI

CONCLUSIONS

Chapter 6.

The main aim of this project was to identify and expand the list of putative biomarkers of neoadjuvant breast chemotherapy using fresh tumour samples in an antibody microarray proteomic approach. Our research group have already demonstrated the feasibility of transition of proteomics based research from the cancer cell lines to clinical tissue samples. In this project, for the first time, the feasibility of working with low sample volumes ($\leq 1\text{ml}$) was explored with an aim to advance the antibody microarray based proteomic research to much smaller tissues (e.g breast cores). Also, pilot immunohistochemistry experiments were carried out for the previously identified but not validated 14-3-3 protein isoforms (epsilon, beta/alpha and zeta/delta) to confirm their clinical relevance. Lastly, using a few excluded breast tumour samples, pilot optimisation experiments were carried out for protein extractions to explore the feasibility of obtaining a required protein yield (1mg/ml) for proteomic studies using smaller clinical tissues.

6.1 SUMMARY FROM MICROARRAY ANALYSIS:

A combined analysis of four antibody microarray experiments from this project and five experiments from the previous project generated a list of 89 differentially expressed proteins (DEPs). Of these 72/89 proteins were eligible for loading onto IPA and 65/72 were mapped onto molecular networks. From the combined microarray (9 experiments) and 2D-PAGE/MS (3 experiments) analysis a total of 122 DEPs were generated and analysed using IPA. The top, most significant, canonical pathways identified was the ERK/MAPK cell signalling, PIP3/AkT cell signalling and 14-3-3 mediated cell signalling pathway. Additionally, ERK5 signalling, P70S6K signalling and Cell Cycle: G2/M DNA Damage Check point Regulation pathways previously

identified as top, most significant pathways were also identified in the combined data re-analysis in this project. The PIP3/AkT pathway from the combined analysis emerged as the most significant pathway with 13 DEPs mapped onto it. Following a thorough data analysis of the combined DEPs and the molecular pathways, three protein candidates were selected and taken forward to the confirmation and clinical validation stages of the biomarker discovery pipeline. These proteins included Vimentin (*VIM*), Akt1 phospho Ser473 (*PKB1*) and FAK phosphoY397 (*PTK2*). Of the three proteins, the differential expression (down regulation) of only vimentin was confirmed in 1/3 samples by western blotting. Previously our research group have confirmed the differential expression of apoptosis-related proteins tBID and Bcl-xL, and 14-3-3 on western blotting. These proteins were identified from five antibody microarray experiments. The differential expression of 14-3-3 theta/tau and tBID was also clinically validated using immunohistochemistry in a small pilot study (MRI-iFEC). The increased expression of 14-3-3 theta/tau, which is an anti-apoptotic protein, was found to be significantly associated with breast chemoresistance. Further, decreased expression of tBID was observed, showing reduced cleavage of BID into its active form (tBID) for apoptosis. The above evidence support increased survival of the cancer cell, by evasion of apoptosis, which is essential for the chemotherapy-resistant phenotype. Therefore, leading from the previous work, 14-3-3 proteins isoforms needed to be validated using a larger archival series for a more extensive downstream analysis.

From the current study, Akt1 phosphoser473 and FAK phosphoY397 proteins were identified and successfully validated in the chemoresistant ER+ (luminal A) subtype. Both these proteins directly or via ERK/MAPK pathway activate the PIP3/AkT pathway resulting in cell proliferation, cell cycle progression and cell survival via inhibition of apoptosis; the above cellular mechanisms mainly responsible for the chemoresistance with these proteins.

6.2 FUTURE CONFIRMATIONS AND VALIDATIONS:

There are several other DEPs highlighted by IPA that warrant future research. These protein candidates include P70S6K, DR4/5, RIP and PKC proteins. Of these, P70S6K was mapped onto 4/6 selected pathways from analysis#2 data, and the other three proteins were found in at least 2 experiments from the combined data analysis. Cancer studies have found P70S6K protein associations with paclitaxel and carboplatin chemotherapy response in advanced ovarian cancers (Carden, Stewart et al. 2012) and with cisplatin-induced cell death in MCF-7 breast cancer cell lines (Dhar, Persaud et al. 2009). Increased levels of P70S6K protein was reported to be associated with drug resistance in both these studies.

6.3 SUMMARY FROM THE NEW MICROARRAY PROTOCOL:

One of the aims of this current study was to advance the antibody microarray proteomic research platform to extend its application to smaller sample volumes. The study was successful in optimising '*Half-Labeling Microarray Protocol*' using **0.5** ml of sample volume. Of the 4 antibody microarray experiments performed in this study, a total of 3/4 experiments were successfully performed using the new protocol. As a result of this advancement, scientists can now use this high-throughput technique with smaller tissue sizes and low lysate volumes for the biomarker discovery process.

6.4 SUMMARY FROM PROTEIN EXTRACTION EXPERIMENTS:

One of the secondary aims of the project was to assess the feasibility for protein extraction and quantification using small sample volumes for microarray analysis. The aim was to optimise protein extraction technique using small breast tissue samples such as breast cores. The results from the pilot work have shown the feasibility to obtain the required 1mg/ml protein

concentration needed for the microarray analysis from a sample size ≤ 0.1 g. Our research group aims to present this research finding to support an ethic application for the breast core biopsy project.

6.5 PROTEOMICS-FUTURE PERSPECTIVE:

6.5.1 Monitoring for Chemoresistance: Intrinsic vs. Acquired

The ability to predict tumour response at the time of diagnosis would benefit both the patient and clinician, allowing the individualisation of treatment and the administration of chemotherapy to only those who are mostly likely to benefit, thus maximising treatment efficacy. In order to achieve this, clinical samples (core biopsy pre-treatment and resection samples post-treatment) had to be collected alongside corresponding relevant clinical information. Comparative proteomic analysis performed on these clinical samples would allow the identification of putative biomarkers associated with both the ‘intrinsic’, (where cancer cells are innately resistant to chemotherapy), and ‘acquired’ (where cancer cells develop resistance during treatment) mechanisms of chemotherapy resistance. If predictive biomarkers of chemotherapy resistance were transferred to the clinic, screening would be performed at the time of diagnosis, to allow subsequent treatment to be tailored accordingly. This may involve the routine screening of formalin-fixed paraffin-embedded (FFPE) core biopsy samples, with an established panel of predictive biomarkers. This is a clinically accepted approach, currently used for routine ER PR and HER2 screening, therefore if a panel of predictive biomarkers was identified it would be relatively simple to incorporate this into an existing routine protocol, without requiring extra patient samples. Also, monitoring for acquired resistance will identify molecular targets that can help understand the mechanism of chemoresistance and aid in developing targeted molecular therapies in future.

6.5.2 Developing Pre-Clinical Models:

To mimic a clinical setting, *in-vitro* breast cancer cell lines models of anthracycline-taxanes chemotherapy resistance should be developed and the identified putative biomarkers of breast chemoresistance analysed using specific protein inhibitors. From the data from our research work, ERK/MAPK and PIP3/AkT pathway protein candidates (e.g. Akt1, 14-3-3, FAK, and P70S6K) appear interesting targets for further explorations. If chemoresistance can be successfully overcome by inhibition of these proteins, an important breakthrough will be achieved in developing novel targeted treatments for the ER+ (luminal A) breast cancer subtype.

6.5.3 Concluding Remarks:

From this study and our previous pilot work, protein extraction, labelling and quantification methods using clinical tissue samples with antibody microarray and 2D-PAGE/MS proteomic techniques have been optimised and successfully used to discover biomarker of breast chemotherapy resistance. Pilot optimisation work for protein extraction & quantification using smaller size tissue samples for using core biopsies in future proteomic experiments has been performed. The current study has been complimentary to the previous work done by our research group and identified two more novel proteins (Akt1 and FAK). Future work utilising core biopsy samples for the discovery of predictive biomarkers of breast intrinsic chemoresistance is currently in the pipeline. Planning for a proof-of-principle study and ethics application has now been completed.

References:

- (2003). "Breast cancer and hormone-replacement therapy in the Million Women Study." Lancet.
- (2005). "Cancer Incidence and Mortality by Cancer Network, ." National Cancer Intelligence Network.
- (2005). "Effects of chemotherapy and hormonal therapy for early breast cancer on recurrence and 15-year survival: an overview of the randomised trials." Lancet **365**(9472): 1687-1717.
- (2009). Advanced breast cancer: diagnosis and treatment, clinical guidelines CG81 NICE.
- (2011). "Data were provided by the Office for National Statistics on request."
- (2012). The NCCN Guidelines Version 1.2012.
- Al-Bazz, Y. O., B. L. Brown, et al. (2009). "Immuno-analysis of phospho-Akt in primary human breast cancers." Int J Oncol **35**(5): 1159-1167.
- Al-Mansouri, L. J. and M. S. Alokail (2006). "Molecular basis of breast cancer." Saudi Med J **27**(1): 9-16.
- Allen, J. D., R. F. Brinkhuis, et al. (1999). "The mouse Bcrp1/Mxr/Abcp gene: amplification and overexpression in cell lines selected for resistance to topotecan, mitoxantrone, or doxorubicin." Cancer Res **59**(17): 4237-4241.
- Antoon, J. W., R. Lai, et al. (2012). "Altered death receptor signaling promotes epithelial-to-mesenchymal transition and acquired chemoresistance." Sci Rep **2**: 539.
- Aoudjit, F. and K. Vuori (2001). "Integrin signaling inhibits paclitaxel-induced apoptosis in breast cancer cells." Oncogene **20**(36): 4995-5004.
- Atkins, D., K. A. Reiffen, et al. (2004). "Immunohistochemical detection of EGFR in paraffin-embedded tumor tissues: variation in staining intensity due to choice of fixative and storage time of tissue sections." J Histochem Cytochem **52**(7): 893-901.
- Bartek, J., C. Lukas, et al. (2004). "Checking on DNA damage in S phase." Nat Rev Mol Cell Biol **5**(10): 792-804.
- Bauer, J. A. (2010). "Identification of markers of taxane sensitivity using proteomic and genomic analyses of breast tumors from patients receiving neoadjuvant paclitaxel and radiation." Clin Cancer Res **16**(2): 681-690.
- Bear, H. D., S. Anderson, et al. (2003). "The effect on tumor response of adding sequential preoperative docetaxel to preoperative doxorubicin and cyclophosphamide: preliminary results from National Surgical Adjuvant Breast and Bowel Project Protocol B-27." J Clin Oncol **21**(22): 4165-4174.
- Bear, H. D., S. Anderson, et al. (2006). "Sequential preoperative or postoperative docetaxel added to preoperative doxorubicin plus cyclophosphamide for operable breast cancer: National Surgical Adjuvant Breast and Bowel Project Protocol B-27." J Clin Oncol **24**(13): 2019-2027.
- Bertucci, F. and D. Birnbaum (2008). "Reasons for breast cancer heterogeneity." J Biol **7**(2): 6.
- Bhattacharyya, M. (2008). "Using MRI to plan breast-conserving surgery following neoadjuvant chemotherapy for early breast cancer." Br J Cancer **98**(2): 289-293.
- Bonnetterre, J., V. Dieras, et al. (2004). "Phase II multicentre randomised study of docetaxel plus epirubicin vs 5-fluorouracil plus epirubicin and cyclophosphamide in metastatic breast cancer." Br J Cancer **91**(8): 1466-1471.
- Braakman, R. B. (2011). "Laser capture microdissection applications in breast cancer proteomics." Methods Mol Biol **755**: 143-154.

- Braakman, R. B., T. M. Luider, et al. "Laser capture microdissection applications in breast cancer proteomics." Methods Mol Biol **755**: 143-154.
- Burcombe, R. J., A. Makris, et al. (2005). "Evaluation of ER, PgR, HER-2 and Ki-67 as predictors of response to neoadjuvant anthracycline chemotherapy for operable breast cancer." Br J Cancer **92**(1): 147-155.
- Burden, D. W. (Sept 2008). "Guide to the Homogenization of Biological Samples." Random Primers(7): 1-14.
- Bustos, D. M. (2012). "The role of protein disorder in the 14-3-3 interaction network." Mol Biosyst **8**(1): 178-184.
- Cancer, A. J. C. o. Breast Cancer Staging.
- Carden, C. P., A. Stewart, et al. (2012). "The association of PI3 kinase signaling and chemoresistance in advanced ovarian cancer." Mol Cancer Ther **11**(7): 1609-1617.
- Carey, L. A., E. C. Dees, et al. (2007). "The triple negative paradox: primary tumor chemosensitivity of breast cancer subtypes." Clin Cancer Res **13**(8): 2329-2334.
- Celis, J. E., J. M. Moreira, et al. (2005). "Towards discovery-driven translational research in breast cancer." FEBS J **272**(1): 2-15.
- Chaney, S. G. and A. Sancar (1996). "DNA repair: enzymatic mechanisms and relevance to drug response." J Natl Cancer Inst **88**(19): 1346-1360.
- Chaudhry, P. and E. Asselin (2009). "Resistance to chemotherapy and hormone therapy in endometrial cancer." Endocr Relat Cancer **16**(2): 363-380.
- Chen, E. I. and J. R. Yates, 3rd (2007). "Cancer proteomics by quantitative shotgun proteomics." Mol Oncol **1**(2): 144-159.
- Chen, G. and D. V. Goeddel (2002). "TNF-R1 signaling: a beautiful pathway." Science **296**(5573): 1634-1635.
- Chen, J., A. R. Gomes, et al. (2010). "Constitutively nuclear FOXO3a localization predicts poor survival and promotes Akt phosphorylation in breast cancer." PLoS One **5**(8): e12293.
- Chen, W. J., H. Wang, et al. (2010). "Multidrug resistance in breast cancer cells during epithelial-mesenchymal transition is modulated by breast cancer resistant protein." Chin J Cancer **29**(2): 151-157.
- Chen, Y. Y., Z. X. Wang, et al. (2009). "Knockdown of focal adhesion kinase reverses colon carcinoma multicellular resistance." Cancer Sci **100**(9): 1708-1713.
- Cheng, J. Q., X. Jiang, et al. (2002). "Role of X-linked inhibitor of apoptosis protein in chemoresistance in ovarian cancer: possible involvement of the phosphoinositide-3 kinase/Akt pathway." Drug Resist Updat **5**(3-4): 131-146.
- Chua, B. T., D. Gallego-Ortega, et al. (2009). "Regulation of Akt(ser473) phosphorylation by choline kinase in breast carcinoma cells." Mol Cancer **8**: 131.
- Chuthapisith, S., R. Layfield, et al. (2007). "Proteomic profiling of MCF-7 breast cancer cells with chemoresistance to different types of anti-cancer drugs." Int J Oncol **30**(6): 1545-1551.
- Craven, R. A., N. Totty, et al. (2002). "Laser capture microdissection and two-dimensional polyacrylamide gel electrophoresis: evaluation of tissue preparation and sample limitations." Am J Pathol **160**(3): 815-822.
- Crown, J., M. O'Leary, et al. (2004). "Docetaxel and paclitaxel in the treatment of breast cancer: a review of clinical experience." Oncologist **9 Suppl 2**: 24-32.
- Daidone, M. G., S. Veneroni, et al. (1999). "Biological markers as indicators of response to primary and adjuvant chemotherapy in breast cancer." Int J Cancer **84**(6): 580-586.

- Dejean, L. M., S. Martinez-Caballero, et al. (2006). "Is MAC the knife that cuts cytochrome c from mitochondria during apoptosis?" Cell Death Differ **13**(8): 1387-1395.
- Denis, F., A. V. Desbiez-Bourcier, et al. (2004). "Contrast enhanced magnetic resonance imaging underestimates residual disease following neoadjuvant docetaxel based chemotherapy for breast cancer." Eur J Surg Oncol **30**(10): 1069-1076.
- DeVita, V. T., Jr. and E. Chu (2008). "A history of cancer chemotherapy." Cancer Res **68**(21): 8643-8653.
- Dhar, R., S. D. Persaud, et al. (2009). "Proteolytic cleavage of p70 ribosomal S6 kinase by caspase-3 during DNA damage-induced apoptosis." Biochemistry **48**(7): 1474-1480.
- Diamandis, E. P. (2010). "Cancer biomarkers: can we turn recent failures into success?" J Natl Cancer Inst **102**(19): 1462-1467.
- Dihazi, H. and G. A. Muller (2007). "Urinary proteomics: a tool to discover biomarkers of kidney diseases." Expert Rev Proteomics **4**(1): 39-50.
- Doyle, L. A., W. Yang, et al. (1998). "A multidrug resistance transporter from human MCF-7 breast cancer cells." Proc Natl Acad Sci U S A **95**(26): 15665-15670.
- Dumitrescu, R. G. and I. Cotarla (2005). "Understanding breast cancer risk -- where do we stand in 2005?" J Cell Mol Med **9**(1): 208-221.
- Ericsson, C. and M. Nister (2011). "Blood plasma handling for protein analysis." Methods Mol Biol **675**: 333-341.
- Farquhar C, M. J., Lethaby A, Suckling JA, Lamberts Q. "Long term hormone therapy for perimenopausal and postmenopausal women." Cochrane Database Syst Rev **2009**.
- Fedier, A., V. A. Schwarz, et al. (2001). "Resistance to topoisomerase poisons due to loss of DNA mismatch repair." Int J Cancer **93**(4): 571-576.
- Fesik, S. W. and Y. Shi (2001). "Structural biology. Controlling the caspases." Science **294**(5546): 1477-1478.
- Filipits, M., R. Malayeri, et al. (1999). "Expression of the multidrug resistance protein (MRP1) in breast cancer." Anticancer Res **19**(6B): 5043-5049.
- Fisher, B., A. Brown, et al. (1997). "Effect of preoperative chemotherapy on local-regional disease in women with operable breast cancer: findings from National Surgical Adjuvant Breast and Bowel Project B-18." J Clin Oncol **15**(7): 2483-2493.
- Fisher, B., J. Bryant, et al. (1998). "Effect of preoperative chemotherapy on the outcome of women with operable breast cancer." J Clin Oncol **16**(8): 2672-2685.
- Frisch, S. M. and H. Francis (1994). "Disruption of epithelial cell-matrix interactions induces apoptosis." J Cell Biol **124**(4): 619-626.
- Fujiwara, A. H., T.; Westley (2000). "Anthracycline Antibiotics " Critical Reviews in Biotechnology **3**(2): 133.
- Gardina, P. J., T. A. Clark, et al. (2006). "Alternative splicing and differential gene expression in colon cancer detected by a whole genome exon array." BMC Genomics **7**: 325.
- Garimella, V., O. Qutob, et al. (2007). "Recurrence rates after DCE-MRI image guided planning for breast-conserving surgery following neoadjuvant chemotherapy for locally advanced breast cancer patients." Eur J Surg Oncol **33**(2): 157-161.
- Geyer, F. C., C. Marchio, et al. (2009). "The role of molecular analysis in breast cancer." Pathology **41**(1): 77-88.
- Ghobrial, I. M., D. J. McCormick, et al. (2005). "Proteomic analysis of mantle-cell lymphoma by protein microarray." Blood **105**(9): 3722-3730.

- Gianni, L., J. Baselga, et al. (2005). "Feasibility and tolerability of sequential doxorubicin/paclitaxel followed by cyclophosphamide, methotrexate, and fluorouracil and its effects on tumor response as preoperative therapy." Clin Cancer Res **11**(24 Pt 1): 8715-8721.
- Glass AG, L. J. J., Carreon JD, Hoover RN (2007). "Breast cancer incidence, 1980-2006: combined roles of menopausal hormone therapy, screening mammography, and estrogen receptor status." J Natl Cancer Inst
- Golubovskaya, V. M., S. Figel, et al. (2012). "A small molecule focal adhesion kinase (FAK) inhibitor, targeting Y397 site: 1-(2-hydroxyethyl)-3, 5, 7-triaza-1-azoniatricyclo [3.3.1.1(3,7)]decane; bromide effectively inhibits FAK autophosphorylation activity and decreases cancer cell viability, clonogenicity and tumor growth in vivo." Carcinogenesis **33**(5): 1004-1013.
- Gorg, A., W. Weiss, et al. (2004). "Current two-dimensional electrophoresis technology for proteomics." Proteomics **4**(12): 3665-3685.
- Gromov, P., J. E. Celis, et al. (2008). "A single lysis solution for the analysis of tissue samples by different proteomic technologies." Mol Oncol **2**(4): 368-379.
- Guarneri, V., K. Broglio, et al. (2006). "Prognostic value of pathologic complete response after primary chemotherapy in relation to hormone receptor status and other factors." J Clin Oncol **24**(7): 1037-1044.
- GuidelinesTM, N. C. P. G. i. O. N. (2012). "Breast Cancer." (1.2012).
- Guiu, S., L. Arnould, et al. (2013). "Pathological response and survival after neoadjuvant therapy for breast cancer: a 30-year study." Breast **22**(3): 301-308.
- Gustafsson, J. A. (1999). "Estrogen receptor beta--a new dimension in estrogen mechanism of action." J Endocrinol **163**(3): 379-383.
- Gygi, S. P., Y. Rochon, et al. (1999). "Correlation between protein and mRNA abundance in yeast." Mol Cell Biol **19**(3): 1720-1730.
- Halder, J., Y. G. Lin, et al. (2007). "Therapeutic efficacy of a novel focal adhesion kinase inhibitor TAE226 in ovarian carcinoma." Cancer Res **67**(22): 10976-10983.
- Haqqani, A. S., J. F. Kelly, et al. (2008). "Quantitative protein profiling by mass spectrometry using label-free proteomics." Methods Mol Biol **439**: 241-256.
- He, J., S. A. Whelan, et al. (2011). "Proteomic-based biosignatures in breast cancer classification and prediction of therapeutic response." Int J Proteomics **2011**: 896476.
- Heidkamp, M. C., A. L. Bayer, et al. (2002). "GFP-FRNK disrupts focal adhesions and induces anoikis in neonatal rat ventricular myocytes." Circ Res **90**(12): 1282-1289.
- Helbich, T. H., M. Rudas, et al. (1998). "Evaluation of needle size for breast biopsy: comparison of 14-, 16-, and 18-gauge biopsy needles." AJR Am J Roentgenol **171**(1): 59-63.
- Hennessy, B. T., G. N. Hortobagyi, et al. (2005). "Outcome after pathologic complete eradication of cytologically proven breast cancer axillary node metastases following primary chemotherapy." J Clin Oncol **23**(36): 9304-9311.
- Herschkowitz, J. I., K. Simin, et al. (2007). "Identification of conserved gene expression features between murine mammary carcinoma models and human breast tumors." Genome Biol **8**(5): R76.
- Hewitt, S. C., J. C. Harrell, et al. (2005). "Lessons in estrogen biology from knockout and transgenic animals." Annu Rev Physiol **67**: 285-308.
- Hilakivi-Clarke, L., C. Wang, et al. (2004). "Nutritional modulation of the cell cycle and breast cancer." Endocr Relat Cancer **11**(4): 603-622.

- Hodgkinson, V. C. (2012). "Pilot and feasibility study: comparative proteomic analysis by 2-DE MALDI TOF/TOF MS reveals 14-3-3 proteins as putative biomarkers of response to neoadjuvant chemotherapy in ER-positive breast cancer." J Proteomics **75**(9): 2745-2752.
- Hodgkinson, V. C., E. L. D, et al. (2012). "Proteomic identification of predictive biomarkers of resistance to neoadjuvant chemotherapy in luminal breast cancer: a possible role for 14-3-3 theta/tau and tBID?" J Proteomics **75**(4): 1276-1283.
- Honjo, Y., C. A. Hrycyna, et al. (2001). "Acquired mutations in the MXR/BCRP/ABCP gene alter substrate specificity in MXR/BCRP/ABCP-overexpressing cells." Cancer Res **61**(18): 6635-6639.
- Hood, J. D. and D. A. Cheresh (2002). "Role of integrins in cell invasion and migration." Nat Rev Cancer **2**(2): 91-100.
- Huanwen, W., L. Zhiyong, et al. (2009). "Intrinsic chemoresistance to gemcitabine is associated with constitutive and laminin-induced phosphorylation of FAK in pancreatic cancer cell lines." Mol Cancer **8**: 125.
- Hudis, C. and S. Modi (2007). "Preoperative chemotherapy for breast cancer: miracle or mirage?" JAMA **298**(22): 2665-2667.
- Huober, J., G. von Minckwitz, et al. (2010). "Effect of neoadjuvant anthracycline-taxane-based chemotherapy in different biological breast cancer phenotypes: overall results from the GeparTrio study." Breast Cancer Res Treat **124**(1): 133-140.
- Iseri, O. D., M. D. Kars, et al. (2011). "Drug resistant MCF-7 cells exhibit epithelial-mesenchymal transition gene expression pattern." Biomed Pharmacother **65**(1): 40-45.
- Ishikawa, T., M. T. Kuo, et al. (2000). "The human multidrug resistance-associated protein (MRP) gene family: from biological function to drug molecular design." Clin Chem Lab Med **38**(9): 893-897.
- Jimenez-Marin, A., M. Collado-Romero, et al. (2009). "Biological pathway analysis by ArrayUnlock and Ingenuity Pathway Analysis." BMC Proc **3 Suppl 4**: S6.
- Johann, D. J., Jr., M. D. McGuigan, et al. (2004). "Clinical proteomics and biomarker discovery." Ann N Y Acad Sci **1022**: 295-305.
- Johnson-Holiday, C., R. Singh, et al. (2011). "CCR9-CCL25 interactions promote cisplatin resistance in breast cancer cell through Akt activation in a PI3K-dependent and FAK-independent fashion." World J Surg Oncol **9**: 46.
- Jones, G., J. Machado, Jr., et al. (2001). "PTEN-independent induction of caspase-mediated cell death and reduced invasion by the focal adhesion targeting domain (FAT) in human astrocytic brain tumors which highly express focal adhesion kinase (FAK)." Cancer Res **61**(15): 5688-5691.
- Jones, R. L. and I. E. Smith (2006). "Neoadjuvant treatment for early-stage breast cancer: opportunities to assess tumour response." Lancet Oncol **7**(10): 869-874.
- Kaufmann, S. H. and W. C. Earnshaw (2000). "Induction of apoptosis by cancer chemotherapy." Exp Cell Res **256**(1): 42-49.
- Keam, B., S. A. Im, et al. (2007). "Prognostic impact of clinicopathologic parameters in stage II/III breast cancer treated with neoadjuvant docetaxel and doxorubicin chemotherapy: paradoxical features of the triple negative breast cancer." BMC Cancer **7**: 203.
- Keen, J. C. and N. E. Davidson (2003). "The biology of breast carcinoma." Cancer **97**(3 Suppl): 825-833.
- Kelley, M. R., Y. W. Kow, et al. (2003). "Disparity between DNA base excision repair in yeast and mammals: translational implications." Cancer Res **63**(3): 549-554.

- Kokkinos, M. I., R. Wafai, et al. (2007). "Vimentin and epithelial-mesenchymal transition in human breast cancer--observations in vitro and in vivo." Cells Tissues Organs **185**(1-3): 191-203.
- Kopf, E., D. Shnitzer, et al. (2005). "Panorama Ab Microarray Cell Signaling kit: a unique tool for protein expression analysis." Proteomics **5**(9): 2412-2416.
- Kopp, F., P. S. Oak, et al. (2012). "miR-200c sensitizes breast cancer cells to doxorubicin treatment by decreasing TrkB and Bmi1 expression." PLoS One **7**(11): e50469.
- Korsching, E., J. Packeisen, et al. (2005). "The origin of vimentin expression in invasive breast cancer: epithelial-mesenchymal transition, myoepithelial histogenesis or histogenesis from progenitor cells with bilinear differentiation potential?" J Pathol **206**(4): 451-457.
- Krebs, T. L., W. A. Berg, et al. (1996). "Large-core biopsy guns: comparison for yield of breast tissue." Radiology **200**(2): 365-368.
- Kumar, R., R. K. Vadlamudi, et al. (2000). "Apoptosis in mammary gland and cancer." Endocr Relat Cancer **7**(4): 257-269.
- Laura Gatti, F. Z. (2005). Overview of Tumour Cells Chemoresistance Mechanisms.
- Leal, C., R. Henrique, et al. (2001). "Apocrine ductal carcinoma in situ of the breast: histologic classification and expression of biologic markers." Hum Pathol **32**(5): 487-493.
- Leder, E. H., J. Merila, et al. (2009). "A flexible whole-genome microarray for transcriptomics in three-spine stickleback (*Gasterosteus aculeatus*)." BMC Genomics **10**: 426.
- Leonessa, F. and R. Clarke (2003). "ATP binding cassette transporters and drug resistance in breast cancer." Endocr Relat Cancer **10**(1): 43-73.
- Li, X., Y. Lu, et al. (2005). "Differential responses to doxorubicin-induced phosphorylation and activation of Akt in human breast cancer cells." Breast Cancer Res **7**(5): R589-597.
- Liang, X. and Y. Huang (2002). "Physical state changes of membrane lipids in human lung adenocarcinoma A(549) cells and their resistance to cisplatin." Int J Biochem Cell Biol **34**(10): 1248-1255.
- Lin, H. J., F. C. Hsieh, et al. (2005). "Elevated phosphorylation and activation of PDK-1/AKT pathway in human breast cancer." Br J Cancer **93**(12): 1372-1381.
- Lipshutz, R. J., S. P. Fodor, et al. (1999). "High density synthetic oligonucleotide arrays." Nat Genet **21**(1 Suppl): 20-24.
- Liu, E. T. and C. Sotiriou (2002). "Defining the galaxy of gene expression in breast cancer." Breast Cancer Res **4**(4): 141-144.
- Longley, D. B., D. P. Harkin, et al. (2003). "5-fluorouracil: mechanisms of action and clinical strategies." Nat Rev Cancer **3**(5): 330-338.
- Loo, C. E., H. J. Teertstra, et al. (2008). "Dynamic contrast-enhanced MRI for prediction of breast cancer response to neoadjuvant chemotherapy: initial results." AJR Am J Roentgenol **191**(5): 1331-1338.
- Lorch, J. H., T. O. Thomas, et al. (2007). "Bortezomib inhibits cell-cell adhesion and cell migration and enhances epidermal growth factor receptor inhibitor-induced cell death in squamous cell cancer." Cancer Res **67**(2): 727-734.
- Lv, M., B. Li, et al. (2011). "Predictive role of molecular subtypes in response to neoadjuvant chemotherapy in breast cancer patients in Northeast China." Asian Pac J Cancer Prev **12**(9): 2411-2417.
- Madoz-Gurpide, J., M. Canamero, et al. (2007). "A proteomics analysis of cell signaling alterations in colorectal cancer." Mol Cell Proteomics **6**(12): 2150-2164.

- Mariman, E. C. (2009). "2DE-proteomics meta-data indicate the existence of distinct cellular stress-responsive mechanisms." Expert Rev Proteomics **6**(4): 337-339.
- Masters, S. C., R. R. Subramanian, et al. (2002). "Survival-promoting functions of 14-3-3 proteins." Biochem Soc Trans **30**(4): 360-365.
- Mauri, D., N. Pavlidis, et al. (2005). "Neoadjuvant versus adjuvant systemic treatment in breast cancer: a meta-analysis." J Natl Cancer Inst **97**(3): 188-194.
- May, P. and E. May (1999). "Twenty years of p53 research: structural and functional aspects of the p53 protein." Oncogene **18**(53): 7621-7636.
- Miller, K. D. and G. W. Sledge, Jr. (1999). "Taxanes in the treatment of breast cancer: a prodigy comes of age." Cancer Invest **17**(2): 121-136.
- Mitra, S. K. and D. D. Schlaepfer (2006). "Integrin-regulated FAK-Src signaling in normal and cancer cells." Curr Opin Cell Biol **18**(5): 516-523.
- Moler, E. J., M. L. Chow, et al. (2000). "Analysis of molecular profile data using generative and discriminative methods." Physiol Genomics **4**(2): 109-126.
- Murillo-Ortiz, B., E. Perez-Luque, et al. (2008). "Expression of estrogen receptor alpha and beta in breast cancers of pre- and post-menopausal women." Pathol Oncol Res **14**(4): 435-442.
- Newman, L. A., H. M. Kuerer, et al. (2001). "Adverse prognostic significance of infraclavicular lymph nodes detected by ultrasonography in patients with locally advanced breast cancer." Am J Surg **181**(4): 313-318.
- Nigg, E. A. (1995). "Cyclin-dependent protein kinases: key regulators of the eukaryotic cell cycle." Bioessays **17**(6): 471-480.
- Nuki, G. and P. A. Simkin (2006). "A concise history of gout and hyperuricemia and their treatment." Arthritis Res Ther **8 Suppl 1**: S1.
- Olopade, O. I., M. O. Adeyanju, et al. (1997). "Overexpression of BCL-x protein in primary breast cancer is associated with high tumor grade and nodal metastases." Cancer J Sci Am **3**(4): 230-237.
- Olsson, B., H. Zetterberg, et al. "Biomarker-based dissection of neurodegenerative diseases." Prog Neurobiol **95**(4): 520-534.
- Osborne, C., P. Wilson, et al. (2004). "Oncogenes and tumor suppressor genes in breast cancer: potential diagnostic and therapeutic applications." Oncologist **9**(4): 361-377.
- Partridge, S. C., J. E. Gibbs, et al. (2002). "Accuracy of MR imaging for revealing residual breast cancer in patients who have undergone neoadjuvant chemotherapy." AJR Am J Roentgenol **179**(5): 1193-1199.
- Pathmanathan, N. and R. L. Balleine (2013). "Ki67 and proliferation in breast cancer." J Clin Pathol **66**(6): 512-516.
- Peppercorn, J., C. M. Perou, et al. (2008). "Molecular subtypes in breast cancer evaluation and management: divide and conquer." Cancer Invest **26**(1): 1-10.
- Perou, C. M., T. Sorlie, et al. (2000). "Molecular portraits of human breast tumours." Nature **406**(6797): 747-752.
- Petit, T., M. Wilt, et al. (2004). "Comparative value of tumour grade, hormonal receptors, Ki-67, HER-2 and topoisomerase II alpha status as predictive markers in breast cancer patients treated with neoadjuvant anthracycline-based chemotherapy." Eur J Cancer **40**(2): 205-211.
- Petrak, J., R. Ivanek, et al. (2008). "Deja vu in proteomics. A hit parade of repeatedly identified differentially expressed proteins." Proteomics **8**(9): 1744-1749.

- Pitteri, S. J. and S. M. Hanash (2007). "Proteomic approaches for cancer biomarker discovery in plasma." Expert Rev Proteomics **4**(5): 589-590.
- Prat, A. and C. M. Perou (2011). "Deconstructing the molecular portraits of breast cancer." Mol Oncol **5**(1): 5-23.
- Quinn, D. I., S. M. Henshall, et al. (2005). "Molecular markers of prostate cancer outcome." Eur J Cancer **41**(6): 858-887.
- Radetzki, S., C. H. Kohne, et al. (2002). "The apoptosis promoting Bcl-2 homologues Bak and Nbk/Bik overcome drug resistance in Mdr-1-negative and Mdr-1-overexpressing breast cancer cell lines." Oncogene **21**(2): 227-238.
- Radhakrishnan, V. M., C. W. Putnam, et al. (2011). "P53 suppresses expression of the 14-3-3 gamma oncogene." BMC Cancer **11**: 378.
- Ramu, A., D. Glaubiger, et al. (1983). "Plasma membrane lipid structural order in doxorubicin-sensitive and -resistant P388 cells." Cancer Res **43**(11): 5533-5537.
- Reed, J. C. (1999). "Dysregulation of apoptosis in cancer." J Clin Oncol **17**(9): 2941-2953.
- Riley, T., E. Sontag, et al. (2008). "Transcriptional control of human p53-regulated genes." Nat Rev Mol Cell Biol **9**(5): 402-412.
- Ring, A. E., I. E. Smith, et al. (2004). "Oestrogen receptor status, pathological complete response and prognosis in patients receiving neoadjuvant chemotherapy for early breast cancer." Br J Cancer **91**(12): 2012-2017.
- Rouzier, R., C. M. Perou, et al. (2005). "Breast cancer molecular subtypes respond differently to preoperative chemotherapy." Clin Cancer Res **11**(16): 5678-5685.
- Sandhu, R., J. S. Parker, et al. (2010). "Microarray-Based Gene Expression Profiling for Molecular Classification of Breast Cancer and Identification of New Targets for Therapy." Lab Medicine **41**(6): 364-372.
- Satoh, J. (2012). "Molecular network analysis of human microRNA targetome: from cancers to Alzheimer's disease." BioData Min **5**(1): 17.
- Satoh, T. H., T. A. Surmacz, et al. (2003). "Inhibition of focal adhesion kinase by antisense oligonucleotides enhances the sensitivity of breast cancer cells to camptothecins." Biocell **27**(1): 47-55.
- Sedmak, J. J. and S. E. Grossberg (1977). "A rapid, sensitive, and versatile assay for protein using Coomassie brilliant blue G250." Anal Biochem **79**(1-2): 544-552.
- Selvakumaran, M., D. A. Pisarcik, et al. (2003). "Enhanced cisplatin cytotoxicity by disturbing the nucleotide excision repair pathway in ovarian cancer cell lines." Cancer Res **63**(6): 1311-1316.
- Shaaban AM, S. J., West CR (2002). "Histopathologic types of benign breast lesions and the risk of breast cancer." Am J Surg Pathology.
- Shao, C., Y. Wang, et al. "Applications of urinary proteomics in biomarker discovery." Sci China Life Sci **54**(5): 409-417.
- Shou, J., H. R. Qian, et al. (2006). "Optimization and validation of small quantity RNA profiling for identifying TNF responses in cultured human vascular endothelial cells." J Pharmacol Toxicol Methods **53**(2): 152-159.
- Simstein, R., M. Burow, et al. (2003). "Apoptosis, chemoresistance, and breast cancer: insights from the MCF-7 cell model system." Exp Biol Med (Maywood) **228**(9): 995-1003.
- Smith, L., O. Qutob, et al. (2009). "Proteomic identification of putative biomarkers of radiotherapy resistance: a possible role for the 26S proteasome?" Neoplasia **11**(11): 1194-1207.

- Smith, L., M. B. Watson, et al. (2006). "The analysis of doxorubicin resistance in human breast cancer cells using antibody microarrays." Mol Cancer Ther **5**(8): 2115-2120.
- Sommers, C. L., S. E. Heckford, et al. (1992). "Loss of epithelial markers and acquisition of vimentin expression in adriamycin- and vinblastine-resistant human breast cancer cell lines." Cancer Res **52**(19): 5190-5197.
- Sorlie, T., C. M. Perou, et al. (2001). "Gene expression patterns of breast carcinomas distinguish tumor subclasses with clinical implications." Proc Natl Acad Sci U S A **98**(19): 10869-10874.
- Sorlie, T., C. M. Perou, et al. (2001). "Gene expression patterns of breast carcinomas distinguish tumor subclasses with clinical implications." Proc Natl Acad Sci U S A **98**(19): 10869-10874.
- Sotiriou, C., S. Y. Neo, et al. (2003). "Breast cancer classification and prognosis based on gene expression profiles from a population-based study." Proc Natl Acad Sci U S A **100**(18): 10393-10398.
- Sotiriou, C., P. Wirapati, et al. (2006). "Gene expression profiling in breast cancer: understanding the molecular basis of histologic grade to improve prognosis." J Natl Cancer Inst **98**(4): 262-272.
- Stavrovskaya, A. A. (2000). "Cellular mechanisms of multidrug resistance of tumor cells." Biochemistry (Mosc) **65**(1): 95-106.
- Steger, G. G. and R. Bartsch (2011). "Trends and Novel Approaches in Neoadjuvant Treatment of Breast Cancer." Breast Care (Basel) **6**(6): 427-433.
- Sun, Y. F., X. R. Yang, et al. "Circulating tumor cells: advances in detection methods, biological issues, and clinical relevance." J Cancer Res Clin Oncol **137**(8): 1151-1173.
- Takimoto CH, C. E. (2008). "Principles of Oncologic Pharmacotherapy" Cancer Management: A Multidisciplinary Approach.
- Therasse, P., S. G. Arbuck, et al. (2000). "New guidelines to evaluate the response to treatment in solid tumors. European Organization for Research and Treatment of Cancer, National Cancer Institute of the United States, National Cancer Institute of Canada." J Natl Cancer Inst **92**(3): 205-216.
- Tsujimoto, Y., L. R. Finger, et al. (1984). "Cloning of the chromosome breakpoint of neoplastic B cells with the t(14;18) chromosome translocation." Science **226**(4678): 1097-1099.
- Tsutsumi, K., T. Kasaoka, et al. (2008). "Tumor growth inhibition by synthetic and expressed siRNA targeting focal adhesion kinase." Int J Oncol **33**(1): 215-224.
- Tzivion, G., V. S. Gupta, et al. (2006). "14-3-3 proteins as potential oncogenes." Semin Cancer Biol **16**(3): 203-213.
- van 't Veer, L. J., H. Dai, et al. (2002). "Gene expression profiling predicts clinical outcome of breast cancer." Nature **415**(6871): 530-536.
- van de Vijver, M. J., Y. D. He, et al. (2002). "A gene-expression signature as a predictor of survival in breast cancer." N Engl J Med **347**(25): 1999-2009.
- van Nimwegen, M. J., S. Verkoeijen, et al. (2005). "Requirement for focal adhesion kinase in the early phase of mammary adenocarcinoma lung metastasis formation." Cancer Res **65**(11): 4698-4706.
- Vazquez, A., L. F. Grochola, et al. (2010). "Chemosensitivity profiles identify polymorphisms in the p53 network genes 14-3-3tau and CD44 that affect sarcoma incidence and survival." Cancer Res **70**(1): 172-180.

- Villedieu, M., E. Deslandes, et al. (2006). "Acquisition of chemoresistance following discontinuous exposures to cisplatin is associated in ovarian carcinoma cells with progressive alteration of FAK, ERK and p38 activation in response to treatment." Gynecol Oncol **101**(3): 507-519.
- Vogelstein, B., D. Lane, et al. (2000). "Surfing the p53 network." Nature **408**(6810): 307-310.
- von Minckwitz, G., S. Kummel, et al. (2008). "Intensified neoadjuvant chemotherapy in early-responding breast cancer: phase III randomized GeparTrio study." J Natl Cancer Inst **100**(8): 552-562.
- Wajant, H. (2002). "The Fas signaling pathway: more than a paradigm." Science **296**(5573): 1635-1636.
- Wang, B., K. Liu, et al. (2010). "14-3-3Tau regulates ubiquitin-independent proteasomal degradation of p21, a novel mechanism of p21 downregulation in breast cancer." Mol Cell Biol **30**(6): 1508-1527.
- Watermann, D. O., B. Gabriel, et al. (2005). "Specific induction of pp125 focal adhesion kinase in human breast cancer." Br J Cancer **93**(6): 694-698.
- Weiss, W. and A. Gorg (2008). "Sample solubilization buffers for two-dimensional electrophoresis." Methods Mol Biol **424**: 35-42.
- West, K. A. and P. A. Dennis (2011). "Starting with the ABCs: Akt in breast cancer." Mol Cancer Ther **10**(11): 2031.
- Westlake S, C. N. (2008). "Cancer incidence and mortality: trends in the United Kingdom and constituent countries, 1993 to 2004." Health Statistics Quarterly.
- Wolmark, N., J. Wang, et al. (2001). "Preoperative chemotherapy in patients with operable breast cancer: nine-year results from National Surgical Adjuvant Breast and Bowel Project B-18." J Natl Cancer Inst Monogr(30): 96-102.
- Wu, C. C. and M. J. MacCoss (2002). "Shotgun proteomics: tools for the analysis of complex biological systems." Curr Opin Mol Ther **4**(3): 242-250.
- Xiong, M., X. Fang, et al. (2001). "Biomarker identification by feature wrappers." Genome Res **11**(11): 1878-1887.
- Yamamoto, D., Y. Sonoda, et al. (2003). "FAK overexpression upregulates cyclin D3 and enhances cell proliferation via the PKC and PI3-kinase-Akt pathways." Cell Signal **15**(6): 575-583.
- Yamashita, H., M. Nishio, et al. (2004). "Coexistence of HER2 over-expression and p53 protein accumulation is a strong prognostic molecular marker in breast cancer." Breast Cancer Res **6**(1): R24-30.
- Yi, W., J. Peng, et al. (2013). "[Differential protein expressions in breast cancer between drug sensitive tissues and drug resistant tissues]." Zhong Nan Da Xue Xue Bao Yi Xue Ban **38**(2): 148-154.
- Yoshioka, T., M. Hosoda, et al. (2013). "Prognostic significance of pathologic complete response and Ki67 expression after neoadjuvant chemotherapy in breast cancer." Breast Cancer.
- Zepeda-Castilla, E. J., E. Recinos-Money, et al. (2008). "[Molecular classification of breast cancer]." Cir Cir **76**(1): 87-93.
- Zheng, W. Q., J. Lu, et al. (2001). "Variation of ER status between primary and metastatic breast cancer and relationship to p53 expression*." Steroids **66**(12): 905-910.
- Zhou, B. P., Y. Liao, et al. (2001). "Cytoplasmic localization of p21Cip1/WAF1 by Akt-induced phosphorylation in HER-2/neu-overexpressing cells." Nat Cell Biol **3**(3): 245-252.

- Zhu, C., I. Rawe, et al. (2008). "Differential protein expression in human corneal endothelial cells cultured from young and older donors." Mol Vis **14**: 1805-1814.
- Zong, Y., S. Zhang, et al. (2007). "Forward-phase and reverse-phase protein microarray." Methods Mol Biol **381**: 363-374.

Appendix 1: The full clinico-pathological, and therapy response details of the breast tumour samples collected for the research project between January 2008 to June 2011 from the Hull and East Yorkshire Hospitals NHS Trust breast unit. A total of n=50 fresh tumour samples were collected and the clinical information details including the tumour grade, IHC determined receptor status, pre and post treatment MRI/US tumour sizes, chemotherapy administered, final histopathological size and therapy response as determined using the RECIST criteria are outlined in the table below (refer sections 2.3 and 2.3.1)

Ductal / Lobular	Grade	Molecular Subtype	Tumour size pre-chemotherapy		Therapy administered	Tumour size post-chemotherapy		Tumour size (pathology)	Response (% increase/reduction)
			MRI	US		MRI	US		
Ductal	Grade 3 (poor)	ER+ PR- HER2-.	-	24mm mass + diffuse area	ECx4 Docetaxel x 4	-	many nodules max 4mm. Diffuse area of 90mm	max overall 120mm composed of nodules/foci of varying size	Progression (based on metastasis) Non-responder
Ductal	Grade 3 (poor)	ER+ PR+ HER2-	80mm all quadrants surrounded by smaller satellite lesions	54mm	ECx4 Docetaxel x 4	50mm responded partially	-	max 19mm	76.3% reduction responder
Lobular	Grade 2 (mod)	ER+ PR+ HER2-.	-	24mm	EC x4 Docetaxel x4	no sig reduction in size	12-20mm diffuse & difficult to measure	15mm max made of small foci	37.5% reduction responder
Ductal	Grade 3 (poor)	ER- PR- HER2+	-	30mm	neoTANGO. EC x 6 only	-	29mm	97mm	Stable disease non-responder
Ductal	Grade 2 (mod)	ER+ PR+ HER2-.	26mm	16mm	neoTANGO ECx4 and Paclitaxel x4	17mm	2 patches with overall area 30mm	27mm	3.8% increase Non-responder

Ductal	Grade 1 (well) from resection	ER+ PR+ HER2-	42mm + 2nd lesion of 11mm	37mm	neoTANG O arm1B ECx4 then PAC+GEM x4	'no residual tumour' 0mm	9mm	Multifocal. Largest focus 16mm but whole area 35mm . Clinically 'partial response': tumour not shrunk, but broken into smaller fragments	16.7% reduction Non-responder
Ductal	Grade 3 (poor)	ER- PR- HER2+	66mm	-	EC x4 Docetaxel x4	10mm	-	15mm largest index. Overall 37mm	43.9% reduction responder
Ductal	Grade 2 (mod)	ER- (+ in core) PR- HER2- CK5/6+ CK14-	40mm	-	neoTANG O arm 2b Pac +Gem.x4, EC x 4	27mm and a new lesion of 10mm. Fragmented tumour spread over 50mm	-	38mm	5% reduction non-responder progressive disease (due to new lesion)
Ductal	Grade 2 (mod)	ER+ PR+ HER2-	70mm	35mm	neoTANG O arm1B ECx4 then PAC+GEM x4 (20% reduced PAC for cycles 3&4)	34mm	-	25mm	64.3% reduction responder
Ductal	Grade 3 (poor)	ER- PR- HER2-	48mm	max 34mm	EC x 4 Docetaxel x 4	27mm	-	no tumour cells remaining. Isolated cells in lymphatic channel 0mm	100% reduction responder

Ductal	Grade 3 (poor)	ER+ PR+ HER2-	40mm	33mm	EC x 4, D x 2 (reduced by 20%) unwell	-	24mm	18mm	55% reduction responder
Ductal	Grade 3 (poor)	ER- PR- HER2-	55mm	13.7mm	neoTANG O arm 1a EC x4 and Paclitaxel x 4	-	8mm & 'something else' at 38mm	no. of foci in residual tumour; largest at 15mm & 11 more foci of 1-2mm. = 30mm altogether	45.5% reduction Responder
Ductal	Grade 3 (poor)	ER+ PR+ HER2+	25mm	37mm	EC x 4 (no response, size increase - early surgery)	-	during EC - 28mm	27mm 'minimal effects of chemotherapy' reported	8% increase non-responder
Ductal (core) Metaplastic (resection)	Grade 3 (poor)	ER - PR- HER2?	46mm	33mm	EC x 4 Docetaxel x 4	25mm	-	chemotherapy changes', poorly differentiated, metaplastic type 5mm	89.1% reduction responder
Ductal	Grade 1 (well) from resection	ER+ PR+ HER2-	42mm	9mm	EC x 4 Docetaxel x 4	33mm	-	max 25mm effects of chemotherapy reported	40.5% reduction responder
Ductal	Grade 3 (poor)	ER+ PR+ HER2? (HER2 not tested)	30mm and a 2nd lesion of 10mm	29mm	EC x 4, D x 2 (2nd at 20% reduced dose) could not tolerate side effects	21mm	16mm	main lesion 18mm 'apparent chemotherapy effects'	40% reduction responder
Ductal	Grade 3 (poor)	ER- (core 3/8 +ve)	28mm	23mm	EC x 4. D x 1 (no	-	30mm	22mm	21.4% reduction

		PR- HER2 + CK5/6 +			response)				non-responder
Ductal	Grade 1 (well)	ER+ PR+ HER2 -	39mm	35mm	EC x 4 Docetaxel x 4	22mm	-	12mm	69.2% reduction responder
Ductal	Grade 1 (well)	ER+ PR+ HER2?	31mm	-	EC x 4 Docetaxel x 4	after EC 22mm	-	26mm	16.1% reduction non-responder
Lobular	Grade 2 (mod)	ER+ PR+ HER2-	48mm	45mm	EC x 3. no response so abandoned	-	41mm	at least 60mm 'no evidence of chemotherapy effects'	25% increase non-responder
Ductal	Grade 3 (poor)	ER+ PR+ HER2-	32mm	-	EC x 4, D x 2 (side effects)	16mm	-	7mm	78.1% reduction responder
Ductal	Grade 3 (poor)	ER+ PR- HER2-	28mm nodule. Whole area 75mm	24mm	EC x 2. progressed - early surgery	nodule 38mm. 62mm overall new axillary and intramammary malignant lymph nodes (progression)	26mm	max 48mm	71.4% increase non-responder progression based on metastasis rather than size

Ductal	Grade 3 (poor)	ER- PR- HER2-CK 5/6+ CK14-	-	35 mm 'solid mass'	EC x 4 4.increase in size	-	54mm	52mm	54.3% increase non-responder
Ductal	Grade 2 (mod)	ER+ PR+ HER2-	Max diameter 90mm multifocal	-	EC x 4 Docetaxel x 4	-	-	overall field of malignancy 125mm. Multifocal	38.9% increase Non-responder.
Ductal	Grade 2 (mod)	ER+ PR+ HER2 -	25mm	40mm	ECx4 Docetaxel x 2 (side-effects)	13mm	16mm	13mm	48% reduction responder
Ductal	Grade 2 (mod)	ER+ PR+ HER2-	25mm	24mm	EC x 4 Docetaxel x 4	16mm	-	7mm	72% reduction Responder
Ductal	Grade 3 (poor)	ER+ PR- HER2+	-	35mm	EC x 4 Docetaxel x 4	26mm	-	'no residual cancer' 0mm	100% reduction Responder
Ductal	Grade 2 (mod)	ER+ PR- HER2-.	50mm (mixed invasive and DCIS)	40mm	EC x 4 Docetaxel x 4	40mm	25mm	20mm inc. DCIS (high grade)	60% reduction responder
Ductal	Grade 2 (mod)	ER+ PR- HER2-	26mm max but 2 other areas 15mm away (multifocal)	27mm	EC x 4, D x 3 but 2 and 3 were at 25% - dose (ill) but good response seen	13mm	-	14mm	46.2% reduction responder

Lobular	Grade 2 (mod)	ER+ PR+ HER2-	66mm	-	EC x 4 Docetaxel x 4	Decreased in volume by 65% after EC. No further red. After D 50mm	-	Multifocal. Largest focus 7mm. Extensive LCIS. Involves all 4 quadrants	24.2% reduction non-responder. Stable disease
Ductal	Grade 3 (poor)	ER- PR- HER2+	-	28mm	EC x 4 Docetaxel x 4	40mm ('lack of uptake')	-	no residual disease 0mm	100% reduction responder
Ductal	Grade 3 (poor)	ER+ PR+ HER2+	Only have Pre-treatment CT scan. 29mm	T1 14mm T2 12mm total 26mm	had surgery & chemo previously on other breast. ECx2 (already received. Doc x 4 (side effects so last 2 doses reduced by 25%	T1 16mm T2 19mm take total = 35mm	After EC: 11.5 and 7 (total 18.5) After D: 13mm and 6mm (total 19)	3 lesions T1 10mm T2 10mm T3 6mm + 20mm DCIS. Multifocal	26.9 % reduction. Stable disease
Ductal	Grade 2 (mod)	ER+ PR+ HER2-	extensive' (no size) clinically 40mm mammogram 20mm +	no size (u5)	EC x 4, Docetaxel x 4 but at 25% - dose	Considerable tumour present. Area 50mm but	mid docetaxel: T1 10mm T2 15mm	Mastectomy. High grade DCIS. Size of tumour + DCIS = 40mm T1 30mm (max). T2 10mm (max)	

			20mm			fragme nted			
Tubular (core was ductal)	Grade 2 (mod)	ER+ PR+ HER2-	extensive malignancy 78mm	2 x foci of diffuse change. Whole area 27mm	EC x 4 Docetaxel x 4	Frage nted. 24mm for largest	-	Grade 1 Tubular. 20mm	74.4% reduction responder
Ductal	Grade 2 (mod)	ER+ PR+ HER2+ luminal B	80mm diffuse thickening extensive malignancy	multifocal lesion largest 33mm	EC x 4. Docetaxel x 2 at full dose & docetaxel x 2 at 20% - dose	57mm	-	Partial response to chemotherapy'. 33 mm tumour	58.8% reduction Responder
Ductal	Grade 3 (poor)	ER+ PR- HER2-. Luminal	max 47mm + another of 8mm. + suspicious lesion in other breast	Multifocal. 43mm	EC x 4, docetaxel X 1 at full dose. Docetaxel - by 20% (severe reaction) for 2,3&4	good respons e' 21mm	-	5mm residual cancer	89.4% reduction Responder
Ductal	Grade 2 (mod)	ER+ PR+ (core) HER2+ (PR in resection was negative)	43mm multifocal	40mm possibly another focus	EC x 4 Docetaxel x 4	max diamet er of 30mm	-	15mm. ER+ PR-	65.1% reduction Responder
Ductal	Grade 3 (poor)	ER+ PR+ HER2+	30mm	25mm	ECx4. Dx2. 3rd cycle reduced	20mm	-	no residual cancer 0mm. Complete regression	100% reduction responder

					by 20% (toxicities). no cycle 4				
Lobular	Grade 2 (mod)	ER+ PR+ HER2-	60mm max diameter	-	EC x 6 (had bone metastasis at start - palliative chemo)	No significant alteration' at least 54mm	-	47mm minimum.	21.7% reduction Non-responder
Lobular	Grade 2 (mod)	ER+ PR+ HER2-	max 56mm fragmented	diffuse area max 34mm	EC x 4 Docetaxel x 4	20mm	-	partial regression & response to chemo'. 3 ops; 1 (wide local) 26mm ; 2 (surgery to remove more tumour) 22mm; 3 (mastectomy).total of 48mm	14.3% reduction non-responder
Lobular	Grade 2 (mod)	ER+ PR+ HER2-	2 lesions. T1 23mm & T2 24mm. 47mm total	2 lesions; 23mm and 16mm. Area of 50mm total	EC x 4 Docetaxel x 4	-	-	max 32 mm	31.9% reduction Responder
Ductal	Grade 3 (poor)	ER - PR - HER2- E-cadherin +	extensive disease' 47mm	'diffuse'	EC x 5 (#6 abandoned - no response)	-	After 2/3 cycles 40mm. After 4th 'no change'	Mastectomy. Large foci 24mm. Extensive overall 40mm malignancy	14.9% reduction non-responder
Ductal	Grade 3 (poor)	ER- PR- HER2- CK5/6/14 +	max 82mm	2 separate lesions. Largest 42mm	ECx4. Docetaxel x 1 (tumour progressed and	Overall volume unchanged. "not respon	'no change"	(bilateral mastectomy) RHS: 2 lesions. Largest 47mm overall area 115mm	40.2% increase non-responder

					developed new tumour in other breast)	ded"			
Ductal	Grade 1 (well)	ER+ PR+ HER2-	40mm	6mm	EC x 4 Docetaxel x 1 then Docetaxel 2-4 at 20% reduced dose	good response' 2 lesions of 10mm each, but overall 30mm	-	15mm	62.5% reduction responder
Ductal	Grade 2	ER+ PR- HER2-	> 40mm	34mm	4 x EC, 2 x Docetaxel (no evidence of good response)	54mm (reported progression)	-	overall 57mm	progressive disease
Lobular	Grade 2	ER+ PR+ HER2-	28mm	-	EC x 4, D x 4 (complete)	little change in volume, fragmented 25mm	-	28mm invasive, plus LCIS	stable disease
Ductal	Grade 3	ER+ PR+ HER2+	(not done)	30mm	EC x 4, D x 4 (complete)	lesion 13mm plus 27mm DCIS	(mid treatment 18.6.10: 50mm, 13.8.10: 40mm)	Largest residual focus 10mm. Overall extent of malignancy 38mm	progressive disease

Ductal		ER+ PR+ HER2-	53mm	30mm	EC x 4, D x 4	46mm	(mid 15mm)	36mm	Partial Responder
Ductal	Grade 1 (well)	ER+ PR+ HER2-	28mm	40mm	EC x 4 Docetaxel x 4	-	36mm	26mm	7.1% reduction Non- responder
Ductal	Grade 2 (mod)	ER+ PR+ HER2-	93mm	43mm	EC x 4 Docetaxel x 4	fragme nted disease over max area of 87mm	-	60mm	35.5% reduction responder

Appendix 2: The list of 725 Antibodies (Panorama Antibody Microarray XPRESS Profiler). All 725 have human, mouse and rat reactivity and coated in duplicates on the nitrocellulose slide; section 2.7.1).

	ANTIBODY	SIGMA No.	P/M	Reactivity		
				Human	Mouse	Rat
1	14-3-3	T5942	M	y	y	y
2	Acetylated Protein	A5463	P	y	n/d	n/d
3	Actin	A5060	P	y	y	y
4	Actin	A3853	M	y	y	y
5	Actin, α -Smooth Muscle	A5228	M	y	y	y
6	β -Actin	A1978	M	y	y	y
7	β -Actin	A2228	M	y	y	y
8	β -Actinin	A5044	M	y	y	d/n
9	Actopaxin	A1226	P	y	n/d	n/d
10	AP2	A7107	M	y	n/d	n/d
11	β 1 and β 2-Adaptins	A4450	M	y	n/d	y
12	I-Afadin	A0349	P	y	y	y
13	AFX	A8975	P	y	n/d	n/d
14	AFX (FOXO4)	A5854	M	y	n/d	n/d
15	AKR1C3	A6229	M	y	n/d	n/d
16	Aly	A9979	M	y	n/d	n/d
17	β -Amyloid	A8354	M	y	n/d	n/d
18	Amyloid Precursor Protein, C-Terminal	A8717	P	y	y	y
19	Amyloid Precursor Protein, N-Terminal	A8967	P	y	y	y
20	Amyloid Precursor Protein, KPI Domain	A8842	P	y	y	y
21	Androgen Receptor	A9853	P	y	n/d	y
22	Annexin V	A8604	M	y	n/d	n/d
23	Annexin VII	A4475	M	y	y	y
24	Anti Cy3+Cy5	C0992	M	NA	NA	NA
25	AOP1	A7674	M	y	y	y
26	AP-1	A5968	P	y	n/d	n/d
27	AP-2	A0844	P	y	n/d	n/d
28	AP Endonuclease	A2105	M	y	y	y
29	Apaf1, N-Terminal	A8469	P	y	y	n/d
30	Apoptosis Inducing Factor (AIF)	A7549	P	y	y	n/d
31	APRIL, Extracellular Domain	A1726	P	y	n/d	n/d
32	APRIL, Extracellular Domain 2	A1851	P	y	n/d	n/d
33	ARC, C-Terminal	A8344	P	y	n/d	n/d
34	ARNO (Cytohesin-2)	A4721	M	y	n/d	y
35	Arp1/Contractin	A5601	P	y	y	y
36	ARP2	A6104	M	y	y	y
37	ARP3	A5979	M	y	y	y
38	ARTS	A3720	P	y	n/d	n/d
39	ARTS	A4471	M	y	n/d	n/d
40	ASAP1/Centaurin β 4	A4227	P	y	y	y
41	ASC-2	A5355	M	y	n/d	n/d
42	ASPP1	A4355	M	y	y	n/d
43	ASPP2	A4480	M	y	y	n/d

44	ATF-1	A7833	P	y	n/d	n/d
45	ATF2	A4086	P	y	n/d	n/d
46	phospho-ATF-2 (pThr ^{69,71})	A4095	M	y	y	y
47	ATM	A6093	M	y	n/d	n/d
48	Anti Cy3+Cy5	C0992	M	NA	NA	NA
49	ATM	A6218	M	y	n/d	n/d
50	Aurora-B	A5102	P	y	y	y
51	BACE-1	B0806	P	y	n/d	n/d
52	BACH1	B1310	P	y	y	y
53	BAD	B0559	M	y	n/d	n/d
54	BAF57	B0436	P	y	y	n/d
55	BAK	B5897	P	y	n/d	n/d
56	BAP1	B9303	M	y	n/d	n/d
57	Bax	B3428	P	y	n/d	n/d
58	Bax	B8429	M	y	y	y
59	Bax	B8554	M	y	n/d	n/d
60	Bax	B9054	M	n/d	y	n/d
61	Bcl-10	B7806	M	y	n/d	n/d
62	Prion protein	P0110	M	y	y	y
63	Bcl-10	B0431	P	y	y	y
64	Seladin	S4697	M	y	n/d	n/d
65	Bcl-2	B9804	P	n/d	y	y
66	Bcl-2	B3170	M	y	n/d	n/d
67	Bcl-x	B9304	P	y	n/d	n/d
68	Bcl-x _L	B9429	M	y	y	y
69	BID	B4305	P	y	n/d	n/d
70	BID	B3183	P	n/d	y	n/d
71	Bim	B7929	P	y	y	y
72	Anti Cy3+Cy5	C0992	M	NA	NA	NA
73	CDK5	C6118	M	y	y	n/d
74	Bmf, N-Terminal	B1684	P	y	y	n/d
75	Bmf, C-Terminal	B1559	P	y	y	n/d
76	BNIP3	B7931	M	y	n/d	n/d
77	BOB.1/OBF.1	B7810	M	y	y	n/d
78	Brg1/hSNF2 β	B8184	P	y	n/d	n/d
79	BTK, C-Terminal	B0811	P	y	n/d	n/d
80	BTK, N-Terminal	B0686	P	y	n/d	n/d
81	BUB1	B0561	M	y	n/d	n/d
82	BUBR1	B9310	M	y	n/d	n/d
83	c-Abl	A5844	M	y	y	y
84	c-Cbl	C9603	P	y	n/d	n/d
85	c-erbB-2	E2777	M	y	n/d	n/d
86	c-erbB-3	E8767	M	y	n/d	n/d
87	c-erbB-4	E5900	M	y	n/d	n/d
88	phospho-c-Jun (pSer ⁶³)	J2128	P	y	y	n/d
89	phospho-c-Jun (pSer ⁷³)	J2253	P	y	y	n/d
90	c-Myc	M4439	M	n/d	n/d	n/d
91	c-Myc	C3956	P	n/d	n/d	n/d

92	Uvomorulin/E-Cadherin	U3254	M	y	y	n/d
93	N-Cadherin	C2542	M	y	y	y
94	N-Cadherin	C2667	M	n/d	n/d	n/d
95	Pan Cadherin	C1821	M	y	y	y
96	Anti Cy3+Cy5	C0992	M	NA	NA	NA
97	Calbindin-D-28K	C7354	P	y	n/d	y
98	Calcineurin (γ -Subunit)	C1956	M	y	n/d	y
99	Caldesmon	C6542	M	y	n/d	n/d
100	Calmodulin	C7055	M	n/d	n/d	y
101	Calnexin	C4731	P	y	y	y
102	Calponin	C2687	M	y	y	y
103	Calreticulin	C4606	P	y	n/d	n/d
104	Calretinin	C7479	P	y	n/d	y
105	Claspin	C7867	P	y	n/d	n/d
106	CaM Kinase IV (CaMKIV)	C2851	P	y	y	y
107	CaM Kinase Kinase (CaMKK γ)	C7099	P	n/d	n/d	y
108	CaM Kinase II α (CaMKII α)	C6974	P	y	y	y
109	CaM Kinase IV (CaMKIV)	C9973	P	y	n/d	n/d
110	CASK/LIN2	C4856	P	y	n/d	n/d
111	Casein Kinase 2 β	C3617	M	y	y	y
112	Caspase 2	C7349	P	y	n/d	n/d
113	Caspase 3	C9598	P	y	n/d	n/d
114	Caspase 3, Active	C8487	P	y	y	y
115	Caspase 4	C4481	P	y	n/d	n/d
116	Caspase 4	C3392	M	y	n/d	n/d
117	Caspase 5	C6979	M	y	n/d	n/d
118	Caspase 6	C7599	P	y	n/d	n/d
119	Caspase 7	C7724	P	y	n/d	n/d
120	Anti Cy3+Cy5	C0992	M	NA	NA	NA
121	Caspase 7	C1104	M	y	n/d	n/d
122	Caspase 8	C3101	P	y	n/d	n/d
123	Caspase 8	C2976	P	y	n/d	n/d
124	Caspase 8	C4106	M	y	n/d	n/d
125	Pro-Caspase 8	C7849	P	y	n/d	n/d
126	Caspase 9	C7729	P	y	n/d	y
127	Caspase 9	C4356	M	y	n/d	n/d
128	Caspase 10	C8351	P	y	n/d	n/d
129	Caspase 10	C1229	M	y	n/d	n/d
130	Caspase 11	C1354	M	n/d	y	n/d
131	Caspase 12	C7611	M	y	y	n/d
132	Caspase 13 (ERICE)	C8854	P	y	y	y
133	Catalase	C0979	M	y	y	y
134	α -E-Catenin	C8114	P	y	n/d	y
135	N-Catenin	C8239	P	n/d	y	n/d
136	Catenin	C2081	P	n/d	n/d	n/d
137	β -Catenin	C7207	M	y	n/d	n/d
138	β -Catenin	C7082	M	y	n/d	n/d
139	phospho- β -Catenin (pThr ⁴¹)	C8616	M	y	n/d	n/d

140	phospho- β -Catenin (pSer ³³ /pSer ³⁷)	C4231	M	y	y	y
141	phospho- β -Catenin (pSer ⁴⁵)	C5615	M	y	y	y
142	phospho- β -Catenin (pSer ³³)	C2363	M	y	n/d	n/d
143	δ -Catenin/NPRAP	C4864	P	n/d	y	y
144	Anti Cy3+Cy5	C0992	M	NA	NA	NA
145	Cathepsin D	C0715	M	y	n/d	n/d
146	Cathepsin L	C2970	M	y	y	y
147	Caveolin-1	C3237	P	y	y	y
148	CD40	C5987	M	y	n/d	n/d
149	Cdc14A	C2238	M	y	n/d	n/d
150	Cdc25c	C0349	M	y	n/d	n/d
151	Cdc25A	C9479	M	y	n/d	n/d
152	Cdc27	C7104	M	y	y	y
153	Cdc6	C0224	M	y	n/d	n/d
154	Cdc7 Kinase	C6613	M	y	n/d	n/d
155	Cdh1	C7855	M	y	n/d	n/d
156	Cdk1 ^{p34cdc2}	C4973	P	y	y	n/d
157	Negative Control	NA	M	NA	NA	NA
158	Cdk4	C8218	M	y	y	y
159	Cdk6	C8343	M	y	y	y
160	Cdk-7/cak	C7089	M	y	n/d	n/d
161	TBP	T1827	M	y	n/d	n/d
162	CENP-E	C7488	P	y	n/d	n/d
163	Centrin	C7736	P	y	n/d	n/d
164	Chk1	C9358	P	y	n/d	n/d
165	Chk2	C9108	M	y	n/d	n/d
166	Chk2	C9233	M	y	n/d	n/d
167	Chondroitin Sulfate	C8035	M	y	y	y
168	Anti Cy3+Cy5	C0992	M	NA	NA	NA
169	Ciliated Cell Marker	C5867	M	y	n/d	n/d
170	CIN85	C8116	P	y	y	y
171	Casein Kinase 2 α	C5367	M	y	y	y
172	Clathrin Light Chain	C1985	M	y	y	y
173	Clathrin Heavy Chain	C1860	M	y	y	y
174	CNPase	C5922	M	y	y	y
175	Cofilin	C8736	P	y	y	y
176	Coilin	C1862	M	y	n/d	n/d
177	Collagen, Type IV	C1926	M	y	n/d	n/d
178	Connexin 32	C3470	P	y	y	y
179	Negative Control	NA				
180	Connexin- 32	C6344	M	y	y	y
181	Connexin- 43	C8093	M	y	y	y
182	Connexin- 43	C6219	P	y	y	y
183	β -COP	G6160	M	y	n/d	y
184	Cortactin	C6987	P	y	y	y
185	Corticotropin Releasing Factor	C5348	P	y	y	y
186	COX II	C9354	M	y	n/d	n/d
187	Crk-L	C0978	P	y	y	n/d

188	Crk II	C0853	P	y	y	n/d
189	Csk	C7863	P	y	n/d	y
190	CtBP1, N-Terminal	C9491	P	y	y	n/d
191	CtBP1, C-Terminal	C8741	P	y	y	n/d
192	Anti Cy3+Cy5	C0992	M	NA	NA	NA
193	CUG-BP1	C5112	M	y	y	y
194	Cyclin A	C4710	M	y	y	n/d
195	Cyclin B ₁	C8831	P	y	y	n/d
196	Cyclin D ₁	C5588	P	y	n/d	y
197	Cyclin D ₁	C7464	M	y	y	n/d
198	Cyclin D ₂	C7339	M	y	y	n/d
199	Cyclin D ₃	C7214	M	y	y	y
200	Cyclin H	C5351	P	y	n/d	n/d
201	Cystatin A	C3095	M	y	n/d	n/d
202	Cytohesin-1	C8979	M	y	n/d	n/d
203	Cytokeratin peptide 4	C5176	M	y	n/d	n/d
204	Cytokeratin CK5	C7785	M	y	n/d	n/d
205	Cytokeratin peptide 7	C6417	M	y	n/d	n/d
206	Cytokeratin 8.12	C7034	M	y	n/d	n/d
207	Cytokeratin 8.13	C6909	M	y	n/d	n/d
208	Cytokeratin peptide 13	C0791	M	y	n/d	n/d
209	Cytokeratin Peptide 17	C9179	M	y	n/d	y
210	Cytokeratin peptide 18	C1399	M	y	n/d	n/d
211	Cytokeratin peptide 19	C6930	M	y	n/d	n/d
212	Pan Cytokeratin	C2931	M	y	y	y
213	DAPK	D2178	M	y	n/d	n/d
214	phospho-DAPK (pSer ³⁰⁸)	D4941	M	y	n/d	n/d
215	DAP Kinase 2	D3191	P	y	y	y
216	Anti Cy3+Cy5	C0992	M	NA	NA	NA
217	Daxx	D7810	P	y	n/d	n/d
218	DcR1	D3566	P	y	y	y
219	DcR2	D3188	P	y	n/d	n/d
220	DcR3	D1814	P	y	y	y
221	DEDAF	D3316	P	y	y	y
222	Desmin	D1033	M	n/d	y	y
223	Desmosomal Protein	D1286	M	y	n/d	n/d
224	Dextrin/ADF	D8940	P	y	y	y
225	Dnase I	D0188	P	n/d	n/d	n/d
226	Dnase II	D1689	P	y	n/d	n/d
227	DNMT1	D4567	P	y	y	y
228	DNMT1	D4692	P	y	y	n/d
229	DOPA Decarboxylase	D0180	M	y	n/d	y
230	DP2	D7438	M	y	n/d	n/d
231	DR3	D3563	P	y	n/d	n/d
232	Negative Control	NA				
233	DR4	D3813	P	y	n/d	n/d
234	DR5	D3938	P	y	n/d	n/d
235	DR6	D1564	P	y	n/d	n/d

236	DRAK1	D1314	P	y	y	y
237	Dystrophin	D8168	M	y	y	y
238	Dystrophin	D8043	M	y	y	y
239	E2F1	E9026	P	y	n/d	n/d
240	Anti Cy3+Cy5	C0992	M	NA	NA	NA
241	E2F1	E8901	M	y	y	y
242	E2F2	E8776	M	y	n/d	n/d
243	E2F3	E8651	M	y	n/d	n/d
244	E2F4	E8526	M	y	n/d	n/d
245	E6AP	E8655	M	y	y	y
246	EGF receptor	E3138	M	y	n/d	n/d
247	ERK5 (Big MAPK-BMK1)	E1523	P	y	y	n/d
248	Elastin	E4013	M	y	n/d	n/d
249	ELKS	E4531	M	y	y	y
250	Endothelial Cell Protein C Receptor	E6280	M	y	n/d	n/d
251	Endothelial Cells	E9653	M	y	n/d	n/d
252	Endothelin	E0771	M	y	n/d	y
253	Epidermal Growth Factor	E2520	M	y	n/d	n/d
254	Episialin (EMA)	E0143	M	y	n/d	n/d
255	ERP57	E5031	M	y	y	n/d
256	Estrogen Receptor	E0521	P	y	n/d	n/d
257	Estrogen Receptor	E1396	P	y	n/d	n/d
258	Exportin T	E1531	M	y	y	y
259	Ezrin	E8897	M	y	y	y
260	F1A	F3428	P	y	y	y
261	FADD	F8053	M	y	n/d	n/d
262	Focal Adhesion Kinase (pp125 ^{FAK})	F2918	P	y	y	y
263	FAK Phospho (pSer ⁷⁷²)	F9051	P	y	y	y
264	Anti Cy3+Cy5	C0992	M	NA	NA	NA
265	phospho-FAK Phospho (pSer ⁹¹⁰)	F9301	P	y	y	y
266	phospho-FAK (pTyr ³⁹⁷)	F7926	P	y	y	y
267	phospho-FAK (pTyr ⁵⁷⁷)	F8926	P	y	y	n/d
268	Falkor/PHD1	F5303	M	n/d	y	n/d
269	Fas (CD95/Apo-1)	F4424	M	y	n/d	n/d
270	Fas Ligand	F2051	M	y	n/d	n/d
271	Fas Ligand	F1926	M	y	n/d	n/d
272	FBI-1/PAKEMON	F9429	P	y	y	y
273	Fibroblast Growth Factor-9	F1672	M	y	y	n/d
274	Fibronectin	F0791	M	y	n/d	n/d
275	Fibronectin	F3648	P	y	n/d	n/d
276	Fibronectin	F7387	M	y	y	n/d
277	Filamin	F1888	M	n/d	n/d	n/d
278	Filensin	F1043	M	y	y	n/d
279	FKHR (FOXO1a)	F6928	M	y	n/d	n/d
280	FKHRL1 (FOXO3a)	F2178	P	y	y	n/d
281	FKHRL1 (FOXO3a)	F1304	M	y	n/d	n/d
282	FLIP γ/δ , C-Terminal	F9925	P	y	y	n/d
283	FOXC2	F1054	P	y	y	n/d

284	FOXP2	F6304	P	y	y	y
285	FANCD2	F0305	P	y	y	y
286	FXR2	F1554	M	y	n/d	n/d
287	FRS2 (SNT-1)	F9052	P	y	y	y
288	Anti Cy3+Cy5	C0992	M	NA	NA	NA
289	G9a Methyltransferase	G6919	P	y	n/d	n/d
290	Glutamic Acid Decarboxylase 65 (GAD 65)	G4913	P	y	y	y
291	Glutamic Acid Decarboxylase 65 (GAD 65)	G5038	P	y	y	y
292	Glutamic Acid Decarboxylase (GAD65/67)	G5163	P	y	y	y
293	GADD 153 (CHOP-10)	G6916	P	y	y	n/d
294	GAP1 ^{IP4BP}	G6666	M	y	n/d	n/d
295	GAPDH	G8795	M	y	y	y
296	GATA-1	G0290	P	y	n/d	n/d
297	Gelsolin	G4896	M	y	n/d	n/d
298	Gemin 2	G6669	M	y	y	y
299	Gemin 3	G6544	M	y	n/d	n/d
300	GFAP (Glial Fibrillary Acidic Protein)	G9269	P	y	n/d	y
301	GFAP (Glial Fibrillary Acidic Protein)	G3893	M	y	n/d	y
302	Growth Factor Independence-1 (GFI)	G6670	M	y	y	y
303	Glutamate receptor NMDAR 2a	G9038	P	y	y	y
304	Glutamine Synthase	G2781	P	n/d	n/d	y
305	Glycogen Synthase Kinase-3 β (GSK-3 β)	G7914	P	y	n/d	y
306	Glycogen Synthase Kinase-3 (GSK-3)	G4414	M	y	y	y
307	Glycogen Synthase Kinase-3 (GSK-3)	G6414	M	y	y	y
308	Granzyme B	G1044	M	y	n/d	n/d
309	Grb-2	G2791	M	y	y	y
310	GRK 2	G7670	M	n/d	n/d	y
311	GRP1	G6541	M	y	n/d	y
312	Anti Cy3+Cy5	C0992	M	NA	NA	NA
313	GRP 75	G4170	P	y	y	y
314	GRP78/BiP	G8918	P	y	y	n/d
315	GRP94	G4420	P	y	y	d/n
316	hABH1	A8103	M	y	n/d	d/n
317	hABH2	A8228	M	y	n/d	d/n
318	hABH3	A8353	M	y	y	y
319	hBRM/hSNF2 α	H9787	P	y	n/d	n/d
320	HAT1 (Histone acetyltransferase 1)	H7161	P	y	y	n/d
321	HDAC-1	H3284	P	y	y	y
322	HDAC-1	H6287	M	y	y	n/d
323	HDAC-2	H3159	P	y	y	y
324	HDAC-2	H2663	M	y	y	y
325	HDAC-3	H6537	M	y	y	n/d
326	HDAC-3	H3034	P	y	y	y
327	HDAC-4	H9411	P	y	y	y
328	HDAC-4	H9536	P	y	y	y
329	Negative Control	NA				
330	HDAC-5	H4538	M	y	y	y
331	HDAC-5	H8163	P	y	y	y

332	HDAC-6	H2287	P	y	y	n/d
333	HDAC-7	H2537	P	y	y	y
334	HDAC-7	H6663	M	y	y	n/d
335	HDAC-8	H6412	M	y	n/d	n/d
336	Anti Cy3+Cy5	C0992	M	NA	NA	NA
337	HDAC-10	H3413	P	y	y	y
338	HDAC-11	H2913	M	y	n/d	n/d
339	HDRP/MITR	H9163	P	y	y	n/d
340	Heat Shock Factor 1	H4163	P	y	y	y
341	Heat Shock Factor 2	H6788	P	y	n/d	y
342	Heat Shock Protein 25	H0148	M	y	y	y
343	Heat Shock Protein 27	P1498	P	y	n/d	n/d
344	Heat Shock Protein 27/25	H2289	P	y	y	y
345	Heat Shock Protein 70	H5147	M	y	n/d	y
346	Heat Shock Protein 90	H1775	M	y	y	y
347	Heat Shock Protein 110	H7412	P	y	y	y
348	Heat Shock Protein 110	H7287	P	n/d	y	y
349	Acetyl Histone H3 (Ac-Lys ⁹)	H9286	P	y	y	n/d
350	Acetyl Histone H3 (Ac-Lys ⁹)	H0913	M	y	y	n/d
351	Acetyl- & phospho-Histone H3 (Ac-Lys ⁹ , Ser ¹⁰)	H9161	P	y	y	n/d
352	Acetyl- & phospho-Histone H3 (Ac-Lys ⁹ , Ser ¹⁰)	H0788	M	y	n/d	n/d
353	Dimethyl Histone H3 (diMe-Lys ⁴)	D5692	P	y	y	n/d
354	Dimethyl Histone H3 (diMe-Lys ⁹)	D5567	P	y	n/d	n/d
355	methyl-Histone H3 (Me-Lys ⁹)	H7162	P	y	n/d	n/d
356	phospho-Histone H2AX (pSer ¹³⁹)	H5912	P	y	y	n/d
357	phospho-Histone H3 (pSer ¹⁰)	H6409	M	y	n/d	n/d
358	phospho-Histone H3 (pSer ²⁸)	H9908	M	y	y	n/d
359	phospho-Histone H3 (pSer ¹⁰)	H0412	P	y	n/d	n/d
360	Anti Cy3+Cy5	C0992	M	NA	NA	NA
361	SUV39H1 Histone Methyl Transferase	S8316	M	y	y	n/d
362	HMG-1	H9537	M	y	y	y
363	hMps1	M5818	M	y	n/d	n/d
364	hnRNP-A1	R4528	M	y	y	y
365	hnRNP-A1	R9778	M	y	n/d	n/d
366	hnRNP-A2/B1	R4653	M	y	y	y
367	hnRNP-C1/C2	R5028	M	y	n/d	n/d
368	hnRNP-K/J	R8903	M	y	n/d	n/d
369	hnRNP-L	R4903	M	y	y	n/d
370	hnRNP-Q	R5653	M	y	y	y
371	hnRNP-U	R6278	M	y	n/d	n/d
372	hnRNP M3-M4	R3777	M	y	y	y
373	hPlk1	P5998	M	y	y	y
374	hPlk1	P6123	M	y	y	y
375	hSNF5/INI1	H9912	P	y	n/d	n/d
376	iASPP	A4605	M	y	y	n/d

377	IFI-16	I1659	M	y	n/d	n/d
378	IB	I0505	P	y	y	y
379	IKK	I6139	P	y	n/d	n/d
380	ILK	I0783	M	y	y	y
381	ILK	I1907	P	y	y	y
382	ILP2	I4782	P	y	y	y
383	Negative Control	NA				
384	Anti Cy3+Cy5	C0992	M	NA	NA	NA
385	Importin-1	I9658	M	y	y	n/d
386	Importin-3	I9783	M	y	y	y
387	Importin-5/7	I9908	M	y	y	n/d
388	INCENP	I5283	P	y	y	y
389	ING1	I3659	M	y	n/d	n/d
390	β -Internexin	I0282	M	y	n/d	y
391	JAB 1	J3395	P	y	y	y
392	JAB 1	J3020	P	y	y	y
393	JAK 1	J3774	M	y	n/d	n/d
394	c-Jun N-Terminal Kinase	J4500	P	y	y	y
395	JNK, Activated (Diphosphorylated JNK)	J4750	M	y	y	y
396	KCNK9 (TASK-3)	K0514	M	y	n/d	n/d
397	Kaiso	K4263	M	y	y	y
398	KIF17	K3638	P	n/d	y	y
399	KIF3A	K3513	P	y	y	y
400	KSR	K4261	M	n/d	y	n/d
401	Ku Antigen	K2882	M	y	n/d	n/d
402	L1CAM	L4543	M	y	n/d	n/d
403	l/s-Afadin	A0224	P	y	y	y
404	Laminin	L9393	P	y	n/d	n/d
405	Laminin-2 (α -2 Chain)	L0663	M	y	y	n/d
406	LAP2 (TMPO)	L3414	M	y	n/d	n/d
407	Leptin	L3410	P	y	y	n/d
408	Anti Cy3+Cy5	C0992	M	NA	NA	NA
409	LIM Kinase 1	L2290	P	y	y	y
410	LIN-7	L1538	P	n/d	n/d	y
411	LIS1	L7391	M	y	y	y
412	LKB1	L7917	P	y	y	y
413	LDS1	L4793	P	y	y	y
414	Mad1	M8069	M	y	n/d	n/d
415	Mad2	M8694	M	y	n/d	n/d
416	MADD	M5683	P	y	y	n/d
417	MAFF	M8194	P	y	n/d	n/d
418	MAGI-1	M5691	P	n/d	n/d	y
419	MAGI-2	M2441	P	n/d	n/d	y
420	MAP Kinase, Activated/Monophosphorylated (Phosphothreonine ERK-1&2)	M7802	M	y	n/d	y
421	MAP Kinase, Monophosphorylated Tyrosine	M3682	M	y	n/d	y
422	MAP Kinase, Activated (Diphosphorylated ERK-1&2)	M9692	M	y	y	y

423	MAP Kinase, Monophosphorylated Threonine	M3557	M	y	y	y
424	MAP Kinase (ERK-1)	M7927	P	y	y	y
425	MAP Kinase (ERK1+ERK2)	M5670	P	y	y	y
426	MAP Kinase Activated Protein Kinase-2 (MAPKAPK-2)	M3550	P	y	y	n/d
427	MAP Kinase Phosphatase-1 (MKP-1)	M3787	P	y	n/d	n/d
428	MAPK non phosphorylated ERK	M3807	M	y	n/d	y
429	MAP Kinase 2 (ERK-2)	M7431	M	y	y	y
430	MAP Kinase Kinase (MEK, MAPKK)	M5795	P	y	y	y
431	MAP2 (2a+2b)	M2320	M	n/d	n/d	y
432	Anti Cy3+Cy5	C0992	M	NA	NA	NA
433	MAP1	M4278	M	n/d	y	y
434	MAP1 (Light Chain)	M6783	M	n/d	n/d	y
435	MAP1b	M4528	M	y	y	y
436	MAP2	M9942	M	y	y	y
437	MBD1	M6569	P	y	n/d	n/d
438	MBD2a	M7568	P	y	y	n/d
439	MBD2a,b	M7318	P	y	y	n/d
440	MBD4	M9817	P	n/d	y	n/d
441	MBDin/XAB1	M1944	P	y	n/d	n/d
442	MBNL 1	M3320	M	y	y	n/d
443	MCH	M8440	P	y	n/d	n/d
444	Mcl-1	M8434	P	y	n/d	n/d
445	MDC1	M2444	M	y	n/d	n/d
446	MDM2	M8558	M	n/d	y	n/d
447	MDM2	M4308	M	y	y	y
448	MDM2	M7815	M	y	y	n/d
449	MDMX	M0445	M	y	n/d	n/d
450	MeCP2	M9317	P	y	n/d	n/d
451	MeCP2	M7443	M	y	y	y
452	MeCP2	M6818	M	y	y	y
453	MEKK4	M7194	M	y	y	y
454	Melanocortin-3 Receptor	M4937	P	n/d	n/d	y
455	MGMT	M3068	M	y	n/d	n/d
456	Anti Cy3+Cy5	C0992	M	NA	NA	NA
457	Mint2	M3319	P	n/d	n/d	y
458	LRRK2 (PARK8)	L3044	M	y	y	n/d
459	MRP1	M9192	M	y	n/d	n/d
460	MRP2	M3692	M	y	n/d	n/d
461	MSH	M0939	P	y	n/d	n/d
462	MSH6	M2445	P	y	y	y
463	MSH6	M2820	P	y	y	n/d
464	MSK-1	M5437	P	y	n/d	y
465	MTA 2	M7569	M	y	y	y
466	MTA1	M1320	M	y	y	y
467	MTA1	M7693	P	y	n/d	n/d
468	MTA2/MTA1L	M7818	P	y	n/d	n/d
469	MTA3L	M0819	P	y	n/d	n/d

470	MTBP	M3566	P	y	n/d	n/d
471	mTOR	T2949	P	y	y	y
472	Munc-18-1	M2694	P	n/d	y	y
473	Munc-13/1	M6194	M	n/d	y	y
474	MyD88	M9934	P	y	y	n/d
475	Myosin	M1570	M	y	y	y
476	Myosin I β (Nuclear)	M3567	P	y	y	y
477	Myosin IIA	M8064	P	y	n/d	y
478	Myosin IX/Myr5	M5566	P	n/d	n/d	y
479	Negative Control	NA				
480	Anti Cy3+Cy5	C0992	M	NA	NA	NA
481	Myosin Light Chain Kinase	M7905	M	y	y	Y
482	Myosin Va	M4812	P	n/d	n/d	y
483	Myosin Va	M5062	P	n/d	n/d	y
484	Myosin VI	M0691	M	y	y	y
485	Myosin VI	M5187	P	n/d	n/d	y
486	NBS1 (Nibrin)	N9287	M	y	n/d	n/d
487	NBS1 (Nibrin)	N3037	P	y	n/d	n/d
488	NBS1 (Nibrin)	N3162	P	y	n/d	y
489	Nck-2	N2911	M	y	n/d	y
490	Nedd 8	N2786	M	y	n/d	n/d
491	Nerve Growth Factor- β	N3279	M	y	y	n/d
492	Nerve Growth Factor Receptor	N5408	M	y	n/d	n/d
493	Nerve growth factor receptor (NGFR p75)	N3908	P	n/d	n/d	y
494	Neurabin I	N4412	P	n/d	y	y
495	Neurabin II (C-terminal)	N5037	P	n/d	y	y
496	Neurabin-II	N5162	P	n/d	y	y
497	Neurofibromin	N3662	M	y	y	y
498	Neurofilament 160	N2787	M	y	y	y
499	Neurofilament 200	N4142	P	y	y	y
500	Neurofilament 200	N0142	M	y	y	y
501	Neurofilament 200	N5389	M	y	n/d	n/d
502	Neurofilament 68	N5139	M	y	n/d	n/d
503	Neurofilament 160/200	N2912	M	y	y	y
504	Anti Cy3+Cy5	C0992	M	NA	NA	NA
505	NF-kB	N8523	M	y	y	n/d
506	NAK (NF κ B-Activating Kinase)	N2661	M	y	n/d	y
507	NG2	N8912	M	n/d	n/d	y
508	Nicastrin	N1660	P	y	n/d	n/d
509	Nitric Oxide Synthase, Brain (b-NOS)	N2280	M	y	n/d	y
510	Nitric Oxide Synthase, Brain (b-NOS)	N7155	P	y	n/d	y
511	Nitric Oxide Synthase, Endothelial (e-NOS)	N9532	M	y	y	y
512	Nitric Oxide Synthase, Endothelial (e-NOS)	N3893	P	y	y	y
513	Nitric Oxide Synthase, Endothelial (e-NOS)	N2643	P	y	y	n/d
514	Nitric Oxide Synthase, Inducible (i-NOS)	N7782	P	n/d	y	y
515	Nitric Oxide Synthase, Inducible (i-NOS)	N9657	M	n/d	y	y
516	Notch1	N6786	M	y	y	n/d
517	Nitrotyrosin	N0409	P	y	n/d	n/d

518	NTF2	N9527	M	y	y	y
519	Nuf2	N5287	M	y	n/d	n/d
520	O-GlcNAc Transferase	O6264	P	y	y	y
521	OP-18/Stathmin	O0138	P	y	n/d	y
522	Ornithine Decarboxylase (ODC)	O1136	M	y	y	n/d
523	p115/TAP	P3118	M	n/d	n/d	Y
524	p120 ^{ctn}	P1870	P	y	n/d	n/d
525	p130 ^{CAS}	C0354	P	y	y	y
526	p14 ^{arf}	P2610	M	y	n/d	n/d
527	p16 ^{INK4a/CDKN2}	P0968	M	y	n/d	n/d
528	Anti Cy3+Cy5	C0992	M	NA	NA	NA
529	p19 ^{INK4d}	P4354	M	y	n/d	n/d
530	p21WAF1/Cip1	P1484	M	y	y	n/d
531	p300/CBP	P2859	M	y	y	y
532	p34 ^{cdc2}	C3085	M	y	y	n/d
533	p35 (Cdk5 Regulator)	P9489	P	y	n/d	y
534	p38 MAP Kinase, Non-Activated	M8432	M	y	y	y
535	p38 MAPK	M0800	P	n/d	y	y
536	p38 MAPK activated (diphosphorylated p38)	M8177	M	y	y	y
537	Negative Control	NA				
538	p53	P5813	M	y	n/d	n/d
539	p53	P6874	M	y	n/d	n/d
540	phospho-p53 (pSer ³⁹²)	P8982	P	y	y	n/d
541	p53DINP1/SIP	P4868	P	y	y	y
542	p53R21	P4993	P	y	y	y
543	p53 BP1	B4561	P	y	y	y
544	p53 BP1	B4436	P	y	y	n/d
545	p57 ^{kip2}	P2735	M	y	y	n/d
546	p63	P3362	M	y	y	n/d
547	p63	P3737	M	y	y	y
548	PABP	P6246	M	y	n/d	n/d
549	PAD14	P4749	P	y	n/d	n/d
550	phospho-PAK1 (pThr ²¹²)	P3237	M	y	y	y
551	Par-4 (Prostate Apoptosis Response-4)	P5367	P	y	y	y
552	Anti Cy3+Cy5	C0992	M	NA	NA	NA
553	Parvin	P5746	M	y	n/d	n/d
554	Parkin	P6248	M	y	y	y
555	PARP	P7605	P	y	n/d	n/d
556	Paxillin	P1093	M	y	n/d	y
557	PCAF	P7493	P	y	n/d	n/d
558	Proliferating Cell Nuclear Antigen (PCNA)	P8825	M	y	n/d	n/d
559	PDK 1	P3110	P	y	n/d	n/d
560	Pen-2	P5622	P	y	n/d	n/d
561	Peripherin	P5117	M	y	y	y
562	Peroxiredoxin 3	P1247	P	y	n/d	n/d
563	PERP	P5243	P	y	n/d	n/d
564	Phospholipase A2 group V	P5242	M	y	n/d	n/d

565	Phosphoserine	P5747	M	y	y	y
566	Phosphothreonine	P6623	M	y	y	y
567	Phosphotyrosine	P1869	M	y	y	y
568	Phospholipase C 1 (PLC 1)	P8104	P	y	y	n/d
569	PhosphatidylSerine Receptor (PSR)	P1495	P	y	y	n/d
570	Negative Control	NA				
571	PIAS-x	P9498	M	y	n/d	n/d
572	Negative Control	NA				
573	PINCH-1	P9371	M	y	y	y
574	Protein Kinase B Akt1	P2482	M	y	y	y
575	Protein Kinase B Akt1	P1601	P	y	y	y
576	Anti Cy3+Cy5	C0992	M	NA	NA	NA
577	phospho-PKB (pSer ⁴⁷³)	P4112	P	n/d	y	y
578	phospho-PKB (pThr ³⁰⁸)	P3862	P	n/d	y	y
579	Protein Kinase C (PKC)	P5704	M	y	y	y
580	Protein Kinase C α	P4334	P	n/d	y	y
581	Protein Kinase C β_1	P3078	P	n/d	n/d	y
582	Protein Kinase C β_1	P6959	M	n/d	n/d	y
583	Protein Kinase C β_2	P3203	P	n/d	n/d	y
584	Protein Kinase C β_2	P2584	M	n/d	n/d	y
585	Protein Kinase C	P8083	M	n/d	n/d	y
586	Protein Kinase C δ	P8333	P	n/d	n/d	y
587	Protein Kinase C ϵ	P8458	P	n/d	n/d	y
588	Protein Kinase C ζ	P0713	P	n/d	y	y
589	Protein Kinase C η	P8090	P	y	n/d	n/d
590	Protein Kinase D	P3987	P	y	y	n/d
591	PKR	P0244	P	y	n/d	n/d
592	Plakoglobin (Catenin)	P8087	M	y	n/d	n/d
593	Platelet-Derived Growth Factor Receptor β	P7679	M	y	n/d	n/d
594	Plectin	P9318	M	n/d	n/d	y
595	PML	P6746	M	y	y	n/d
596	Presenilin-1 (S182)	P7854	P	y	y	y
597	Prion Protein	P5999	M	n/d	y	y
598	PRMT1	P6871	P	y	n/d	n/d
599	PRMT1	P6996	P	y	y	y
600	Anti Cy3+Cy5	C0992	M	NA	NA	NA
601	PRMT2	P0748	M	y	n/d	n/d
602	PRMT3	P9370	M	y	y	y
603	PRMT4	P4995	P	y	n/d	n/d
604	PRMT5	P0493	M	y	y	y
605	PRMT6	P6495	P	y	n/d	n/d
606	PRMT6	P2996	M	y	n/d	n/d
607	Proliferating Cell Protein Ki-67	P6834	M	y	n/d	n/d
608	Protein Phosphatase 1	P7979	P	y	n/d	n/d
609	Protein Phosphatase 1	P7607	M	y	y	y
610	Protein Phosphatase 2A (PP2A)	P8998	M	y	y	n/d
611	Protein S	P4555	P	y	n/d	n/d

612	Protein Tyrosine Phosphatase PEST	P9109	M	y	y	y
613	PSF	P2860	M	y	y	n/d
614	PTEN	P7482	P	y	n/d	y
615	PTEN	P3487	M	y	y	y
616	PUMA/bbc3, C-Terminal	P4618	P	y	y	n/d
617	PUMA/bbc3, N-Terminal	P4743	P	y	n/d	n/d
618	Pyk2	P3902	P	y	y	y
619	AP2 beta	9856A	M	y	n/d	n/d
620	phospho-Pyk2 (pTyr ^{579/580})	P6989	P	y	n/d	n/d
621	alpha 2AP	9981A	M	y	n/d	n/d
622	Negative Control	NA				
623	Rab5	R7904	M	y	y	y
624	Anti Cy3+Cy5	C0992	M	NA	NA	NA
625	Rab 7	R8779	M	y	y	y
626	Rab9	R5404	M	y	y	y
627	RAD1	R5029	P	y	n/d	n/d
628	Rad17 (C-terminal)	R8029	P	y	n/d	d/n
629	Raf-1/c-Raf	R2404	M	y	y	y
630	Raf-1	R5773	P	y	n/d	y
631	phospho-c-Raf (pSer ⁶²¹)	R1151	P	y	y	y
632	RAIDD, Internal Domain	R9775	P	y	n/d	n/d
633	RAIDD	R5275	P	y	n/d	n/d
634	RALAR	R8529	M	y	y	y
635	Ran	R4777	M	y	y	n/d
636	PIASy	P0104	M	y	n/d	n/d
637	RAP1	R8154	M	y	n/d	n/d
638	RbAp48/RbAp46	R3779	P	y	n/d	n/d
639	Reelin	R4904	P	n/d	y	y
640	Retinoblastoma	R6775	P	y	n/d	n/d
641	phospho-Retinoblastoma (pSer ⁷⁹⁵)	R6878	M	y	y	y
642	RhoE	R6153	M	y	y	n/d
643	RICK, C-Terminal	R9650	P	y	y	y
644	RIP (Receptor Interacting Protein)	R8274	P	y	n/d	n/d
645	RNase L	R3529	M	y	n/d	n/d
646	ROCK-1	R6028	P	y	y	y
647	ROCK-2	R8653	P	y	y	n/d
648	Anti Cy3+Cy5	C0992	M	NA	NA	NA
649	Rsk1	R5145	P	y	y	y
650	S-100	S2644	P	y	n/d	y
651	S-100 (Subunit)	S2407	M	y	n/d	n/d
652	S-100 (β-Subunit)	S2532	M	y	n/d	y
653	S-Nitrosocysteine	N5411	P	y	y	y
654	S6 Kinase	S4047	P	y	y	y
655	SAPK3	S0315	P	y	y	y
656	Spectrin (α and β)	S3396	M	y	n/d	n/d
657	Serine/Threonine Protein Phosphatase 2 A/A	P8109	P	y	y	y
658	Serine/Threonine Protein Phosphatase 1β	P7484	P	y	y	y
659	Serine/Threonine Protein Phosphatase 1α1	P7609	P	y	y	y

660	Serine/Threonine Protein Phosphatase 2 A/B	P5359	P	y	y	y
661	Serine/Threonine Protein Phosphatase 2 A/B' pan2	P8359	P	n/d	n/d	y
662	Serine/Threonine Protein Phosphatase 2C	P8609	P	y	y	n/d
663	AP2 gamma	A3108	M	y	n/d	n/d
664	SGK	S5188	P	y	n/d	n/d
665	SH-PTP2 (SHP-2)	S3056	P	y	n/d	n/d
666	Siah2	S7945	M	y	y	n/d
667	Sin3A, N-terminal	S4445	P	y	y	y
668	Sin3A, C-Terminal	S6695	P	y	n/d	n/d
669	Sir2	S5313	P	n/d	y	n/d
670	SIRP1 (SHPS-1)	S1311	P	n/d	y	y
671	Sirt1	S5196	M	n/d	y	n/d
672	Anti Cy3+Cy5	C0992	M	NA	NA	NA
673	SKM1 (Skeletal Muscle Type 1)	S9568	M	n/d	y	y
674	Beta tubulin III (neuronal)	8578T	M	y	y	y
675	SLIPR/MAGI-3	S1190	P	n/d	n/d	y
676	SLIPR/MAGI-3	S4191	M	n/d	n/d	y
677	Smad4 (DPC4)	S3934	M	y	n/d	n/d
678	SMC1L1	S6446	P	y	n/d	n/d
679	SMN	S2944	M	y	y	n/d
680	-SNAP, C-terminus	S9444	P	y	y	y
681	SNAP-23	S2194	P	n/d	y	n/d
682	SNAP-25	S9684	P	n/d	y	y
683	SNAP- 29	S2069	P	n/d	y	y
684	Sos1	S2937	P	y	n/d	n/d
685	Sp1	S9809	P	y	n/d	n/d
686	Spred-2	S7320	P	y	y	y
687	Striatin	S0696	P	n/d	y	y
688	Substance P Receptor	S8305	P	y	y	y
689	SMAC/Diablo	S0941	P	y	y	n/d
690	SUMO-1	S8070	P	y	n/d	n/d
691	SUMO-1 (C-terminal)	S5446	P	y	n/d	n/d
692	Survivin	S8191	P	y	n/d	n/d
693	Synaptotagmin	S2177	P	y	y	n/d
694	Synaptopodin	S9442	P	n/d	n/d	y
695	Synaptopodin	S9567	P	n/d	n/d	y
696	Anti Cy3+Cy5	C0992	M	NA	NA	NA
697	SynCAM	S4945	P	n/d	y	y
698	1 Syntrophin	S4688	P	n/d	n/d	y
699	1 Syntrophin	S4813	P	n/d	n/d	y
700	Syntaxin	S0664	M	n/d	n/d	y
701	Syntaxin 6	S9067	M	y	y	y
702	Syntaxin 8	S8945	P	n/d	n/d	y
703	Synuclein	S3062	P	y	n/d	y
704	Negative Control	NA				
705	Tal	T1075	P	y	y	y
706	Tal	T1200	P	y	y	y

707	TAP	T1076	M	y	n/d	n/d
708	Tau	T9450	M	y	y	y
709	phospho-Tau (pSer ^{199/202})	T6819	P	y	y	y
710	Tau	T5530	M	y	n/d	n/d
711	Tenascin	T2551	M	y	n/d	n/d
712	Thimet Oligopeptidase 1	T7076	M	y	n/d	n/d
713	TIS7	T2576	M	y	y	n/d
714	Tumor Necrosis Factor Soluble Receptor II	T1815	M	y	n/d	n/d
715	Tob	T2948	M	y	n/d	n/d
716	TOM22	T6319	M	y	n/d	n/d
717	Topoisomerase-I	T8573	M	y	n/d	n/d
718	TRAIL	T3067	M	y	n/d	n/d
719	TRAIL	T9191	P	y	n/d	n/d
720	Anti Cy3+Cy5	C0992	M	NA	NA	NA
721	Transforming Growth Factor- β , pan	T9429	P	y	n/d	n/d
722	Transportin 1	T0825	M	y	y	y
723	TRF1	T1948	M	y	n/d	n/d
724	Tropomyosin	T2780	M	y	y	y
725	Tropomyosin (Sarcomeric)	T9283	M	y	n/d	y
726	Tryptophane Hydroxylase	T0678	M	y	n/d	y
727	TSG101	T5826	P	y	y	y
728	Tubulin	T6074	M	y	y	y
729	Tubulin	T6199	M	y	y	y
730	Tubulin	T5201	M	y	y	y
731	β -Tubulin I	T7816	M	y	y	y
732	Tubulin I+II	T8535	M	y	y	y
733	Tubulin III	T5076	M	y	n/d	y
734	β -Tubulin IV	T7941	M	y	y	y
735	Tubulin	T5326	M	y	y	y
736	Tubulin	T3559	P	y	n/d	n/d
737	Tubulin	T3320	P	y	n/d	y
738	ϵ -Tubulin	T1323	M	y	y	n/d
739	Tubulin, Polyglutamylated	T9822	M	y	y	y
740	Tubulin, Tyrosine	T9028	M	y	n/d	n/d
741	Tumor Necrosis Factor- α	T8300	P	y	n/d	n/d
742	Tumor Necrosis Factor- α	T2824	M	n/d	y	y
743	Nanog	N3038	M	y	n/d	n/d
744	Anti Cy3+Cy5	C0992	M	NA	NA	NA
745	TWEAK Receptor/Fn-14	T9700	M	y	n/d	n/d
746	Tyrosin hydroxylase	T2928	M	y	n/d	y
747	U2AF ⁶⁵	U4758	M	y	y	y
748	Ubiquitin	U0508	M	y	y	y
749	Ubiquitin C-terminal Hydrolase L1	U5133	P	y	y	y
750	Ubiquitin C-terminal Hydrolase L1	U5258	P	y	y	y
751	Pinin	P0084	M	y	n/d	n/d
752	Vanilloid Receptor-1	V2764	P	n/d	n/d	y
753	VDAC/Porin	V2139	P	y	y	y

754	Vascular Endothelial Growth Factor Receptor-1 (VEGFR-1)	V4762	M	y	n/d	n/d
755	Vesicular GABA Transporter	V5764	P	n/d	y	y
756	VGLUT 1	V0389	P	y	n/d	n/d
757	VGLUT 2	V2639	P	n/d	n/d	y
758	Vimentin	V6389	M	y	n/d	y
759	Vinculin	V4505	M	y	y	n/d
760	Vitronectin	V7881	M	y	n/d	n/d
761	WAVE	W0392	P	y	y	y
762	WSTF	W3516	P	y	y	n/d
763	Y14	Y1253	M	y	n/d	n/d
764	ZAP-70	Z0627	M	y	y	d/n
765	Zip Kinase	Z0134	P	y	n/d	n/d
766	Zyxin	Z0377	M	y	y	y
767	GAPDH	G8795	M	y	y	y
768	Anti Cy3+Cy5	C0992	M	NA	NA	NA

Appendix 3: The list of differentially expressed proteins identified in the experiment #1c; sample #16B^{CS} vs #1B^{CR} (*Half-Labeling Protocol*). A total of n=24 proteins were identified with a fold change of ≥ 1.8 as listed below (Refer: Table 47 in thesis).

Protein	ID	Log ratio	Fold change
14-3-3	T5942	-1.658	-3.15
BclXI	B9429	1.362	2.57
Calbindin D 28K	C7354	-2.398	-5.27
CDK5	C6118	-0.944	-1.92
CUGBP1	C5112	-1.169	-2.24
Cytokeratin Peptide 4	C5176	-1.328	-2.51
Dystrophin	D8043	0.914	1.88
E2F6	E1532	-1.458	-2.74
FAK pTyr577	F8926	-0.989	-1.98
FANCD2	F0305	0.965	1.95
HDAC2	H3159	0.846	1.79
HDAC6	H2287	0.915	1.88
ILK	I1907	1.048	2.06
MDMX	M0445	0.852	1.8
Mint2	M3319	-2.012	-4.03
NFkB	N8523	-0.905	-1.87
p19INK4d	P4354	-1.344	-2.53
Pan Cytokeratin	C2931	1.077	2.1
PRMT2	P0748	-1.833	-3.56
SynCAM	S4945	-0.982	-1.97
Tau pSer199 202	T6819	-0.99	-1.98
Transforming Growth factor beta pan	T9429	-1.682	-3.2
TWEAK Receptor	T9700	-1.465	-2.76
Zyxin	Z0377	-1.108	-2.15

Appendix 4: The list of differentially expressed proteins identified from the combined experiments #2 and #2b (*Full and Half-Labeling Protocols*); sample #38^{CS} vs #15. A total of n=13 proteins were identified with a fold change of ≥ 1.8 as listed below from both the experiments (Refer: Table 47 in thesis).

Protein	ID	Log ratio	Fold Change
PRMT2	P0748	-1.545	-2.91
Anti Cy3/5	C0992	-1.43	-2.69
FAK pTyr577	F8926	-1.038	-2.05
FANCCD2	F0305	0.9	1.86
G9a Methyltransferase	G6919	-0.998	-1.99
GRANZYME B	G1044	0.869	1.826
ILK	I1907	1.037	2.05
LIM Kinase 1	L2290	-0.858	-1.81
MeCP2	M9317	0.898	1.86
Pan cytokeratin	C2931	1.484	2.79
DR4	D3813	0.84	1.79
ROCK1	R6028	0.975	1.96
ZAP70	Z0627	-0.909	-1.87

Appendix 5: The list of differentially expressed proteins identified in the experiment #3; sample #12B^{CS} vs #1^{CR} (*Half-Labeling Protocol*). A total of n=15 proteins were identified with a fold change of ≥ 1.8 as listed below (Refer: Table 47 in thesis).

Proteins	ID	Log ratio	Fold change
14 3 3	T5942	-2.401	-5.28
ARC	A8344	0.921	1.89
BclxL	B9429	0.999	1.99
Csk	C7863	1.287	2.44
DR4	D3813	1.468	2.76
E2F6	E1532	-0.972	-1.96
FANCD2	F0305	1.039	2.05
G9a Methyltransferase	G6919	-1.203	-2.3
MSK1	M5437	1.775	3.42
p19INK4d	P4354	-1.101	-2.14
Pan Cytokeratin	C2931	1.12	2.17
Pinin	P0084	1.182	2.26
Rab7	R8779	-1.113	-2.16
RNaseL	R3529	-1.171	-2.25
SNX6	S6324	2.416	5.33

Appendix 6: The list of 72 differentially expressed proteins identified and mapped onto IPA from the combined analysis #1 (9 x AbMA experiments TH+VH combined data). Refer to section 4.2.1 in the thesis.

Proteins	Gene Names
14- 3-3	YWHAQ
Annexin V	ANXA5
Chondroitin sulfate	ACAN
Protein Kinase Ba	AKT1
Mint2	APBA2
BclxL	BCL2L1
BID	BID
Calbindin D 28K	CALB1
CDK5	CDK5
p19INK4d	CDKN2D
Centrin	CETN1
IKKa	CHUK
Csk	CSK
CUGBP1	CUGBP1
Dystrophin	DMD
Desmosomal protein	DSC1
E2F6	E2F6
Epidermal Growth Factor	EGF
G9a Methyl Transferase	EHMT2
FANCD2	FANCD2
GRANZYME B	GZMB
Dimethyl Histone H3/Acetyl Histone H3 AcLys9	H3F3A
HDAC4	HDAC4
HDAC6	HDAC6
ILK	ILK
Cytokeratin peptide 4	KRT4
LIM Kinase 1	LIMK1
PINCH 1	LIMS1
SAPK3	MAPK12
Tau pSer199 202	MAPT
MDMX	MDM4
MeCP2	MECP2
Ki-67	MKI67
cMyc	MYC
MyD88	MYD88
NFkB	NFKB1
ARC	NOL3
Pinin	PNN

Protein Kinase Cb2/Protein Kinase Cb1	PRKCB
PRMT2	PRMT2
FAKpTyr577	PTK2
Rab7	RAB7A
RALAR	RALA
Reelin	RELN
RIP	RIPK1
RNaseL	RNASEL
ROCK1	ROCK1
Rsk1	RPS6KA1
MSK1	RPS6KA5
S6 Kinase	RPS6KB1
Sir2	SIRT1
hSNF5 INI1	SMARCB1
SNX6	SNX6
Sp1	SP1
DRAK1	STK17A
TBP	TBP
Transforming Growth factor beta pan	TGFB1
DR4	TNFRSF10A
TWEAK receptor	TNFRSF12A
TRAIL	TNFSF10
Transportin 1	TNPO1
Tropomyosin	TPM1
Munc13 1	UNC13A
ZAP70	ZAP70
Zyxin	ZYX

Appendix 7: The list of 125 differentially expressed proteins identified and loaded onto IPA from the combined analysis #2 (9 x AbMA experiments + 2x 2D-PAGE/MS + 3 Literature proteins combined data). Refer to section 4.2.2 in the thesis.

Proteins	Gene Names
14 3 3	YWHAQ
14-3-3 protein epsilon	YWHAE
14-3-3 protein gamma	YWHAG
14-3-3 protein theta	YWHAQ
14-3-3 protein zeta/delta	YWHAZ
Activator of 90 kDa heat shock protein ATPase homolog 1	AHSA1
Adenine phosphoribosyltransferase	APRT
Annexin A3	ANXA3
Annexin V	ANXA5
Apolipoprotein A1	APOA1
ARC	NOL3
ATP synthase subunit beta, mitochondrial	ATP5B
Barrier-to-autointegration factor	BANF1
BclxL	BCL2L1
BID	BID
Calbindin D 28K	CALB1
CDK5	CDK5
Cellular retinoic acid-binding protein 2	CRABP2
Centrin	CETN1
Chloride intracellular channel protein 1	CLIC1
Chondroitin sulfate	ACAN
cMyc	MYC
Coactosin-like protein	COTL1
Creatine kinase B-type	CKB
Csk	CSK
CUGBP1	CUGBP1
Cytokeratin peptide 4	KRT4
Cytokeratin 19	KRT19
Desmosomal protein	DSC1
Dimethyl Histone H3/Acetyl Histone H3 AcLys9	H3F3A
DR4	TNFRSF10A
DRAK1	STK17A
Dystrophin	DMD
E2F6	E2F6
Epidermal Growth Factor	EGF
FAKpTyr577	PTK2
FANCD2	FANCD2

Ferritin light chain	FTL
G9a Methyl Transferase	EHMT2
Glutathione S-transferase omega-1	GSTO1
Glutathione S-transferase P	GSTP1
Glycerol-3-phosphate dehydrogenase [NAD+], cytoplasmic	GPD1
GRANZYME B	GZMB
HDAC4	HDAC4
HDAC6	HDAC6
HEBP2 protein (fragment)	HEBP2
highly similar to Heat-shock protein beta-6	HSPB6
Histone-binding protein RBBP4	RBBP4
hSNF5 INI1	SMARCB1
HSP27	HSBP1
IKKa	CHUK
ILK	ILK
Inorganic pyrophosphatase	PPA1
Isoform 1 of Acyl-protein thioesterase 1	LYPLA1
Isoform 1 of Alpha-1-antitrypsin	SERPINA1
Isoform 1 of Eukaryotic translation initiation factor 5A-1	EIF5A
Isoform 1 of Nucleoside diphosphate kinase A	NME1
Isoform 2 of F-actin-capping protein subunit beta	CAPZB
Isoform 2 of Tropomyosin alpha-3 chain	TPM3
Isoform 2 of Tropomyosin alpha-4 chain	TPM4
Isoform 3 of Tropomyosin alpha-1 chain	TPM1
Isoform Long of 14-3-3 protein beta/alpha	YWHAB
Isoform Long of Proteasome subunit alpha type-1	PSMA1
Keratin, type I cytoskeletal 19	KRT19
Keratin, type II cytoskeletal 8	KRT8
Ki-67	MKI67
LIM Kinase 1	LIMK1
Macrophage-capping protein	CAPG
MDMX	MDM4
MeCP2	MECP2
Microfibril-associated glycoprotein 4	MFAP4
Microtubule-associated protein RP/EB family member 1	MAPRE1
Mint2	APBA2
MSK1	RPS6KA5
Munc13 1	UNC13A
MyD88	MYD88
Myosin regulatory light chain 12B	MYL12B

NFkB	NFKB1
p19INK4d	CDKN2D
peroxiredoxin 3 isoform b	PRDX3
PINCH 1	LIMS1
Pinin	PNN
Platelet-activating factor acetylhydrolase IB subunit beta	PAFAH1B2
PRMT2	PRMT2
Prohibitin	PHB
Proteasome activator complex subunit 1	PSME1
proteasome activator subunit 2	PSME2
Proteasome subunit beta type-3	PSMB3
Protein disulfide-isomerase	P4HB
Protein Kinase Ba	AKT1
Protein Kinase Cb2/Protein Kinase Cb1	PRKCB
Protein SEC13 homolog	SEC13
Rab7	RAB7A
RALAR	RALA
Reelin	RELN
Rho GDP-dissociation inhibitor 1	ARHGDI1
Rho GDP-dissociation inhibitor 2	ARHGDI2
Ribonuclease inhibitor	RNH1
RIP	RIPK1
RNaseL	RNASEL
ROCK1	ROCK1
Rsk1	RPS6KA1
S6 Kinase	RPS6KB1
SAPK3	MAPK12
Serum amyloid P-component	APCS
Sir2	SIRT1
SNX6	SNX6
Sorcin	GCL
Sp1	SP1
Stathmin	STMN1
Tau pSer199 202	MAPT
TBP	TBP
T-complex protein 1 subunit beta	CCT2
TRAIL	TNFSF10
Transforming Growth factor beta pan	TGFB1
Transportin 1	TNPO1
Transthyretin	TTR
Tropomyosin	TPM1

Tubulin-specific chaperone A	TBCA
Tumor protein, translationally-controlled 1	TPT1
TWEAK receptor	TNFRSF12A
Vimentin	VIM
ZAP70	ZAP70
Zyxin	ZYX

